Fundamentals of torrefaction of biomass and its environmental impacts

by

Raimie Hebriyah Haji Ibrahim

Submitted in accordance with the requirements for the degree of

Doctor of Philosophy

The University of Leeds

School of Process, Environmental and Materials Engineering

October 2013

The candidate confirms that the work submitted is his/her own, except where work which has formed part of jointly-authored publications has been included. The contribution of the candidate and the other authors to this work has been explicitly indicated below. The candidate confirms that appropriate credit has been given within the thesis where reference has been made to the work of others. Further details of the jointly-authored publications and the contributions of the candidate and the other authors to the work are listed below.

Chapter 5 is based on the publication and a conference paper as listed below:

IBRAHIM, R.H.H., L.I. DARVELL, J.M. JONES and A. WILLIAMS. 2013. Physicochemical characterisation of torrefied biomass. *Journal of Analytical and Applied Pyrolysis*. **103**, pp.21-30.

IBRAHIM, R.H.H., L.I. DARVELL, J.M. JONES and A. WILLIAMS. 2012. Physicochemical characterisation of torrefied biomass. 19th International Symposium on Analytical and Applied Pyrolysis, Linz, Austria.

I was the lead author and lead conductor and coordinator of most experiments and all experimental data respectively. The study of investigated biomass fuels using XPS was carried out in Molecular and Nanoscale Physics, Faculty of Physics and Astronomy, University of Leeds with the help of Dr. Benjamin Johnson. TEM analysis was carried out in Institute of Materials Research, Faculty of Engineering, with the help of Dr. Michael Ward. The metal analysis was conducted at TES Bretby Ltd.

Chapter 6 is based on a conference paper:

IBRAHIM, R.H.H., Z. TAO, L.I. DARVELL, J.M. JONES and A. WILLIAMS. The influence of particle sizes of biomass on torrefaction. 2012. Proceeding of Sustainable Energy. 21-23 Nov 2012: ***International Energy Conference***, Brunei Darussalam and 10th Sustainable Energy and Environment (SEE) Forum. pp. 208-216.

I was the lead author. Most of the experimental work on the first half of the chapter on the investigation of the effect of particle sizes of biomass fuels on torrefaction using TGA was carried out by Zhiwen Tao, an MSc student under my supervision (May-Jun 2012), while I worked on the calibration of the permanent gases (H_2O, CO_2 and CO) for the FTIR. FTIR was used simultaneously with the TGA. For the other half of the chapter, I carried out most

of the work that deals with the simulation of torrefaction work using a program, FG-Biomass model.

ACKNOWLEDGEMENTS

In the name of Allah, the most Gracious, the most Merciful.

Praise to Allah, with His shower of blessings.

I would like to acknowledge a number of people who have guided and supported me throughout the course of this work as without them, I would not be able to produce this thesis. First and foremost, I would like to express my sincerest gratitude to my supervisors, Prof. Jenny Jones and Prof. Alan Williams. They have provided me endless guidance, invaluable support and always make sure that I was on the right track. Words of encouragement that came from these two wonderful people gave me the confidence in my work.

I would also like to express my gratitude to my colleagues, Leilani Darvell, Abby Saddawi, Bijal Gudka, Xiao Mian, Femi Akinrinola, Patrick Biller and Simon Lloyd, who also have played a major part in building up my confidence working with this project especially in the lab. They make me feel very grateful to be a part of the research group and I am lucky to have met these great people. Most of them have graduated and left for jobs and I wish them the very best of luck in their future undertakings.

My thanks also goes to Zhiwen Tao, an MSc student, who have worked hard in collecting data used in this thesis. I would like to thank Prof. Jenny Jones again for giving me faith to assist him throughout his lab-work during the summer in 2012.

I would like to acknowledge the Energy Programme, who are the Research Councils UK cross council initiative led by Engineering and Physical Sciences Research Council (EPSRC) and contributed to by Economic and Social Research Council (ESRC), National Environment Research Council (NERC), Biotechnology and Biological Sciences Research Council (BBSRC) and Science and Technology Facilities Council (STFC), as well as the scholarship received from Brunei's Ministry of Education for the financial support.

A big thank you to my beloved family, especially my parents for their great love and words of encouragement, and to my friends, both in Leeds and back in Brunei, for always there for me in the good and tough times. Every moment I had in Leeds will be cherished. Finally, I would also like to thank my other half for being understanding, patient and for giving me his continuous support in whatever I do.

ABSTRACT

In response to the EU 2020 target, the markets of biomass energy are developing rapidly and becoming more international. At the same time, there have been concerns with biomass in terms of its characteristics such as high moisture content, poor grindability behaviour, low calorific value and problems in relation to transport, handling and storage. Torrefaction is a pre-thermal treatment that has the potential to improve these characteristics. This thesis covers four areas of investigation work. The first chapter shows how torrefaction has improved the physical and chemical properties of biomass. Torrefied fuels became more hydrophobic, contain higher energy yields and have grindability behaviours that resemble those of low rank coals. Furthermore, microscopic and spectrometric studies were carried out to gain a better insight into any changes in morphology and chemical composition of torrefied biomass. The overall results indicate that careful optimization is required to maximize the benefits of torrefaction whilst maintaining a good energy yield. Torrefaction is still in the development stage and so underpinning knowledge and science is still required. The second chapter examines how different sizes of biomass ($\geq$ 5x5x5 mm) could influence torrefaction. The presence of mass and heat transfer limitations was suggested to explain the observed significant changes. The third chapter provides a short investigation on how torrefied biomass fuels react in response to combustion, where the heating rate of the flame and the rate of char combustion were estimated. Torrefaction in relation to health and safety concerns as well as environmental issues are still unknown. The next chapter provides a preliminary study of an environmental impact assessment was reviewed using any information that is readily available. Several areas of interests that cover from raw materials to the environmental fates of products of torrefaction were considered. Finally, a series of recommendations for future work are discussed at the end of the thesis.

Table of contents

Fundamentals of torrefaction of biomass and its environmental impacts

Acknowledgements iv

Abstract vi

Table of contents vii

List of tables xv

List of figures xvii

List of publications xxvi

List of abbreviations xxvii

Chapter 1: Introduction 1

1.1 Introduction 1

1.1.1 Oil 3

1.1.2 Coal 3

1.1.3 Natural gas 4

1.2 Energy challenges 4

1.2.1 Climate change 5

1.2.2 Energy security 5

1.3 The implication of renewable sources of energy in the UK 5

1.3.1 Electricity 6

1.3.2 Heat 7

1.3.3 Transportation 8

1.4 Biomass as a potential renewable source of energy 8

1.4.1 Renewability benefits 9

1.4.2 Environmental benefits 10

1.4.3 Sociopolitical benefits 10

1.5 Biomass Task Force Report 10

1.6 UK Biomass Strategy 11

1.7 Short Rotation Coppice (SRC) 12

1.8 Short Rotation Forestry (SRF) 12

1.9 Energy crops: Herbaceous and woody crops 13

1.9.1 Definition of energy crops 13

1.9.2 Herbaceous energy crops 14

1.9.3 Woody crops 16

1.10 Biomass composition 20
1.10.1 Cellulose 20
1.10.2 Hemicellulose 21
1.10.2.1 Hemicellulose in grasses and herbaceous crops 21
1.10.2.2 Hemicellulose in hardwoods 23
1.10.2.3 Hemicellulose in softwoods 23
1.10.3 Lignin 23
1.11 Biomass characterisation 25
1.11.1 Fuel characteristics: Proximate analysis 25
1.11.2 Fuel characteristics: Ultimate analysis 29
1.12 Current uses of biomass energy in the UK 30
1.13 Problems of biomass as a renewable source of energy 34
1.14 Biomass pre-treatment technologies 36
1.15 Torrefaction 37
1.15.1 Definition of torrefaction 38
1.15.2 Differences between carbonization, pyrolysis and torrefaction 39
1.15.3 Process diagram (Heat Integration) 39
1.15.4 Torrefaction reaction 40
1.16 Mass and energy balance 44
1.17 Torrefaction approaches 46
1.17.1 Fixed bed torrefier 46
1.17.2 TG-FTIR 46
1.17.3 Model development 48
1.18 Applications of torrefied biomass 49
1.19 Status of torrefaction 50
1.19.1 Directly heated reactors 51
1.19.2 Indirectly heated reactors 51
1.20 Overview of project initiatives 53
1.21 Economic value of torrefaction 55
1.22 Current challenges for market implementations of torrefaction technologies 56
1.22.1 Technical challenges 56
1.22.2 Macroeconomic challenges 57
1.23 Regulatory issues 57

Chapter 2: Aims and Objectives 58
2.1 Project overview 58
2.2 Group project aims and objectives 59
2.3 Research aims and objectives 59
Chapter 3: Literature Review 62
3.1 The behaviour of lignocellulosic materials to pyrolysis 62
3.2 Mechanisms of torrefaction 63
3.2.1 Differences found in deciduous, coniferous and herbaceous crops 64
3.2.2 Rate kinetics 67
3.3 Physical and chemical changes of biomass fuels upon torrefaction 72
3.3.1 Colour 72
3.3.2 Particle size and shape 73
3.3.3 Mass loss 74
3.3.4 Moisture, ash, volatile and fixed carbon content 74
3.3.5 Carbon, nitrogen, hydrogen and oxygen contents, Higher heating value (HHV) and Van Krevelen plot 76
3.4 The influence of temperature and residence time on biomass fuels 77
3.5 The influence of particle size on torrefaction 78
3.6 The investigation of grindability characteristics of biomass subject to different conditions 83
3.7 The study of energy properties of torrefied biomass fuels 87
3.8 The assessment of hydrophobicity of raw and treated biomass fuels 88
3.9 Comparison between the combustion behaviour of raw and torrefied biomass 90
3.10 The investigation of the liquid products (tar and condensables) and non-condensables products of torrefaction 93
3.11 The use of FG-Biomass model to predict torrefaction 96
3.12 Conclusions 98
Chapter 4: Experimental Procedures 101
4.1 Samples 101
4.2 Sample preparation for torrefaction using TGA-FTIR 101
4.3 Torrefaction procedures 102
4.3.1 Torrefaction using the bench scale reactor 102
4.4 Fuel characterisation 106
4.4.1 Proximate analysis using British Standard methods 107
4.4.1.1 Moisture content, M_{ad} 107

4.4.1.2 Ash content, A_d 108
4.4.1.3 Volatile matter content, V_d 108
4.4.1.4 Fixed carbon content, *FCC* 109
4.4.2 Proximate analysis using the Thermogravimetric Analyser (TGA) 109
4.4.3 Ultimate analysis 109
4.4.4 Calorific value determination 110
4.4.5 Energy yield, η_E 112
4.4.6 Hydrophobicity 112
4.4.7 Density 112
4.4.8 Grindability tests 113
4.4.8.1 Calibration of Retsch PM 100 ball mill 113
4.4.8.2 Particle size distribution 115
4.4.9 Ash metal analysis 115
4.5 Morphology of raw and torrefied biomass 116
4.5.1 Determination of surface area (BET method) 116
4.5.2 Scanning Electron Microscopy and Energy Dispersive X-ray Detection SEM-EDX Detection 116
4.5.3 Transmission Electron Microscopy (TEM) 117
4.5.4 Transmission Fourier Transform Infra Red (FTIR) 118
4.5.4.1 Preparation of KBr pellets 118
4.5.4.2 Running the samples 118
4.5.5 X-ray Photoelectron Spectrometer (XPS) 118
4.6 Analysis of liquid products 120
4.6.1 Aqueous fraction 120
4.6.1.1 Total organic carbon content (TOC) 120
4.6.1.2 pH 120
4.6.2 Tar fraction 121
4.6.2.1 Karl Fischer titration 121
4.6.2.2 Liquid-GC-MS 121
4.7 Torrefaction using the TGA-FTIR 122
4.8 Analysis of volatile products (Permanent gases and low molecular weight volatiles) 124
4.9 Single Particle Combustion of woody biomass 126
4.10 Functional-Group (FG) Biomass model 126
Chapter 5: An investigation of the properties and characterisation of products of torrefaction 133

5.1 Introduction 133
5.2 Results and discussion 135
5.2.1 Temperature profile 135
5.2.2 Mass balances 137
5.2.2.1 Mass yields 137
5.2.2.2 Overall mass balance 138
5.2.3 Standard fuel analysis 138
5.2.4 Physical characterisation 143
5.2.4.1 Hydrophobicity 143
5.2.4.2 Grindability of torrefied biomass 146
5.2.4.3 Density 150
5.2.5 Morphological changes to the structure of solid torrefied biomass fuels 151
5.2.5.1 Surface area 151
5.2.5.2 Electron microscopy 151
5.2.6 Chemical properties of solid torrefied biomass 152
5.2.6.1 FTIR analysis 152
5.2.6.2 XPS measurements 155
5.2.7 Analysis of liquid products 157
5.3 Conclusions 159
Chapter 6: The Investigation of the influence of particle sizes on products from torrefaction of biomass 161
6.1 Introduction 161
6.2 Results and discussion 166
6.2.1 Fuel analyses of raw willow and eucalyptus (*E.Gunnii*) 166
6.2.2 Themogravimetric analysis (TGA-FTIR) 167
6.2.2.1 Mass loss and temperature profile 167
6.2.2.2 Influence of temperature and residence time on torrefaction using a TGA in terms of rate of mass loss 169
6.2.2.3 Influence of particle sizes on the pyrolysis of torrefied biomass 171
6.2.2.4 Properties of torrefied solid product 172
6.2.2.4.1 Proximate analysis (Moisture, ash, volatile and char contents) 172
6.2.2.4.2 Ultimate analysis (C, H, N contents) and calorific values 174
6.2.2.5 Gas evolution profile 175
6.2.3 Comparison between the product distribution obtained experimentally 182

and as predicted in FG-Biomass model

6.2.3.1 Overall mass balance 182

6.2.3.2 Mass yields of torrefied biomass 187

6.2.3.3 Ultimate analysis 188

6.2.4 Influence of particle size on temperature distribution as predicted by the FG-Biomass model 191

6.3 Conclusions 196

Chapter 7: The study of a single particle combustion of willow (*Salix spp.*) and eucalyptus (*Eucalyptus Gunnii*) 197

7.1 Introduction 197

7.2 Combustion of biomass 197

7.2.1 The chemistry of combustion of solid biomass fuels 198

7.2.1.1 Heating and drying 198

7.2.1.2 Devolatisation and volatile combustion 199

7.2.1.3 Char combustion 200

7.2.1.4 Char burnout 202

7.3 Single particle combustion studies 202

7.3.1 Determination of rate of devolatisation 203

7.3.2 Determination of rate of char combustion 204

7.4 Results and discussion 204

7.4.1 Four stages of single particle combustion 204

7.4.2 Combustion behaviour with respect to torrefaction 205

7.4.3 Ignition delay 205

7.4.4 Volatile combustion 207

7.4.5 Char combustion 207

7.4.6 Rate of devolatisation and char combustion 209

7.5 Conclusions 213

Chapter 8: Environmental Impact Assessment of Torrefaction of Biomass 214

8.1 Introduction 214

8.2 Biomass and air quality 216

8.3 Lifecycle assessment (LCA) 217

8.4 Environmental impacts of biomass production 218

8.4.1 Soil quality 219

8.4.2 Water pollution 220

8.4.3 Air pollution 220

8.4.4 Biodiversity 221
8.4.5 Greenhouse gases 221
8.5 Brief summary of the environmental impacts of biomass use in industries for energy 221
8.6 Emission controls 226
8.7 Biomass sustainability 226
8.8 Potential of biomass energy in the future 227
8.9 Overview of environmental impact assessment (EIA) 228
8.10 Environmental impact assessment of torrefaction of biomass 231
8.10.1 Screening 233
8.10.2 Scoping 233
8.10.2.1 Raw materials 233
8.10.2.1 Torrefaction plant 235
8.10.2.3 Stages involved before, during and after torrefaction 236
8.10.2.3.1 Heating and drying 238
8.10.2.3.2 Torrefaction 243
8.10.2.4 Torrefied biomass materials 246
8.10.2.5 Environmental fates of volatiles 248
8.10.2.6 Environmental risk assessment and its mitigation measures as well as alternative options 252
8.11 Conclusion 252
Chapter 9: Summary of conclusions and discussion of further work 260
9.1 Introduction 260
9.2 An investigation of the properties and characterisation of products of torrefaction 260
9.3 The investigation of the influence of particle sizes on products from torrefaction of biomass 261
9.4 The study of a single particle combustion of willow (*Salix spp.*) and eucalyptus (*E. Gunnii*) 261
9.5 Environmental impact assessment of torrefaction of biomass 262
9.6 Future work 263
9.6.1 An investigation of the properties and characterisation of products of torrefaction 263
9.6.2 The investigation of the influence of particle sizes on products from torrefaction of biomass 263
9.6.3 The study of a single particle combustion of willow (*Salix spp.*) and eucalyptus (*E. Gunnii*) 264

9.6.4 Environmental impact assessment of torrefaction of biomass 264

References 265

Appendices

Appendix 5.1. Temperature profile of biomass fuels upon torrefaction. 281

Appendix 5.2. Ash elemental composition (%m/m). 283

Appendix 5.3. Grindability performance of biomass. 284

Appendix 5.4. FTIR Spectra of raw and torrefied willow and eucalyptus samples. 286

Appendix 5.5. X-ray Photoelectron Spectroscopy survey spectra of eucalyptus samples. 287

Appendix 5.6. List of components contained in tar, obtained from torrefaction of hardwood and softwood. 288

Appendix 6.1. A procedure to conduct a torrefaction/pyrolysis simulation using an FG-Biomass model. 290

Appendix 6.2. Calculated volumes of willow and eucalyptus samples. 291

Appendix 6.3. Mass yields of torrefied willow and eucalyptus, obtained from TGA-FTIR 294

Appendix 6.4. Yields of products of torrefaction of biomass as predicted by FG-Biomass model. 295

Appendix 8.1. Potential stakeholders and sources of environmental information (EA, 2002). 296

List of tables

Table 1.1	Total production of fuels based in UK equivalent to million tonnes of oil, according to the UK Energy Brief 2013 (DECC, 2013a)	3
Table 1.2	Countries that use biomass in the industrial sector (IEA, 2013a).	9
Table 1.3	Types of biomass and their examples (James and Howes, 2006).	14
Table 1.4	Overview of reactor technologies and some of the associated companies (IEA, 2012a).	52
Table 3.1	Evolution of volatiles during the pyrolysis of wood (Güllü and Demirbaş, 2011).	72
Table 3.2	Three factor design approach to the experimental work (Bridgeman *et al*., 2010).	78
Table 4.1	Conditions used in this study.	104
Table 4.2	Calculated and measured HHV of different conditions of torrefied willow (Bridgeman *et al*., 2010).	111
Table 5.1	Mass yields of torrefied biomass that were treated at different conditions, A, B and C as tabulated in Table 4.1 (dry basis).	138
Table 5.2	Proximate analysis of raw and torrefied biomass samples.	140
Table 5.3	Ultimate analysis of raw and torrefied biomass samples (daf basis).	141
Table 5.4	Calculated HGI_{equiv} values of raw and torrefied biomass samples, where the m (%) represents the values of mass that passed through the 75 μm sieve as displayed in Equation 5.1.	147
Table 5.5	BET Total surface areas of raw and torrefied biomass samples (size fraction of < 0.25 mm).	151
Table 5.6	Identified components in the tar fraction from torrefied willow.	159
Table 6.1	Cubes and their respective radii.	163
Table 6.2	Radius and the mean radius of each specific shell.	165
Table 6.3	Fuel characteristics of raw willow and eucalyptus (*E. Gunnii*).	166
Table 6.4	Proximate analysis of torrefied willow and eucalyptus obtained from pyrolysis.	174
Table 6.5	Energy yields of torrefied willow and *E. Gunnii* (dry ash free basis).	177
Table 6.6	Characteristics wavenumbers of evolved volatiles during torrefaction of	178

biomass.

Table 6.7	Distribution of products (daf) in terms of % mass obtained from the torrefaction of willow and eucalyptus as simulated by FG-Biomass model.	183
Table 6.8	Yields of torrefied biomass fuels, tars and permanent gases against radius of particle size of willow and eucalyptus after torrefaction at conditions A, B and C.	185
Table 6.9	Percentage yields (daf) of the remaining products of torrefaction (condensable organics), obtained from the torrefaction of willow and eucalyptus at condition A. **Appendix 6.4** displays the yields obtained from that of those biomass fuels at conditions B and C.	186
Table 6.10	Ultimate analysis (daf basis) in terms of torrefied willow and eucalyptus (cubes) as predicted by the FG-Biomass model.	192
Table 7.1	Predicted char burnout of torrefied willow.	213
Table 8.1	Potential benefits and consequences of different aspects of bioenergy development (Thornley, 2006).	216
Table 8.2	Emissions and their origin when treated with combustion (Hustad *et al*., 1995).	224
Table 8.3	Description of each step involved in the EIA process (Glasson *et al*., 2005).	232
Table 8.4	Ash contents and High Heating Value (HHV), both at dry basis, of biomass before and after water washing at 60°C as determined by Deng *et al* (2013).	238
Table 8.5	Emissions of volatile organic compounds from drying of softwood (Samuelsson *et al*., 2006).	241
Table 8.6	Composition of condensed liquids upon torrefaction of Lauan (Chen *et al*., 2011).	245
Table 8.7	Environmental fate of identified pollutants (Source: International Programme of Chemical Safety (INCHEM) & PubChem Compounds Database (PUBCHEM)).	249
Table 8.8	Identification of impact (health and environmental) of torrefaction process according to activity associated with the plant.	254
Table 8.9	Environmental risks based on Nurminen (2012) and suggested mitigation measures.	257

List of figures

Figure 1.1	World energy consumption from 2000 to 2040, which the unit is in quadrillion Btu (EIA, 2013).	2
Figure 1.2	World energy consumption in terms of fuels from 1987 to 2012, according to the BP Statistical Review of World Energy 2013.	2
Figure 1.3	Renewable sources of energy used in the UK and the percentages shown were based on their usages in 2012 (DECC, 2013a).	6
Figure 1.4	Progress against the 2009 Renewable Energy Directive (DECC, 2013a).	7
Figure 1.5	Photo images of herbaceous crops (Lewondowski *et al*., 2000).	16
Figure 1.6	Photo images of hardwood trees (Source: www.2020site.org/trees/).	18
Figure 1.7	Photo images of softwoods and their respective needle-like leaves (Source: www.2020site.org/trees/).	20
Figure 1.8	Structure of cellulose (Sjöstörm, 1981).	21
Figure 1.9	Lignocellulosic compositions of biomass and their respective hemicellulose composition, at dry basis (Pauly and Keegstra, 2008).	22
Figure 1.10	Chemical structures of xylose, mannose, arabinose and galactose (Sjöstörm, 1981).	22
Figure 1.11	Principal structure of glucuronoxylan in hardwood, in which the sugar units are *β*-D- Xylopyranose (Xyl*p*) and 4-O-methyl-α-D-glucopyranosyluronic acid (Glc*p*A). R is an acetyl group (CH_3CO) (Sjöstörm, 1981).	23
Figure 1.12	Principal structure of galactoglucomannans in softwood, in which the sugar units are *β*-D-glucopyranose (Glc*p*), *β*-D-mannopyranose (Man*p*) and *β*-D-galactopyranose (Gal*p*). R is CH_3CO or H (Sjöstörm, 1981).	24
Figure 1.13	Principal structure of arabinoglucuronoxylan in softwood, where the sugar units are *β*-D- Xylopyranose (Xyl*p*) and 4-O-methyl-α-D-glucopyranosyluronic acid (Glc*p*A) and α-L-arabinofuranose (Ara*f*) (Sjöstörm, 1981).	24
Figure 1.14	Principal components that make up the structure of lignin (Brett & Waldron, 1996).	25
Figure 1.15	Stages involved in the solid fuel combustion (Brown, 2003).	26
Figure 1.16	A typical diagram of a thermogravimetric analysis of a biomass.	26
Figure 1.17	Van Krevelen diagram of solid fuels (McKendry, 2002)	30
Figure 1.18	A schematic flow diagram of options of co-firing (Livingston, 2012).	32

Figure 1.19	Options for co-firing in a coal-fired boiler, where a) represents indirect co-firing and b) parallel co-firing (Basu, 2013).	34
Figure 1.20	Overview of heat integration options (IEA, 2012a).	39
Figure 1.21	Processes involved in the reactor (Bergman *et al*., 2005b).	43
Figure 1.22	Main physico-chemical reactions during the heating of lignocellulosic components at torrefaction (Bergman *et al*., 2005b).	44
Figure 1.23	Mass and energy balance of the torrefaction process, where E and M represent the energy and mass units (Bergman *et al*., 2005b).	45
Figure 1.24	Overall mass and energy balances of torrefaction of willow at temperature and reaction time of a) 250°C and 30 min and b) 300°C and 10 min (Prins *et al*., 2006a).	45
Figure 1.25	The arrangement of four thermocouples (T5, T6, T7 and T8) inside a reactor for temperature control (Phanphanich and Mani, 2011).	47
Figure 1.26	Laboratory torrefaction unit as illustrated in Phanphanich and Mani (2011).	47
Figure 1.27	A schematic diagram of torrefaction experiment as set up in Chen *et al* (2011).	48
Figure 3.1	Pyrolysis of hemicellulose, cellulose and lignin as observed in a thermogravimetric analyser, where their mass losses and rates of mass loss of were recorded (Yang *et al*., 2007).	63
Figure 3.2	a) Thermogravimetric analysis and b) derivative thermogravimetric of hemicellulose (left), cellulose (middle) and lignin (right) at three torrefaction temperatures (230, 260 and 290ºC with a residence time of 1 hour) (Chen *et al*., 2011).	64
Figure 3.3	Condensable volatile yields of produced during the torrefaction of willow and larch at 230°C and 250°C with residence times of 50 min and 30 min respectively (Prins *et al*., 2006a).	65
Figure 3.4	Non-condensable volatile yields produced during the torrefaction of willow and larch (Prins *et al*., 2006a).	66
Figure 3.5	Decomposition of various biomass compounds at 267°C (Prins *et al*., 2006b).	68
Figure 3.6	Comparison of experimental and modelled relative weight of willow upon torrefaction at 270°C, 280°C, 290°C and 300°C with a heating rate of 10°C min^{-1} (Prins *et al*., 200ba).	70
Figure 3.7	Comparison of experimental and modelled relative weight of willow upon torrefaction at 260°C with various heating rate of 10, 50 and 100°C min^{-1} (Prins *et al*., 2006b).	70

Figure 3.8	Images of willow: a) untreated; b) low temperature, short residence time; c) low temperature, long residence time; d) high temperature; short residence time; e) high temperature, long residence time (Bridgeman *et al*., 2010).	72
Figure 3.9	Images of raw eucalyptus (RE), torrefied eucalyptus (TRE) at 240°C and 280°C respectively (Arias *et al*., 2008).	73
Figure 3.10	SEM images of raw (left) and torrefied (right) *E.Saligna* at 280ºC with a residence time of 5 hrs (Almeida *et al*., 2010).	74
Figure 3.11	Mass loss during torrefaction of reed canary grass at different temperatures (Bridgeman *et al*., 2008).	75
Figure 3.12	The change in the moisture, volatile and ash contents of torrefied rice husks (Pimchuai *et al*., 2010).	75
Figure 3.13	Changes in carbon, hydrogen and oxygen upon torrefaction at increasing temperatures (Bridgeman *et al*., 2008).	76
Figure 3.14	Van Krevelen diagram for coals, raw and torrefied biomass fuels, where A-D represents the severity of torrefaction conditions. Table 3.2 provides the description for such conditions, where A as the least severe and D as the most severe (Bridgeman *et al*., 2008).	77
Figure 3.15	Mass yields of solid, gas and tar after pyrolysis at 800°C (Chen *et al*, 2010).	79
Figure 3.16	Weight loss curves of torrefaction of pine as obtained from TGA at a) 300°C and b) 280°C (Peng *et al*., 2012).	81
Figure 3.17	Schematic representation of the breakdown of biomass when stress is applied (Bergman *et al*., 2005a).	85
Figure 3.18	Specific energy consumption for grinding of untreated and torrefied pine chips and logging residues (Phanphanich and Mani, 2011).	86
Figure 3.19	Grindability behaviour of different particle sizes against power consumption (Bergman *et al*., 2005a).	86
Figure 3.20	Particle size distribution curves for untreated and torrefied Miscanthus (A – D), where A was treated at 290ºC with a residence time of 10 mins, B at 240ºC with a residence time of 60 mins, C at 240ºC with a residence time of 10 mins and D at 290ºC with a residence time of 60 mins, alongside four standard reference coals of known HGI 32, 49, 66 and 92 (Bridgeman *et al*., 2010).	87
Figure 3.21	An infra-red spectrum of bamboo that was torrefied at 220, 260 and 280ºC (Rousset *et al*., 2011).	90
Figure 3.22	ATR-FTIR spectra of torrefied wheat straw samples, where the reduction of O-H bands decreased with increased temperature at 3500-3000 cm^{-1} (Shang *et al*., 2012).	91

Figure 3.23	Combustion characteristics between torrefied and raw wood (Pentananunt *et al*., 1990).	92
Figure 3.24	Duration of a) volatile combustion and b) char burnout of raw and torrefied willow particles (523 and 563 K) (Bridgeman *et al*., 2008).	93
Figure 3.25	Evolution of volatile products during the torrefaction of reed canary grass at 290°C as detected in the FTIR (Bridgeman *et al*., 2008)	95
Figure 3.26	Main components contained in condensed liquid, namely a) phenol, b) eugenol, c) vanillin and d) 7,9-dihydroxy-3-methoxy-1-methyl-6H-dibenzo[b,d]pyrane-6-one (Chen *et al*., 2011)	96
Figure 3.27	Comparison between the results of TG-FTIR and FG-DVC model for evolution rates and yields obtained from pyrolysis of wood pellets (de Jong *et al*., 2003).	98
Figure 4.1	Woody biomass samples used in this study.	101
Figure 4.2	A longitudinal rig furnace that is equipped with three temperature zones to allow maximum temperature control used for torrefaction.	103
Figure 4.3	How biomass fuels are positioned inside the reactor tube. The biomass shown in the above picture is eucalyptus.	103
Figure 4.4	How thermocouples are arranged in the tube. The longest (1) thermocouple is located near to the glass wool on the left. The second (2) goes to the other wool and the last (3) one is 20 cm away from the second as pointed out in the figure.	103
Figure 4.5	Apparatus used for the collection of liquid products.	105
Figure 4.6	Perkin Elmer Autosystem XL Gas chromatograph that was used to detect the permanent gases (CH_4, CO_2 and CO).	105
Figure 4.7	Flow diagram of different types of analysis carried out for characterisation of torrefied products, where M_1, M_2, M_3 and M_4 represent the masses of biomass before torrefaction and its respective products.	106
Figure 4.8	TGA Q5000 analyser.	109
Figure 4.9	CE Instruments Flash EA 1112 Series elemental analyser.	110
Figure 4.10	The set up to test the hydrophobicity of the biomass fuels.	112
Figure 4.11	The set up to determine the density of each biomass fuel.	113
Figure 4.12	a) Retsch cutting mill SM 100, b) Stack of sieves of 600, 355, 212, 150, 75 and 53 µm on an Retsch Mechanical Sieve Shaker AS 200 Basic for particle size distribution experiment and c) Retsch PM 100 ball mill, that is equipped with 20 steel balls and 500 mL milling cup.	114

Figure 4.13	Calibration curve of the Retsch PM100 mill (500 mL) using four standard coals of known HGI values of 32, 49, 66 and 92.	115
Figure 4.14	Quantachrome Instruments NOVA 2200 Multi-station Any-gas Sorption Analyser Standard Model v10.03, where sample tubes were warmed in the pair of jackets as shown in the figure.	116
Figure 4.15	Camscan 4 SEM with Oxford Instruments INCA 250 EDX system and HKL automated electron backscattered diffraction (EBSD) that were used to take SEM images.	117
Figure 4.16	Transmission Electron Microscopy (TEM) analyser.	117
Figure 4.17	SPECAC instrument that was used to make pellets. The top right shows the KBr discs of raw and torrefied willow and eucalyptus of different treatment conditions. While the bottom right is the spectrometer where pellets are placed.	119
Figure 4.18	Thermo Scientific ESCALAB 250 X-ray Photoelectron Spectrometer.	119
Figure 4.19	TOC analyser.	120
Figure 4.20	Mettler Toledo Titrator Karl Fischer V20 for measuring the water content in tars.	121
Figure 4.21	Equipments used to detect components in liquid products from torrefaction.	122
Figure 4.22	Netzsch STA 449C Jupiter simultaneous analyser (as shown on the left), coupled to a Nicolet Magma-IR 560 Spectrometer (as shown on the far right) via a heated gas transfer line. The middle picture shows how big the crucible is to allow a particle as big as 8x8x8 mm to fit in.	123
Figure 4.23	Typical temperature profile that is programmed for torrefaction of biomass at three conditions A, B (both at 270°C with a residence time of 30 and 60 min respectively) and C (at 290°C with a residence time of 30 min).	123
Figure 4.24	Calibration plots of water, carbon monoxide and carbon dioxide for FTIR.	125
Figure 4.25	Instruments used in conducting the single particle combustion of biomass.	126
Figure 4.26	Input requirements for willow as provided by the AFR.	127
Figure 4.27	Input requirements of eucalyptus as provided by the AFR.	128
Figure 4.28	a) The setting of the heating regime and b) the temperature profile as resulted from the set up.	130
Figure 4.29	a) Predicted char yield as simulated by the FG-Biomass as a result of torrefaction of willow and b) the evolution rate of char during the torrefaction.	131

Figure 4.30	Lists of yields and evolution rates of torrefied products as predicted from the simulated torrefaction of willow.	132
Figure 4.31	Evolution rate of elements of torrefied char.	132
Figure 5.1	Temperature profiles of torrefaction of softwood at conditions A, B (270°C with a residence time of 30 and 60 min respectively) and C (290°C with a residence time of 30 min).	136
Figure 5.2	Overall mass balance of torrefaction of willow, hardwood and softwood treated at 290°C with a residence time of 30 min.	139
Figure 5.3	Van Krevelen plot of raw and torrefied biomass alongside anthracite and lignite.	142
Figure 5.4	Energy yield against mass yield for all torrefied biomass (dry basis) where the line represents the indication of the performance index of the fuels.	143
Figure 5.5	Variation in moisture uptake (as measured by the water immersion test) with the mass yield of the raw and torrefied willow and eucalyptus samples (treatments A, B, and C).	144
Figure 5.6	Relationship between moisture uptake (as measured by the water immersion test) and a) energy yield; b) high heating value; of raw, and torrefied willow and eucalyptus (treatments A, B, and C).	145
Figure 5.7	Cumulative particle size distributions resulting from milling tests of the raw biomass samples compared with standard reference coals of HGI 32, 49, 66 and 92.	147
Figure 5.8	Cumulative particle size distributions resulting from milling tests of raw and torrefied eucalyptus under conditions A, B and C and compared with standard reference coals of known HGI values.	149
Figure 5.9	Relationships of HGI_{equiv} against a) the C content (dry ash free basis), b) the mass yield, (dry basis) and c) the energy yield (dry basis) of the raw and torrefied biomass fuels.	150
Figure 5.10	SEM images of raw and torrefied a) willow and b) eucalyptus.	152
Figure 5.11	FTIR spectra of raw and torrefied willow and eucalyptus.	153
Figure 5.12	Zoom on spectra between 2000 and 500 cm^{-1}.	154
Figure 5.13	XPS spectra of untreated eucalyptus and torrefied eucalyptus sample C, where a) and c) are the C 1s and O 1s XPS spectra of raw eucalyptus; b) and d) are the C 1s and O1s XPS spectra of torrefied eucalyptus.	156
Figure 5.14	Chromatogram of tar produced from the torrefaction of willow, hardwood and softwood.	158
Figure 6.1	Data in the ‘sphere.out’ after running the Sphere program.	165

Figure 6.2 Typical mass loss and temperature profile during torrefaction of willow and eucalyptus. Two stages of mass loss and change in temperature can be seen, labelled (1) and (2). 167

Figure 6.3 Rates of mass loss and temperature profile as recorded by the software during torrefaction of willow of different sizes (cubes) at condition B, when the final temperature was set to 270ºC with a reaction time of 60 min. 168

Figure 6.4 Mass yield (dry basis) of willow and *E.Gunnii* of different particle sizes for torrefaction at treatments A, B and C (270°C, 30 min, 270°C, 60 min and 290ºC, 30 min respectively). 170

Figure 6.5 DTG of the decomposition of a) willow and b) *E.Gunnii* of particle size 7x7x7 mm for treatments A, B and C (at 270ºC with residence times 30 and 60 min and at 290ºC with residence time 30 min respectively), c) cubes and cuboids of willow and d) those of eucalyptus treated at condition C in helium at 10ºC min^{-1}. 171

Figure 6.6 TGA and DTG curves for the pyrolysis of raw and torrefied willow and eucalyptus of different particle sizes from treatment C, in helium at 10ºC min^{-1}. 173

Figure 6.7 Plots of volatile, fixed carbon and ash contents of different particle sizes of torrefied a) *E.Gunnii* and b) willow (treatment C) against particle volume. Note that the volumes were calculated according to the density of the biomass fuels as displayed in **Appendix 6.2**. 176

Figure 6.8 Typical evolution profile of volatile products during torrefaction of willow and eucalyptus of treatment C. This plot was taken from the torrefaction of willow (7x7x7 mm). 178

Figure 6.9 Evolution profiles of carbon dioxide obtained from torrefaction of willow (7x7x7 mm) at increasing torrefaction conditions (A, B and C). 179

Figure 6.10 Evolution profiles of a) carbon dioxide, b) acetaldehyde, c) methane and d) methanol obtained from torrefaction of cubes of willow at condition C. 180

Figure 6.11 Plots of water, carbon monoxide and carbon dioxide from torrefaction of willow (a-c) and eucalyptus (d-f) at conditions A, B and C. 181

Figure 6.12 Simulated overall mass balances of willow and eucalyptus upon torrefaction at condition A. 183

Figure 6.13 a) Char yields of torrefied biomass of different particle sizes against time, b) tar yields, c) and d) yields of permanent gases (carbon dioxide and carbon monoxide respectively) obtained from the torrefaction of willow of increasing particle sizes (5, 6, 7 and 8 mm). 184

Figure 6.14 Mass yields (dry ash free basis) determined from torrefaction of willow by the reactor, TGA-FTIR and FG-Biomass model at increasing conditions: a) A, b) B and c) C. It is important to note that the sample 189

size torrefied in the reactor was 40 x 20 x 10 mm, while those in the other two were cubes of 5 mm, 6 mm, 7 mm and 8 mm.

Figure 6.15 Mass yields (dry ash free basis) determined from torrefaction of eucalyptus by the reactor, TGA-FTIR of different particle sizes and FG-Biomass model. 190

Figure 6.16 Carbon and oxygen contents of torrefied willow (a and b respectively) and eucalyptus (c and d respectively) at conditions A, B and C. 193

Figure 6.17 a) The effect of particle size on the temperature of torrefaction and b) The zoom version of the plot in a) from 0-500 s. The condition applied was 270°C with a reaction time of 60 min. 194

Figure 6.18 Temperature-time distribution within a spherical particle of a)-d) different cubes of willow treated at condition A and e) that of 8 mm treated at condition A and C. 195

Figure 7.1 Wood pyrolysis model (Lu *et al*., 2008). 199

Figure 7.2 (a – e) Images taken during the combustion of willow C. 205

Figure 7.3 Ignition delays of raw and torrefied a) willow and b) eucalyptus where the mass refers to the masses of each fuel before the combustion experiment. 206

Figure 7.4 Durations of volatile combustion of raw and torrefied a) willow and b) eucalyptus. 207

Figure 7.5 Durations of char combustion of raw and torrefied a) willow and b) eucalyptus. 209

Figure 7.6 Char yields of raw a) willow and b) eucalyptus that upon pyrolysis treatment at different heating rates that ranged from 100 to 1000 K s^{-1}. 210

Figure 7.7 The evolution rates of char of raw a) willow and b) eucalyptus (wt% s^{-1}, daf) plotted with time upon pyrolysis at different heating rates. 211

Figure 7.8 Conversion factor as a function of time upon pyrolysis of torrefied willow. 212

Figure 8.1 An illustration of the main lifecycle stages for a bioenergy system (Bird *et al*., 2006). The green circle represents the carbon cycle, while the grey arrows demonstrate the input and outputs from the bioenergy system. 218

Figure 8.2 Potential impacts of biomass production due to non-sustainability of biomass practices (Brown, 2003). 219

Figure 8.3 Products formed during the combustion of biomass (Williams *et al*., 2012). 223

Figure 8.4 Potential environmental impacts of converting bio-renewable resources into heat and power (Brown, 2003). 225

Figure 8.5 Key steps in the Environmental Impact Assessment process (Glasson *et al*., 2005). 230

Figure 8.6 An example of an environment risk assessment profile that consists of probabilities and consequences of the identified environmental hazards (DEFRA, 2011). 230

Figure 8.7 Overview of heat integration options (Koppejan *et al*., 2012). The red dashed lines represent the boundaries at which those enclosed in the red box are discussed in this section. 236

Figure 8.8 Terpenes (Sell, 2003). 240

Figure 8.9 Amounts of organic compound groups released from the drying of pine bark and peat in steam dryers (Fagernäs and Sipilä, 1997). 242

Figure 8.10 Pellets of spruce and torrefied spruce of increasing temperatures (250, 275 and 300°C) (Stelte *et al*., 2011). 248

List of publications

IBRAHIM, R.H.H., L.I. DARVELL, J.M. JONES and A. WILLIAMS. 2013. Physicochemical characterisation of torrefied biomass. *Journal of Analytical and Applied Pyrolysis*. **103**, pp.21-30.

IBRAHIM, R.H.H., L.I. DARVELL, J.M. JONES and A. WILLIAMS. 2012. Physicochemical characterisation of torrefied biomass. 19th International Symposium on Analytical and Applied Pyrolysis, Linz, Austria.

IBRAHIM, R.H.H., Z. TAO, L.I. DARVELL, J.M. JONES and A. WILLIAMS. The influence of particle sizes of biomass on torrefaction. 2012. Proceeding of Sustainable Energy. 21-23 Nov 2012: ***International Energy Conference***, Brunei Darussalam and 10th Sustainable Energy and Environment (SEE) Forum. pp. 208-216.

List of abbreviations

C-H	Alkane Group
C=C	Alkene Group
A_d	Ash content
ar	As received
ATR	Attenuated Total Reflectance Fourier Transform Infra-Red
BE	Binding Energy
BEC	Biomass Energy Centre
CEN/TS	British Standard
Btu	British thermal unit
BET	Brunauer, Emmett and Teller method
CV	Calorific Value
CO_2	Carbon Dioxide
C-C=O	Carbon to a carbonyl
CO	Carbon Monoxide
C=O	Carbonyl Group
CEC	Commission of the European Communities
DECC	Department of Energy and Climate Change
DEFRA	Department of Environment Food and Rural Affairs
DTI	Department of Trade and Industry
DTG	Derivative Thermogravimetric Analysis
DTA	Differential Thermal Analysis
DCM	Dichloromethane
daf	dry ash free basis
EBSD	Electron Back-Scattered Diffraction
EDX	Energy Dispersive X-ray
ECN	Energy Research Centre of the Netherlands
η_E	Energy Yield
EMC	Equilibrium Moisture Content
EU	European Union
C-O-C	Ether group
C-O-R	Ether connected to an alkyl group
FCC	Fixed Carbon Content

fps	frames per second
FTIR	Fourier Transform Infra-Red
FG-DVC	Functional-Group, Depolymerisation, Vaporisation, Cross-linking
GC	Gas Chromatography
GHG	Greenhouse Gases
GDP	Gross Domestic Product
HGI	Hardgrove Grindability Index
HHV	Higher Heating Value
h	hour
O-H	Hydroxyl Group
ICP	Inductively Coupled Plasma
Liquid-GC-MS	Liquid-Gas Chromatography-Mass Spectrometry
LHV	Low Heating Value
η_m	Mass Yield
CH_4	Methane
CH_3OH	Methanol
M_{ad}	Moisture Content
MW	Molecular Weight
NNFCC	National Non Food Crops Centre
n.d	no date
C-O	Non-Carbonyl Group
C-COO	Non-Carbonyl Oxygen atoms
NA	Not Applicable
ND	Not Detected
OLS	Ordinary Least Squares Regression
PLS	Particle Least Squares Regression
POST	Parliamentary Office of Science and Technology
KBr	Potassium Bromide
RE	Raw Eucalyptus
RCG	Reed Canary Grass
RHI	Renewable Heat Incentive
RO	Renewable Obligation
RTFO	Renewable Transport Fuel Obligation

RT	Retention Time
SEM	Scanning Electron Microscopy
SRC	Short Rotation Coppice
STA	Simultaneous Thermogravimetric Analyser
TGA	Thermogravimetric Analyser
TGA-FTIR	Thermogravimetric Analyser coupled with Fourier Transform Infra-Red
TOP	Torrefaction and Pelletisation
TOC	Total Organic Carbon
TRE	Torrefied Eucalyptus
TEM	Transmission Electron Microscopy
UNFCCC	United Nation Framework Convention on Climate Change
USA	United States of America
V_d	Volatile Matter Content
H_2O	Water
WS	Wheat Straw
WCI	World Coal Institute
XPS	X-ray Photoelectron Spectroscopy

CHAPTER 1

INTRODUCTION

1.1 Introduction

The world energy consumption is expected to increase by 56% from 2010 to 2040 as shown in Figure 1.1 (EIA, 2013). According to the International Energy Outlook 2013, this increase is due to the economic growth and expanding population especially in the countries that is outside the Organization for Economic Cooperation and Development (OECD), known as non-OECD (EIA, 2013). Furthermore, the energy use in the non-OECD increases by 90% while in the OECD is just 17% (EIA, 2013).The BP Statistical Review of World Energy (2013) provided statistics based on 2012, where oil remains the world's leading fuel, accounted for 33.1% of global energy consumption, followed by natural gas, coal, hydroelectricity, nuclear energy and renewables (see Figure 1.2). Here, the renewables include wind, geothermal, solar, biomass and wastes. The International Energy Outlook 2013 pointed out that renewable energy and nuclear power are becoming the world's fastest growing energy sources, each by 2.5% per year even though fossil fuels still continue to supply almost 80% of the world energy through 2040 (EIA, 2013). In addition to that, natural gas is the fastest growing fossil fuel in the outlook (EIA, 2013). The BP Statistical Review of World Energy (2013) reported that the Asia Pacific region accounted the most of the global energy consumption (40%) and 69.9% of global coal consumption. Moreover, Europe and Eurasia is the leading region for the consumption of nuclear power and renewables. While Middle East consumed the most percentage of natural gas (50%, while other countries consumed a percentage that ranged from 10-30%) and its proportion was similar to that of oil. South and Central America are the leading regions for the consumption of hydroelectricity.

In UK, the extraction of oil and gas still remains the major contributor to the economy, followed by the electricity sector (DECC, 2013a). In 2012, it was reported that the energy industries contribute 3.5% of GDP to the UK economy (DECC, 2013a). 46% of the UK economy is accounted from the oil and gas extraction, while electricity (with renewables included) accounted for 27% of the energy total. In addition to that, Table 1.1 shows that the total production increased rapidly between 1980 and 2000 due to the expansion of oil and gas but later, declined from 2010 to 2012 as the oil and gas fields become dissipated. With

regards to low carbon sources of energy, they contributed 12% of their energy to the country, with two thirds of this came from nuclear energy (DECC, 2013a). The second largest was bioenergy (DECC, 2013a).

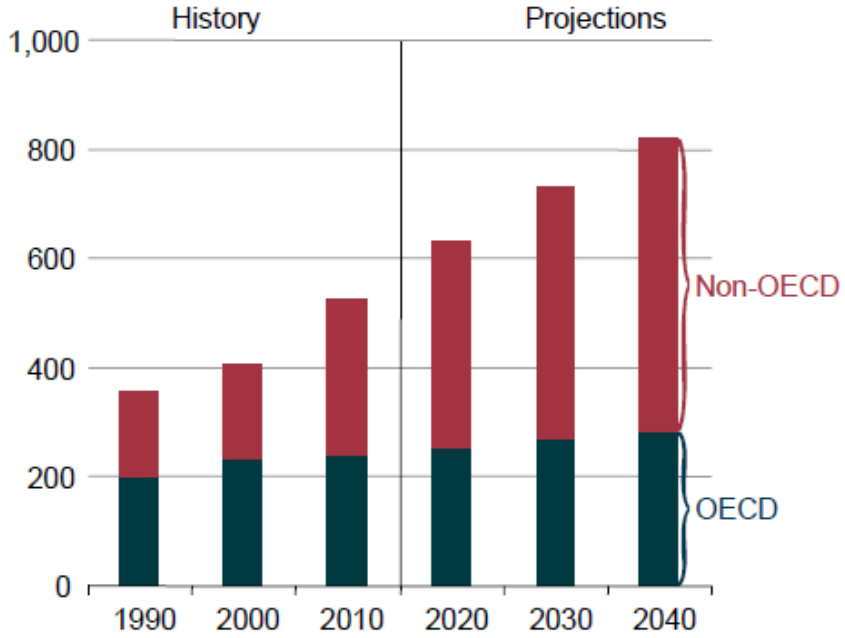

Figure 1.1. World energy consumption from 2000 to 2040, which the unit is in quadrillion Btu (EIA 2013).

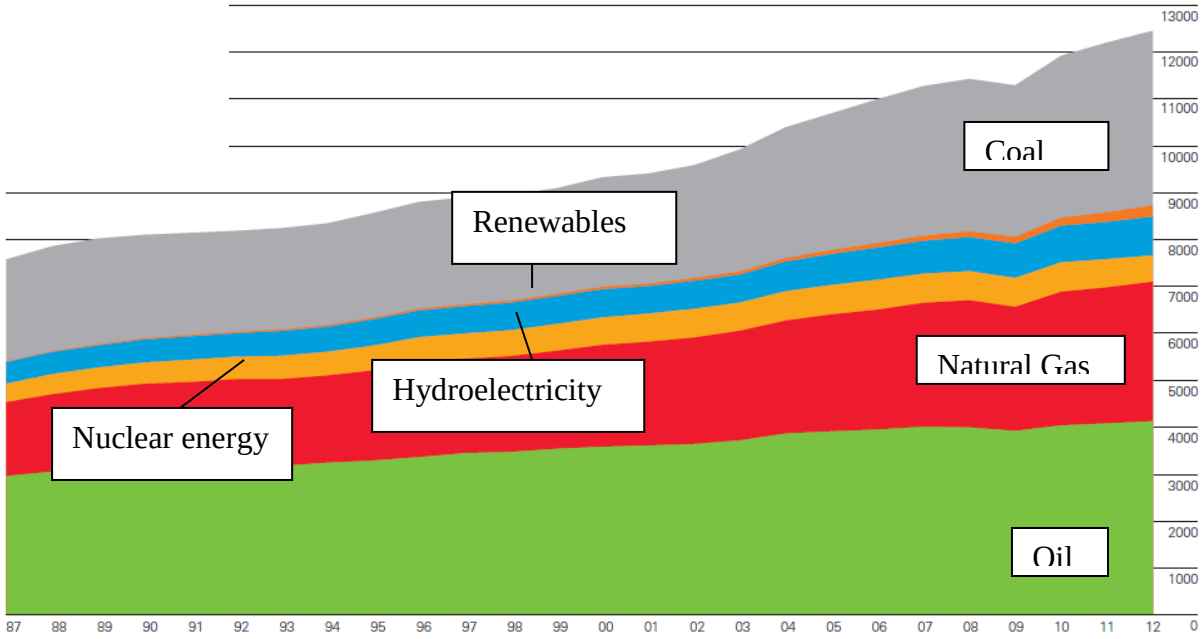

Figure 1.2. World energy consumption in terms of fuels from 1987 to 2012, according to the BP Statistical Review of World Energy (2013).

Table 1.1. Total production of fuels based in UK equivalent to million tonnes of oil, according to the UK Energy Brief 2013 (DECC, 2013a).

	1980	**1990**	**2000**	**2010**	**2011**	**2012**
Petroleum	86.9	100.1	138.3	69.0	56.9	48.8
Natural gas	34.8	45.5	108.4	57.2	45.3	38.9
Coal	78.5	56.4	19.6	11.5	11.6	10.6
Primary electricity	10.2	16.7	20.2	15.1	17.5	17.4
Bioenergy and waste	0.0	0.7	2.3	5.2	5.6	6.4
Total	210.5	219.4	288.7	157.9	136.8	122.1

1.1.1 Oil

The world has witnessed the exponential growth of oil production since 1900. More than 85% of the world's oil production comes from conventional sources (or 'crude oil', which is usually defined as fields that produce light and medium crude oil). The other 15% is from natural gas liquids (a by-product of the extraction of natural gas) (Hughes and Rudolph, 2011).Countries like China and other emerging market economies have pushed the world oil demand higher in the early years of the 21st century (Hughes and Rudolph, 2011). According to the BP Statistical Review of World Energy (2013), the world production of oil has increased by 1.9 million barrels of oil a day, where OPEC members (Middle East, North Africa, West Africa and South America accounted for three quarters of the global increase. The UK Energy Brief 2013 reported that the country's oil production has dropped in 2012 by 68% in comparison to that recorded in 1999 (150.2 million tonnes) due to "*maintenance issues at the Buzzard field at St Fergus associated gas terminal and production constraints on the Elgin area*" (DECC, 2013a).

1.1.2 Coal

Coal is the other one of the world's most important sources of energy. China, US, India, Australia and South Africa are the top five coal producers as they are highly dependent on this resource for their energy needs (WCI, n.d). Other countries would need to import for example, Japan and Korea. Coal has been long used since ancient history and it was during the industrial era in the 18th and 19th centuries that the coal was in higher demand. Global coal consumption and production grew by 2.5% and 2.0% in 2012 respectively (BP Statistical

Review of World Energy, 2013). The World Coal Institute (n.d) reported that coal production has grown fastest in Asia and the global coal production is expected to reach 7 billion tonnes in 2030, with China accounting for around half the increase (54%). In Asia, they use steam coal production for electricity, coking coal for steel production and cement manufacturing. In the UK, the coal production fell to 10.6 million tonnes for 2012 (DECC, 2013a). Last year, it was 11.6 million tonnes. The drop was due to a number of operational and geological issues. On the other hand, imports of coal continue to increase by 10 million tonnes due to a greater demand by electricity generators.

1.1.3 Natural gas

Just like oil and coal, natural gas continues to play its part in meeting the demand for energy worldwide. It has a lower carbon composition, which makes it a more attractive fuel than the two resources especially its ability to produce low amounts of greenhouse gases emissions. According to the International Energy Outlook 2013, the consumption of natural gas increases at an average rate of 1.7% per year and in order to meet the consumption growth, the producers will need to increase supplies around 65% from 2010 to 2040 (EIA, 2013). Much of this increase will be expected to come from non-OECD countries (EIA, 2013). Following that, the BP Statistical Review of World Energy (2013) reported that in 2012, the global natural gas consumption grew by 2.2%, where the US recorded the largest increment in the world, followed by China and Japan. While its production grew by 1.2% and again, the US remained the world's largest producer.

In the UK, the natural gas consumption declined by around 25% below its 2004 peak. In terms of gas production, it has been declining since the peak in 2000. UK relies heavily on gas to provide energy for heating and electricity (POST, 2004). The alarming concern that UK's gas reserves are declining has made it to become a net gas importer on an annual basis. Now, it has increasingly becoming reliant on gas imports to meet demand (DECC, 2012).

1.2 Energy challenges

UK's Energy White Paper 2007 pointed out two long term challenges faced in the world today. Firstly, the need to tackle climate change by reducing greenhouse emissions within UK and abroad and secondly, energy security, as most of the electricity is generated from imported gas, imported coal and nuclear (DTI, 2007).

1.2.1 Climate change

Climate change has been a major global problem since the beginning of the industrial era. Fossil fuels are the main drivers for industrial development worldwide, leading to the continuous emissions of greenhouse gases (GHG) particularly carbon dioxide. More than two thirds of the world's carbon dioxide emissions come from the way the energy is produced and utilised. This creates tension and continues to threaten the stability of the world's climate in relation to global warming, economy and population. There have been many legislations, directives, acts and protocols aiming to stabilize the concentrations of GHG in the atmosphere. One of them is Kyoto Protocol that was adopted in the United Nation Framework Convention on Climate Change (UNFCCC) in 1997 (United Nations, 1998). This was when UK started to set its own target to reduce its GHG emissions by 12.5% by the first Kyoto Protocol commitment period (2008-2012). The UK's commitment in doing this is outlined in the Energy White Paper 2003. According to the document at that time, even though the UK only contributes a global total of 2% of carbon dioxide emissions and actions may have no impact on the climate change, their ambition is for the world's developed economies to reduce greenhouse gases (GHG) emissions by 60% by 2050 (DEFRA, 2003).

1.2.2 Energy security

There is an increasing global demand for energy until today, particularly in the United States and in growing economies such as India and China. Population growth and changes in lifestyles are two major factors contributing to this rise (James & Howes, 2006). With regards to the UK, it is relying mainly on imported energy. The Energy White Paper 2007 sets out a number of factors that are known to add to the risks of energy security: "*(1) abuse of market power, (2) poor energy market information, (3) infrastructure security risks and (4) regulatory uncertainty (particularly concerning government actions to tackle climate change)*" (DTI, 2007).

1.3 The implication of renewable sources of energy in the UK

In January 2008, the European communities proposed a directive to promote the use of energy from clean renewable based sources. The agreement is aimed to establish an overall binding target to achieve reductions in EU greenhouse gases emissions of 20% by 2020 (CEC, 2008). The UK has signed up to the EU target and committed to produce 15% of its energy from renewable sources. As a result, the UK Renewable Energy Strategy was introduced in July 2009. Figure 1.3 illustrates the renewable sources of energy in the UK and

how much they were used in 2012. According to the UK Energy Brief 2013, a total of 9.3 million tonnes of oil equivalent of primary energy use accounted for these renewable sources. 7.0 million tonnes was used to generate electricity, 1.4 million tonnes was for heating and 1.0 million tonnes was used for transportation (DECC, 2013a).

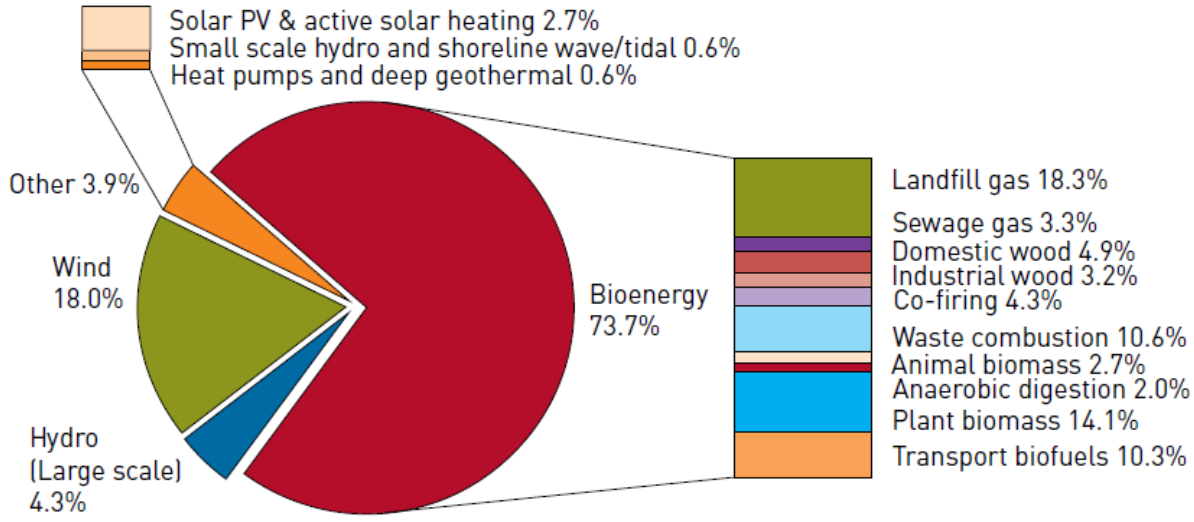

Figure 1.3. Renewable sources of energy used in the UK and the percentages shown were based on their usages in 2012 (DECC, 2013a).

According to the UK Renewable Energy Strategy, targets are placed on three energy sectors: electricity, heat and transport (DECC, 2009).

1.3.1 Electricity

During 2012, renewables accounted for 11.3% of electricity generated in the UK (DECC, 2013a) These renewable sources are promoted under the Renewables Obligations (RO) and since its establishment in 2002, the amount of renewable capacity operating in the UK has increased from 1.8% to 6.6% in 2009 and up to 9% in the quarter of 2011 (EWP, 2011; Ares, 2012a; RO, 2011). To date, there are two incentive schemes for renewables: i) The Renewables Obligation, which acts as the main support scheme for large renewable projects, ii) Feed-in Tariffs (FIT), which was introduced in 2010, that focuses on smaller schemes, to increase microgeneration (Ares, 2012a). The RO places an obligation on UK electricity suppliers to make use of renewables for electricity generation (Ares, 2012a). Suppliers will purchase Renewable Obligation Certificate (ROC) to be issued to an accredited generator for renewable electricity (Ares, 2012a). Some of the renewable electricity technologies are advanced gasification/pyrolysis, co-firing of biomass, dedicated energy crops, energy from

waste with CHP, geothermal, hydroelectricity, solar photovolataic, tidal stream and wave (Ares, 2012a). FIT is a scheme that was introduced by the Government in the *Energy Act 2008* and its aim is "*to provide a simple system to incentivise small domestic and business renewables*" (Ares, 2012b). It pays tariff for every kWh generated and this approach makes electricity suppliers to pay a higher unit price for electricity sourced from renewables (Ares, 2012b).

Figure 1.4 displays the UK progress against the 2009 EU Renewable Energy Directive (RED), where the 4.1% of the final energy consumption was from renewable sources during 2012.

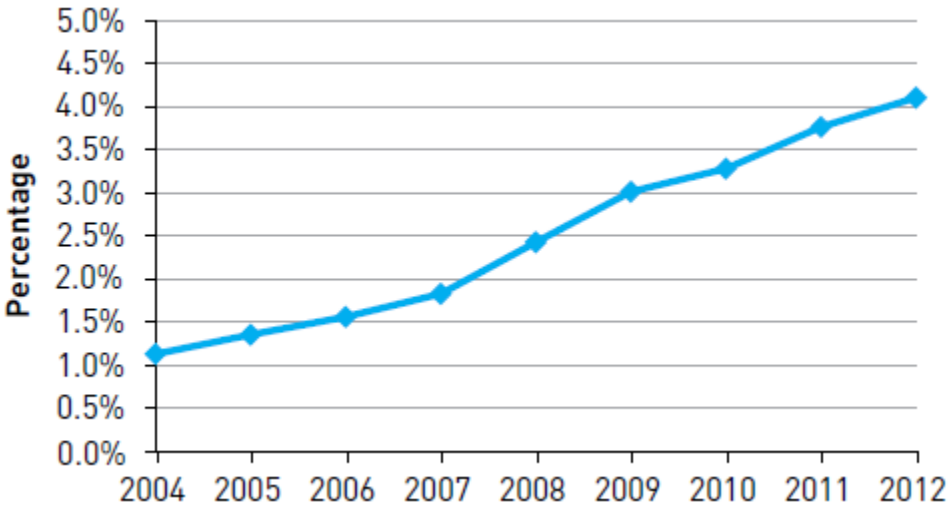

Figure 1.4. Progress against the 2009 Renewable Energy Directive (DECC, 2013a).

1.3.2 Heat

12% of the heat is expected to come from biomass, biogas, solar and heat pump (DECC, 2009). In March 2011, the Government introduced the Renewable Heat Incentive (RHI) policy to revolutionise the way heat is generated and used. Approximately 69% of heat produced comes from gas, followed by 14% from electricity, 10% from oil, 3% from solid fuel and 1.5% from renewables (DECC, 2011). Therefore, the objective of RHI is to increase the amount of heat generated from renewables and encourage the installation of renewable heating equipment, contributing towards carbon reduction goals. Not all technologies will be eligible for RHI. According to DECC (2011), they have to be considered renewable under the Renewable Energy Directive (RED).

1.3.3 Transportation

10% of transportation will be from renewables (DECC, 2009). The Government plays its role in this strategy by supporting the use of electric vehicles and electrification of the rail network. The Renewable Transport Fuel Obligation (RTFO) came into effect in 2008, where "*it places an obligation to fossil fuel suppliers to produce evidence showing that a percentage of fuels for road transport supplied in the UK come from renewable sources and are sustainable or that a substitute amount of money is paid*" (RTFO, 2011). Suppliers that provide 450,000 litres of fuel in a year are obligated, which include those that supply biofuels and fossil fuels (RTFO, 2011).

1.4 Biomass as a potential renewable source of energy

The versatility of biomass as a source of energy for heat, power and transport has been viewed as a source of energy that has the potential to offset fossil fuel use and continues to attract worldwide attention (McKay, 2006; Nowakowski *et al*., 2007). The IEA Bioenergy Task 40 reported that most of the biomass use globally is accounted for inefficient residential use (66%) that is mainly in developing countries for cooking and heating. Industry is the second largest, followed by electricity and transportation. (IEA, 2013a).

Table 1.2 presents a list of countries that uses biomass in the industrial sector, where Brazil, India and the United States present the top three who use the largest amount of biomass (IEA, 2013). With regards to UK, Ares (2013) mentioned that in 2011, 0.6% of its generation of energy comes from dedicated biomass. These fuels include straw and short rotation energy crops and the rest was animal biomass. The author also reported that half of the biomass was imported while the animal biomass is usually home produced. The use of dedicated plant biomass has reached more than double over the past four years (Ares, 2013). On the other hand, UK often uses wood for heating in homes and industry rather than for electricity generation. Therefore, Ares (2013) stated that UK is a net exporter of wood and wood waste for energy.

In the transportation sector, ethanol is the major transport biofuel in the US and Brazil while biodiesel is widely used in EU area (IEA, 2013). Almost half of the global liquid biofuels production are consumed by the US (43%) as recorded in 2011 and interestingly, 87% of the ethanol produced in Brazil is used as fuel (IEA, 2013).

Table 1.2. Countries that use biomass in the industrial sector (IEA, 2013a).

No.	**Country**	**Share of global use (%)**
1	Brazil	18
2	India	16
3	United States	16
4	Nigeria	5
5	Canada	4
6	Thailand	4
7	Indonesia	4
8	Democratic Republic of Congo	3
9	Sweden	2
10	Pakistan	2
11	Finland	2
12	Australia	1
13	Germany	1
14	France	1
15	Japan	1
Other countries		20
World		100

Basu (2013) listed three drivers that motivate the use of biomass and each is described briefly below.

1.4.1 Renewability benefits

Unlike fossil fuels (coal, oil and natural gas), biomass is a renewable source of energy, where it has a lifecycle that grows annually once a crop is cut or within a decade if it was a tree (Basu, 2013). Moreover, if biomass is managed in a sustainable way, it is not likely to deplete through consumption. *Switchgrass* and *Miscanthus* are the two examples of fast-growing plants that can grow in months. Later section will list more of this type of plant that are now increasingly receiving attention for energy production.

1.4.2 Environmental benefits

Biomass offers substantial environmental benefits relevant to managing atmospheric carbon and global climate change (Dayton *et al*., 1999), which could help meet the targets as have been set up in the Kyoto Protocol and the EU target of 20% renewable energy by 2020 (Arias *et al*., 2008). James and Howes (2006) discussed the benefits of biomass fuels from the principles of the carbon cycle. During thermal conversion of biomass, carbon dioxide is released but it is balanced by carbon dioxide absorbed by plant matter whilst they are growing. As a result, biomass is theoretically perceived as carbon neutral and able to reduce net carbon dioxide emissions (McKendry, 2002). In addition to that, biomass has zero to low sulphur content, eliminating the increase emission of SO_2 from the thermal conversion of biomass. However, it is crucial that "*the biomass is produced in a sustainable way as it is only truly renewable if replaced*" (James and Howes, 2006). In addition to that, there have been public concerns on the use of biomass and the impact it has on the environment, food supplies issues and people in developing countries.

The UK Biomass Strategy was published with Energy White Paper 2007 and in response to the 2005 Biomass Task Force Report. This Strategy acknowledges the increase use of biomass in tackling the climate change. The Government will ensure that the implementation of this strategy will not lead to increased deforestation and adversely affect the food security for the developing countries.

1.4.3 Sociopolitical benefits

Biomass offers a great advantage to countries that grow fast-growing trees/plants. A biomass-based power plant is economically viable if the biomass comes from a plantation that is within the radius from the power plant in terms of growing, collecting and harvesting (Basu, 2013). Moreover, local employment can be created and Basu (2013) stated that biomass-based power plant can create up to 20 times more job than that by fossil-fueled power plants.

1.5 Biomass Task Force Report

Biomass Task Force was introduced in 2004 to "*assist Government and the biomass industry in optimising the contribution of biomass energy to renewable energy targets and to sustainable farming and forestry and rural economy objectives*" (DEFRA, 2005). This Task Force was led by Sir Ben Gill. He noticed that biomass is not being fully utilised in the UK and there is an urgent need to address the ignorance about the potential use of biomass. The

objectives of this report are firstly, to identify possible measures for the development of biomass as an energy source; secondly, to engage with energy, agricultural and forestry industries, potential biomass users and other stakeholders to identify barriers and ways to tackle them and lastly, to make recommendations to industry and public sectors (DEFRA, 2005).

Included in the Biomass Task Force report are a series of 42 recommendations, which will not be discussed in detail in this section. They are grouped into three categories: i) delivering biomass energy, which covers biomass-fired heat and electricity generation, from wastes, anaerobic digestion and co-firing; ii) providing strategic leadership, which includes ownership of biomass to government and regulatory issues, where renewables policy in relation to biomass is said to have lack of clarity, over-emphasised and out-dated; and iii) underpinning delivery, such as creating awareness, developing supply chains, development of plan for the use of feedstock, recognition of energy crops, quality standards and certification, biodiversity, where a long-term strategic approach for the development of biomass is needed and training and skills, where there is a need to consider the qualifications and competence schemes for engineers (DEFRA, 2005).

1.6 UK Biomass Strategy

UK Biomass Strategy was published with the Energy White Paper 2007, in response to 2006 Energy Review and 2005 Biomass Task Force Report (DEFRA, 2007). This strategy focuses on the need to expand biomass supplies significantly and sustainably. It discusses UK targets and Government's policies on biomass for energy, transport and industry. It also "*acknowledges that separate strategies have been or are being developed to address the specific conditions that apply in Scotland, Wales and Northern Ireland*" (DEFRA, 2007). Few objectives were laid out in this strategy such as to realise and maximise the potential use of biomass in the UK as well as to support low-carbon technologies in striving to achieve the energy targets towards reducing the GHG emissions. The strategy is also intended to facilitate the development of a competitive and sustainable market and supply chain as well as to contribute to overall environmental benefits and the well-being of the ecosystem through the achievement of multiple benefits from land use (DEFRA, 2007).

1.7 Short Rotation Coppice (SRC)

Short rotation coppice (SRC) is a woody, perennial crop, and the term "Short Rotation" is derived from the frequency of harvesting, that is, every 2 to 3 years (AILE, 2007). SRC is planted once and harvested on a rotation of 3 to 10 years in a 20-year cycle (Brown, 2003; Caslin *et al*., 2011). SRC has been used for study since the mid-1960s to produce fibre for pulp and paper industry (Mitchell *et al*., 1999). Following the oil crisis in the 1970s, the objective switched to produce woody biomass for energy (AILE, 2007). In the UK, willow and eucalyptus are the two genera that have been evaluated for their suitability for use in SRC systems. Mitchell *et al* (1999) commented that SRC should ideally be established on a well-drained, fertile soil that is flat and free from stones to avoid the inhibition of plant growth.

1.8 Short Rotation Forestry (SRF)

In the UK, biomass is playing an important role in reaching the 2020 target. In order to meet the demand, there has to be a rapid increase in the production of energy crops for an increase in wood fuel supply, make better use of agricultural residues and fully exploit waste biomass from dumped into landfills (McKay, 2011). Previous development of woody biomass has put focus on SRC. Even though SRC like willow and poplar have fast growth rates and high productivity, they do not meet the six criteria for an ideal wood as a source of fuel as suggested by Ramsay (2004) as cited in Leslie *et al* (2012):

1) Produce high density wood
2) Have suitable chemical characteristics
3) Exhibit low moisture content
4) Be easily harvested
5) Be harvested using conventional machinery
6) Be capable of being harvested all year round.

SRC willow and poplar were also reported to be very hygroscopic, low density and promote the formation of corrosive substances upon thermal treatment (McKay, 2011). These concerns encourage the development of short rotation forestry (SRF). SRF is receiving current attention as a way of producing wood as a source of fuel. SRF is "*the practice of cultivating fast-growing trees that reach their economically optimum size between eight and 20 years old; each plant produces a single stem that is harvested at around 15 cm diameter*" (McKay, 2011). The differences between SRF and SRC are that the material in SRF is single-

stemmed and the rotation is longer, where it is usually been harvested between 8 and 20 years, as opposed to SRC, where the material is multi-stemmed and has shorter rotations (< 5 years) (Hardcastle, 2006). Some species that can be grown as SRF are alder, ash, birch, sycamore and eucalyptus. Conifers, willow, sweet chestnut, Norway maple, beech, hornbeam and oak are species that are excluded from consideration for SRF due to slower growth and site demands (Hardcastle, 2006). One challenge in operating SRF in Britain is the limited knowledge, data and experience. Hardcastle (2006) commented that SRF has not been widely used, hence, the lack of information. The other challenge is the climate change such as great temperature changes, less rainfall and less extreme summer drought, which could affect the prospects of SRF in this country (Murphy *et al*., 2009 as cited in McKay, 2011).

1.9 Energy crops: Herbaceous and Woody crops

Table 1.3 presents a wide range of types of biomass that are likely to be used in the UK for heat and/or power generation (energy crops, forestry residues, agricultural residues, wood and paper processing residues, imported biomass fuels and waste biomass fuels).

1.9.1 Definition of energy crops

"*Energy crops are annual and perennial species which can be cultivated to produce solid, liquid or gaseous energy feedstocks*" (Montross and Czarena in Crocker, 2010). In other words, they are defined as "*plants grown specifically as a source of carbon and energy for the manufacture of bio-based products*" (Brown, 2003). Crops are planted, harvested once a year for example, switchgrass, or on a 3- to 10-year cycle for example, willow (Brown, 2003; Montross and Czarena in Crocker, 2010).

Previously, energy crops are those that contain significant amounts of one or more of the four energy-rich components, namely, oils, sugars, starches and most importantly, lignocellulose (Brown, 2003). Crops that are abundant in the first three have been grown for food and feed. Lignocellulose is difficult to break down, hence, it is preferably to be used as an energy source (Brown, 2003). As a result, development of energy crop was put more focused on those that are rich in lignocellulose. Lignocellulosic crops are categorised into herbaceous energy crops and woody crops.

Table 1.3. Types of biomass and their examples (James and Howes, 2006).

Biomass types	**Examples**
Energy crops	Wood - Short rotation coppice (Willow) Herbaceous crop - Miscanthus
Forestry residues	Woody residues from felling, thinning and other forestry operations
Agricultural residues	Poultry litter Wheat straw
Wood and paper processing residues	Untreated wood waste from sawmills Paper sludge Contaminated wood wastes such as demolition waste, waste from furniture
Imported biomass fuels	Wood pellets Palm kernel expeller Palm oil processing resides Shea nuts Sunflower Cashew nuts
Waste biomass fuels	Waste derived fuel such as cellulose fibres Food processing residues such as coffee grounds Animal processing residues such as slurry

1.9.1.1 Herbaceous energy crops

"*Herbaceous crops are plants that have little or no woody tissue and usually live for only a single growing season*" (Brown, 2003). Brown (2003) stated that plants that grow annually will die at the end of the growing season and must be replanted in the spring, while those that grow perennially will die back each year in temperate climates but they re-establish themselves each spring from rootstock. He also noted that these types of plants are harvested on annual basis. Grasses have greater potential as energy crops because they contain a rich amount of lignocellulose than other herbaceous plants, hence many works are focused on them.

a) Miscanthus

Figure 1.5 shows an image of *Miscanthus*. *Miscanthus* is a genus of 15 species of rhizomatous grasses (Karp and Halford, 2011). They are perennial crops and harvested every year (Nordh and Dimitriou, 2003). They are usually planted in spring and reach to their maximum height in the summer. The drying stage accelerates during autumn and leaves fall off, providing nutrients for the soil and the canes are usually harvested in the winter. After harvesting, these crops are stored outdoor in piles and covered with plastic foil (Lewondowski *et al*., 2000). In some countries, *Miscanthus* is harvested during spring when the moisture content is 12-15%, where it will then be stored like dry straw (Nordh and Dimitriou, 2003). This growth pattern is repeated every year for the lifetime of the crop. Nordh and Dimitriou (2003) reported that the yields for *Miscanthus* differ depending on how this crop is managed and the location. The average yield is 10-30 tonnes dry matter per hectare (Lewondowski *et al*., 2000). Biomass Energy Centre (BEC) (2007a) stated that *Miscanthus* can be used for energy to produce heat and electricity on large power stations, requiring hundreds of thousands of tonnes of biomass annually. It can also be used on small-scale systems that only require dozen tonnes during winter (BEC, 2007a). Two of the most popular *Miscanthus* are *Miscanthus giganteus* and *Miscanthus sinensis*.

b) Reed canary grass

Reed canary grass (RCG) is another potential rhizomatous energy crop, with a scientific name, *Phalaris arundinacea* as also shown in Figure 1.5 (Lavergne and Molofsky, 2004). It is a 1 to 2 m tall grass and typically grows best under cool and moist conditions. It is known for its fast growth and industries are putting interests into this crop. This is because "*RCG can be grown in an environmentally and economically sound system with low nutrient input to the crop*" (Andersson and Lindvall, n.d.). Its annual production levels are 8-12 tonnes dry matter per hectare (Nordh and Dimitriou, 2003). However, it is an invasive species and therefore, can be difficult to control and maintain. It is usually planted in spring or summer and can be harvested early in the following spring rather than in the growing season (Landström *et al*., 1996). This is when the crop has low water content (10-15%) and a reduced ash as well as mineral contents such as chlorine, potassium and sulphur (Nordh and Dimitriou, 2003). It was suggested that when the plant reaches its mature stage, the lignocellulose contents increase while the mineral contents decrease. Therefore, for biofuel purposes, RCG should be harvested as late as possible (Andersson and Lindvall, n.d.).

Miscanthus

Reed canary grass

Figure 1.5. Photo images of herbaceous crops (Lewondowski *et al*., 2000).

1.9.1.2 Woody crops

Woody crops can be divided into hardwoods and softwoods. Hardwoods include willow, eucalyptus, birch and oak as shown in Figure 1.6. Softwoods include pine and spruce (see Figure 1.7).

a) Willow

Willow, a short rotation coppice, forms the genus *Salix*. It grows very rapidly during the juvenile stage (Murphy *et al*., 1996). This type of tree species is established by plant cuttings from one-year old wood, which are then inserted into the ground in the spring. At the end of the first growing season, they are cut to ground level to promote the growth of multi-stemmed stool (Dawson, 2007). The growth reaches up to 4 m in the first year and continues rapidly to heighten to 6-7 m at harvest in the third year (Dawson, 2007). Moreover, the willow coppice may be harvested six to eight times on a three-year cycle through the crop's lifespan of 15 to 20 years (McCracken, 2006; Dawson, 2007). Willow grows best in mildly acidic soils (pH 5-7) and one important advantage that it has compared to other crops is that less insecticides, fungicides and herbicides are needed in willow coppice plantations (Murphy *et al*., 1996). They are only necessary during the first and second year of the plantation. Dawson (2007) suggested that the yield can be expected to be in the range 7-12 tonnes dry matter (tDM) per hectare per year or 21-36 tDM on a three year harvest cycle.

b) Eucalyptus

Eucalyptus comes from the family, *Myrtaceae*. Many species of Eucalyptus are well grown in numerous countries such as Florida, South Africa, Brazil, Uruguay, Portugal and Venezuela (Gonzalez *et al*., 2011). However, in the UK, Leslie *et al* (2012) stated that there are only a few Eucalyptus species that are able to survive and grow well in the cold climate, namely *Eucalyptus gunnii* and *Eucalyptus nitens*. These two species have very rapid early growth, where their growth rates are 1.5-2.0 m per year and > 2.0 m per year respectively (FCS, 2010). Therefore, they have been used for short rotation coppice (Leslie *et al*., 2012). More interestingly, *E.gunnii* and *E.nitens* are also eligible as candidates for short rotation forestry (McKay, 2011). In central Florida, Eucalyptus is very promising for co-firing in coal-based plants (Rockwood *et al*, 2008).

c) Oak

Quercus is the old Latin name for oak and there are about 450 species known to be found in Europe, Asia, North Africa, North America and South America (Simpfendorfer, 1992). Its family is said to be one of the largest and hardest in the world (Simpfendorfer, 1992). Oak trees can survive up to hundreds of years, of at least 200 years and a maximum of 600 years. The growth rate of oak trees depends on the species, where it varies from slow to rapid. An example of a slow growth oak tree is the white oak, *Quercus alba*, where it grows 10-15 feet within a span of 10-12 years (Simpfendorfer, 1992). An example of a moderate growth oak tree is the Southern red oak tree, *Quercus falcate*, where it grows 25 feet every 20 years. An example of a fast growth oak tree is water oak tree, *Quercus nigra*, where it grows 25 feet every 10 years. Oak woods are widely used for furniture and housing industries (Tumuluru *et al*., 2012). Its sawdust is a by-product available from the timber industry and is said to be valuable for bioenergy purposes (Tumuluru *et al*., 2012).

d) Birch

Birch is a relatively short-lived and broad-leaved deciduous tree of the genus *Betula*, where there are about 60 species found in northern Europe, Asia and North America (Simpfendorfer, 1992). Birch trees are medium-sized trees growing to between 40 and 50 feet. They are considered to be moderate to fast growing trees, where their growth rate is 1.25 feet per year for the first 10-20 years (Simpfendorfer, 1992). Simpfendorfer (1992) suggested that since birch is very short-lived, it is required to be sown within a few days of falling. Silver Birch is the species that is always planted. Interestingly, recent Energy Crops Scheme

is now supporting more hardwood species, where one of them is silver birch, even though it gives lower yield than willow and poplar (BEC, 2007b).

Willow

Eucalyptus

Birch

Oak

Figure 1.6. Photo images of hardwood trees (Source: www.2020site.org/trees/).

e) Pine

Pines are among the most well-known coniferous trees in the genus *Pinus*, with about 70 species. They are mostly found in most of Northern hemisphere, throughout temperate and subtropical regions of the world (Simpfendorfer, 1992). They can also be found past the Equator in parts of Southeast Asia (Simpfendorfer, 1992). These pines are characterised by their needle-shaped leaves and their heights range from 45 to 135 feet. Pine trees are evergreens, in which their leaves do not change in colour in the fall and do not shed in the winter months (2020site, 2012). Viana *et al* (2010) stated that one pine species that is capable

of providing a regular supply to meet fuel demand is *Pinus pinaster* (maritime pine), which is originally from France and Portugal. It has a fast growth rate and is reported to be able to grow well over a wide range of soil and rainfall conditions (FPC, 2006). Another fast growth pine species is *Pinus taeda* (loblolly pine), which is an important source for saw timber and pulp wood. It is abundant in Southern U.S and has been studied for ethanol production and can be economically competitive compared to production of ethanol from corn stover and other lignocellulosic materials (Frederick *et al*., 2008). The other species is Loblolly pine and it is considered a dedicated energy crop, at which there has been a considerable interest in using this pine as a feedstock for the production of transportation fuels (Frederick *et al*., 2008). It was reported in Georgia that short rotation plantation for loblolly pine was carried out intensively (10 to 12 years) and as a result, 26.6 m^3 per hectare per year was produced (Borders and Bailey, 2001 in Gonzalez *et al*., 2011).

f) Spruce

Spruce trees belong to the genus *Picea* and can grow up to 100 feet tall. They have attractive pyramid shape and stiff needles. These coniferous trees can live up to 800 years and are able to tolerate extreme weather conditions (2020site, 2012). They can be found in Europe while most grow in North America. In Sweden, trees are used as raw materials for industrial needs and source of energy, for example *Picea abies* (Norway spruce) (Johansson, 1999). Johansson (1999) reported that spruce plantations grow very fast especially if the soil is very fertile, where the spruce can grow 2 to 3 feet per year on their first 25 years. On a poor soil, it can grow on an average of a foot per year.

g) Larch

Larch is a deciduous in the genus, *Larix* with about ten species identified around Europe, Asia and North America (Simpfendorfer, 1992). Its height can go up to 120 feet. It can survive in cooler temperature Northern hemisphere so they grow mostly in the mountainous regions (2020site, 2012). The leaves are soft, flat-looking needles and shed during autumn. Larch is very hard that it is able to withstand most forest fires. One example of a larch species is the European larch, *Larix decidua*, which has a slow to moderate growth rate (12 to 18 inches per year) and long been used in the timber industry for building constructions and provide heat in homes.

Pine **Spruce** **Larch**

Figure 1.7. Photo images of softwoods and their respective needle-like leaves (Source: www.2020site.org/trees/).

1.10 Biomass composition

Cellulose, hemicellulose, lignin, starch, triglycerides and other classes of organic materials such as resins and terpenes are components that make up a biomass. Out of these, the first three appear to be significant when considering biomass as an energy fuel. They involved actively especially hemicellulose, in thermal decomposition reactions. In a biomass, cellulose is the most abundant component (40-60%), followed by hemicellulose (20-40%) and lignin (10-25%) (Yang *et al.*, 2007). Lignocellulose is the term that is used to describe cellulose, hemicellulose and lignin as a whole. Starch, triglycerides and other classes of organic materials are present in relatively small amounts, thus, they have almost negligible impact in any thermal reactions (Klass, 1998) and will not be described in this section.

1.10.1 Cellulose

Cellulose is a homopolysaccharide, which is composed of β-(1-4)-D-glucopyranose units, linked together by 1, 4-glycosidic bonds without branches (David and Ragaukas, 2010; Yang *et al.*, 2007). Cellulose molecules are completely linear and form strong, crystalline and fibrous structures. Figure 1.8 shows that each glucose unit has three hydroxyl (O-H) groups.

This promotes the formation of hydrogen bonding within the molecule and between cellulose molecules. Thus, further creates a high thermal stability to the structure (Yang *et al*., 2007).

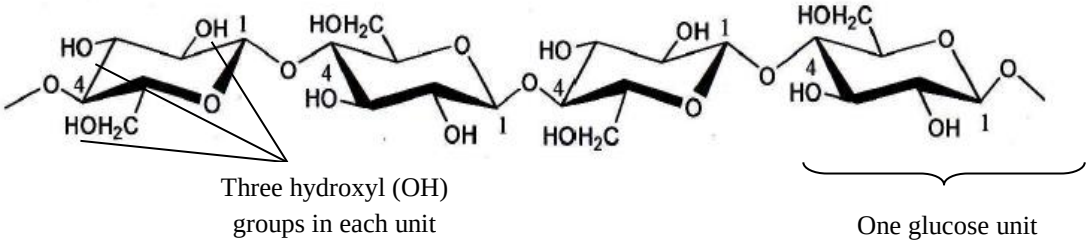

Figure 1.8. Structure of cellulose (Sjöstörm, 1981).

1.10.2 Hemicellulose

Hemicellulose is a heteropolysaccharide, which consists of a mixture of different monosaccharides. These include D-glucose, D-mannose, D-galactose, D-xylose, L-arabinose and D-uronic acids (D-galacturonic acid, D-glucuronic acid) (Lewin and Goldstein, 1991; David and Ragaukas, 2010). Of all these, D-xylose, also known as xylan, is often the most abundant hemicellulose present in a biomass. The backbone of hemicellulose has a linear structure like cellulose. But because hemicellulose has a great number of side chains and functional groups that contain sugars, sugar acids and acetyl esters, these prevent the component from arranging itself in an ordered and linear manner (Brett & Waldron, 1996). The side chains and functional groups create branches in hemicellulose. They are easy to remove from the main stem and prone to degradation, releasing volatiles upon thermal treatment (Yang *et al*., 2007). It is interesting to note that hemicellulose in grasses, herbaceous crops, hardwood and softwood are different in terms of composition and structure.

1.10.2.1 Hemicellulose in grasses and herbaceous crops

Figure 1.9 represents the lignocellulose compositions of different biomass as well as their respective hemicellulose composition. It shows that other plant materials in comparison to hardwood and softwood have a more variety in the hemicellulose composition, which is comprised of xylose, arabinose, galactose and mannose. Chemical structures of the four components can be shown in Figure 1.10.

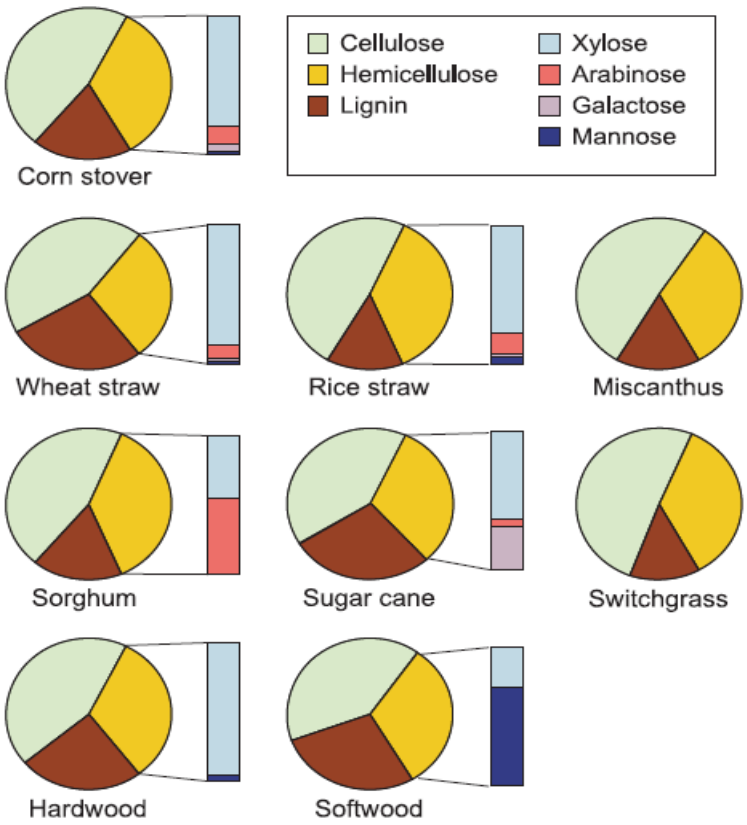

Figure 1.9. Lignocellulosic compositions of biomass and their respective hemicellulose composition, at dry basis (Pauly and Keegstra, 2008).

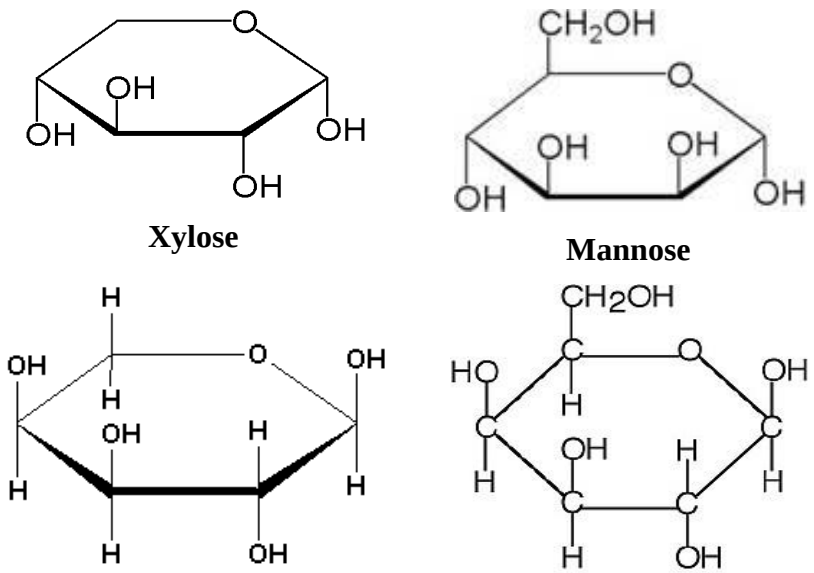

Figure 1.10. Chemical structures of xylose, mannose, arabinose and galactose (Sjöström, 1981).

1.10.2.2 Hemicellulose in hardwood

Hardwood has a high proportion of xylan-based hemicellulose (Sjöstörm, 1981; Bergman *et al*., 2005). Clearly, Figure 1.11 shows that the predominant hemicellulose in hardwood is glucuronoxylan (xylose). Similar to cellulose, the backbone of the hardwood consists of β-D-xylopyranose units, linked by 1, 4-glycosidic bonds. There is also a few percentages of glucomannan (mannose) in hardwoods, which are composed of β-D-glucopyranose and β-D-mannopyranose units linked by the 1, 4-bonds.

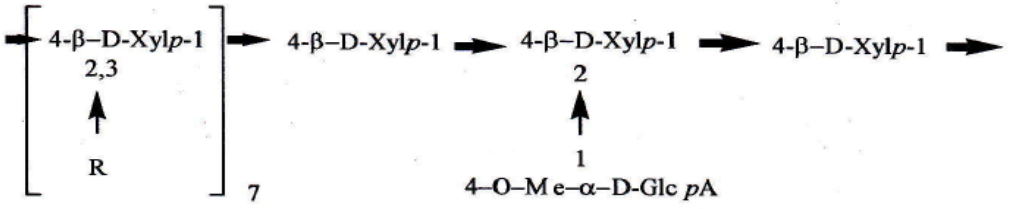

Figure 1.11. Principal structure of glucuronoxylan in hardwood, in which the sugar units are *β*-D- Xylopyranose (Xyl*p*) and 4-O-methyl-α-D-glucopyranosyluronic acid (Glc*p*A). R is an acetyl group (CH_3CO) (Sjöstörm, 1981**)**.

1.10.2.3 Hemicellulose in softwood

The major hemicellulose in softwood is galactoglucomannan (Lewin and Goldstein, 1991; Sjöstörm, 1981). The backbone is linear or slightly branched and composed of 1, 4-linked β-D-glucopyranose, β-D-mannopyranose and *β*-D-galactopyranose units as presented in Figure 1.12. Other than galactoglucomannan, softwood also contains 5-10% of arabinoglucuronoxylan and this structure is made up of 1, 4-linked β-D-xylopyranose, 4-o-methyl-α-D-glucuronic and α-L-arabinofuranose units as shown in Figure 1.13

1.10.3 Lignin

Lignin is described as an amorphous high molecular weight, polyphenolic cross-linked biopolymer and full of aromatic rings with various branches (Yang *et al*., 2007). It acts as a primary binder for cellulosic fibres and consists of three phenylpropane alcohol monomer units as shown in Figure 1.14 (Brett & Waldron, 1996). Interestingly, not only the composition of hemicellulose varies for different types of biomass but lignin as well. The lignin in herbaceous crops or grasses is made up of *p*-cumaril alcohol units (Lewin and Goldstein, 1991; Hon and Shirashi, 2001). In hardwoods, the lignin is composed mostly of

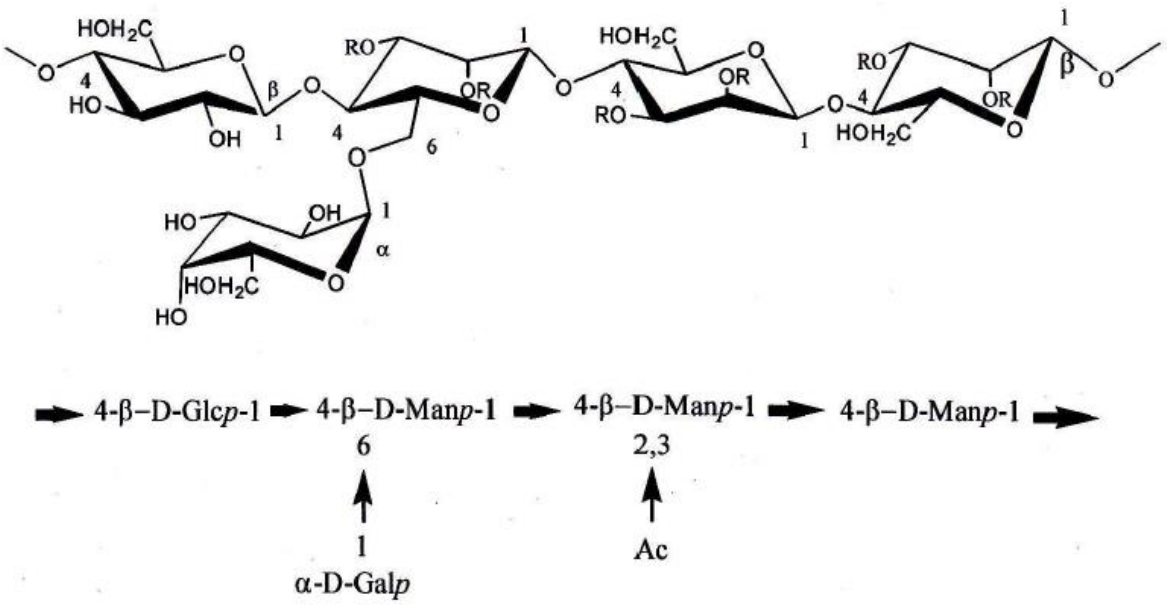

Figure 1.12. Principal structure of galactoglucomannans in softwood, in which the sugar units are *β*-D-glucopyranose (Glc*p*), *β*-D-mannopyranose (Man*p*) and *β*-D-galactopyranose (Gal*p*). R is CH_3CO or H (Sjöstörm, 1981).

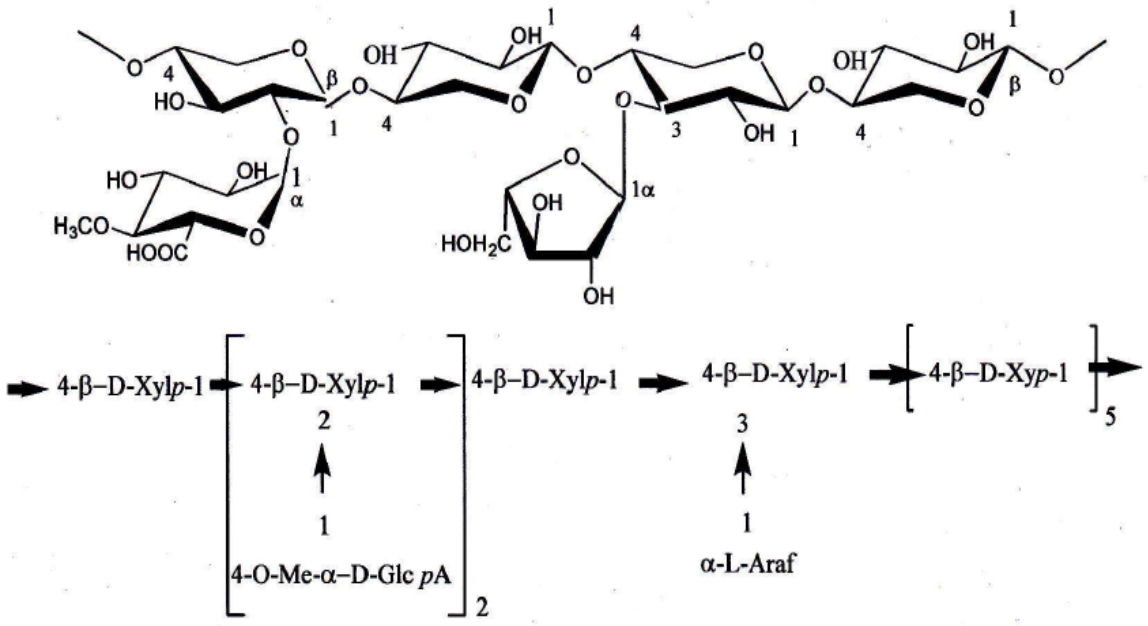

Figure 1.13. Principal structure of arabinoglucuronoxylan in softwood, where the sugar units are *β*-D- Xylopyranose (Xyl*p*) and 4-O-methyl-α-D-glucopyranosyluronic acid (Glc*p*A) and α-L-arabinofuranose (Ara*f*) (Sjöstörm, 1981).

guaicyl- and syringylpropane units, which are made up of coniferil and sinapil alcohols while in softwoods, the lignin has guaicylpropane units that are mainly made up of coniferil alcohols (Freudenberg and Neish, 1968; Lewin and Goldstein, 1991; Hon and Shirashi,

2001). These units are linked together by a wide variety of bonds including carbon-carbon bonds. Lignin is very strong and hydrophobic. Even though it is the least abundant compared to the other two main components, Bridgeman *et al* (2007) stated that lignin is one of the most persistent biological molecules and highly resistant to natural degradation such as enzymatic attack.

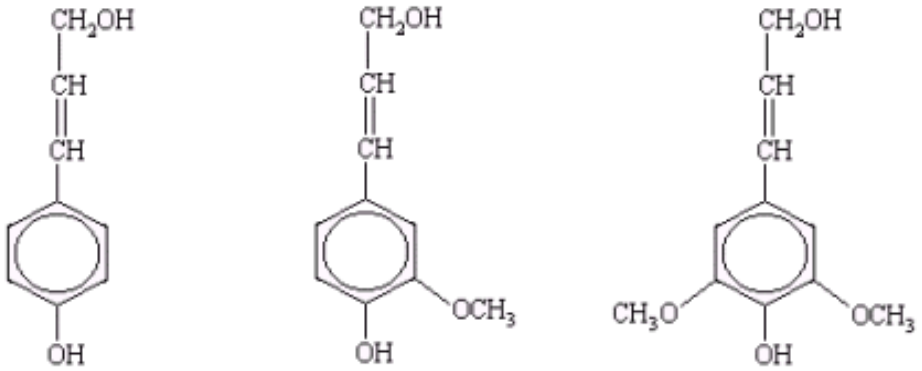

p-cumaril alcohol coniferil alcohol sinapil alcohol

Figure 1.14. Principal components that make up the structure of lignin (Brett & Waldron, 1996).

1.11 Biomass characterisation

Proximate and ultimate analyses are two standard analyses that are used to provide information about the fuel's characteristics as to whether the biomass would be ideal to be used as a fuel for energy and also, when it comes to designing a proper biomass utilisation system such as a gasifier and combustor.

1.11.1 Fuel characteristics: Proximate analysis

Proximate analysis measures the physical and chemical parameters of a biomass, which can be obtained by means of heating a weighted sample in an oven/furnace under a controlled temperature or in a thermogravimetric analysis (TGA). TGA involves the combustion of a biomass that is comprised of four stages: drying, pyrolysis, volatile combustion and char combustion, as shown in Figure 1.15 (Brown, 2003). What happens to the biomass at each stage determines the characteristics of the fuel and this type of analysis provides the information about the moisture, volatile matter, fixed carbon and ash contents of the fuel.

Upon analysis, the results can be corrected to a dry or dry ash free basis except moisture content.

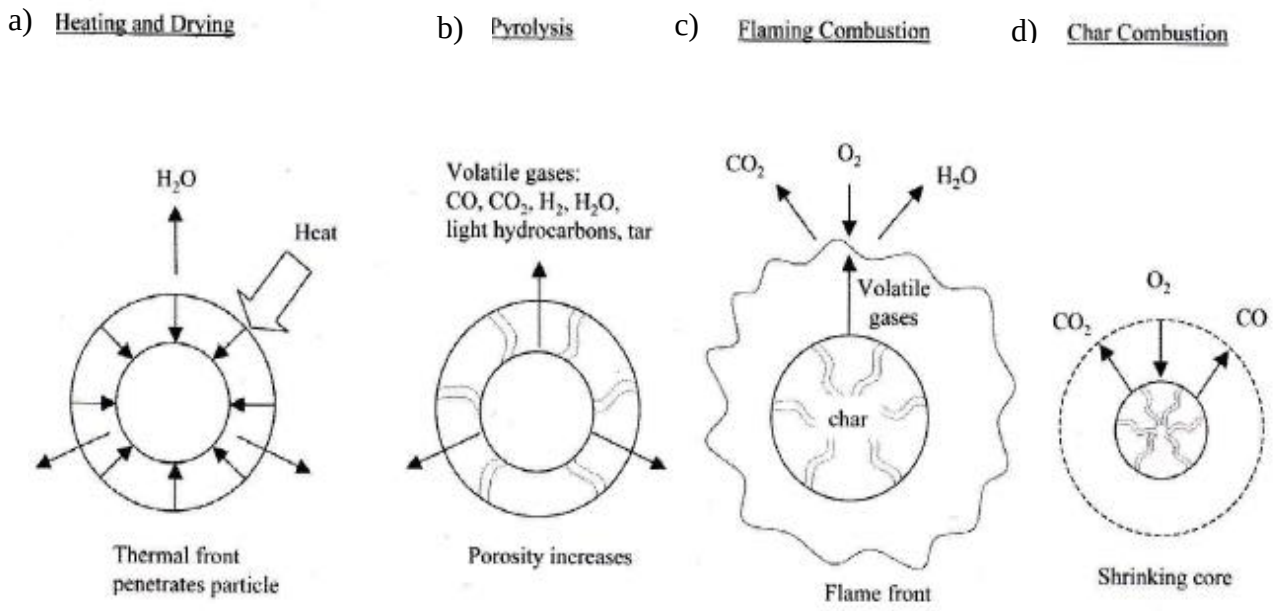

Figure 1.15. Stages involved in the solid fuel combustion (Brown, 2003).

Figure 1.16 is an example of a result from the TGA, which represents the change in mass against time that takes place throughout each stage. In general, it can be seen that the biggest change in mass takes place during the devolatisation stage, which will be explained in more detail shortly.

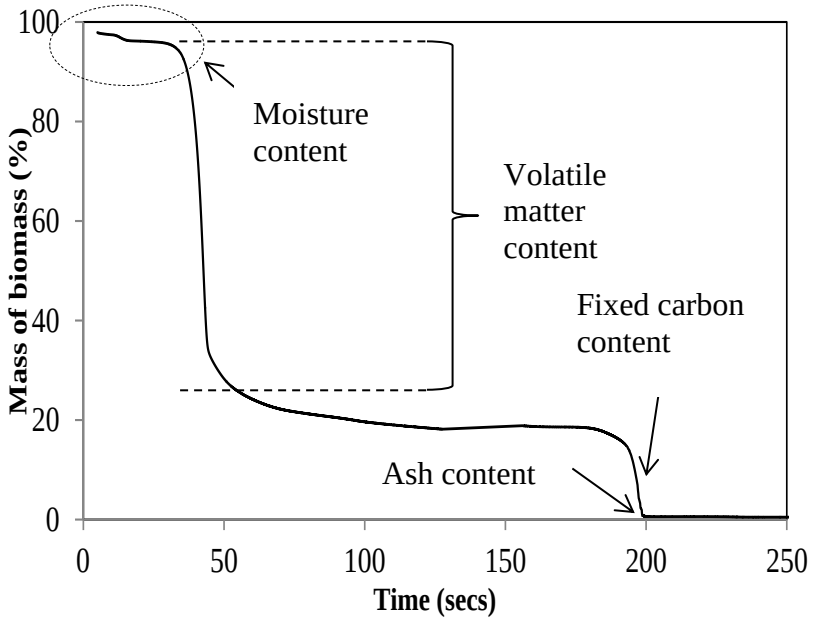

Figure 1.16 A typical diagram of a thermogravimetric analysis of a biomass.

Figure 1.15 a) illustrates the drying stage, after the heat was introduced and the temperature has reached the boiling point of water. Drying stage determines the moisture content of the biomass because it only involves the removal of moisture. The loss of water led to a slight mass loss as shown in Figure 1.16. In terms of biomass as a feedstock for combustion, gasification or other thermochemical processing, moisture content is a very crucial parameter (Murphy *et al*., 1996). Dealing with biomass can be difficult because it readily absorbs moisture when it is exposed to air and degrades gradually upon long storage. The moisture content depends on the type of biomass, location as to where it is planted, when it was harvested, the storage conditions and the duration of storage (Murphy *et al*., 1996). The moisture content of a biomass fuel can go as high as 90% (Basu, 2013). If the moisture content is high, a great amount of heat energy is required for evaporation during biomass thermal processes and Basu (2013) stated that the energy used for evaporation is non-recoverable. Drying is an energy intensive process. This parameter is also important in milling for pelletisation and co-firing purposes.

Volatile matter studies the amount of components in the biomass that are converted and liberated as volatiles at high temperatures (Montross and Czarena in Crocker, 2010). Volatile matter content is important in designing burners and gasifiers for biomass (Brown, 2003). The second stage shown in Figure 1.15 b) represents pyrolysis and it involves a series of thermally driven chemical reactions. This is when lignocellulose materials start to degrade at above 200°C. Decomposition of organic molecules takes place, producing a large variety of volatile compounds, such as carbon dioxide, carbon monoxide, water, methane and high molecular weight compounds (Brown, 2003). Pyrolysis follows the thermal front through the particle and allows the release of volatile compounds, creating pores that penetrate through to the surface of the particle. The content of the volatile matter depends on the heating rate and temperature it is heated (Basu, 2013).

Figure 1.15 c) shows that in the presence of oxygen and sufficient temperature flame, the volatile or flame combustion takes place, in which carbon dioxide and water are the final products (Brown, 2003). At the end of pyrolysis, a porous carbonaceous residue, char remains and again, in the presence of oxygen, char combustion takes over (Figure 1.15 d)). Brown (2003) stated that the char oxidation is governed by mass transfer of oxygen instead of chemical kinetics. Oxygen may react with the char in two ways; at the surface of the particle and results in a shrinking core reaction or it may penetrate into the pores and increase the

porosity of the char while the diameter remains constant (Brown, 2003). Char is a carbon residue of pyrolysis (devolatisation). It is not a pure carbon, nor a fixed carbon of the biomass. It contains the remaining volatiles, ash and the fixed carbon. The fixed carbon content is the amount of carbon contained in the char that is left after volatile materials are driven off. Moreover, it includes "*the elemental carbon in the original fuel plus any carbonaceous residue formed while heating, in the determination of volatile matter*" (Basu, 2013). An increase in the fixed carbon content indicates that the biomass is suitable for energy production (Pierre *et al*., 2011; Basu, 2013).

Ash content is the non-combustible inorganic residue left after the biomass is burnt. The ash content is related to the inorganic matter in a biomass, where the contents of inorganic metal can be measured using inductively coupled plasma spectrometry (ICP) with mass spectrometric detection. Silica content can be analysed using a spectrophotometer as carried out in Bridgeman *et al* (2007).

Fertilisers are important for optimum performance of crop growth and maintaining the fertility of the soil (Brown, 2003). The major nutrients are nitrogen in the form of nitrate, ammonia and urea, phosphorus and alkali metals such as potassium, sodium and calcium, all in the form of salts (Brown, 2003). They are added into the plant tissues for rapid growth. Annual crops contain larger amounts of these nutrients than perennial crops and they remain in the biomass when harvest (Brown, 2003).

The ash composition is crucial for a biomass as a fuel. The ash content does not represent the original inorganic matter in the biomass fuel as some of the composition of the ash undergoes oxidation during burning. Alkali metals (mainly calcium, potassium and sodium) contained in the ash exist as oxides after volatile and char combustion. Inorganic matter does not deliver energy content. The greater the ash content, the lower the energy content. High contents of potassium and sodium may be beneficial for catalysing the conversion to gaseous or liquid fuels (Murphy *et al*., 1996; Nowakowski *et al*., 2007). However, alkali vapours may react with sulphur and silica and form compounds that have low melting points and result in deposits on the heat transfer surfaces (Murphy *et al*., 1996; Brown, 2003). This create a serious concern as it leads to fouling and slagging that can damage the thermal reaction system and combustion equipment such as boiler tubes and corrosion at the surfaces (Dayton *et al*., 1999; Davidsson *et al*., 2007; Nowakowski *et al*., 2007; Werkelin *et al*., 2010).

"*Slagging is the partial or complete melting of ash, while fouling is the accumulation of sticky ash particles on heat exchange surfaces*" (Brown, 2003). Slagging is usually found in the radiant section of the furnace, while fouling occurs in the cooler region in the furnace, where the heat exchange equipment is located (Murphy *et al*., 1996).

1.11.2 Fuel Characteristics: Ultimate analysis

Ultimate analysis studies the elemental composition that makes up a biomass. The contents of carbon, hydrogen, oxygen, nitrogen and sulphur are usually analysed as they are the five most abundant elements present in solid fuels. The percentages of each element are usually presented on a dry, ash free basis. Chemical properties are important for the energy efficiency, environmental concerns and ash related operating problems (Murphy *et al*., 1996).

Friedl *et al* (2005) studied the correlation between C, H and O contents and the calorific values of fuels. Calorific value (CV), which is also known as the heating value is described as "*an expression of the energy content evolved when burnt in air*" (McKendry, 2002). Friedl *et al* (2005) stated that the determination of heating values is important for the design and control of power plants. The CV can be expressed in two forms: the higher heating value (HHV) or gross calorific value (GCV) and the lower heating value (LHV) or net calorific value (NCV). The HHV includes the total energy released when a fuel is burnt in air and therefore includes the latent heat from water vapour. The LHV is defined as "*the amount of heat released by fully combusting a specified quantity less the heat of vapourisation of the water in the combustion product*" (Basu, 2013). As most energy conversion technologies do not recover the latent heat, the LHV is the appropriate value to use for energy (McKendry, 2002).

A Van Krevelen diagram is a plot that is often used to classify (rank) coals The lower the O:C or H:C ratio that is present in the fuel, the higher the heating value, then the better is the fuel. For example, Figure 1.17 shows that anthracite has a high carbon content than lignite, therefore, it can be said that the anthracite is of higher rank than lignite. However, it is important to note that in a formal system, the ranking is not based on the C content or where the fuel is positioned in the Van Krevelen diagram, but rather on how it behaves as a fuel such as during combustion or how much heat is released when it is burned (Schobert, 1990).

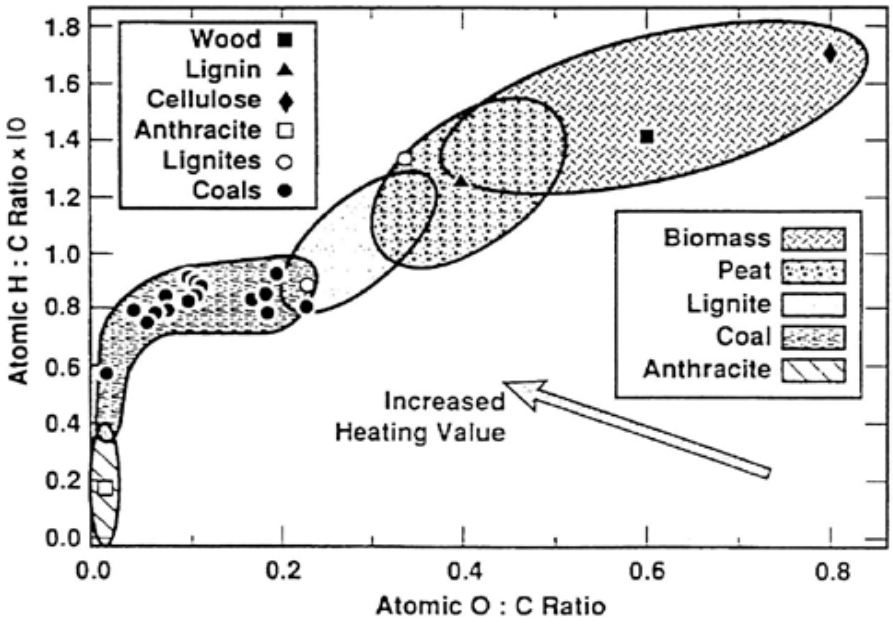

Figure 1.17. Van Krevelen diagram of solid fuels (McKendry, 2002).

1.12 Current uses of biomass energy in the UK

Biomass is currently used for heat and/or power generation in the UK. There are four main approaches for utilising biomass, namely i) combustion in dedicated boilers, ii) pyrolysis, iii) gasification and iv) co-firing with fossil fuels, where dedicated combustion and co-firing as the two most common approaches.

1) Combustion

Combustion is the oldest biomass thermal conversion treatment that involves incineration, direct firing and burning with air (Klass, 1998). This process leads to the formation of carbon dioxide and water vapour. Stages that involve in combustion of biomass are displayed in Figure 1.15 and already explained in Section 1.11.1. The flame temperature can exceed 2000°C, depending on the heating value and moisture content of the fuel, the amount of air to burn the fuel and the construction of the furnace (Brown, 2003). A combustor is the device that is used to convert the chemical energy of fuels into high temperature exhaust gases, where the heat from the gases can be utilised for power generation (Brown, 2003). Combustors include grate-fired systems, suspension burners and fluidised beds. Fluidised bed combustors are the recent innovation and they are developed since 1980s especially for industrial applications. An incomplete combustion can however, lead to large emissions of

pollutants, formation of tars and raise environmental concerns (Williams *et al*., 2012). This is a consequence of biomass having high volatile matter (Murphy *et al*., 1996). Moreover, Brown (2003) stated that burning high-moisture fuels can affect the performance of combustion for two reasons. Firstly, the energy imbalance to recover the energy required to evaporate the moisture with the energy to cool the water vapour in the exhaust gases. Secondly, this type of fuels does not combust well because the process of fuel drying suppresses fuel temperatures to below those required for ignition. With that, biomass that contains 30% moisture is unacceptable in most boilers. Another problem that can affect combustion is serious slagging and fouling due to the presence of high alkali metals and silica contents in the fuel. Alkali metals exist as oxides and the vapours combine with sulphur and silica, forming compounds that have low melting points.

2) Pyrolysis

This process involves a decomposition of biomass at high temperatures (500-900°C) under inert atmosphere to produce a solid char, liquid and non-condensable gases (for example, CO_2, H_2O, CO, C_2H_2, C_2H_4). The liquid product (known as tar) is the main of interest in pyrolysis. It contains up to 20% water and consists mainly of homologous phenolic compounds. Basu (2013) stated that the product of pyrolysis depends on the design of the pyrolyser, composition of biomass and the following parameters, that is, heating rate, final temperature and residence time. Based on the heating rates, here are two types of pyrolysis. If it is a slow pyrolysis, which operates at 200-800°C and long residence times, more char yield will be produced. Fast pyrolysis at low temperatures (below 650°C) yields more vapours and condense to liquids while that at high temperatures (up to 1000°C) yields more gases (Murphy *et al*., 1996; Brown, 2003). Based on the biomass composition, the individual constituents that make up lignocellulose have different temperature ranges for initiation of pyrolysis. They respond differently as well. Cellulose is a primary source of condensable vapours while hemicellulose yields more non-condensable gases and less tar. While lignin degrades slowly, making a contribution to the char yield. Based on temperature, the amount of non-condensable gases increases and the composition varies with increase in temperature.

3) Gasification

Gasification is defined as an endothermic process that uses high temperatures (750-850°C) to convert solid carbonaceous fuels into flammable gas mixtures (Brown, 2003). In combustion, the main products are carbon dioxide and water vapour but for gasification, the gas mixtures,

which are also known as producer gases, consist of carbon monoxide, hydrogen, methane, small amounts of nitrogen, carbon dioxide and higher hydrocarbons. Biomass has a very high volatile content and high reactivity char, which makes it suitable as an ideal gasification fuel (Brown, 2003). Low temperatures and high pressures favour the formation of methane, while high temperatures and low pressures favour the formation of hydrogen and carbon monoxide (Brown, 2003).

4) Co-firing biomass in coal-fired boilers

Co-firing is a process where biomass is burned together with coal and this approach is receiving attention globally. It is an alternative to completely replace coal with biomass fuel in a boiler (Brown, 2003). Co-firing has been carried out in the UK since the introduction of Renewable Obligations in April 2002 (Drax, 2011). Most of the coal-fired power stations practice direct co-firing with biomass. By substituting part of coal with biomass, a significant amount of carbon dioxide emissions can be reduced, provided that the biomass is produced sustainably. Industries that generate biomass wastes can also use co-firing instead of landfilling. Furthermore, co-firing can help to reduce sulphur emissions from boilers since biomass has a low sulphur content. With that, ash-fouling can also be reduced.

The following are six basic options available for the direct co-firing of biomass at coal-fired stations as suggested by Livingston (2012) in Figure 1.18.

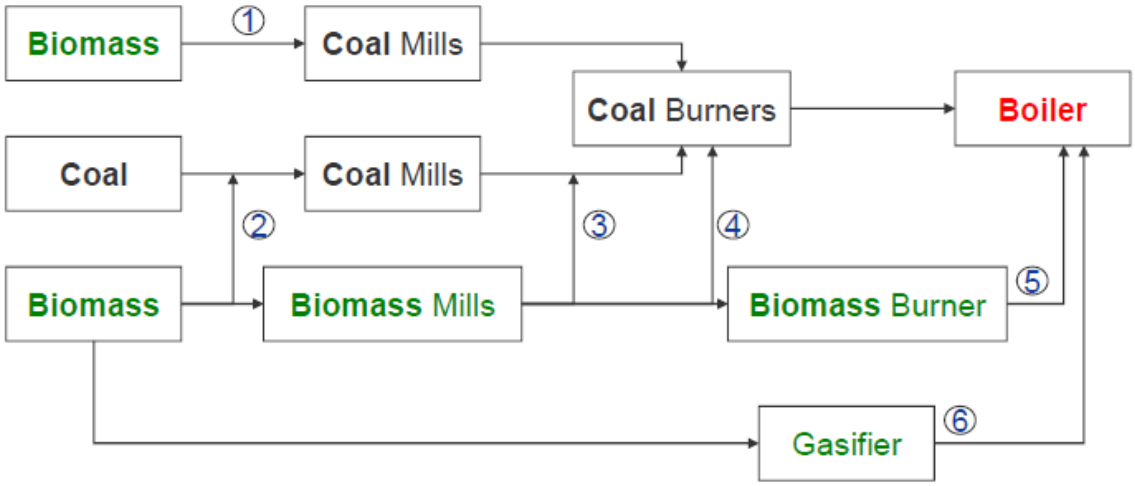

Figure 1.18. A schematic flow diagram of options of co-firing (Livingston, 2012).

Option (1): Milling biomass in coal mills

The first option involves milling biomass in coal mills, where these mills have to be operated in cold primary air to avoid combustion. There are a few plants around Europe that have converted their coal firing plants to 100% wood pellet firing such as in Vasthamnsverket in Helsingborg, Sweden, Unit 9 at Amer Centrale in the Netherlands, Hasselby Heat and power plant, Sweden and very soon, Drax Power station, UK. One drawback of this first option is the fact that biomass has a high volatile matter content and release combustible volatiles at temperatures above 180°C, which can lead to explosion and mill fires. Therefore, it is important to control the flow rate and temperature of the primary air.

Option (2): Co-firing by pre-mixing and co-milling

Livingston (2012) reported that this second option of pre-mixing biomass with coal and further processing these mixtures to coal mills has been the preferred approach for coal-power stations that are doing this for the first time. In Britain, there are several mills used for example, ball mills, tube mills, roller mills, and vertical spindle ball and ring. One disadvantage is that biomass tends to accumulate in the mill so it takes longer time, and this means more energy is required for biomass to clear from the mill. Biomass is well-known for its high moisture content, so wet biomass may have impact on the mill heat balance.

Options (3) – (5): The direct injection of pre-milled biomass

There are three basic direct injection co-firing options listed by Livingston (2012):

i. Into the pulverised coal pipework *(3)*, in which this option is only applicable to limited biomass materials and power plants,
ii. Into modified coal burners or directly into the furnace with no combustion air *(4)*, in which this encompasses the full conversion of existing coal-fired power stations by taking coal out of the energy mix and delivers a cost effective form of renewable power to burn biomass only and
iii. Through new, dedicated biomass burners *(5)*, where these are plants that are dedicated to burn solely biomass. Since they are newly built, they are considered as a more expensive option compared to the first two (Drax, 2011).

Option (6): Gasification of biomass

This is an indirect option for co-firing. Figure 1.19 a) shows a schematic diagram of the gasification co-firing. It involves the installation of separate biomass gasifier and boiler but it

is too expensive and complex to be implemented in UK (Livingston, 2012). Basu (2013) stated that the gasifier does not interfere with the operation of the coal-firing system, therefore, this approach offers a high degree of fuel flexibility. One disadvantage is the evaporation of alkali in the biomass that can cause fouling and corrosion of boiler tubes (Basu, 2013).

The other option is parallel co-firing, which involves the installation of a completely separate biomass-fired boiler to produce steam (Figure 1.19 b)). Basu (2013) described that this option uses low temperature and pressure from the biomass boiler instead of using the high pressure steam from the main boiler. This approach avoids fouling and corrosion but this operation is also expensive.

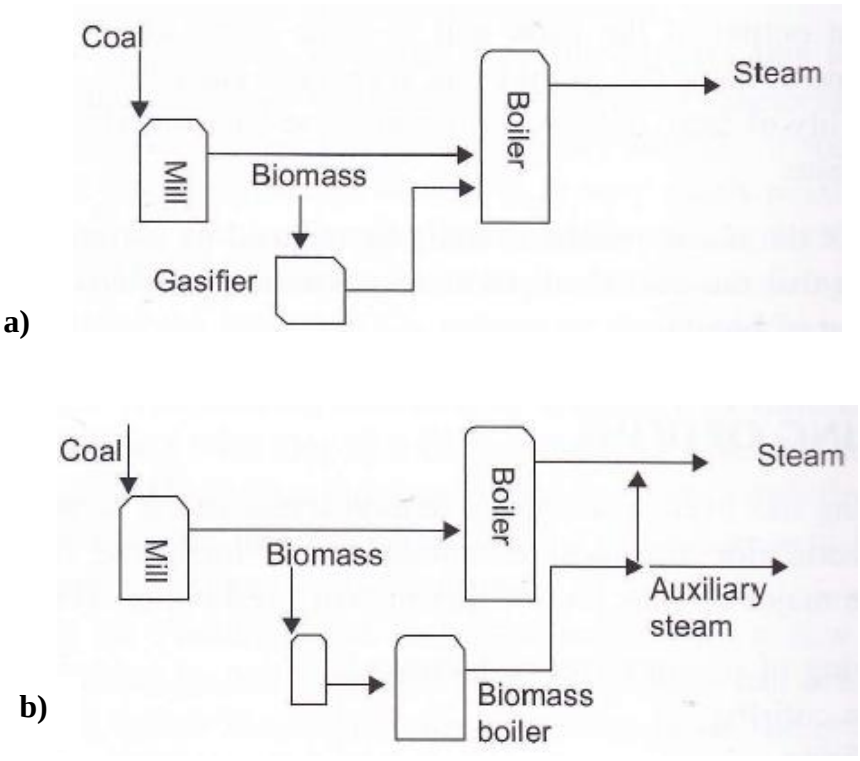

Figure 1.19. Options for co-firing in a coal-fired boiler, where a) represents indirect co-firing and b) parallel co-firing (Basu, 2013).

1.13 Problems of biomass as a renewable source of energy

Biomass is known as the world's fourth largest energy resource after oil, coal and gas. It is also one of the most economical of all renewable technologies to construct compared to wind, solar and tidal power generations. Furthermore, biomass is readily available and plentiful. It has been estimated that sources of biomass could be enough to supply the world with 10-20% of its primary energy requirements by 2050 (Drax, 2011). However, there are a number of

areas that needs to be put into consideration before setting this fuel to a larger scale and placing it as one of the sustainable sources of energy (Bergman *et al*., 2005a), which in turn leads to the necessity for pre-treatment processes. IEA (2013b) has recently provided a report on the "Health and Safety Aspect of Solid Biomass Storage, Transportation and Feeding". Risks are identified that are associated with self-heating, off-gassing and dust explosions. Various accidents have already happened and led to production loss, capital investments and even loss of life (IEA, 2013b). These risks will be briefly reviewed in this section followed by the behaviour of biomass fuels with respect to entrained fuel-gasification and co-firing.

a) Self-heating

Self-heating is described as the first step that initiates a spontaneous combustion (IEA, 2013b). The report pointed out that when materials are milled, they are prone to three reactions, that is heat generating processes from biological metabolic reactions (microbiological growth), exothermic chemical reactions (chemical oxidation) and heat-producing physical processes (for example moisture absorption). The degree as to which these processes take place depends on various factors for example moisture content. Biomass is well known for its hydrophilic nature. Its total moisture content can vary up to 60% depending on the type of biomass. Even if the biomass is dried, it still has the tendency to reabsorb moisture quickly from the atmosphere, provided that they are stored outdoor. Long term storage can be problematic as excess moisture allows microbial respiration activity to take place and leads to self-heating. It is advised to avoid storage in piles if the material's tendency of self-heating is not known. Furthermore, storing biomass with moisture contents of 15% (wet basis) should be avoided and limited duration of storage is recommended.

b) Off-gassing from lignocellulosic biomass

Off-gassing refers to the emission of volatiles from wood pellets along the supply chain. Volatiles consist of condensable gases such as aldehydes, ketones, low molecular carboxylic acids and terpenes. It was reported that such emissions are released during high temperature drying and can lead to further reactions during storage such as hydrolysis and oxidation. Non-condensables also emit during storage such as carbon monoxide, carbon dioxide and methane. Some of these gases are flammable and can be toxic at certain concentrations. Carbon dioxide, for example, can reduce the oxygen level of the storage room and can cause health risks.

c) Dust and gas explosions

IEA (2013b) discussed that for a dust cloud explosion to occur, there are five factors that need to be present. Factors include dispersion of dust particles, containment of dust cloud, ignition source, combustible dust and oxygen. There are several regulations that have been introduced and they differ in countries. In Europe, "Atmospheriques Explosives (ATEX) regulation is an implementation of Directives issued by the European Union and this is a mandatory since July 2003. In America, NFPA guidelines are used, which are intended to eliminate the risks. The IEA (2013b) report described the ATEX and NFPA in more detail.

d) The behaviour of biomass in coal mills

With regards to entrained-flow gasification and co-firing purposes, this issue is related to the grindability of the biomass. Biomass is so tenacious and fibrous that coal mills are not able to be utilised effectively. It also consumes high energy for example, when using hammer mills. Mucsi (2008) reported that 5% of the total energy consumption of developed countries is used for crushing and pulverising materials such as biomass. Currently, biomass derived pellets are used for co-firing but they are expensive and require costly storage facilities to avoid the deterioration of those pellets. Hardgrove Grindability Index (HGI) is developed as an empirical test or a predictive tool and commonly used to determine the milling capacity of pulverisers to grind materials to a particle size that is necessary for an effective combustion (Rubiera *et al*., 1999). The rule of thumb is that the higher the HGI value, the easier the grinding. Mani *et al* (2004) reported that the energy consumption to mill biomass depends on the biomass's particle size, moisture content and properties. Moisture content is an important factor during the milling. As what the authors concluded, "*the higher the moisture content, the higher the specific energy consumption*".

1.14 Biomass pre-treatment technologies

Biomass fuels are usually prepared in some way prior to being used in energy conversion processes (Murphy *et al*., 1996). There is no specific technology that can serve all production plants. In other words, the effectiveness of a pre-treatment depends on the type of feedstock (hardwoods, softwoods, herbaceous crops, agricultural residues) being processed (NNFCC, 2009). A number of pre-treatment methods that aim to reduce the problems associated with biomass have been developed to improve the energy conversion efficiency. Pre-treatment of biomass refers to a number of technologies, which can modify the biomass either by

changing the content of hemicellulose, cellulose and lignin or the characteristics of the biomass to improve its efficiency (NNFCC, 2009).

According to NNFCC (2009) and Harmsen *et al* (2011), some of the pre-treatment technologies comprise of:

a) mechanical pre-treatment, which aims to reduce the particle size of biomass and such treatments include milling, chipping and grinding. This type of approach is often required to make the handling easier and to increase the surface:volume ratio. Densification is the other pre-treatment to overcome problems like high transportation cost. This process can reduce storage problem, improve transportation and energy efficiency,

b) thermal pre-treatment, for example, drying that are used in gasifiers and combustion equipment (Murphy *et al*., 1996). Drying produces a more homogeneous fuel and this aids in controlling the process (Murphy *et al*., 1996),

c) chemical pre-treatment involves destruction of the biomass that is initiated by chemical reactions. Such treatments are (i) acid-based to allow the breakdown of lignin and hemicellulose to access the cellulose using mineral acids and (ii) alkali-based to induce the breakdown of bonds, which link hemicellulose to lignin using calcium hydroxide, and

d) biological pre-treatment that make use of enzymes from bacteria, fungi and other microorganisms to break down the hemicellulose and lignin fraction of the biomass. This treatment requires low energy and mild conditions but the progression is usually very slow.

1.15 Torrefaction

Torrefaction is one of the thermal pre-treatment technologies. It comes from the French word '*torrefier'*, which means to roast coffee. Torrefaction was first practiced in France in the 1930s to develop a suitable gasifier fuel from biomass. Unfortunately, the markets did not see any economic value to the product until in the 1980s when the oil prices went up that it was then recognised as a suitable reducing agent for metallurgy industries (Essendelft *et al*., 2013). Pechiney, a French company, conducted a demonstration plant using an indirectly heated screw reactor and had an output capacity of 12000 tons per year of torrefied biomass (Bergman *et al*, 2005a). Unfortunately, the plant faced problems, which forced it to close

down in the early last decade. For the last ten years, there has been a growing interest in torrefaction due to the advantages it can serve as a very useful technology to pre-treat biomass, which will be briefly discussed in Section 1.18. In a number of exploratory studies, torrefaction is normally tested using either thermogravimetric analysis equipment or small scale reactors (Bridgeman *et al*., 2008; 2010; Medic *et al*., 2012; Phanphanich & Mani, 2011). Torrefaction work has also emerged to large pilot scale units for example in Reuter West power plant, Berlin by Vattenhall, where 4300 tonnes of torrefied biomass were co-fired in 2011 and 60,000 tonnes of it were produced in Topell, The Netherlands per year in 2012. More companies are interested in doing such demonstrations and they are listed in the later sections. For now, it can be said that these large scale trials are still under development and with that, information and experience on storage, conveying and handling is still not sufficient.

1.15.1 Definition of torrefaction

Torrefaction is a thermochemical treatment at a temperature range above 200°C up to 300°C under nitrogen or inert atmosphere. This process is normally characterised by a slow heating rate (as slow as 5°C min^{-1}) at a desired residence time (typically 10-60 min). This approach is able to retain approximately 70% of the initial biomass weight and about 80-90% of the biomass's original energy content (Lipinsky *et al*., 2002; Pentananunt *et al*., 1990). 30% of the mass is converted to volatiles and 10-20% of the energy content is contained in the torrefied gases (Bergman *et al*., 2005a).

Coal has had prolonged use in energy production because of its higher energy density and its ease of production and transportation at a low cost compared to biomass. It has a lower O:C ratio, which results in a higher calorific value. McKendry (2002) clearly explained that the higher proportions of oxygen and hydrogen compared with carbon in a biomass than coal reduces the energy value of the biomass fuel. However, torrefaction has the solution to this problem. Upon this treatment, literature reviews such as Bridgeman *et al* (2008) and Sadaka and Negi (2009) have shown that the torrefied biomass contains a lower amount of oxygen and hydrogen, which in turn, improves the calorific value and has similar compositions as that of low-rank coal such as lignite.

1.15.2 Differences between carbonization, pyrolysis and torrefaction

Carbonization, pyrolysis and torrefaction are the three processes that involved thermal degradation of biomass and sometimes can be confusing. Their main difference is the product of interest. Basu (2013) mentioned that the objective of pyrolysis is to maximize the liquid production and minimize the char yield. Carbonization is aimed to maximize fixed carbon and minimize hydrocarbon content of the solid product, while torrefaction is aimed to maximize energy and mass yields of the solid product that also contains low O:C and H:C ratios (Basu, 2013). Moreover, even though carbonization is similar to torrefaction for example in terms of heating rates, there are some important differences between the two. Carbonization involves high temperature (> 300°C) and drives away most of the volatiles, while torrefaction retains them and only drives away the low energy density volatiles (Basu, 2013). In addition to that, carbonization requires a certain amount of oxygen that allows sufficient combustion for heat supply and torrefaction would prefer to take place in an inert environment.

1.15.3 Process diagram (Heat Integration)

Figure 1.20 illustrates the basic concept of torrefaction and how thermal energy required for drying and torrefaction can be implemented in three ways as described in IEA (2012a):

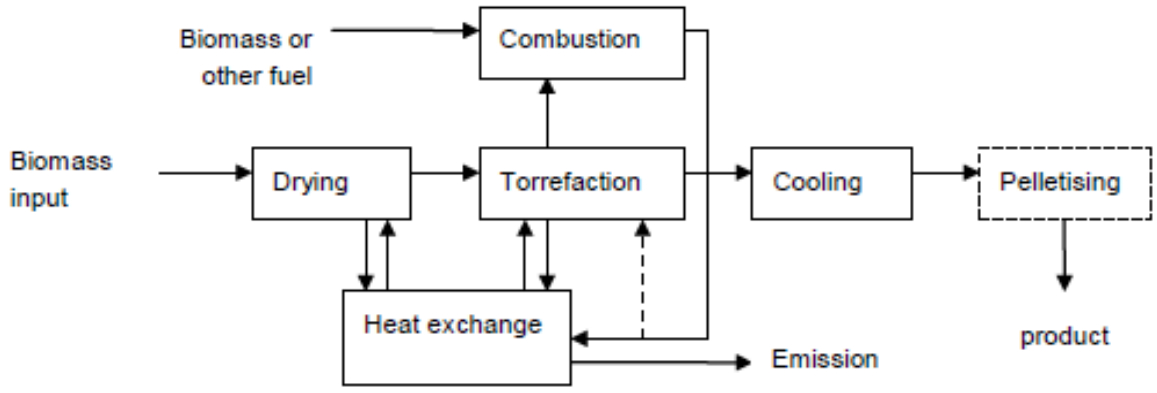

Figure 1.20. Overview of heat integration options (IEA, 2012a).

1) "*Recirculation of the flue gas to directly heat the torrefaction process*"

This option involves the efficient transfer of heat from the flue gas directly to the biomass. However, the gas may contain a high volume of oxygen that will reduce the efficiency of torrefaction. The other advantage to this option is the requirement of high investments for flue gas pipes in case of recycling large volumes of flue gases.

2) "*Recirculation of the torrefaction gas to directly heat the torrefaction process*"

The way the heat is transferred is similar to option 1. But the volume of torrefaction gas is smaller than flue gas, which makes the recycling more compact. However, torrefaction gas contains various amounts of organic products, therefore, recycling it will increase the concentration of the organics, leading to accumulation of tars.

3) "*Recirculation of supercritical (steam) to directly or indirectly heat the torrefaction process*"

Here, the steam is obtained from the boiler that is fired with torrefaction gas. Since the gas is now saturated with moisture (from steam), it has a lower calorific value and leads to inefficient combustion of volatiles. If the steam flow is contaminated by volatiles and tars, these mixtures can condensate and may lead to corrosion and fouling of equipment. If it is indirectly contact with biomass, there is a risk of carbonisation and heat may be transferred inefficiently.

1.15.4 Torrefaction reaction

According to Bergman *et al* (2005a), the following are five main stages that take place in the torrefaction reactor (Figure 1.21), while Basu (2013) described each stage in relation to the energy required, Q.

1) *Initial heating*

This is when the biomass starts to heat up from room temperature and evaporation of moisture takes place. The energy required, Q_{ph} is $M_f C_{pw}$ $(100 - T_0)$. Heat may be lost from the drier, hence, the heat required can be represent as Q_{pd}, where

$$Q_{pd} = \frac{M_f C_{pw} (100 - T_0)}{h_{upd}} \qquad (1.1)$$

where, C_{pw} is the specific heat of biomass (as received), M_f is the mass of the raw biomass and T_0 is the feed temperature. h_{upd} is the heat utilisation efficiency factor of the system to account for the heat loss.

2) *Pre-drying*

Temperature rises to above 100°C and allowed the release of the water content from the biomass at a constant rate. This is usually done in approximately 60 min. In Basu (2013), the energy required for this stage is defined as Q_d, that is LM_fM. If the heat utilisation efficiency of the dryer section, h_{ud} is taken into account, the energy required is

$$Q_d = \frac{LM_fM}{h_{ud}} \quad (1.2)$$

where, L is the latent heat of vapourisation (~2260 kJ kg^{-1}) of water at 100°C and M is the moisture fraction of the biomass (as received).

3) *Post-drying and intermediate heating*

The biomass is assumed to be free of moisture. Some mass loss is expected, which is not only from the loss of moisture but also from the release of light volatile organic compounds due to the degradation of hemicellulose. The energy (Q_{pdh}) demand at this stage is relatively low because it only requires heat that is sufficient to the drier biomass.

$$Q_{pdh} = \frac{M_f\,(1\text{-}M)\,C_{pd}\,(T_t\text{-}100)}{h_{u,\,pdh}} \quad (1.3)$$

where, C_{pd} is the specific heat of the dry biomass, $h_{u,\,pdh}$ is the heat utilisation efficiency and T_t is torrefaction temperature.

4) *Torrefaction*

When temperature reaches 200°C, torrefaction starts. In general, hemicellulose is the most reactive component, followed by lignin, and cellulose is the most thermostable (Bergman *et al*., 2005a). Devolatisation and decarbonisation of hemicellulose mainly take place at lower torrefaction temperature. At higher temperature, hemicellulose extensively decomposes into volatiles. Lignin and cellulose often show limited devolatisation and decarbonisation.

The degree of torrefaction depends on the desired reaction temperature and the time the biomass is subjected to torrefaction (residence time). The energy required is defined as Q_{tor},

$$Q_{tor} = H_{loss} + M_f\,(1\text{-}M)X_t \quad (1.4)$$

where, X_t is a factor that determines the amount of heat absorbed during torrefaction. H_{loss} is the amount of heat loss to the atmosphere from torrefaction that is a function of reactor design.

5) *Solid cooling*

When a desired residence time is reached, the solid is allowed to cool to below 200°C or room temperature, during which at this period, there will be no occurrence of further mass loss. The extracted energy, Q_{cool}, may be in the form of hot air or vapourised liquid such as steam, which could be used to provide energy for drying or pre-heating the biomass.

$$Q_{cool} = M_f (1 - M) MY_{db} C_{pt} (T_t - T_p) \quad (1.5)$$

where, T_t is the torrefaction temperature, T_p is the desired final temperature, MY_{db} is the mass yield of the biomass after torrefaction and C_{pt} represents the specific heat capacity of the torrefied biomass.

It is important to note that the reactor's residence time is often mistaken with the reaction time of torrefaction. Figure 1.21 clarifies this confusion, in which the reaction time covers $t_{tor,h}$ and t_{tor}, where $t_{tor,h}$ is the heating time for torrefaction from 200°C to the desired final temperature and t_{tor} is the reaction time at the desired temperature (Bergman *et al*., 2005b).

Bergman *et al* (2005a) defined a set of temperature regimes comprising of four stages of decomposition that take place during the torrefaction process as can be seen in Figure 1.22. The figure also shows the torrefaction temperature regime, where the blue line splits it into a low and high temperature regime (Bergman *et al*., 2005a). In general, hemicellulose is the most reactive component, which is the dominant one that is responsible for the mass loss during this process. The stage labelled A is the drying period, where the release of most of the moisture content takes place. The stage labelled B occurs in lignin, where the softening of this component occurs. Bergman *et al* (2005a) commented that this stage gives densification to the biomass as the softened lignin makes a good binder. The stage labelled C is where the temperature increases. This is when some parts of the hemicellulose started to decompose, releasing low molecular weight volatiles. In relation to this regime, cellulose and lignin may undergo minor decomposition but this does not cause any much effect on the mass loss. Increasing the temperature above 200ºC, entering to the stage labelled D is when further

devolatisation due to more decomposition of hemicellulose occurs. At even higher temperature above 250ºC, leads to a more extensive devolatisation and carbonisation to the hemicellulose. Cellulose and lignin continue to experience slower degradation over a wider temperature range than hemicellulose.

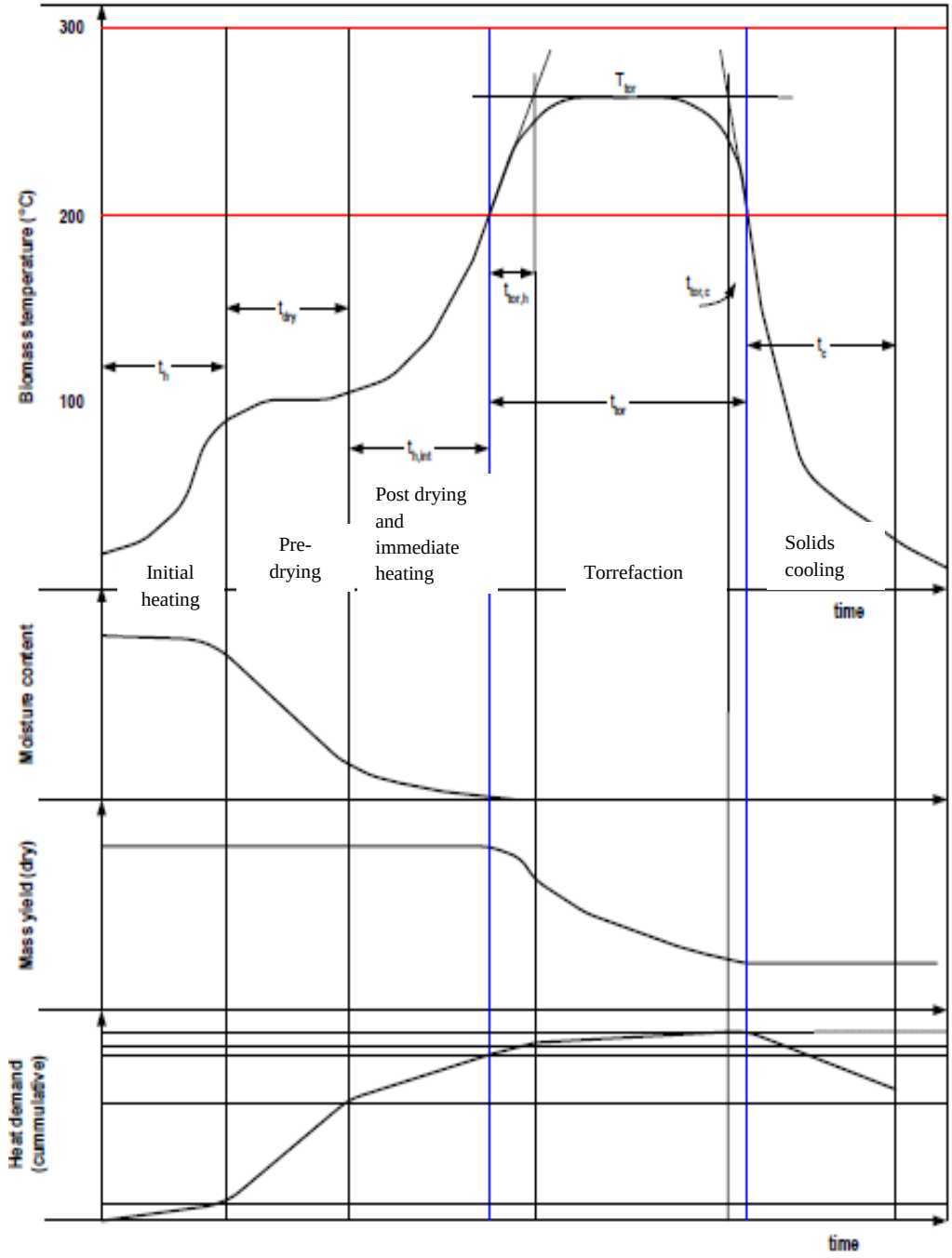

Figure 1.21. Processes involved in the reactor (Bergman *et al*., 2005a).

1.16 Mass and energy balance

Figure 1.23 illustrates the typical mass and energy balances of torrefaction of biomass as presented in Bergman *et al* (2005a). A considerable energy densification can be achieved via torrefaction when 70% of the mass yield and about 80-90% of energy yield can be retained (Bergman *et al*., 2005a). 30% of the mass is removed in the form of volatiles (torrefaction gases, where some would call it 'torgas'), which contain 10-20% of the energy content of the biomass. IEA (2012a) stated that the energy contained in the torgas can be used to drive off moisture in the dryer. Prins *et al* (2006a) provided a mass and energy balances for torrefaction of willow as shown in Figure 1.24. Temperature plays a more of a significant role in torrefaction than residence time. The figure shows that even though the residence time is set longer in Figure 1.24 a), increasing the temperature still produces a lower mass yield of biomass (67%) as seen in 1.24 b). Moreover, increasing the temperature releases more volatiles. This results in a lower energy balance, where 95% and 79% of the respective energy input is retained in the torrefied biomass.

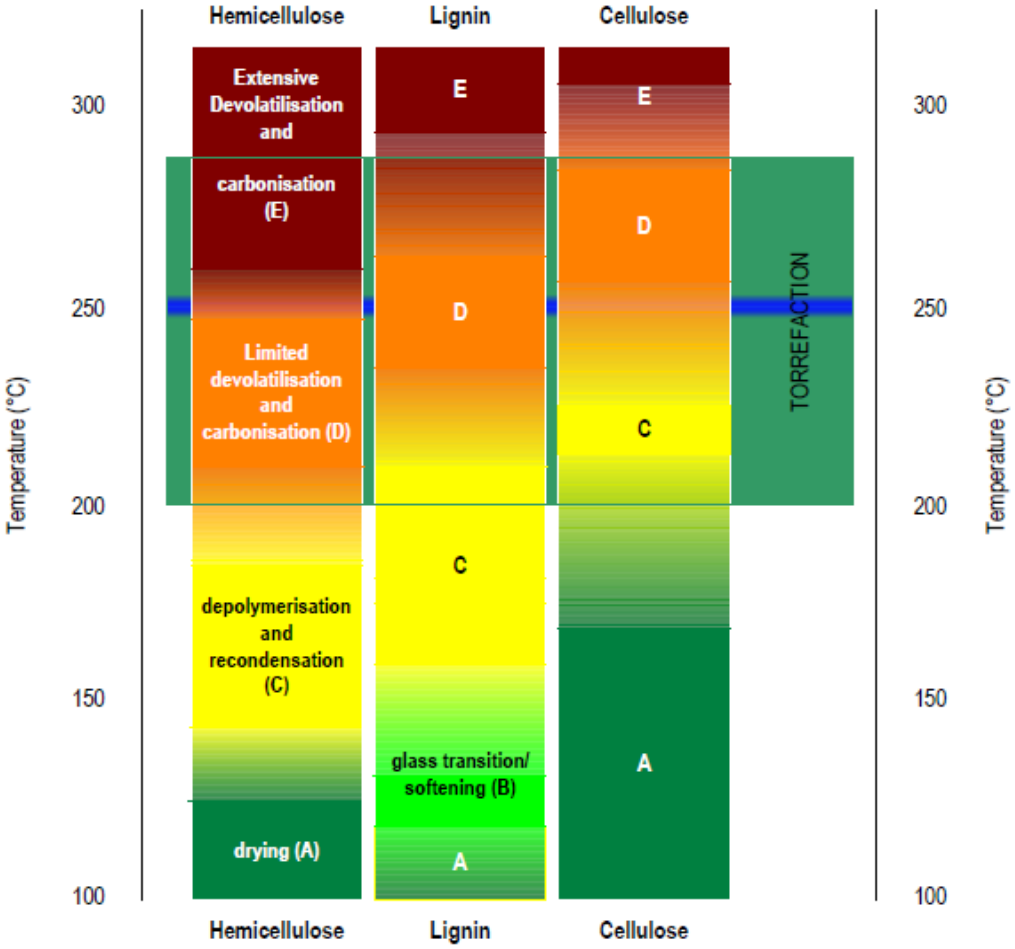

Figure 1.22. Main physico-chemical reactions during the heating of lignocellulosic components at torrefaction (Bergman *et al*., 2005a).

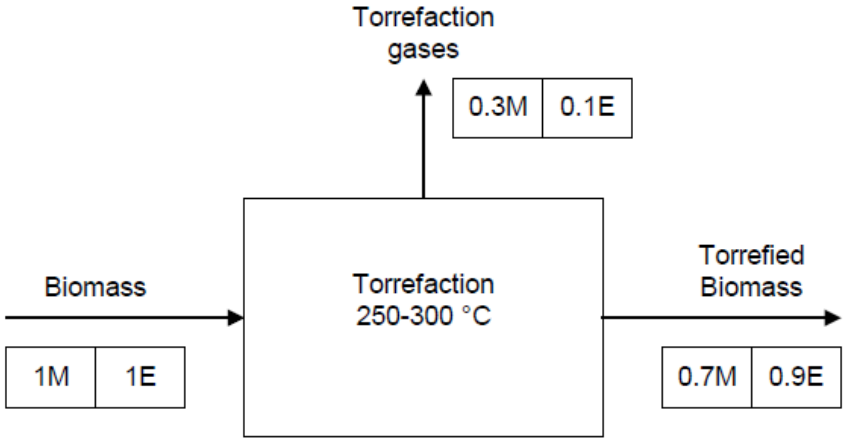

Figure 1.23. Mass and energy balance of the torrefaction process, where E and M represent the energy and mass units (Bergman *et al*., 2005a).

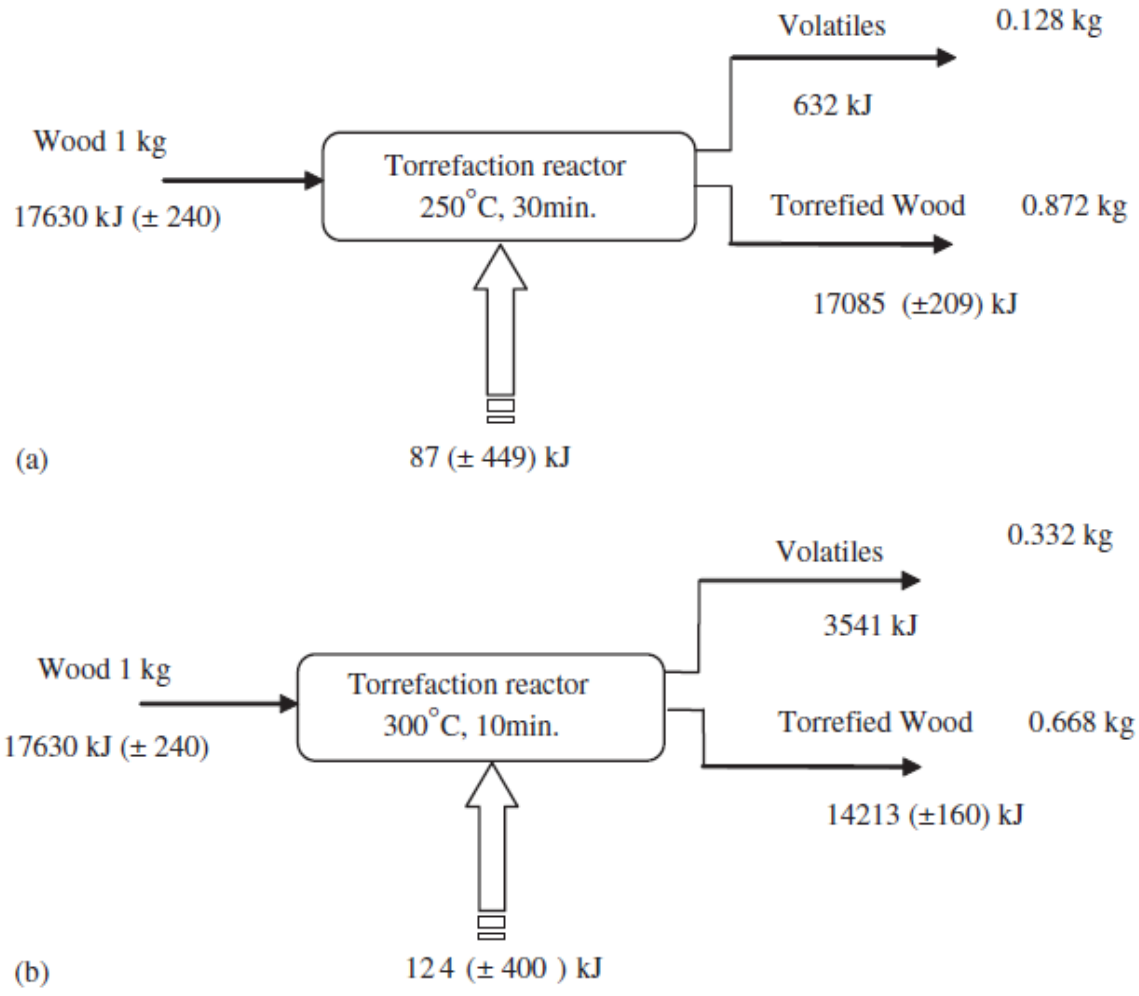

Figure 1.24. Overall mass and energy balances of torrefaction of willow at temperature and residence time of a) 250°C and 30 min and b) 300°C and 10 min (Prins *et al*., 2006a).

1.17 Torrefaction approaches

1.17.1 Fixed bed torrefier

Fixed bed torrefier is used in a laboratory-based and bench scale in carrying out torrefaction of biomass that comes in large particle sizes (that have diameters of bigger than 1 cm). Laboratory-based scale torrefaction usually consists of the torrefier (furnace), which is equipped with thermocouples that are arranged at different heights and connected to a temperature controller in order to measure and monitor the temperature inside the biomass bed and reactor as clearly can be illustrated for example in Figure 1.25.

Inert gases such as argon (Prins *et al*., 2006a) and nitrogen (Pentananunt *et al*., 1990; Bridgeman *et al*., 2010; Chen *et al*., 2011; Phanphanich and Mani, 2011; Wannapeera *et al*., 2011; Medic *et al*., 2012) were continuously supplied inside the reactor in a controlled manner by a valve and flowmeter to eliminate oxygen and hence, to avoid oxidation and ignition (Bridgeman *et al*., 2010; Phanphanich and Mani, 2011). After torrefaction, the torrefied biomass will be taken out of the furnace for cooling as to stop the thermal process. Apart from that, during torrefaction, volatiles are also released. Hence, determination of such products may be of interests in some studies. At the other end of the reactor, where volatiles evolved, are condensers that are immersed in cold water bath to collect any potential condensables as shown in Figure 1.26 (Phanphanich and Mani, 2011; Wannapeera *et al*., 2011). Non-condensables are usually collected in a gas bag and immediately injected to a gas chromatography (Wannapeera *et al*., 2011). Some studies would use flasks to collect liquids and gases as illustrated in Figure 1.27 (Chen *et al*., 2011).

1.17.2 TG-FTIR

The TG-FTIR is another laboratory-based approach that comprised of a thermogravimetric analyser (TG) coupled with a Fourier-Transform Infra-red (FTIR) spectrometer, which are aimed to analyse evolved volatiles. TG-FTIR was first developed at Advanced Fuel Research, Inc (AFR), USA for the study of slow pyrolysis of coal and biomass. Volatiles that can be measured include carbon monoxide, carbon dioxide, water, methane, ethylene, formaldehyde, acetaldehyde, formic acid, acetic acid, methanol, hydrogen cyanide, ammonia, acetone and phenol, while tar can be determined by difference.

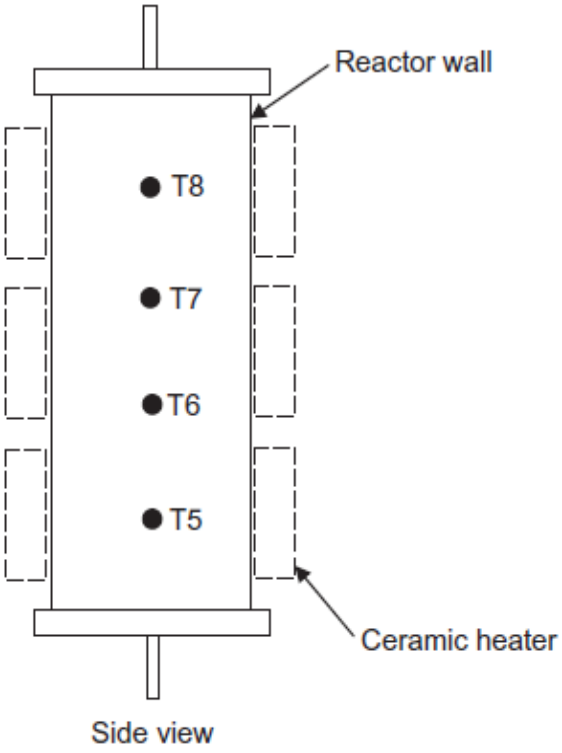

Figure 1.25. The arrangement of four thermocouples (T5, T6, T7 and T8) inside a reactor for temperature control (Phanphanich and Mani, 2011).

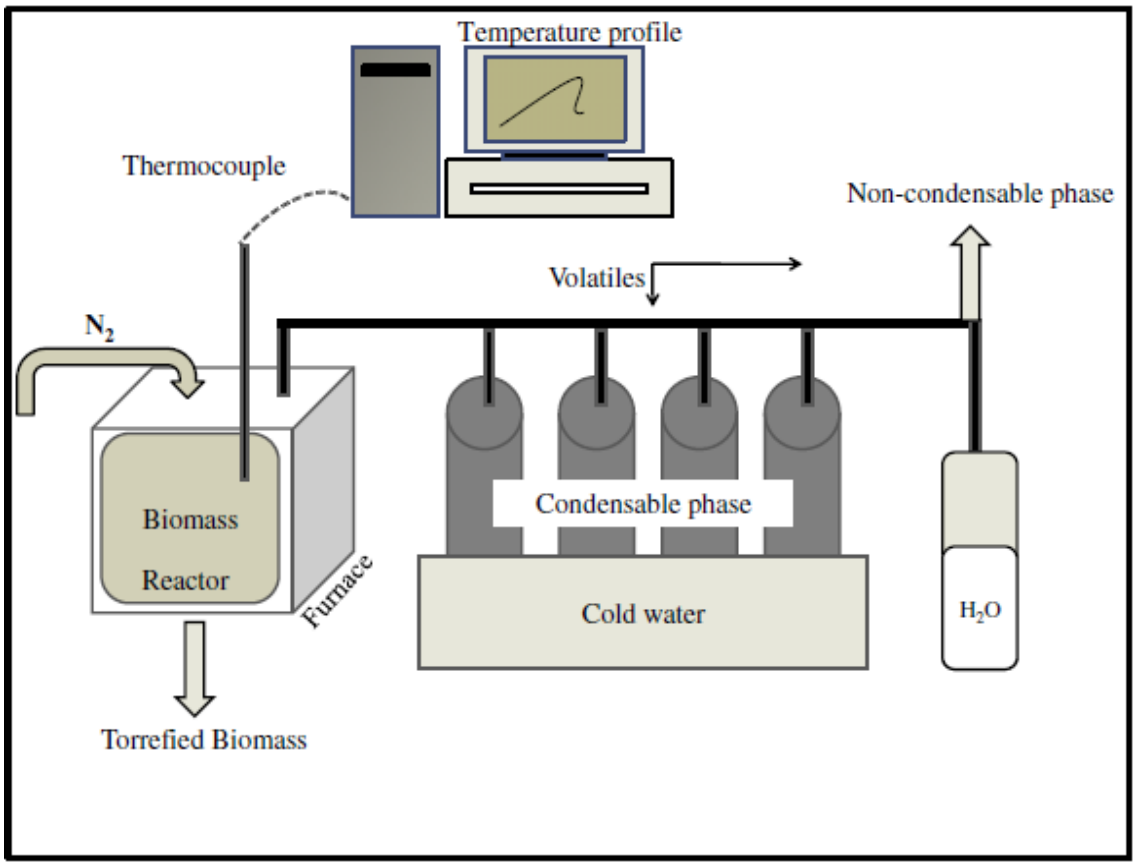

Figure 1.26. Laboratory torrefaction unit as illustrated in Phanphanich and Mani (2011).

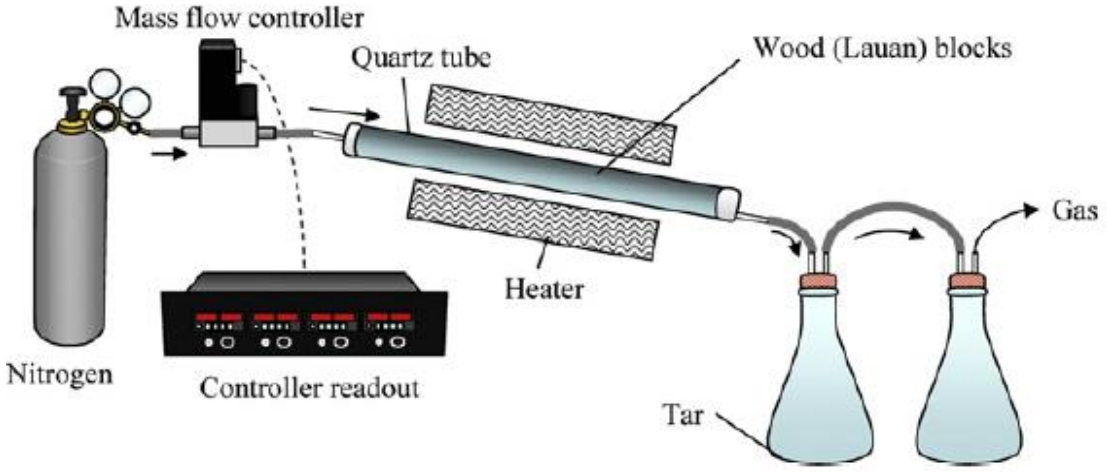

Figure 1.27. A schematic diagram of torrefaction experiment as set up in Chen *et al* (2011).

1.17.3 Model development

When biomass is treated with pyrolysis, significant amounts of fixed nitrogen species, namely ammonia and hydrogen cyanide, are released from biomass-bound nitrogen (de Jong *et al*., 2003). These species may oxidised and form pollutant species, nitrogen oxides (Leppälahti and Koljonen in de Jong *et al*., 2003). de Jong *et al* (2003) suggested that the knowledge of nitrogen evolution from biomass pyrolysis needs to be well understood in order to reduce such harmful emissions. Solomon *et al* (1991) reported that due to the lack of data, together with the large variety and huge diversity of biomass feedstocks, it is difficult to deal with modelling the emission behaviour of biomass thermal conversion processes. Hence the introduction of FG-Biomass model as studied in de Jong *et al* (2003).

Before FG-Biomass model, FG-DVC model, which stands for Functional Group–Devolatilisation, Vaporisation, Cross-linking was first developed by the AFR (Solomon *et al*., 1987; 1991; de Jong *et al*., 2003). This model functions to predict the distribution of products from coal thermal decomposition. The FG is used to describe the evolution of volatiles and compositions of the elemental and functional groups, while the DVC is applied to quantify macromolecular fragments (de Jong *et al*., 2003). This model was then extended for biomass. de Jong *et al* (2003) stated that there are two differences in these models. One is where FG-Biomass favours the evolution gas and tars and de-emphasises DVC. Second is where tar is treated as volatiles in biomass, while in FG-DVC Biomass model, tar competes for the precursor material with gaseous species.

FG-Biomass is a pyrolysis model that is developed by the AFR. Wójtowicz *et al* (2011) stated that FG-Biomass model considers biomass as those that contain functional groups within the main polymers, namely cellulose, hemicellulose and lignin, which thermally degrade via torrefaction and form volatiles. This model also can predict the yields and compositions of solids, liquids and gases from torrefaction that can be carried out at different parameters (temperature and residence time) and recently, particle sizes (Wójtowicz *et al*., 2011).

1.18 Applications of torrefied biomass

Upon treatment, torrefied biomass has improved characteristics, especially in terms of grindability, hydrophobicity and energy density, which will be elaborated in Chapter 3. These values give positive impacts on transportation and storage. As a result, torrefied wood can be made suitable for a number of industrial applications. Chapter 3 examines the research in torrefaction but some applications are worthy of highlighting here.

1) Entrained-flow gasification (EFG)

One major challenge in entrained-flow gasification of biomass is the size reduction. Bergman *et al* (2005b) reported that torrefaction provides solutions to problems that concern with EFG. The biomass has lost its tenacity with torrefaction, making pulverisation easier and improved fluidisation behaviour when introduced to the EF gasifier. Torrefied biomass produces a smooth fluidisation regime when tested using a feeding system. A good fluidisation quality and a positive gasifier performance can be achieved if there is no gas bubbles formed when the bed of particles is aerated (Bergman *et al*., 2005b). Bergman *et al* (2005b) stated that the absence of gas bubbles creates a continuous flow of fuel particles to the stationary flame present in the entrained-flow gasifier and a biomass that is torrefied does that. Furthermore, torrefaction provides an advantage to EFG in terms of transport and storage due to the improved hydrophobicity of the biomass (Bergman *et al*., 2005b).

2) Production of biopellets (densification by means of pelletisation)

Densification of biomass by means of pelletisation (producing biopellets) improves the purpose of biomass for heat and power (Bergman, 2005). Biopellets are made up of small particles and can be easily crushed in mills. However, to make biopellets are expensive and requires great care because these pellets are vulnerable to water. Bergman (2005) studied the combination of torrefaction and pelletisation process (TOP). The mechanical strength of

torrefied pellets was assessed using crushing tests and the results showed that the torrefied pellets can withstand about twice the force exerted compared to conventionally produced pellets before breakage. Bergman (2005) explained that the change in the chemical structure of the biomass during torrefaction leads to the formation of more lignin content by 10-15% and this acts as the binding agent. Hydrophobicity of pellets was also examined via water immersion for 15 hrs. Pellets of untreated biomass showed rapid swelling while torrefied pellets did not experience such behaviour. In conclusion, TOP process produced high quality biopellets and has great economical potential in comparison to conventional biopellets.

3) Co-firing of biomass

Carbon dioxide emissions from coal-fired power station can be reduced by co-firing with biomass in these existing power stations (Bergman *et al*., 2005a). However, there are issues arise due to the differences between the nature of coal and biomass. Biomass is well-known for its fibrous nature and tenacity to grind to produce powders that can be burned in a coal-fired power station. In Netherlands, power stations are currently utilising conventional biopellets, which are not only expensive but also has limited availability and this creates further problem. When torrefaction is applied, grindability is improved, providing an advantage for co-firing purposes. Fuel handling is now not a problem as the addition of torrefied biomass into the feeder system is able to improve the mill capacity. The fuel quality of the torrefied biomass is also offering advantages to co-firing. The chemical composition is more comparable to that of coal, making them to have a similar caloric value. Moreover, torrefied biomass has a very limited water uptake due to the destruction of O-H groups in the biomass. Briefly, torrefaction is an attractive technology that can contribute to the increase of biomass co-firing rates in the existing coal-fired power stations (Bergman *et al*., 2005a).

1.19 Status of torrefaction

For the past five years, there has been a significant increase of interest in torrefaction as a pre-treatment technology for biomass fuels. In 2012, there are at least 40-50 torrefaction initiatives that have been identified in Europe and North America (IEA, 2012a). Most of these installations aim to demonstrate the technical and feasibility of torrefaction as a feasible pre-treatment option. Some would require several thousand tonnes of fuel for large commercial scale tests, where only a few seemed promising. Even though there is still no winning technology identified, there will be several viable torrefaction technologies capturing

the market over time (IEA, 2012a). Due to confidentiality and the high commercial interest, it is not easy to obtain data that are up-to-date and reliable.

Reactor technologies were modified to perform torrefaction and the important ones, with the companies involved, with specific type of torrefaction reactor they use are listed in Table 1.4. According to Dhungana *et al* (2012), the reactors can be classified into two categories: directly heated and indirectly heated. Directly heated reactors allow heat to be directly in contact with the biomass. The heating media can be a hot gas, hot solids, superheated steam or electromagnetic radiation. Indirectly heated reactors do otherwise but one disadvantage is the inconsistency of heating the biomass in the reactors.

1.19.1 Directly heated reactors

Convective reactor is the most common reactor used for torrefaction. The hot gas that passes through the biomass may be completely inert or contains a low level of oxygen. In a fixed bed reactor, the particles are stationary while in a moving bed, the particles move either by gravity or force of a mechanical device like augur. These particles move with respect to the wall of the reactor that can be horizontal, vertical or inclined (Dhungana *et al*., 2012). The heat transfer is usually through solid-gas convection. Fluidized bed involves the flow of gas through a bed of granular heat carrier solids. These heated solids are able to heat up fresh biomass fuels that dropped amongst them. The dominant heat transfer is particle-to-particle and the transfer is higher than that in convective bed. Microwave is also another directly heated type of reactor. It uses microwave irradiation and a typical microwave oven/reactor usually works at 2.45 GHz. Microwave reactor is different from other directly heated reactors, where the former heats the biomass from within while the latter heats the biomass externally.

1.19.2 Indirectly heated reactors

Rotary drum involves heat transfer from the hot drum wall to the biomass. Dhungana *et al* (2012) described that this type of reactor does not need to be oxygen free and that the volatiles are not diluted by the gas passing through it. In screw or stationery shaft, the torrefaction reactor is stationery. The rotating screw moves the biomass through the reactor and along its length. The heat transfer is similar to that in the rotary drum where the hot outer wall of the reactor heats the biomass indirectly.

Table 1.4. Overview of reactor technologies and some of the associated companies (IEA, 2012a).

Reactor technologies	Companies involved
Rotating drum	CDS (IK), Torr-Coal (NL), BIO3D (FR), EBES AG (AT), 4Energy Invest (BE), BioEndev/ETPC (SWE), Atmosclear S.A. (CH), Andritz, EarthCare Products (USA)
Screw reactor	BTG (NL), Biolake (NL), FoxCoal (NL), Agri-tech Producers (US)
Herreshoff oven / Multiple Hearth Furnace	CMI-NESA (BE), Wyssmont (USA)
Torbed reactor	Topell (NL)
Microwave reactor	Rotawave (UK)
Compact moving bed	Andritz/ECN (NL), Thermya (FR), Buhler (D)
Belt dryer	Stramproy (NL), Agri-tech Producers USA)
Fixed bed	NewEarth Eco Technology (USA)

Dhungana *et al* (2012) provides a quantitative comparison of four different types of reactors (convective heating type reactor, fluidised bed reactor, rotary drum reactor and microwave reactor) and examined how each reactor could affect the quality of the biomass in terms of mass yield, energy yield and energy density. They found out that the rotary drum reactor yields torrefied biomass that has the highest energy density, however the lowest mass and energy yield in comparison to convective and fluidised bed reactors. Since microwave reactor heats the biomass internally, the authors discovered that the core of the biomass heated very fast but the surface remained cold. The biomass experienced a large non-uniform heating, where the core was over-torrefied and the exterior remain unaffected.

In the development of torrefaction technologies, the goal is to produce a torrefied biomass fuel that can be converted to pellets or briquettes that can be handled and are durable enough to be stored outside and withstand the weather conditions. For large scale handling, this is still remains to be proven. There are also challenges with the torrefied biomass fuel in terms of difficulty to compact and dust from the torrefied fuel is active and prone to explosion in high concentrations. With regards to outdoor storage and leaching, the concerns are yet to be dealt with. Environmental impact due to leaching from outdoor storage must be well

understood. Dhungana *et al* (2012) discussed that at this stage, there is no commercial market that is fully developed for torrefied biomass, so the price is still uncertain. Torrefaction projects are largely based on clean biomass resources such as clean waste wood. Seems like waste streams and residues have gain attention as feedstock for torrefaction due to their low prices and high availability. However, they have unfavourable chemical compositions, concerns like ash fouling, emissions and efficiency that need to be resolved. Regulators may have to discuss with the energy producers on how waste derived torrefaction fuels could be used in existing facilities.

"*Product quality standards and specific test methodologies for torrefied materials are currently under development by ISO Technical Committee 238, expected to be published during spring 2013 as part of the ISO 17225 Standard, and criteria for sustainability is under development by ISO / PC 248*" (IEA 2012a). Furthermore, since torrefied biomass fuels have similar characteristics as those of low rank coals, safety classification under International Maritime Organisation (IMO) is required especially if they are to be transported by ocean vessels.

1.20 Overview of project initiatives

Developers, who are involved in torrefaction initiatives are as follows (IEA, 2012a):

- Topell B.V. (Topell)

Topell B.V. collaborates with TorfTech Ltd, a British company, which owns the Torbed reactor. In Duiven, the Netherlands, the first full scale demonstration plant consists of multiple stacks of Torbed reactors and was built in 2010. It has a production capacity of 60 kton/year and is running at about 65-85% of design capacity in mid-2012.

- Green Investment (SGI)

SGI is a spin-off company of the Stramproy Group and its most important investor is the Belgian company 4Energy Invest, which also develops another torrefaction technology in Amel, Belgium. A construction of torrefaction demonstration plant has finalised in Steenwijk, with a production capacity of 45 kton/year. The installation is based on modified belt dryer, fed with wood and integrated with a biomass combustion based CHP unit. Unfortunately, a fire broke out in February 2012 and re-operated in the summer of 2012.

- Torr-Coal B.V.

Torr-Coal is a relatively small company that developed a rotating drum torrefaction technology. The installation was built in Dilson-Stokkem (Belgium) with a production capacity of 35 kton/year. The company is planning to add two production lines based on Solid Recovered Fuels (SRF), where a washing process is developed to remove chlorine and sulphur contents.

- BioLake B.V.

BioLake is a consortium of the Dutch research organisation ATO and have developed a pilot plant based on a rotating screw reactor with Technical University of Eindhoven. They used 1 ton/hr of straw as feedstock.

- Airex Energy

Airex Energy is a division of Airex Industries that developed Carbon FX technology in Quebec, Canada. There are two stages of drying using hot flue gas and torrefaction takes place in cyclonic reactor. The volatiles produced will be converted to heat and used for drying biomass while the solid end-product will be pelletised. The next developmental step is to scale up the process to 2 ton/hr by the end of 2013.

- Andritz technology

Andritz technology has developed two processes. The Andritz ACB (Accelerated Carbonised Biomass) technology is intended for production capacities of 50,000-250,000 tonnes of torrefied briquettes per year, while the Andritz ECN technology is intended for that of 700,000 tonnes of torrefied pellets per year.

a) Andritz/ACB torrefaction technology

This torrefaction technology uses woody and herbaceous biomass and the plant is based on rotary drum reactor. The demonstration plant is built in Frohnleiten, Austria since 2011, with an added briquetting capability in 2012.

b) Andritz/ECN torrefaction technology

This technology uses wood chips as feedstock and the processes involve drying of biomass fuels in a conventional rotary drum dryer, followed by torrefaction in a vertical column

torrefier. After torrefaction, the fuel is allowed to cool and later, hammer-milled, ready for palletisation.

- New Biomass Energy

New Biomass Energy is a company that is based in Quitman, Mississippi, USA. They have been producing torrefied woody biomass fuels since 2011 and compact the products to briquettes and pellets. They also have been conducting experiments using *Miscanthus*. The company is currently operating with two parallel reactors, each with a capacity of 2.5-3 t/hr. Two larger reactors are currently in construction, each with a capacity of 6-8 t/hr and will be operational in 2013. There are a few challenges that remain for example, bringing torrefied biomass to clients in an economic and safe manner, torrefied biomass pellets require some weather protection to remain intact, large storage facilities are needed for large volumes of shipment and dusts that are generated are quite explosives especially in high concentrations. At present, the company has a permit to ship thousands of tons of torrefied pellets for test burning in power plants and continues to produce torrefied fuels for future deliveries.

- Earth Care Products Inc.

Earth Care Products, Inc (ECP) is based in Independence, Kansas. Its torrefaction system has a production capacity of 20,000 t/yr. They use rotary drum reactor in conducting torrefaction. After torrefaction, the torrefied fuel undergoes a cooling stage. The cooler consists of a screw conveyer held inside a continuously-circulated water jacket, where the water at ambient temperature, circulated through the jacket. Once cooled, it proceeds to densification.

1.21 Economic value of torrefaction

The economic assessment of torrefaction is based on a case study that was conducted by the Topell Energy (IEA, 2012a). They compared the financial perspectives between torrefied wood pellets and wood pellets and consider all process steps from the biomass resource to the pellet production. All in all, it shows that the production costs for torrefied pellets are higher than those for wood pellets (IEA, 2012a). However, great savings can be achieved in transportation and end use. With that, it was concluded that there could be a business case for torrefaction. Because torrefied pellets have similar characteristics to those of low rank coals, this enables higher co-firing percentages to power plants for torrefied pellets than wood

pellets (IEA, 2012a). Basu (2013) stated that the commercial use of torrefaction is relatively new, therefore, there is only a limited data available on its capital cost.

1.22 Current challenges for market implementations of torrefaction technologies

The information in this section is mainly based on the report obtained from the IEA Bioenergy Task 32 that describes the status of torrefaction technologies (IEA, 2012a).

1.22.1 Technical challenges

a) Flexibility of feedstock

Particle size and moisture content of feedstock are the two main criteria that seemed to limit the flexibility to be used in current developing torrefaction technologies. The accepted particle size is 5-20 mm and the moisture content not to exceed 15% in order to avoid incomplete combustion of wet torrefaction gases and minimise the process residence time. Agricultural residues such as straw have low bulk density and need large reactors, which leads to high capital costs and more difficult to operate. That is why most torrefaction projects use woody biomass instead of those residues.

b) Treatment of torrefaction gases

Torrefaction evolves volatiles such as carbon dioxide, carbon monoxide and other condensable organics such as acetic acid and formic acid. These gases are usually de-dusted using a cyclone before they are released as fuels to dry incoming biomass. Any presence of heavy tars in the gases may condense in the pipework, leading to operational problems. Therefore, insulation of pipework is necessary. Biomass fuels that have high contents of fluorine, chlorine and sulphur, the burner flue gases has to be treated using an activated coal filter or wet precipitator. Clean biomass fuels will have to use dust filters instead.

c) Process control and the quality and consistency of torrefied products

A well-controlled temperature profile and residence time in a torrefier is important to achieve an efficient process and optimal product quality. If the torrefaction process is based on an indirect heating, it will be more difficult to control, resulting heterogeneity in the products.

1.22.2 Macroeconomic challenges

One of the barriers for torrefaction development is when power producers are not willing to take all promoted quality aspects into consideration when negotiating prices (IEA, 2012a). There is no doubt that they are interested in the torrefied fuels but they would prefer to avoid costs for handling and storage as well as that is related to ash processing and the avoidance of NO_x and SO_x emissions. One of the main reasons is that these torrefied fuels have not been standardised in terms of health and safety requirements, milling behaviour, combustion behaviour (IEA, 2012a). With that, large co-firing scale for torrefied fuels is not yet possible. However, recently, a large funded project, 'SECTOR', was introduced to tackle several existing issues that hamper large scale use of torrefied materials (IEA, 2012a).

1.23 Regulatory issues

There is limited experience in issuing environmental permits for torrefaction installations (IEA, 2012a). No extensive environmental impact assessment study is required since biomass is not regarded as waste. However, it is important that the CEN, ISO and national product standards to include torrefied biomass (IEA, 2012a). Then this can provide confidence to deal with both producers and end users of the products.

CHAPTER 2

AIMS AND OBJECTIVES

2.1. Project overview

Torrefaction is a developing research area that is receiving attention and believed to become a leading technology. Many laboratory scale studies have focussed on the understanding this process on how it affects the characteristics of biomass fuels that ranged from woody biomass to agricultural residues and recently, microalgae (Wu *et al*, 2012). Influence of important parameters, namely temperature, residence time and particle sizes of biomass on torrefaction were the fundamental interests of investigation (Bridgeman *et al*., 2008; 2010; Wannapeera *et al*., 2011). Standard analyses such as proximate and ultimate analysis of torrefied biomass were the main characteristics studied and authors usually compared their findings to raw biomass. There are few in depth studies of the torrefied biomass in terms of physical properties such as grindability, hydrophobicity, surface area and looked into its images microscopically. This thesis covers these characteristics and investigates torrefied biomass in more depth using microscopic and spectrometries studies. This thesis also includes the study of products of torrefaction in response to different particle sizes of biomass fuels. A model, FG-Biomass is also put into test to simulate the slow pyrolysis (torrefaction). In addition, the preliminary study of an environmental impact assessment of torrefaction of biomass is conducted and a short investigation on how raw and torrefied biomass fuels behave during combustion are also studied here.

This research is funded by the Energy Programme (Grant EP/H048839/1). The Energy Programme is a Research Councils UK cross council initiative led by Engineering and Physical Sciences Research Council (EPSRC) and contributed to by Economic and Social Research Council (ESRC), National Environment Research Council (NERC), Biotechnology and Biological Sciences Research Council (BBSRC) and Science and Technology Facilities Council (STFC).

2.2. Group project aims and objectives

Torrefaction group that represents University of Leeds and together with the support from other interested parties such as Alstom Power Ltd, have come up with several objectives. Individuals are assigned either to carry out such objectives or to continue what is left in order to achieve the project aims.

The group project aims are listed as follows:

- To examine the feasibility of using coal milling technology for thermally pre-treated (torrefied) biomass.
- To provide an initial assessment of the combustion properties of torrefied biomass.
- To validate torrefaction model based on FG Biomass.

The group project objectives are:

- To prepare thermally treated biomass from different size fractions.
- To characterise the fuels and determine the extent of conversion to establish the maximum particle size that can be converted with operating conditions.
- To examine nitrogen partitioning during the process.
- To characterise the treated material for Hardgrove Grindability Index (HGI), density, surface area.
- To produce high heating rate chars from different size fractions obtained from drop-tube furnace.
- To determine the reactivities of the chars from different size fractions obtained from drop-tube furnace.

2.3. Research aims and objectives

This section provides a list of more focused aims and objectives that are specifically targeted to accomplish for the development of this thesis.

The aims are:

- To investigate the influence of fundamental parameters (temperature, residence time and particle sizes) on the behaviour of biomass fuels when treated with torrefaction
- To examine the nature of products of torrefaction in terms of composition, physical and chemical characteristics and their response to combustion (particularly for torrefied

biomass) as well as to provide comparisons between the products obtained from torrefaction and when the biomass fuels are untreated.

- To provide a summary of environmental impact assessment of torrefaction of biomass fuels.

In order to achieve such aims, the objectives are set as follows:

- To determine the standard fuel characterisation of torrefied biomass fuels in terms of proximate and ultimate analysis.
- To provide a relationship between the elemental composition of biomass fuels and energy yields with increase severity of torrefaction.
- To analyse the rate of decomposition of biomass fuels during torrefaction using TGA method.
- To assess the morphology changes experienced by torrefied biomass fuels using electronic methods such as X-ray Photoelectron Spectroscopy (XPS), Scanning Electron Microscopy (SEM) and Transmission Electron Microscopy (TEM) as well as its surface area using the Brunauer, Emmett and Teller (BET) method.
- To examine the grindability behaviour of torrefied biomass fuels using the Hardgrove Grindability tests.
- To determine the Hardgrove Grindability Index of torrefied biomass fuels in comparison to reference standard coals.
- To investigate the changes in the chemical structures of torrefied biomass fuels and tar product using Fourier Transform Infrared Spectroscopy (FTIR).
- To analyse the behaviour of torrefied biomass fuels when treated with combustion in terms of duration of volatile and char combustion..
- To determine the approximate heating rate of the flame experienced by the biomass particles based on devolatisation.
- To determine the predicted rate of char combustion from combustion of torrefied biomass fuels.
- To investigate the characteristics of tar and other liquid products of torrefaction of biomass fuels particularly on willow, softwood and hardwood.
- To investigate torrefaction using a thermogravimetric analyser (TGA), coupled to an FTIR via a heated transfer line.

- To investigate the yields and composition of products of torrefaction in response to different particle sizes of biomass fuels using TGA-FTIR.
- To make use of FG-biomass model to simulate pyrolysis.
- To provide an overall mass balance of biomass fuels subject to torrefaction.
- To compare the nature of products of torrefaction as predicted by the FG-Biomass model and those obtained experimentally (reactor and TGA-FTIR).
- To study the temperature distribution within a spherical biomass particle during torrefaction of biomass fuels (willow and eucalyptus) of different particle sizes and increase severity of torrefaction.
- To produce a summary of the hazards and environmental impacts of torrefaction of biomass fuels.
- To identify the potential hazards that can occur during drying, different stages of torrefaction process and cooling.
- To identify the potential hazards that can occur with regards to torrefied biomass fuels.
- To identify the environmental fates of the volatiles to air, soil and water.
- To provide an environmental risk profile based on the probability and consequences of hazards.
- To suggest mitigation measures to address the identified environmental impacts.

CHAPTER 3

LITERATURE REVIEW

3.1 The behaviour of lignocellulosic materials to pyrolysis

The cell wall of a biomass is made up of three main components, namely hemicellulose, cellulose and lignin. Cellulose is the most abundant, which covers 40-60%, followed by hemicellulose (20-40%) and lignin (10-25%). These contents differ depending on the type of biomass, for example, willow, a woody crop, has more lignin (20.0%) and less hemicellulose (14.1%) contents than wheat straw, an agricultural residue, which contains 7.7% and 30.8% of the respective contents (Bridgeman *et al*., 2008). Furthermore, the biomass contents are differed on how they are structured (Bergman *et al*., 2005a). For instance, hardwoods contain xylan-based hemicellulose while softwoods are dominantly comprised of mannan-based hemicellulose (Sjöstörm, 1981). Such differences can be observed in Figure 1.11-1.13. Understanding how these lignocellulosic components behave upon thermal treatment is crucial. They comprise the bulk of the mass of the biomass, therefore, their conversion is necessary to realise the potential as a renewable source of energy.

Figure 3.1 demonstrates the degradation of lignocellulose during pyrolysis in terms of mass and the rate of mass loss as studied in Yang *et al* (2007). The figure shows how hemicellulose starts to degrade at the earliest time and this degradation becomes rapid at 220-315ºC. As illustrated in Figure 1.10, hemicellulose consists of various saccharides such as xylose, mannose, glucose and galactose and has many branches, which makes it vulnerable to break from the main stem (Yang *et al*., 2007). At 315-400ºC, a more significant mass loss and faster rate of decomposition than that of hemicellulose is observed due to cellulose decomposition. Cellulose consists of a long polymer of glucose without branches, which gives it a very strong structure and degrades at higher temperatures than hemicellulose (Yang *et al*., 2007). Lignin is the most difficult to breakdown. It degrades gradually over the temperature range 150-900°C. Its decomposition occurs at a gentle rate over a very wide range of temperatures. Lignin is made up of aromatic rings with various branches and cross-linkages, which explains the gradual degradation (Yang *et al*., 2007).

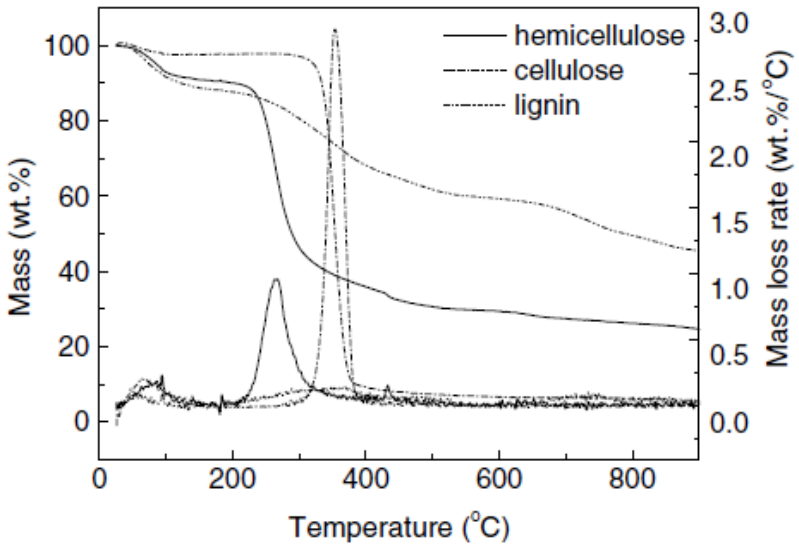

Figure 3.1. Pyrolysis of hemicellulose, cellulose and lignin as observed in a thermogravimetric analyser, where their mass losses and rates of mass loss of were recorded (Yang *et al*., 2007).

Yang *et al* (2007) also looked into the main gaseous products and volatile organic compounds during the pyrolysis, which comprise of carbon dioxide, carbon monoxide, methane and some organics (a mixture of acids, aldehydes, alkanes and ethers). These gases were reported to be released mainly at low temperatures from the degradation of hemicellulose and to a lesser extent, cellulose.

3.2 Mechanisms of torrefaction

Torrefaction takes place at a low pyrolysis temperature range (200-290ºC). Exploratory studies have shown that this thermal treatment has a great impact on the behaviour of the cell wall in the biomass particularly hemicellulose (Prins *et al*., 2006a).

Chen *et al* (2011) carried out torrefaction processes that focussed on these lignocellulosic materials using thermogravimetry with increasing temperatures (230, 260, 290ºC), followed by pyrolysis until the temperature reached 800ºC. The results were analysed by means of thermogravimetric analysis (TGA), derivative thermogravimetric (DTG) and differential thermal analysis (DTA). As in agreement with Yang *et al* (2007), the TGA shown in Figure 3.2 a) indicates that the hemicellulose starts to degrade slightly during torrefaction even at a temperature as low as 230ºC (Chen *et al*., 2011). The DTG peak observed in Figure 3.2 b) for hemicellulose at 230ºC was the least intense, which also indicates it has the slowest rate of mass loss in comparison to the other peaks upon torrefaction at 260 and 290ºC. The other

peaks showed that the increased in intensity were of ten-folds (20-22 wt%/ºC). A significant rate of degradation due to cellulose occurred at the highest torrefaction temperature (23 wt%/ºC), while only to a less extent for that of lignin (about 3 wt%/ºC). Cellulose would take more energy for it to degrade and often responds at higher temperatures (Yang *et al*., 2007). Even though, lignin did not seem to show any significant change, its decomposition did take place yet gradually over a wide range of temperature and at a very low mass loss rate during pyrolysis heading towards 800ºC (Chen *et al*., 2011).

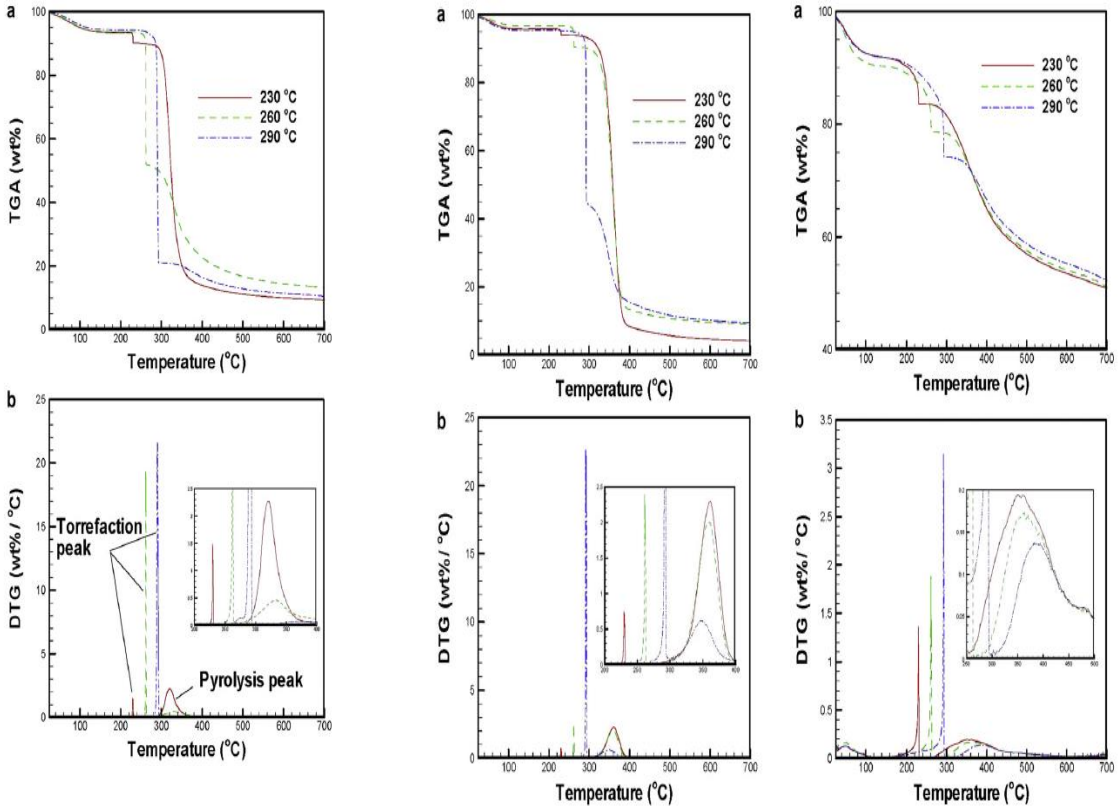

Figure 3.2. a) Thermogravimetric analysis and b) derivative thermogravimetric of hemicellulose (left), cellulose (middle) and lignin (right) at three torrefaction temperatures (230, 260 and 290ºC with a residence time of 1 hour) (Chen *et al*., 2011).

3.2.1 Differences found in deciduous, coniferous woods and herbaceous crops

Different biomass behaves differently upon thermal treatment. Prins *et al* (2006a) studied the differences in the torrefaction of two deciduous woods (willow and beech), coniferous wood (larch) and a herbaceous crop (straw) at three increasing temperatures and decreasing residence times (230ºC, 50 min; 250ºC, 30 min; 270ºC, 15 min). The results showed that temperature plays an important role in this torrefaction process, where the solid yield decreased with increased temperature. In brief, larch produced the largest yield, followed by

willow, beech and straw. At 270°C and a residence time of 15 min, the solid yield of torrefied larch was about 92%, while that of torrefied willow was about 83%. This difference can be explained in relation to the hemicellulose structures of both deciduous and coniferous woods as described in Section 3.1. Larch has a greater proportion of glucomannan and it is less reactive, in comparison to willow that has a larger amount of glucoxylan, which behaves very reactively towards thermal treatment (Prins *et al.*, 2006a). The authors also investigated the yields of volatiles and their compositions obtained from the torrefaction process. Figure 3.3 and 3.4 show the production of a greater yield of condensable volatiles (for example, acetic acid and methanol) and permanent non-condensable gases (that is, carbon dioxide and carbon monoxide) during the torrefaction of willow than larch. These differences can be explained by the lower degree of devolatization in larch due to its lower glucoxylan content than in willow. Volatile products from the slow pyrolysis of softwoods are found to be mainly water, carbon dioxide, carbon monoxide and acetic acid (Aho *et al.*, 2008).

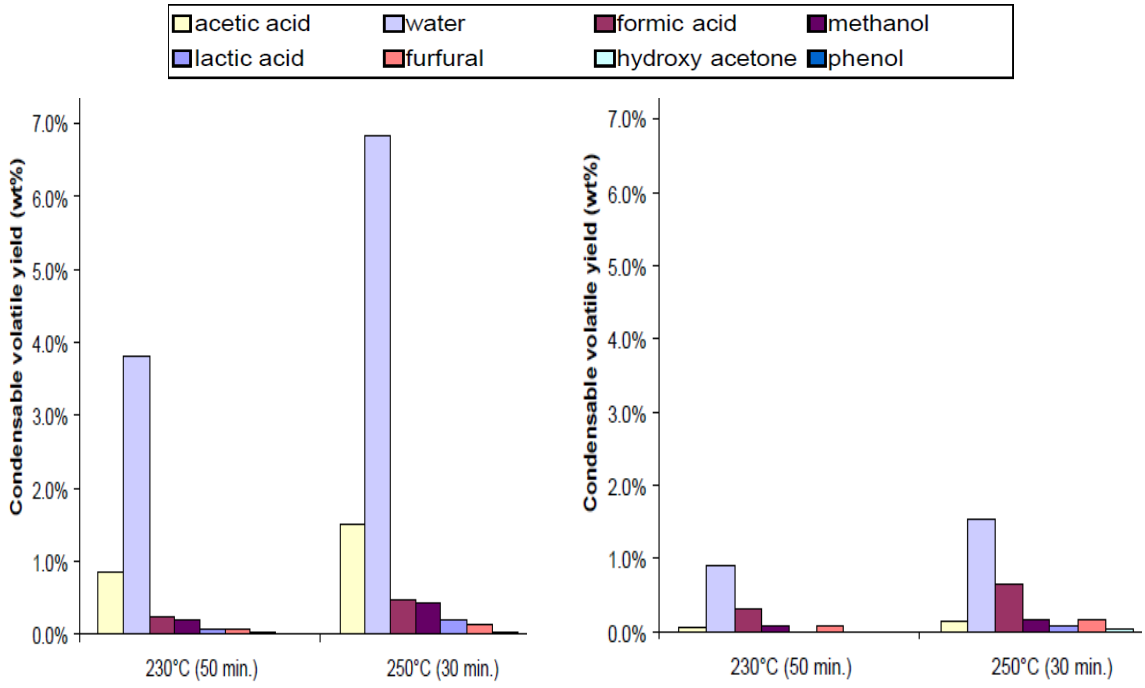

a) Willow b) Larch

Figure 3.3. Condensable volatile yields produced during the torrefaction of willow and larch at 230°C and 250°C with residence times of 50 min and 30 min respectively (Prins *et al.*, 2006a).

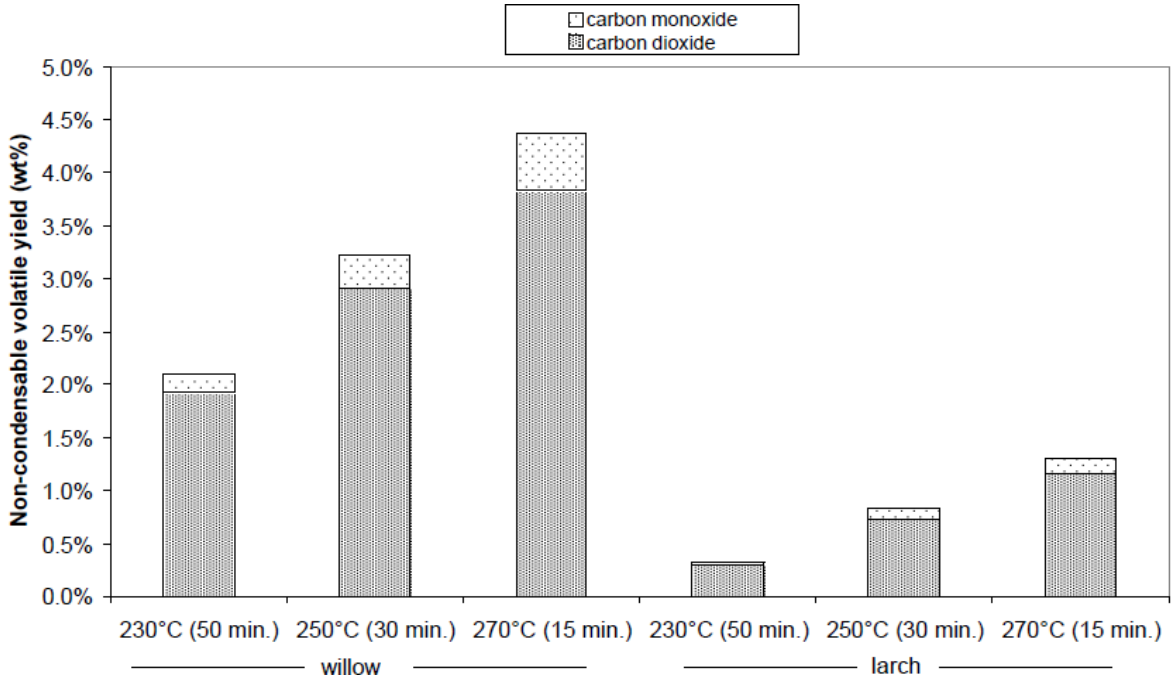

Figure 3.4. Non-condensable yields produced during the torrefaction of willow and larch (Prins *et al*., 2006a).

Bridgeman *et al* (2008) conducted a similar study that they compared the characteristics of willow, reed canary grass and wheat straw, that were torrefied at 230-290ºC. To begin with, raw reed canary grass (RCG) and wheat straw (WS) has about twice (29.7% and 30.8% respectively) of the hemicellulose content compared to raw willow (16.1%). When these fuels were torrefied, the results showed that torrefied WS experienced the greatest changes in the elemental composition followed by torrefied RCG and willow. Changes were more pronounced at 290ºC. For example, the change in carbon content of torrefied WS was about 14%, while that of torrefied RCG and willow was only about 8-9%. When a Van Krevelen diagram was plotted, torrefied wheat straw was seen to have its composition closest to that of lignite. However, mass and energy yields of WS were calculated to be the lowest than those of RCG and willow. The mass yields of torrefied WS, RCG and willow were 55.1%, 61.5% and 72.0% accordingly, while the energy yields of the respective fuels were 65.8%, 69.0% and 79.2%. The authors concluded that herbaceous species are more affected than woody biomass upon torrefaction in terms of composition, mass and energy yields. Note that RCG and WS have similar hemicellulose content but they behaved differently in terms of yields and characteristics. This is again, largely due to the difference in structure of hemicellulose in both fuels as described in Section 1.10.2.1 and displayed in Figure 1.9.

Tapasvi *et al* (2012) investigated the torrefaction behaviour of a hardwood (birch) and softwood (spruce) using a batch reactor that is equipped with a TGA. This study is somewhat different than previously reviewed. This experiment designed an experimental matrix, which focused on the effect of torrefaction on four parameters: the type of fuel, residence time (30 and 60 min), size of the samples (10 and 40 mm) and temperature (225 and 275°C). As a result, 16 different torrefied samples were prepared and analysed. In terms of sizes, solid yields increased with particle sizes even though only slight differences were reported that could be due to the heat and mass transfer limitations. With regards to the different types of fuel, the DTG curves showed that birch has a higher devolatization rate than spruce. Following that, birch produced lower mass yield than spruce. For example, when both at 40 mm were treated at 275°C for a residence time of 60 min, birch produced 63.5% while spruce yielded 75.8%. Another interesting finding is how different types of biomass can affect the evolution of CO/CO_2. It was earlier stated that the evolution of volatiles in birch is higher than in spruce but these authors also discovered that birch produced lower CO/CO_2 ratio than spruce at 275°C. Deng *et al* (2009) explained that when the ratio increased, this could be due to the decomposition of cellulose and to a little extent, lignin. Hence, the authors concluded that the difference in this ratio between the two fuels is likely due to the lower lignin and greater cellulose content in birch than spruce.

3.2.2 Rate kinetics

Studying the thermal decomposition of wood can be complex because wood contains various components. With regards to torrefaction and the potential of torrefied biomass as an attractive renewable fuel, it is important to fully understand the chemical and physical processes that occur during the thermal process (Prins *et al*., 2006b). Rate kinetics is one of the areas of research interests apart from reaction mechanism, optimisation of the process conditions and selection of particle size of biomass (Prins *et al*., 2006b). Many literatures have studied the kinetics and models that mainly dealt with pyrolysis temperature range above 300°C on the decomposition of the lignocellulose components (van der Stelt *et al*., 2011) but those involves torrefaction is slowly receiving attention (Prins *et al*., 2006; Bates *et al*., 2012; Peng *et al*., 2012).

Prins *et al* (2006b) examined the determination of weight loss kinetics of wood by torrefaction in a thermogravimetric analyser (TGA). The type of biomass is a crucial parameter in reaction kinetics as its lignocellulosic components will determine its behaviour

upon torrefaction. For example, hardwoods and softwoods may not have much difference in their lignocellulosic composition but the content of hemicellulose in each type of biomass is. As repeatedly mentioned, hardwoods contain a higher proportion of glucoxylan while softwoods contain the lower reactive glucomannan and arabinogalactan. Therefore, the thermal behaviour of these two types of biomass fuels became the main case study in Prins *et al* (2006b).

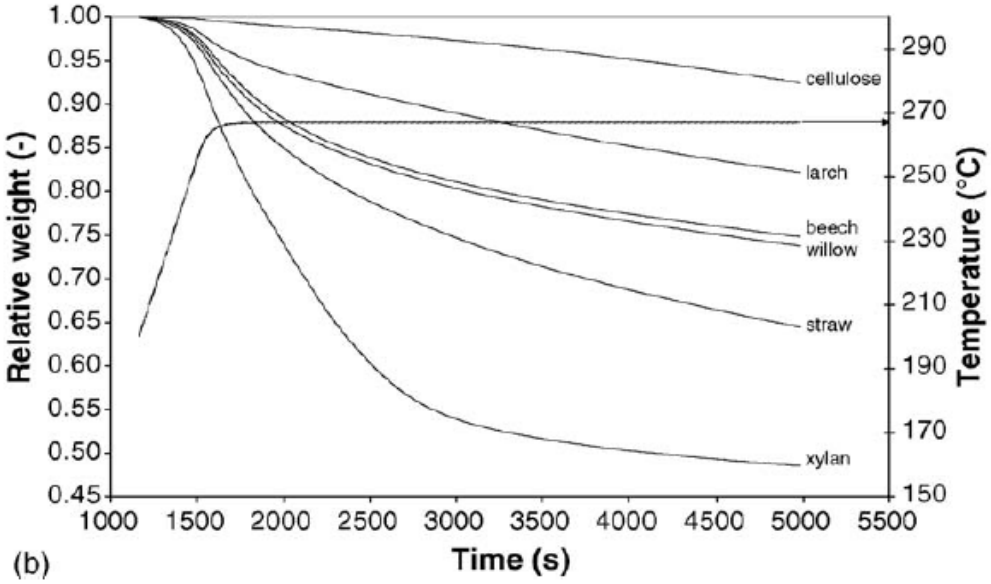

Figure 3.5. Decomposition of various biomass compounds at 267°C (Prins *et al*., 2006b).

Figure 3.5 shows that cellulose had the most limited weight loss. Another model component investigated in this study was xylan, which demonstrated the highest reactivity. Beech and willow are both hardwoods so they probably have similar composition, hence exhibited similar thermal reactivity. Larch has a slower degradation due to the low reactivity component, mannan. Straw may have a higher xylan content than in hardwoods but its high content of mineral matter may also explain its great mass loss (Prins *et al*., 2006b).

Prins *et al* (2006b) developed the kinetic model for the torrefaction of willow based on the model defined by Di Blasi and Lanzetta (1997). Di Blasi and Lanzetta (1997) modelled the rate kinetics (Equation 3.1) by a combination of two-step mechanism with parallel reactions for the formations of solids and volatiles, where A is the hemicellulose component, B is the intermediate product that has a reduced degree of depolymerisation and C is the torrefied biomass. V1 and V2 represent volatiles evolved from the first and second stages of pyrolysis respectively. k_1, k_2, k_{v1} and k_{v2} are the four Arrhenius kinetic parameters that were used to measure the mass loss data experimentally. Prins *et al* (2006) then used the below equation to

verify whether it can be used to describe the weight loss kinetics for torrefaction of biomass fuels.

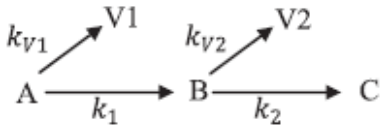

(3.1)

They stated that different types of biomass will have different char yields and kinetic parameters. Therefore, they compared the char yields and reaction rates of the first and second step for willow with those for xylan that was previously studied in Di Blasi and Lanzetta (1997). They found out that the first reaction stage is faster (A → B + V1) than the second stage (B → C + V2). Figure 3.6 shows the simulation of the mass loss of willow which indicates that the first stage was completed within 15-60 min and resulted in a solid mass loss of 16-30% for temperatures between 250-300°C, while the second stage took several hours to complete and produced 42-48% of mass loss. Prins *et al* (2006b) concluded that the mass loss during the first stage is primarily due to the decomposition of hemicellulose and the mass loss progressed further due to the breakdown of cellulose, minor lignin decomposition and charring of the remaining hemicellulose at higher temperatures. These findings are supported by studies that used TGA to investigate the thermal behaviour of the lignocellulose components (Chen and Kuo, 2011).

Figure 3.7 illustrates the predicted char yields has shown good agreement with the experimental data (Prins *et al.*, 2006b). Willow experienced a slower first reaction due to its lower hemicellulose content than the xylan. The great weight loss in the second reaction is likely due to the decomposition of other reactions, including cellulose. The model was also tested for higher heating rates up to 100°C min^{-1} and the trend of weight loss is predicted accurately with the experimental results. They suggested that above 300-320°C, fast thermal cracking of cellulose produces tar, therefore thermal treatment below 300°C is recommended for torrefaction.

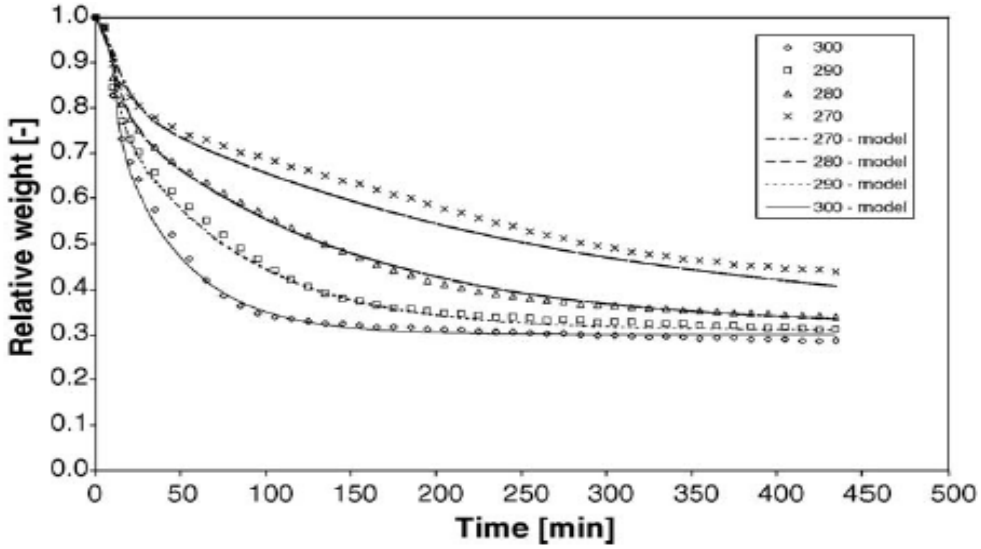

Figure 3.6. Comparison of experimental and modelled relative weight of willow upon torrefaction at 270°C, 280°C, 290°C and 300°C with a heating rate of 10°C min^{-1} (Prins *et al*., 2006b).

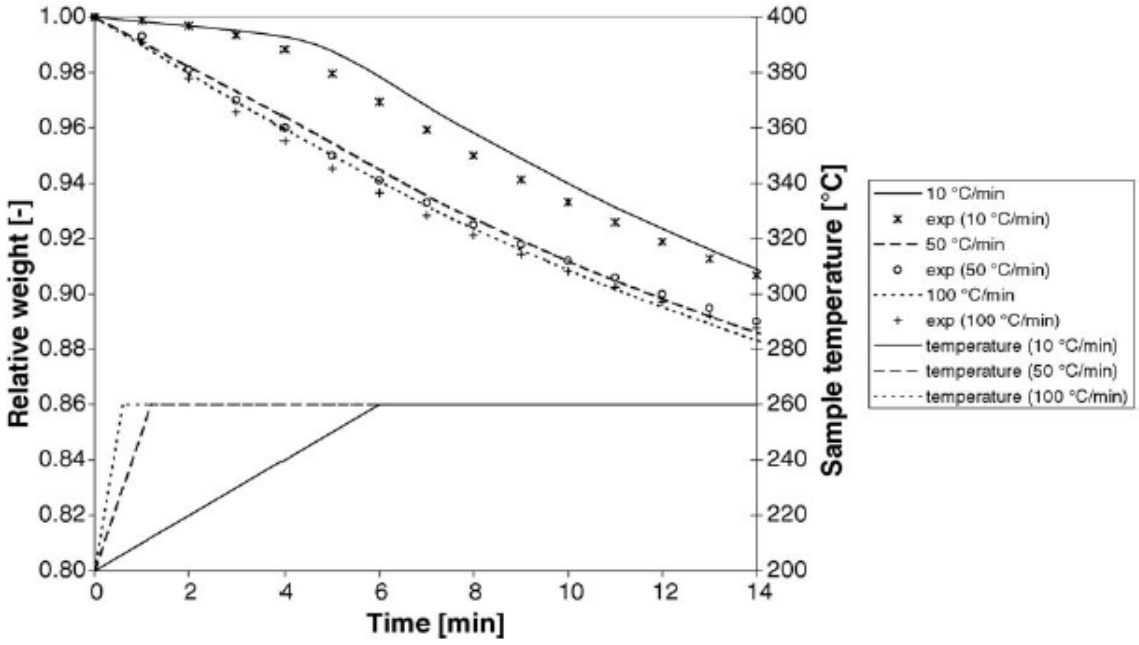

Figure 3.7. Comparison of experimental and modelled relative weight of willow upon torrefaction at 260°C with various heating rate of 10, 50 and 100°C min^{-1} (Prins *et al*., 2006b).

Prins *et al* (2006b) also discussed the importance of particle size in torrefaction process. The rate of heat transfer to and within the particle has to be fast to minimise the residence time. This is also to ensure that the temperature of the biomass is the same as that in the surrounding. Torrefaction involves convective heat transfer from the reactor to the surface of the biomass by convection, followed by conduction of the heat into the core of the biomass and finally the reaction within it (Basu, 2013). Prins *et al* (2006b) used parameters, namely

Biot (Bi) and pyrolysis (Py) numbers to achieve a desired kinetic control, which could influence torrefaction. Biot number is the ratio between the heat convection and conduction rates while pyrolysis number is the ratio of heat convection rate and reaction rate. To avoid heat transfer limitations, firstly, the Biot number has to be small, where the heat conduction within the particle is faster than the heat going into the particle, and secondly, the pyrolysis number has to be large, where the heat convection rate is faster than the chemical reaction rate. If the particle size is small, the internal heat transfer can be ignored and the reaction will be dominantly controlled by rate (Prins *et al*, 2006b; Basu, 2013). If it is large, torrefaction will be controlled by conduction and may lead to a higher temperature in the interior of the biomass (Basu, 2013). This explains the inconsistency of temperature profiles during torrefaction as will be illustrated in the later sections. The effect of particle size on torrefaction kinetics will be discussed again in the later section.

$$\mathrm{Bi} = \frac{\alpha \mathrm{Lc}}{\lambda} = \frac{\text{particle external convective heat transfer rate}}{\text{particle internal conductive heat transfer rate}} \qquad (3.1)$$

where α is the convection heat transfer coefficient in W m^{-2} K^{-1}, Lc is the ratio of the particle volume to surface area in m and λ is the thermal conductivity of particles in W m^{-1} K^{-1} (Peng *et al*., 2012).

$$\mathrm{Py} = \frac{\alpha}{k_i \rho C_p L_C} = \frac{\text{particle external convective heat transfer rate}}{\text{particle internal reaction rate}} \qquad (3.2)$$

where ρ is the particle density in kg m^{-3}, C_p is the heat capacity of particles in J kg^{-1} K^{-1}, k_i is the global reaction rate in s^{-1}, and *i* is the *i*th reaction group (Peng *et al*., 2012).

Bates *et al* (2012) also developed the kinetics model by Bates and Lanzetta for the evolution of volatiles composition during torrefaction. V1 and V2 were modelled with a set of identifiable chemical components, namely, acetic acid, water, formic acid, methanol, lactic acid, furfural, hydroxyl acetone, carbon dioxide and carbon monoxide (Bates *et al*., 2012). In the study, provided that the temperature range is limited (230-300°C), the compositions of V1 and V2 were assumed to be constant and are fitted to the experimental data as tabulated in Bates *et al* (2012). Volatiles from the first phase are expected to represent primarily hemicellulose decomposition products and those from the second phase should come from products of cellulose decomposition. 18 parameters, which are referred to as compositional

coefficients, were used in the model. They represent the mass fraction contribution to V1 and V2 of the nine volatiles. The results showed that acetic acid, water and carbon dioxide were the abundant compounds in V1, while the remaining was found much more in V2, especially methanol and lactic acid. The authors stated that these results were in agreement with experimental data from torrefaction of biomass from literature, Güllü and Demirbaş (2011). These authors studied the evolution of volatiles in terms of three temperature zones (A-C) during the pyrolysis of wood (beech and spruce) at a heating rate of 2-4 K s^{-1} and a residence time of 300-500 s. The results are tabulated in Table 3.1. V1 agrees with those in zones A and B, while V2 comes close to those in zone C.

Table 3.1. Evolution of volatiles during the pyrolysis of wood (Güllü and Demirbaş, 2011).

Zone	Temperature range	Volatiles
A	< 200°C	Water, carbon dioxide, formic acid, acetic acid, glyoxal
B	200-260°C	Water, carbon dioxide, formic acid, glyoxal and carbon monoxide
C	260-500°C	Methane, formaldehyde, formic acid, acetic acid, methanol and hydrogen

3.3 Physical and chemical changes of biomass fuels upon torrefaction

3.3.1 Colour

One apparent change in a torrefied biomass is the colour. Studies have shown that the colour changed to a more intense brown with increased torrefaction condition whether it is increase in temperature and longer residence time (Bridgeman *et al*, 2010; Phanphanich and Mani, 2011). Figure 3.8 illustrates the changes in colour for woody biomass fuels at various conditions.

Figure 3.8. Images of willow: a) untreated; b) low temperature, short residence time; c) low temperature, long residence time; d) high temperature; short residence time; e) high temperature, long residence time (Bridgeman *et al*., 2010).

3.3.2 Particle size and shape

The other observable transformation is the difference in particle size and shape. Arias *et al* (2008) looked into these changes using an optical microscope to get a deeper insight of the structural modification of eucalyptus that was subjected to torrefaction (at 240°C and 280°C with a residence time of 3 h). Figure 3.9 shows that the raw biomass fuel started off as being highly fibrous in nature and it became more spherical and less fibrous when torrefied. Particle sizes also decreased with increased conditions (temperature and residence time). When a sieving process was conducted, a large number of small particles were able to pass through the sieves, which indicate the reduction in size for torrefied biomass and was assumed to have become more spherical.

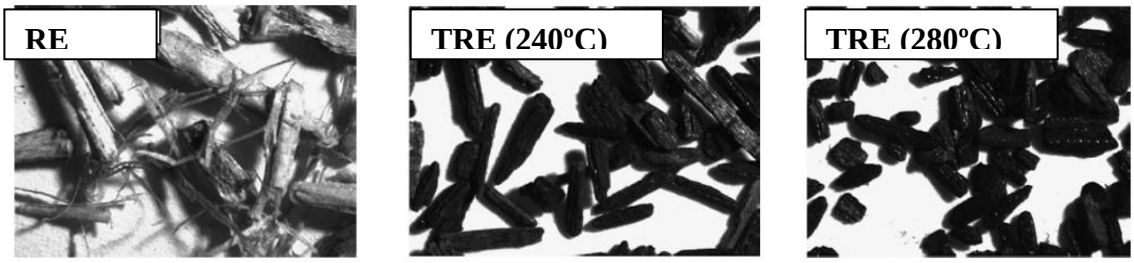

Figure 3.9. Images of raw eucalyptus (RE), torrefied eucalyptus (TRE) at 240°C and 280°C respectively (Arias *et al*., 2008).

These changes can be explained by the transformation in the structure of hemicellulose. Repellin *et al* (2010) stated that torrefaction leads to the shrinkage of the lignocellulosic material, thus, creates stress in the wood fibres and favours cracks. Almeida *et al* (2010) examined raw and torrefied *Eucalyptus Saligna* (*E.Saligna*) via Scanning Electron Microscopy (SEM) and the results can be observed in Figure 3.10. Here, damage to the structure with several fractures appeared in the most fragile tissues, while the raw *E.Saligna* was seen to be strong and intact.

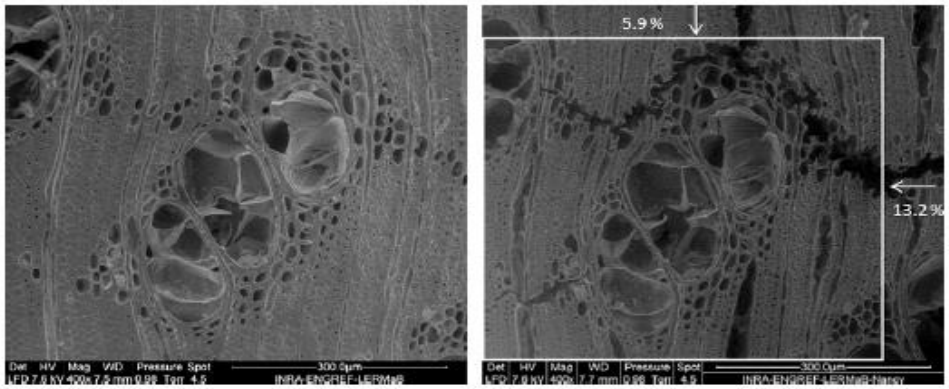

Figure 3.10. SEM images of raw (left) and torrefied (right) *E.Saligna* at 280ºC with a residence time of 5 hrs (Almeida *et al*., 2010).

3.3.3 Mass loss

Figure 3.11 illustrates the reduction of the percentage mass of reed canary grass (RCG) with increasing temperature, from 230 to 290°C (Bridgeman *et al*., 2008). This change was not only primarily due to the loss of moisture via evaporation during the drying stage but also because of the further release of reaction water vapour and the production of volatiles from the degradation of hemicellulose and minor decomposition of cellulose throughout the treatment process.

3.3.4 Moisture, ash, volatile and fixed carbon content

Apart from the colour, particle size and shape, physicochemical properties of interest in a biomass also include the contents of moisture, ash, volatile matter and fixed carbon. This can be determined from proximate analysis. It is one of the two fundamental standard fuel analysis that provides an indication for the suitability of a biomass fuel to be utilised for energy purposes. The changes obtained from proximate analysis of torrefied biomass fuels have been widely studied in Bourgois and Guyonnet (1988), Pentananunt *et al* (1990), Felfli *et al* (2005); Blagini *et al* (2006), Bridgeman *et al* (2008; 2010), Sadaka and Negi (2009), Yan *et al* (2009), Almeida *et al* (2010), Pimchuai *et al* (2010), Wannapeera *et al* (2011), Medic *et al* (2012) and Pirraglia *et al* (2012), to name a few. In general, with increased severity of torrefaction condition, the moisture content and volatiles are reduced, while those of ash and fixed carbon increased. Figure 3.12 illustrates the changes in these contents for torrefied rice husks, where the moisture content and volatiles have reduced from 4.0 to 2.5% and 55 to 30% respectively, while the ash content has increased from 20 to 32% when the temperature increased from 250 to 300ºC with a residence time of an hour. In this experiment, temperature is seen to have a more significant influence to the results than

residence time. With a longer residence time, the moisture content continued to decrease, but minor changes were observed in volatile and ash contents.

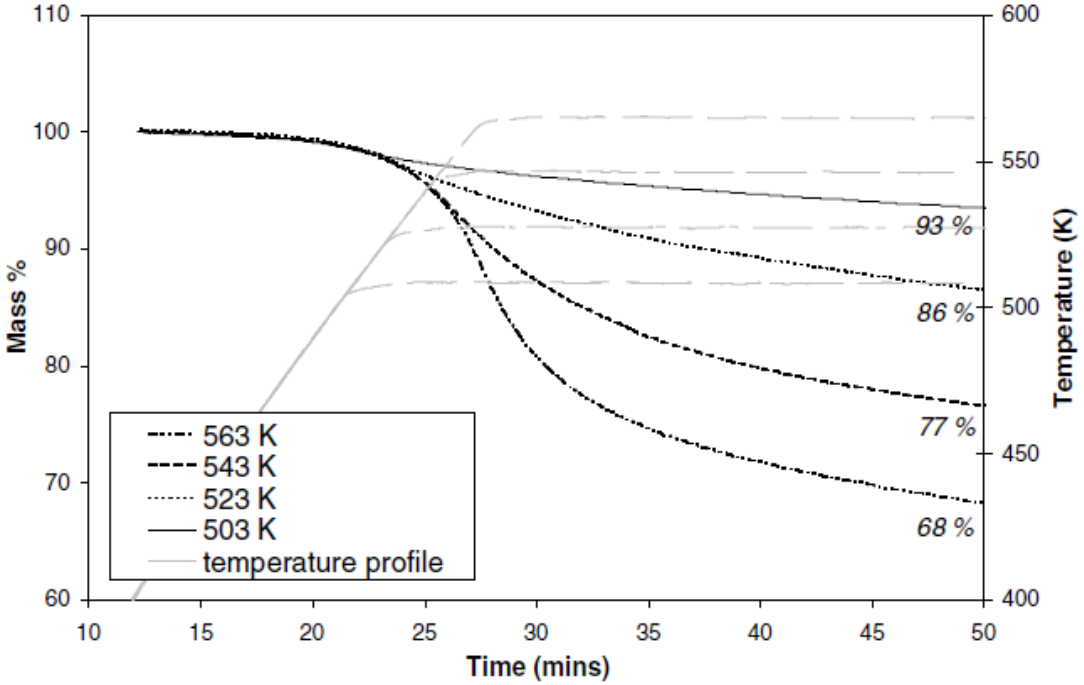

Figure 3.11. Mass loss during torrefaction of reed canary grass at different temperatures (Bridgeman *et al*., 2008).

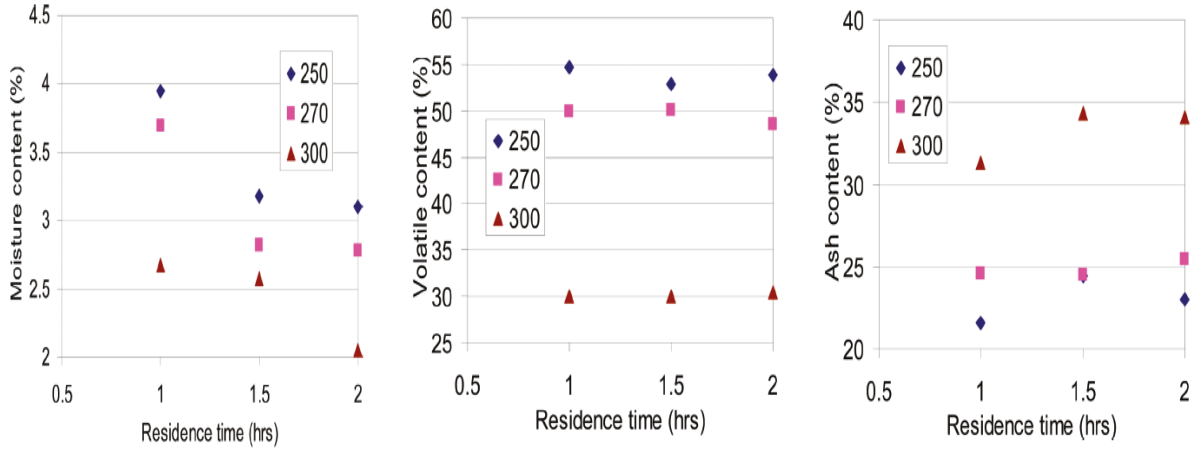

Figure 3.12. The change in the moisture, volatile and ash contents of torrefied rice husks (Pimchuai *et al*., 2010).

3.3.5 Carbon, nitrogen, hydrogen and oxygen contents, Higher heating value (HHV) and Van Krevelen plot

Bridgeman *et al* (2008) stated that the ultimate analysis of a biomass gives an indication to any changes that occur in its chemical composition when it is exposed to torrefaction. Reed canary grass, willow and wheat straw respectively, were torrefied at four final temperatures (230, 250, 270 and 290ºC). Figure 3.13 illustrates the influence of temperature on the carbon, hydrogen and oxygen contents of those three biomass fuels. The carbon content increased, while contents of the other two elements decreased with increased temperature. These values provide useful information for the determination of higher heating value (HHV). The results showed that the HHV increased with increased temperature. For example, willow that was torrefied at 290ºC has a calorific value of 21900 kJ kg^{-1}, while that torrefied at 250ºC was 20200 kJ kg^{-1} and when it was untreated, the calorific value was 20000 kJ kg^{-1}.

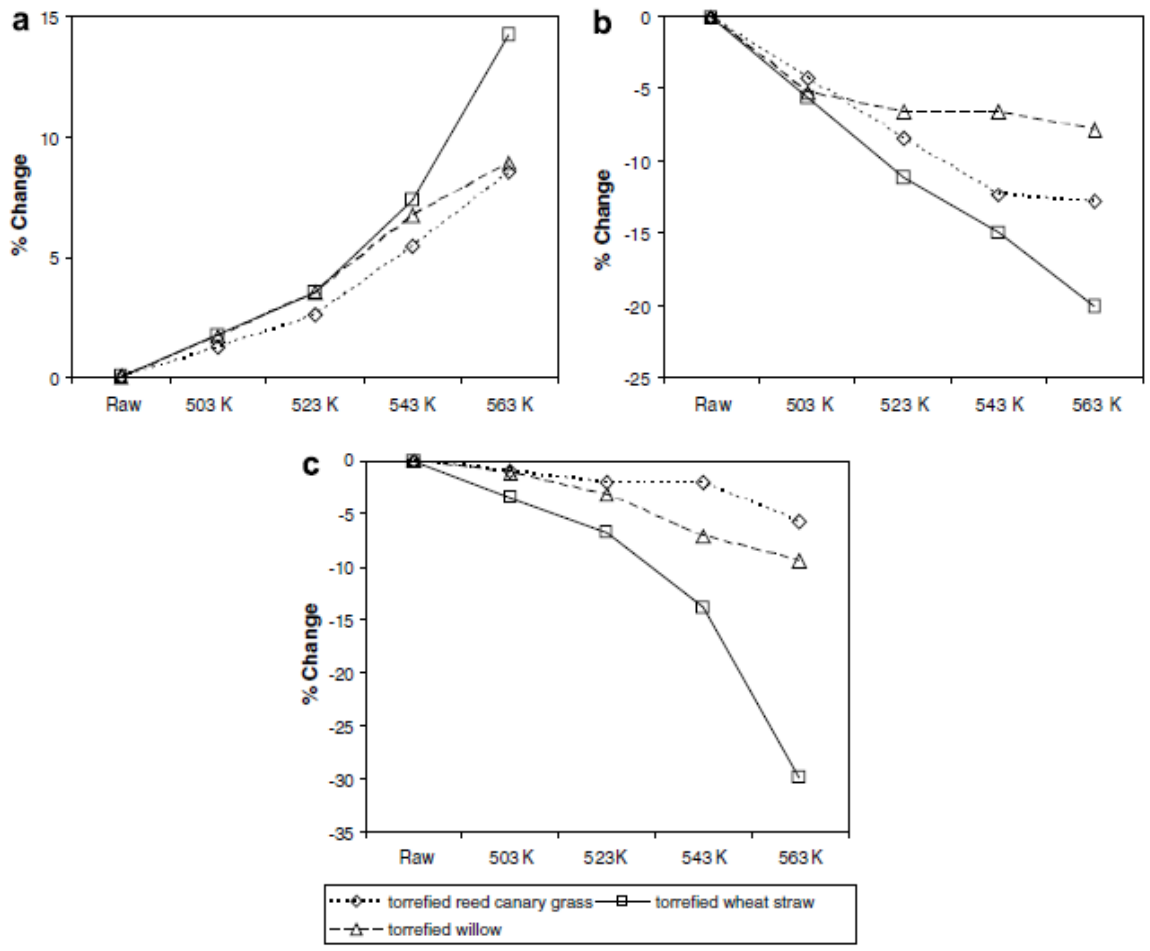

Figure 3.13. Changes in a) carbon, b) hydrogen and c) oxygen upon torrefaction at increasing temperatures (Bridgeman *et al*., 2008).

Another useful information that can be obtained from this analysis is the indication as to how close the torrefied biomass is to low rank coals in terms of chemical composition, and in turn, higher heating value, by plotting a Van Krevelen diagram (Figure 3.14). Many authors have used this technique such as in Bridgeman *et al* (2008), Wu *et al* (2012), van der Stelt *et al* (2011), Rousset *et al* (2011), Prins *et al* (2006), and Phanphanich and Mani (2011). As can be seen in Figure 3.14, those that were torrefied at higher temperatures tend to have similar characteristics, as they are approaching closer to those of low rank coals such as lignite. Therefore, the more severe the torrefaction condition is, the closer the biomass' characteristics are to those of coals. However, one cannot just torrefy the biomass at any high temperature because there is one crucial parameter that needs to be taken into account and that is energy yield. Energy yield has been found to decrease with increasing temperature (Bergman *et al*., 2005a; Bridgeman *et al*., 2010). However, the energy yield can be controlled by carefully adjusting the temperature and residence time during the torrefaction (Wannapeera *et al*., 2011).

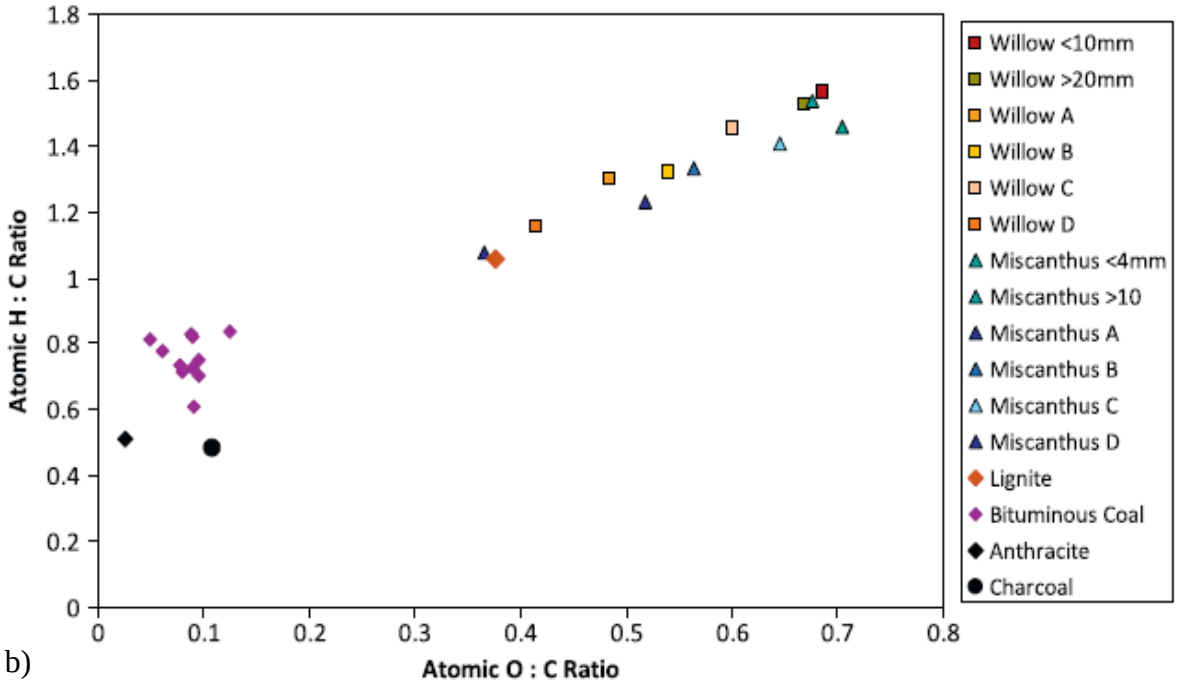

b)

Figure 3.14. Van Krevelen diagram for coals, raw and torrefied biomass fuels, where A-D represents the severity of torrefaction conditions. Table 3.2 provides the description for such conditions, where A as the least severe and D as the most severe (Bridgeman *et al*., 2008).

3.4 The influence of temperature and residence time on biomass fuels

Bridgeman *et al* (2010) stated that the two most critical parameters of torrefaction are temperature and residence time. Particle size is also influential but to a lesser extent. A three

factor design approach was carried out, as tabulated in Table 3.2, using willow and *Miscanthus*.

Table 3.2. Three factor design approach to the experimental work (Bridgeman *et al*., 2010).

Treatment	Temperature (°C)	Residence time (min)	Particle size (mm)
A	290	10	<10 mm; <4 mm
B	230 – 250	60	<10 mm; <4 mm
C	230 – 50	10	>20 mm; >10 mm
D	290	60	>20 mm; >10 mm

As illustrated in Figure 3.11, mass loss is used as an indicator of the severity of the torrefaction conditions (Almeida *et al*, 2010; Bridgeman *et al*., 2008; 2010). According to Bridgeman *et al* (2010), *Miscanthus* experienced more mass loss than the willow for the same condition. In analysing the influence of temperature, time and size, they used differences of the average mass losses within each variable. For example, the difference between high and low temperature average mass loss in willow was 19.4% while that in *Miscanthus* was 24.0%. The difference between long and short residence time was approximately half of that produced by the effect of temperature for both fuels. Differences in mass loss between large and small particles were 3.2% and 2.9% for willow and *Miscanthus* accordingly. In conclusion, temperature was the most significant parameter followed by the residence time and particle size. Following that, fuels that were treated at the most severe condition (D) produced torrefied willow and *Miscanthus* containing the lowest moisture and volatile content and highest fixed carbon and ash content compared to other less torrefied fuels. In terms of elemental analysis, they contained the highest amount of carbon and lowest amounts of oxygen and hydrogen, thus, had the highest calorific value amongst the less treated and raw fuels. Nitrogen content was undetected for *Miscanthus* but there was a slight increase in the torrefied willow.

3.5 The influence of particle size on torrefaction

Particle size is one of the parameters that have influence in torrefaction aside from temperature and residence time. Biomass fuels that are fed into combustors/gasifiers come with different shapes and if they are large particles, the study of particle size becomes more

important (Aylon *et al*., 2005). There are many literatures that have studied and discussed about the effect of particle sizes of biomass in fast and high temperature pyrolysis. Pyrolysis of biomass is complex as it involves two processes: chemical, which includes volatization and char formation and physical, which includes heat and mass transfer (Bahng *et al*., 2011). It also depends on the particle size, shape, temperature, rate of heating and residence time (Bahng *et al*., 2011). In industries, where thick particles are used, pyrolysis process is heat transfer controlled and during this process, these particles tend to trap more condensables due to mass transport limitations (Bahng *et al*., 2011).

Aylon *et al* (2005) studied the devolatisation of tire pyrolysis (up to 550°C) and used particle sizes of 2, 1 and < 1 mm. The results showed that this variable did not seem to have any influence on pyrolysis, at least in the 2 mm range. Chen *et al* (2010) studied the distribution of the products of the pyrolysis at 800°C, at which the solid yield increased but the gas yield decreased with increased size (see Figure 3.15). The tar yield only seemed to increase when the size was greater than 2 mm. This result is in agreement with Aylon *et al* (2005).

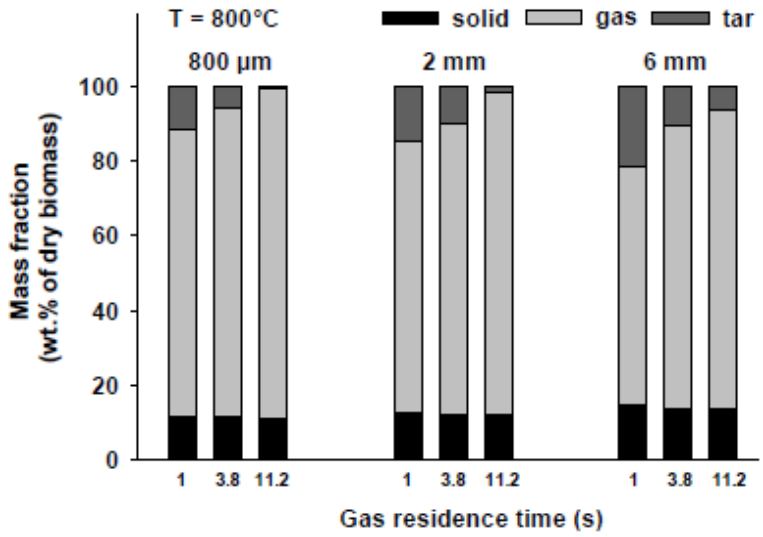

Figure 3.15. Mass yields of solid, gas and tar after pyrolysis at 800°C (Chen *et al*., 2010).

In general, many studies have found that char yields increased linearly with particle size upon pyrolysis (Calahorro et al., 1992; Demirbas, 2004), but mostly were subjected to fast heating rate and the validity of the results would be uncertain if torrefaction is applied (Basu *et al*., 2013). Only recently, that this parameter is receiving more attention than before in torrefaction studies. Particle size was not of importance because previous literatures observed

that it has the least impact on torrefaction (Prins *et al*., 2006b; Bridgeman *et al*., 2010). Torrefaction is an endorthermic reaction, where the heat is absorbed from the hot gas to the particle via thermal conduction. This results in a temperature gradient across the surface boundary and within the particle, which in turn can affect the torrefaction reaction rate. The rate of heat transfer has to be faster than the reaction rate in order to minimise the residence time (Prins *et al*., 2006b). Section 3.2.2 discussed about the use of Biot number (Bi) and pyrolysis number (Py) in order to meet the criteria for absence of heat transfer limitations.

It is important to realise the significance of particle size since biomass rarely comes in uniform sizes when feed to torrefaction plants. For commercial operations, since torrefaction of biomass can save grinding energy (Bridgeman *et al*., 2008), it would be of great interest to use large size biomass as feedstocks and grind them to desired particle sizes after torrefaction. The understanding about the relationship between large particle sizes and torrefaction is therefore, crucial.

Peng *et al* (2012) pointed out the inconsistency of results in the torrefaction data obtained from literature reviews at the same operating conditions (250°C with a residence time of 30 min). Feifli *et al* (2005) reported the weight loss of torrefied wood briquettes was 26% and the HHV was 21.21 MJ kg^{-1}. Bridgeman *et al* (2008) used willow and its mass loss was 10.40% with an HHV of 20.60 MJ kg^{-1}. Wannapeera *et al* (2011) torrefied small samples of Leucaena that has particle sizes of less than 0.075 mm and found that its mass loss was 27.00% and the HHV was 21.20 MJ kg^{-1}. Moreover, Phanphanich and Mani (2010) used pine logging residue chips and the mass loss was 19.99% followed by a HHV of 21.21%. So even though these biomass fuels were treated at the same operating conditions, they produced different results. Other factors such as the type of biomass fuels and heating rate may contribute to the difference but these authors came to realise that particle size can also play a very important role. Therefore, they studied the influence of particle size on torrefaction using the TGA and fixed bed reactor for the torrefaction of softwood, pine. Smaller samples (that were grouped into three: a) <250 μm, (b) 250−500 μm, (c) 500−1000 μm) were tested in the TGA, while those torrefied in the reactor were 0.23, 0.67 and 0.81 mm. The findings in the TGA (Figure 3.16) showed that particle size has a smaller effect on the weight loss of pine than temperature, even though it can be seen that the rate of weight loss decreased with

increased particle size and even more with increased temperature. This effect was also observed in the fixed bed reactor.

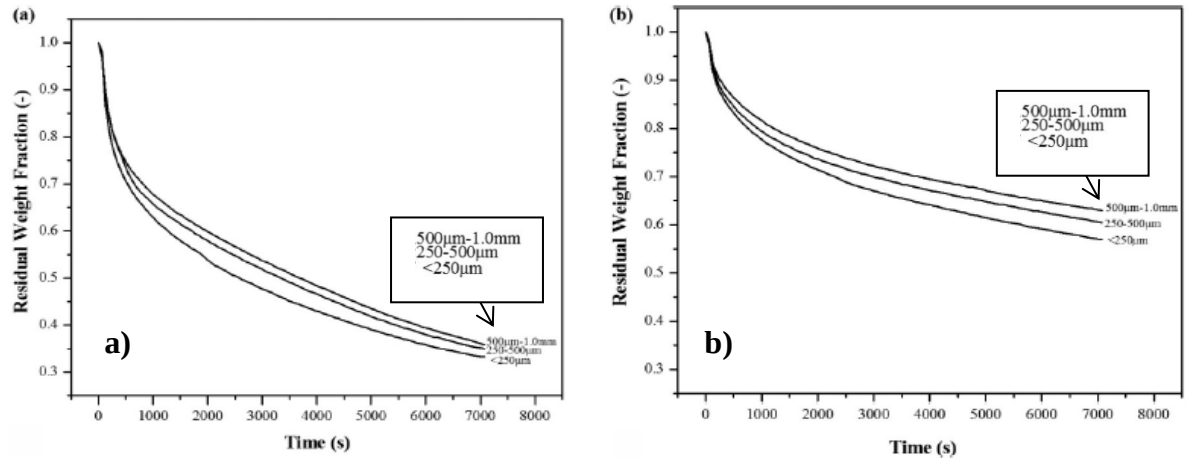

Figure 3.16. Weight loss curves of torrefaction of pine as obtained from TGA at a) 300°C and b) 280°C (Peng *et al*., 2012).

With regards to particle sizes, the smaller particles were reported to experience faster weight losses than larger particles. Peng *et al* (2012) suggested that this could be due to the presence of interparticle heat and mass transfer in large particles. Section 3.2.2 discussed the rate kinetics of pyrolysis of wood as studied by Di Blasi and Lanzetta (1997). Apart from Prins *et al* (2006b) and Bates *et al* (2012), Peng *et al* (2012) has also developed the kinetic model to two equations as follows:

$$\text{wood}_{\text{Fast-reaction group}} \xrightarrow{k_1} \text{volatiles} + \text{chars} \quad (3.3)$$

$$\text{wood}_{\text{Medium-reaction group}} \xrightarrow{k_2} \text{volatiles} + \text{chars} \quad (3.4)$$

where k_1 and k_2 are global reaction rates of fast and medium reaction group respectively. These equations are related to those defined in Di Blasi and Lanzetta (1997), where the fast reaction group refers to the decomposition of hemicellulose content of wood, while the medium reaction group refers to that of cellulose and lignin contents. Peng *et al* (2012) assumed that if the two overall reactions are first order reactions, the residual weight fraction (W_{TGA}) of wood is given by:

$$W_{TGA} = (1 - C_1 - C_2) + C_1 \exp(-k_1 t) + C_2 \exp(-k_2 t) \quad (3.5)$$

where C_1 represents the hemicellulose content and C_2 represents the cellulose and lignin contents of the wood from which observed global reaction rates of both reaction groups can be obtained as equated in (3.6) and (3.7):

$$r_1(\text{obs}) = - C_1 k_1 \exp(-k_1 t) \quad (3.6)$$

$$r_2(\text{obs}) = - C_2 k_2 \exp(-k_2 t) \quad (3.7)$$

where r_1 represents the observed global reaction rates of the fast group and r_2 represents that of the medium reaction group.

Since torrefaction is an endothermic process, Peng *et al* (2012) discussed about the temperature gradient inside a particle during the thermal treatment and how it may affect the torrefaction reaction rate. The authors made use of Biot number (Bi) and pyrolysis number (Py) to examine the substantial temperature gradient within the particles. Due to the small sample sizes that were chosen in this study (< 0.81 mm), they observed the existence of a very small temperature gradient and thus can be neglected.

Wood pyrolysis that leads to a weight loss of more than 70% used the particle shrinking core model (Sreekanth and Kolar, 2009). Torrefaction consists of a narrow and mild temperature range with a low heating rate. Hence, this process can be modeled as a non-shrinking process (Peng *et al.*, 2012). Peng *et al* (2012) stated that for torrefaction with a weight loss of less than 40%, it can be assumed that the diameter of the particle does not change. The analysis showed that the temperature gradient within the particle is negligible, hence the particle can be treated as having a uniform temperature. Apart from that, the authors studied the weight loss of biomass of a particle size of 0.23 mm between torrefaction in the TGA and fixed bed reactor. They used the following model to directly compare the two as shown in equation (3.8). The results showed that the average unit scale factor is 1.29 and they concluded that it could be due to the better mass and heat transfer rates in the fixed bed reactor. This is only true for smaller particle sizes.

$$\text{The unit scale factor, } \Gamma = \frac{\text{global reaction rate obtained from fixed bed unit}}{\text{global reaction rate obtained from TGA}} \quad (3.8)$$

Very recently, Basu *et al* (2013) studied the effect of particle size and shape of biomass fuels on torrefaction, where sizes varied both in terms of length and diameter. For 65 mm length, the diameter varied from 4.76 to 25.4 mm. For the diameter of 4.76 mm, the length varied from 8 to 65 mm. The overall results were discussed in terms of mass and energy yields. Increase in the diameter size showed a decrease in both yields. As predicted, there was an increase in the temperature of the core of the biomass with the increase in the size of diameter. A large diameter particle has a greater wall thickness and hence, a higher thermal resistance. The authors explained that the heat generated by exothermic reaction could not escape , resulting an increase in the core temperature. This have led to a higher degradation, giving lower mass yields. Increase in length however, showed an increase in both mass and energy yields. Basu *et al* (2013) assumed that this effect due to mass transfer limitations rather than heat transfer. The exothermic heat is able to escape readily with increase in length, resulting a no increase in the core temperature.

3.6 The investigation of grindability characteristics of biomass subject to different conditions

Pulverised feedstock particles are necessary for applications in an entrained-flow gasification and co-firing of biomass in a pulverised coal-fired power plant and also in pellet production. Biomass is very fibrous and hygroscopic in nature so it is difficult and costly to get the desired particle size (Bergman *et al*., 2005b). It takes up a lot of energy for the grinding as the fibres and strands of biomass can easily stuck in between the blades of the mill. If the biomass has a high moisture content, pre-drying will be necessary because powdered biomass may clump together and cause further obstacles during milling.

Figure 3.17 is a schematic diagram, which represents the changes occurring in the biomass due to the decomposition of hemicellulose and cellulose upon torrefaction, and what happens when stress such as grinding is applied. The red lines represent the hydrogen bonding between the hemicellulose and the macrofibrils of the cell wall, while the orange lines represent the interweavement of hemicellulose and cellulose (Bergman *et al*., 2005b). Three breakdowns of biomass of different conditions are illustrated (untreated biomass and biomass torrefied at low and high temperatures). The effect is more strongly observed in the structure of biomass that is treated at the higher temperature. Bergman *et al* (2005b) explained that the grinding of untreated biomass causes stress along the fibre orientation and breaks the hemicellulose rather than cellulose fibres. This leads to the formation of needle-like particles

as can be seen in the raw eucalyptus in Figure 3.9. Similar stress is applied to torrefied biomass and produces thinner, shorter and more spherical-shaped particles with increased torrefaction condition compared to the untreated biomass. When biomass is torrefied, the bonds that connect hemicellulose to macrofibrils weaken and more fractures along the macrofibrils are formed. Cellulose depolymerisation may also take place, resulting in the formation of fragile regions.

Arias *et al* (2008) torrefied eucalyptus and noticed that the grindability of torrefied eucalyptus has improved with increased torrefaction temperature. They also observed a reduction in the particle size, as observed by Bergman *et al* (2005b). Phanphanich and Mani (2011) torrefied pine chips and pine logging residue chips at four temperatures (225, 250, 275 and 300ºC) and observed a reduction in the power consumption during grinding. (see Figure 3.18). Torrefaction at 300ºC was able to reduce the power consumption by ten times for pine chips and by six times for logging residues compared to when they are untreated. Figure 3.19 illustrates the grindability behaviour of torrefied biomass (willow, larch and beech), and the required power consumption (Bergman *et al*., 2005b). About 65% of the power consumption was needed to break the untreated willow to a size as small as 0.2 mm. However, this amount was reduced by 50% when the willow was torrefied at 230ºC. It was reduced further at 259ºC and 270ºC.

Hardgrove Grindability Index (HGI) is an indicator to check the extent of the milling capacity of a coal and the difficulty for grinding the coal into smaller particle sizes (Wu *et al*., 2012). Wu *et al* (2012) suggested that for a solid biomass to blend with coal for a pulverised coal-fired power plant, its HGI should not be less than that of coal. Bridgeman *et al* (2010) have made a comparison between the grindability behaviour of raw and torrefied biomass (*Miscanthus*) with that of reference standard coals using an adapted grindability test, HGI. The procedure of this modified version of HGI is used to determine the grindability behaviour of torrefied biomass fuels studied in this thesis. It is well-described in Section 4.4.8. Figure 3.20 demonstrates the changes in the particle distribution curves of *Miscanthus* samples and it shows that *Miscanthus* “D” was reported to have a grindability behaviour closest to coal of known HGI value, 92. The HGI value of *Miscanthus* “D” was 79.

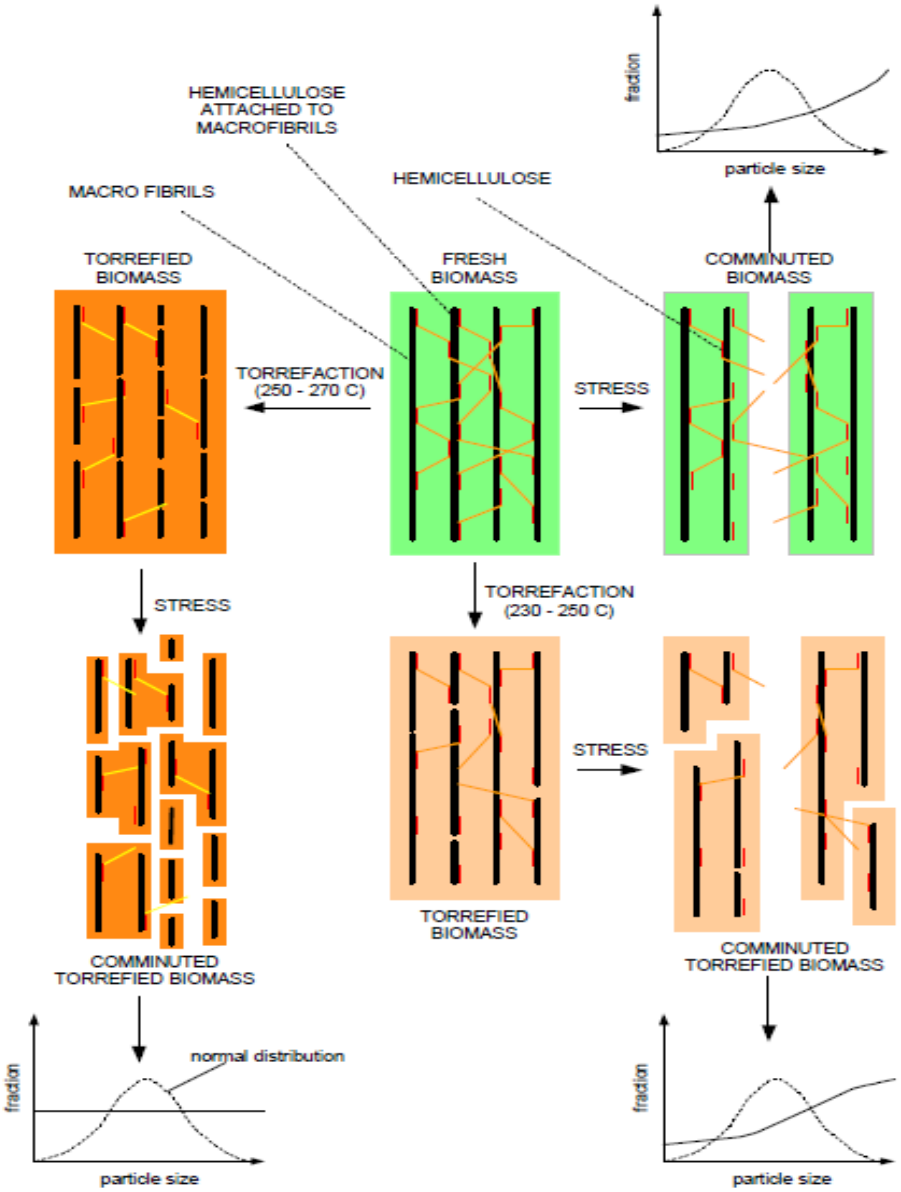

Figure 3.17. Schematic representation of the breakdown of biomass when stress is applied (Bergman *et al*., 2005b).

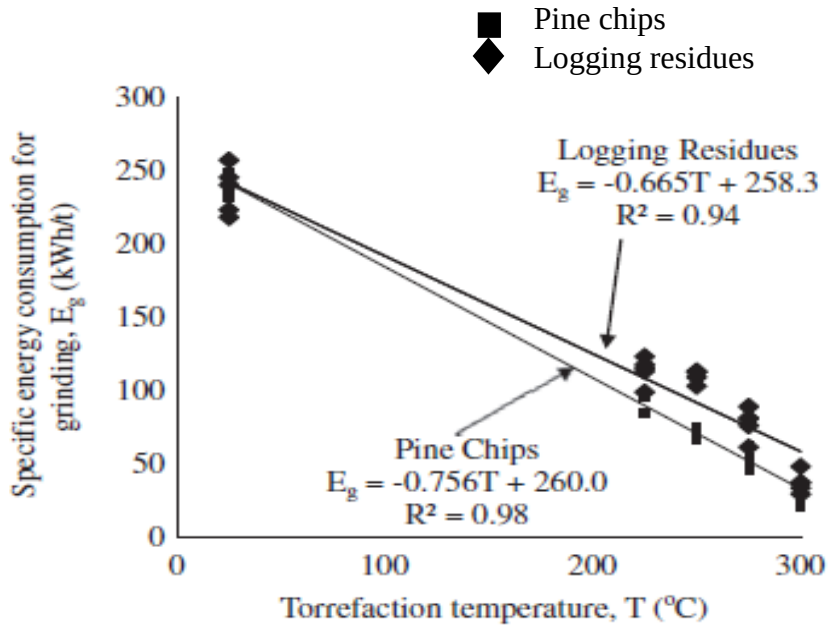

Figure 3.18. Specific energy consumption for grinding of untreated and torrefied pine chips and logging residues (Phanphanich and Mani, 2011).

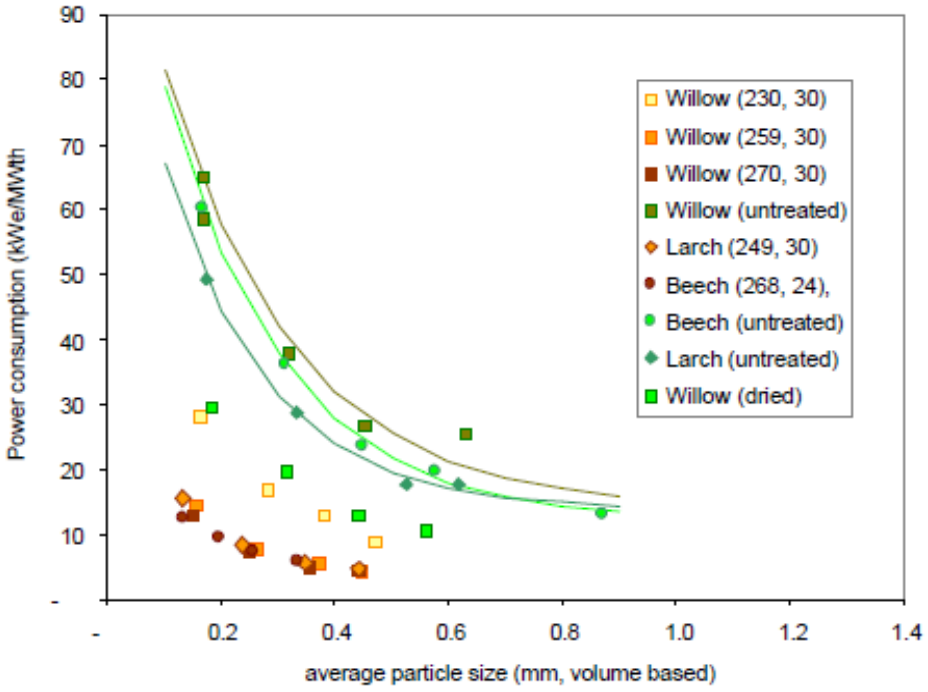

Figure 3.19. Grindability behaviour of different particle sizes against power consumption (Bergman *et al*., 2005b).

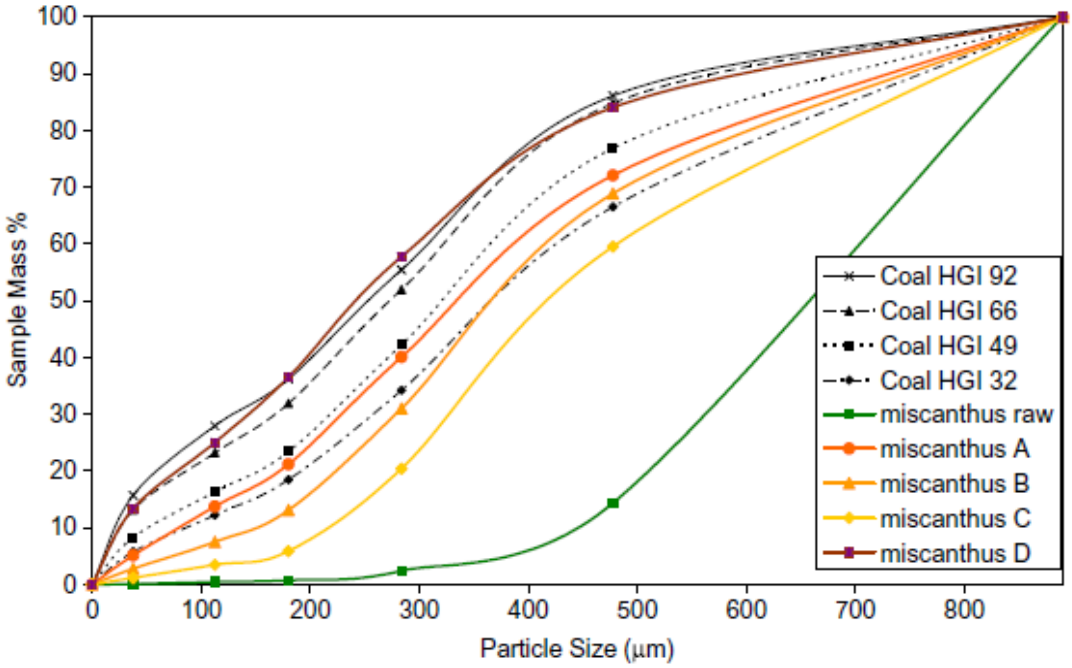

Figure 3.20. Particle size distribution curves for untreated and torrefied Miscanthus (A – D), where A was treated at 290ºC with a residence time of 10 mins, B at 240ºC with a residence time of 60 mins, C at 240ºC with a residence time of 10 mins and D at 290ºC with a residence time of 60 mins, alongside four standard reference coals of known HGI 32, 49, 66 and 92 (Bridgeman *et al*., 2010).

3.7 The study of energy properties of torrefied biomass fuels

Almeida *et al* (2010) emphasized the importance of the energy value of a biomass that it is a relevant parameter if the biomass is intended for energy uses. With torrefaction, studies such as in Rodrigues and Rousset (2009) and Almeida *et al* (2010) have shown that the calorific value (higher heating value) and energy yield increase, which indicates the improvement of the quality of the biomass. These authors also reported that if energy yields are higher than mass yields, it demonstrates the benefits of torrefaction in concentrating biomass energy.

In a typical torrefaction, 70% of the dry mass will be retained as a solid product containing 80-90% of the energy content (heating value) (Arias *et al*., 2010; Pimchuai *et al*., 2010; Bridgeman *et al*., 2008; Chen *et al*., 2011; Medic *et al*., 2012). While the other 30% is converted into torrefaction gases and/or vapours containing 10-20% of the energy content of the biomass (Bergman *et al*., 2005a). Rodrigues and Rousset (2009) studied the effects of torrefaction on the energy properties of *Eucalyptus grandis* wood. The sample was torrefied at 220, 250 and 280ºC. As a result, the heating value increased with increased temperature.

The Higher Heating Value (HHV) increased by 3.93%, 9.56% and 15.74% with respective increased temperatures. The energy yield at the highest temperature (280ºC) was reported to be 92.76%. Almeida *et al* (2010) also investigated the energy properties of two eucalyptus samples (*Eucalyptus grandis* and *Eucalyptus saligna*) at three temperatures, similar to those done by Rodrigues and Rousset (2009). Even though the heating values increased with temperature, the energy yields decreased. Those of torrefied eucalyptus at 220 and 250ºC were above 90% but at 280ºC, the energy yield went down to about 88%. These percentages are still acceptable for energy purposes as they are in agreement with the average energy yield (80-90%) proposed by Bergman *et al* (2005b) and Prins *et al* (2006a). There is no "one size fits all" in determining the operation parameters in order to get a reasonable energy yield as each biomass fuels respond differently to heat. For example, herbaceous crops are more sensitive than woody biomass. At 250ºC, the energy yields of wheat straw and reed canary grass were 83-84% but when they were treated at 270ºC, their energy yields went down significantly to 72% and went further to 55-62% at 290ºC, whereas willow has an energy yield of 92.7% at 250ºC, 85.8% at 270ºC and 79.2% at 290ºC (Bridgeman *et al*., 2008).

3.8 The assessment of hydrophobicity of raw and treated biomass fuels

Raw biomass fuels have very high moisture contents and this is problematic for energy use. Such biomass is not ideally suited for thermal conversion technologies. Lignocellulosic biomass contains hydroxyl groups, which makes it susceptible to moisture absorption as water uptake forms hydrogen bonds with these groups (Yan *et al*., 2009). Torrefaction is able to improve the hydrophobicity property of a biomass (Pimchuai *et al*., 2010) because when it is thermally treated, the hydroxyl groups break down and results in a more hydrophobic solid (Yan *et al*., 2009).

A most common test to check the change in moisture content of a torrefied biomass is by carrying out the proximate analysis that is by simply heating it in the oven for two to three hours at 105ºC, and weigh the biomass before and after drying. Most studies that did torrefaction on a laboratory scale have used this technique and a decrease in the moisture content was observed (Bourgois and Guyonnet, 1988; Pentananunt *et al*., 1990; Arias *et al*., 2008; Bridgeman *et al*., 2008; 2010; Deng *et al*., 2009; Sadaka and Negi, 2009; Phanphanich and Mani, 2011).

Felfli *et al* (2005) torrefied briquettes from wood residues and studied the hydrophobic characteristics by immersing them in water for 17 days and observed their physical changes. As a result, no crumbling was observed and the briquettes remained intact with increased torrefaction condition. They also reported that there was dissolution of impregnated tar in briquettes torrefied at low temperature (220ºC) but nothing found in those treated at 250-270ºC.

Yan *et al* (2009) investigated the hydrophobicity of torrefied loblolly pine and looked into the equilibrium moisture content (EMC) by the static desiccator technique. Loblolly pine was torrefied at temperatures that ranged from 250 to 300ºC and exposed to two environments of different relative humidities (lithium chloride, 11.3% and potassium chloride, 83.6%) at 30ºC. 3 g of each solid sample was initially dried at 105ºC for 24 h and then exposed to those saturated salt solutions for 8-11 days until an equilibrium was reached. The equilibrium was determined when constant mass was observed within three consecutive days. Raw pine was also tested for its hydrophobicity. As a result, the raw biomass has the greatest water uptake. Upon exposure to lithium chloride, its equilibrium moisture content was 3.5%, while the torrefied samples' EMC ranged from 2.2-2.3%. The EMC of raw loblolly was again the highest (15.6%), followed by the sample torrefied at 250ºC (10.4%) and those torrefied at 275 and 290ºC (both having 8.7%) when they were exposed to an environmental in equilibrium with the potassium chloride solution. Shoulaifar *et al* (2012) carried out a similar experiment, where they used different relative humidity levels that ranged from 11 to 98%. Small sample sizes of 90 mg were put in small containers in sealed boxes that contained the saturated salt solutions and these samples were weighed at intervals over two weeks. The decrease in the EMC indicated that the torrefied biomass has become more hydrophobic and one can assumed that it can be stored longer without degrading.

Studies into the reasons for decreased hydrophobicity upon torrefaction are limited during the commencement of this project. Therefore, part of objectives of the project is to investigate the chemical structures of the torrefied biomass through the use of attenuated total reflectance Fourier transform infrared (ATR FT-IR) spectroscopy. However, recently, Rousset *et al* (2011) looked into the hydrophobicity in more depth, in which they studied the changes in the chemical structure of samples during thermal treatment using the ATR FT-IR spectroscopy. Figure 3.21 illustrates a decrease in the intensity of the O-H bands around 3350 cm^{-1} with increased treatment (220-280ºC).

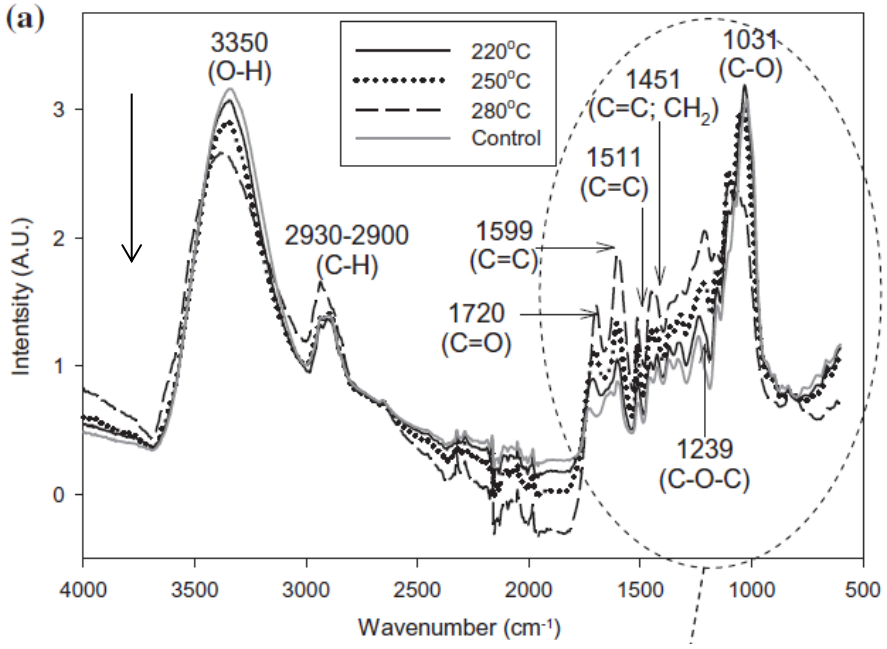

Figure 3.21. An infra-red spectrum of bamboo that was torrefied at 220, 250 and 280ºC (Rousset *et al*., 2011).

More recently, Shang *et al* (2012) also looked into the ATR FT-IR spectroscopy for the determination of any chemical changes in torrefied wheat straw. Wheat straw was torrefied at 200-300ºC with a residence time of 2 hrs. They observed a significant decrease of the O-H band for high temperatures (270-300ºC) as displayed in Figure 3.22. In conclusion, results presented by Rousset *et al* (2011) and Shang *et al* (2012) indicated the occurrence of chemical decomposition of lignocellulose during torrefaction and the reduction in the hydroxyl groups is the one of the main causes for the hydrophobicity of the torrefied biomass.

3.9 Comparison between the combustion behaviour of raw and torrefied biomass

Raw biomass has poor combustion characteristics (Pentananunt *et al*., 1990). It has a high O:C and H:C ratio, resulting a low heating value. Raw biomass fuels also have high moisture contents and they are susceptible to water absorption upon long term exposure. Torrefaction has been shown to have improved the characteristics of biomass in terms of calorific value and hydrophobicity as previously discussed in 3.7 and 3.8 respectively.

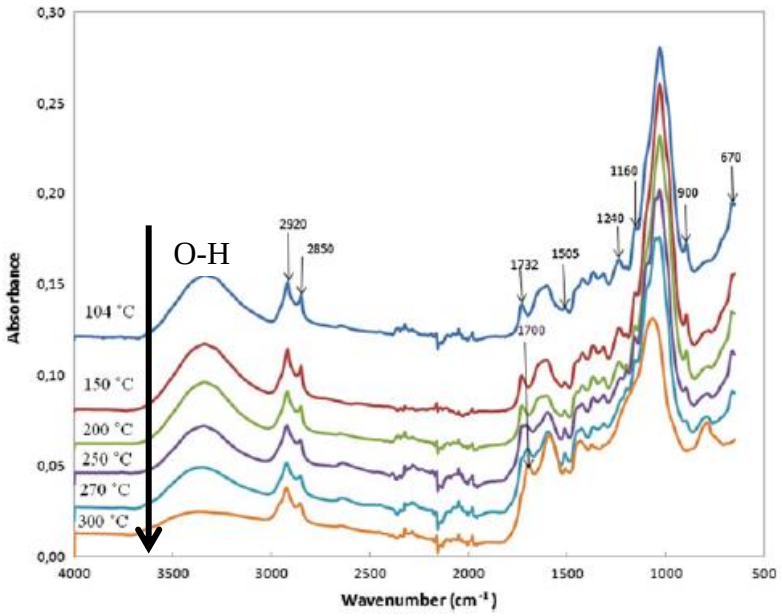

Figure 3.22. ATR-FTIR spectra of torrefied wheat straw samples, where the reduction of O-H bands decreased with increased temperature at 3500-3000 cm^{-1} (Shang *et al*., 2012).

With regards to combustion behaviour, Pentananunt *et al* (1990) carried out a test using methanol flames to compare the combustion characteristics of untreated wood and torrefied wood. The duration of smoking, flame and char combustion were recorded with time as observed in Figure 3.23. The figure shows that when methanol flame was introduced, both samples produced smoke and within the first 5 min, the torrefied wood started to give out flames and stopped smoking on the 10th min. Moreover, the torrefied wood had a faster start of char combustion on the 15^{th} min. The raw wood, however, continued to release smoke almost throughout the burning period even though both samples burned completely at the same time. Furthermore, the raw wood only started to undergo char combustion after the 25^{th} min. With these results, Pentananunt *et al* (1990) concluded that torrefied wood has a higher combustion rate, in which it burns longer without producing much smoke and can serve as a better fuel than wood.

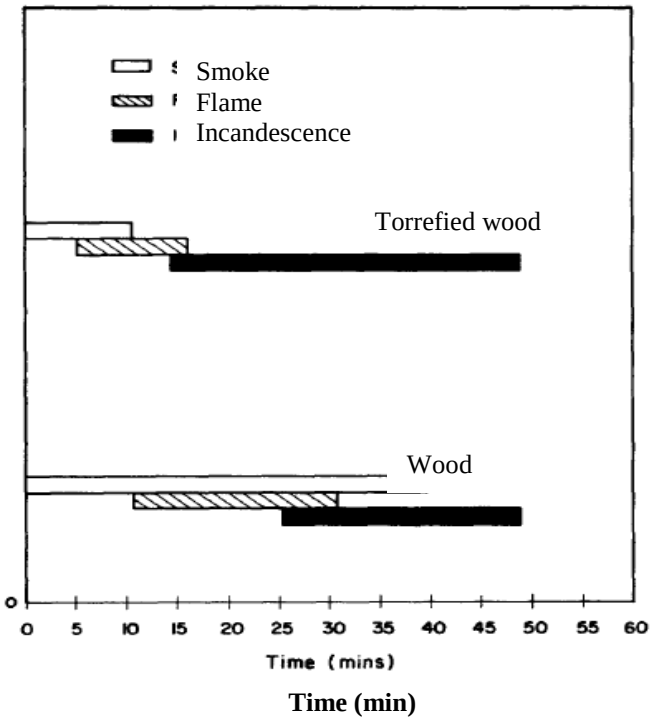

Time (min)

Figure 3.23. Combustion characteristics between torrefied and raw wood (Pentananunt *et al*., 1990).

Bridgeman *et al* (2008) also conducted combustion studies of raw and torrefied willow (particles of 2-4 mm in length) using a Meker burner and natural gas. A steel needle was used to hold each particle adjacent to an R-type thermocouple in a ceramic housing. A Photo-Sonics Phantom V7 high-speed video system was used to record the images of the combusting particles. Images taken were used to observe the combustion behaviour and determine the duration of volatile and char combustion. Figure 3.24 a) and b) illustrate the duration of those two stages of combustion of raw and torrefied willow. The results showed that there was a shorter duration of volatile combustion and longer char combustion for torrefied willow as compared to the raw willow. Bridgeman *et al* (2008) suggested that the overall times for combustions of torrefied willow have increased and this was mainly due to the longer char combustion stage.

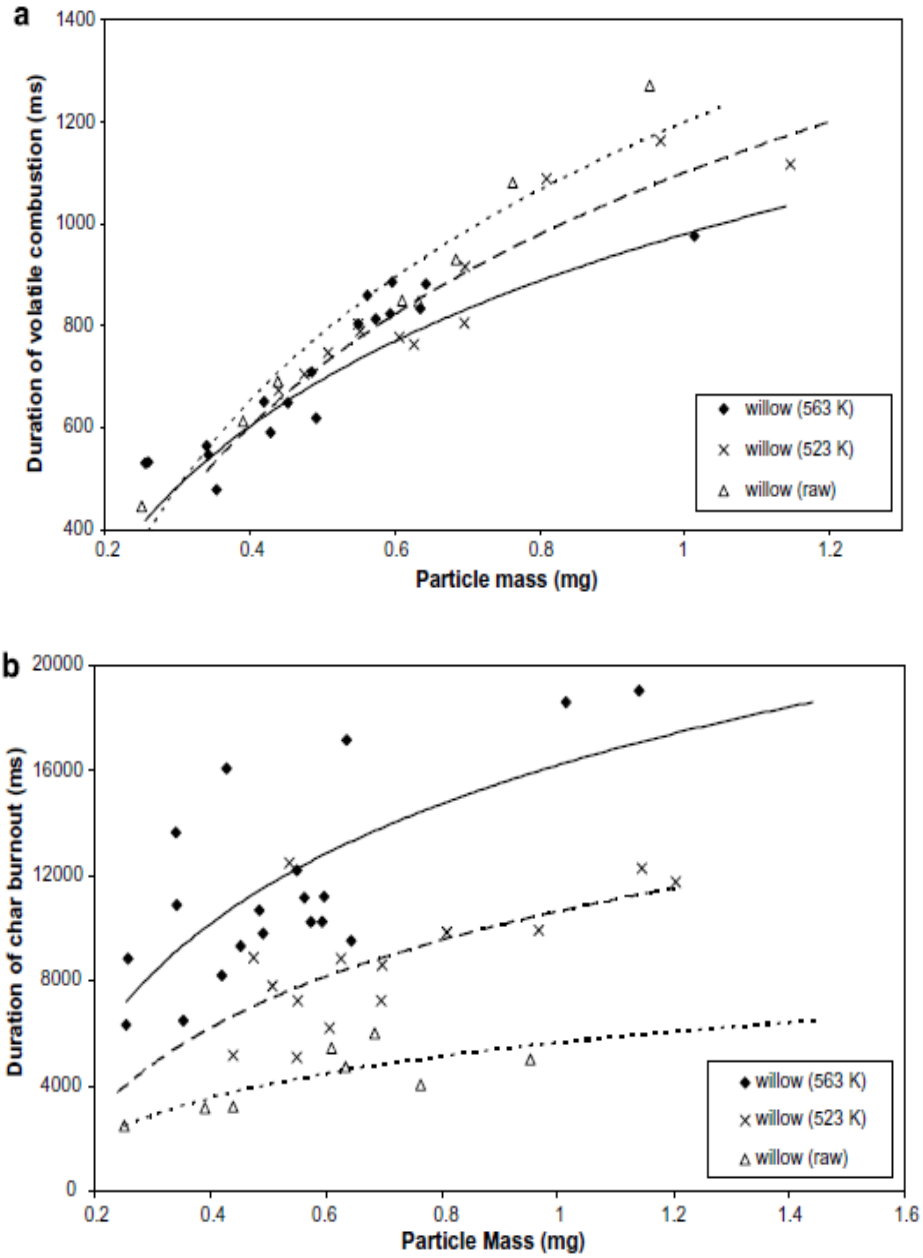

Figure 3.24. Duration of a) volatile combustion and b) char burnout of raw and torrefied willow particles (523 and 563 K) (Bridgeman *et al*., 2008).

3.10 The investigation of the liquid products (tar and condensables) and non-condensable products of torrefaction

Some studies have investigated the composition of volatile products released during torrefaction. Zanzi *et al* (2002) performed torrefaction in a reactor tube that consists of two cylinders, where the sample is placed. Volatiles are cooled in a water condenser, where tar and water phase are condensed, while gases are led through a cotton filter and a gasmeter and eventually, collected in a gas bag. The production of volatile yields ranged from 5-35% (daf

basis), depending on the temperature and residence time as well as the biomass fuels. In terms of volatile composition, this study focused on gaseous products only and were analysed by a gas chromatography specifically for CO_2, CO, N_2, CH_4 and C_2-hydrocarbons (ethane, ethane, ethylene). As a result, carbon dioxide is the most abundant gaseous products compared to the rest. However, the percentage of CO_2 decreased with increased temperature and replaced by the increase in CO, CH_4 and C_2-hydrocarbons. No explanation to this finding is reported in this study. Ferro *et al* (2004) conducted similar torrefaction experiments with agricultural and forest residues and produced similar results on the gaseous compositions. Furthermore, they examined the acidity of the liquid products from the torrefaction of pine at 230ºC to 280ºC. Their results showed an increase acidity of the liquid products from 2 to 3 with increased temperature. They suggested that acetic acid was responsible for the lower pH at the lowest temperature.

Prins *et al* (2006a) provided a detailed description on the instruments they used for collecting and analysing volatile products upon torrefaction of beech, willow, larch and straw. Torrefaction was carried out in a bench-scale unit, which consists of a quartz fixed-bed reactor and used argon to remove volatile products from the reactor. The volatiles were then separated to liquid and gas phases in a cold trap at -5°C, where the gases were collected in a gas bag. Liquid products were diluted with 2-butanol and later analysed with HPLC using a Chrompack Organic Acids column with detection based on refraction index. The gases, on the other hand, were analysed using a Varian Micro GC with a Poraplot Q and a Molsieve column. The results showed that acetic acid and water were the two main liquid products, with smaller quantities of methanol, formic acid, lactic acid, furfural, hydroxyl acetone and traces of phenol. These products were mainly produced from the decomposition of hemicellulose. Water was thought to be released at two mechanisms: during drying and during dehydration reactions between organic molecules (Bridgeman *et al*., 2008). Acetic acid and methanol were respectively formed from acetoxy and methoxy groups attached to hemicellulose sugar monomers and lignin, while other compounds were generated at high temperatures by thermal decomposition of plant polymer monomers (Bergman *et al*., 2005b; Prins *et al*., 2006a; Medic *et al*., 2012). Permanent gases identified were carbon dioxide and carbon monoxide. The release of carbon dioxide can be explained by decarboxylation reaction of acid groups that were attached to hemicellulose (Bergman *et al*., 2005b; Prins *et al*., 2006a; Bridgeman *et al*., 2008; Medic *et al*., 2012).While the formation of carbon

monoxide could be due to the reaction of carbon dioxide and steam with porous char at higher temperatures (White *et al* in Prins *et al*., 2006a).

Recently, Medic *et al* (2012) conducted torrefaction and used glass impingers submerged in an ice bath to separate volatile products to gases and condensable liquids. The gases were then analysed using a GC, that is equipped with a Molsieve 5A and Poraplot U column while the liquid fractions that were collected in glass impingers were separated further to water and organic phases, where they were later analysed using Karl-Fischer method and a GC respectively. Similar results were reported as seen in Prins *et al* (2006a), where they identified the components in volatiles and produced an overall mass balance of torrefaction.

Bridgeman *et al* (2008) torrefied reed canary grass (RCG) at four temperatures (230, 250, 270 and 290ºC) using TGA-FTIR. They looked into the evolution of volatile products with the FTIR and the absorbance of each chosen volatiles is presented in Figure 3.25. In this study, water was the major product, followed by carbon dioxide. Other gaseous products found were carbon monoxide and methane, while condensable organics were formaldehyde, acetaldehyde, acetic acid, formic acid, acetone and methanol. Bridgeman *et al* (2008) also found traces of phenol, furfural and ammonia for the highest temperature.

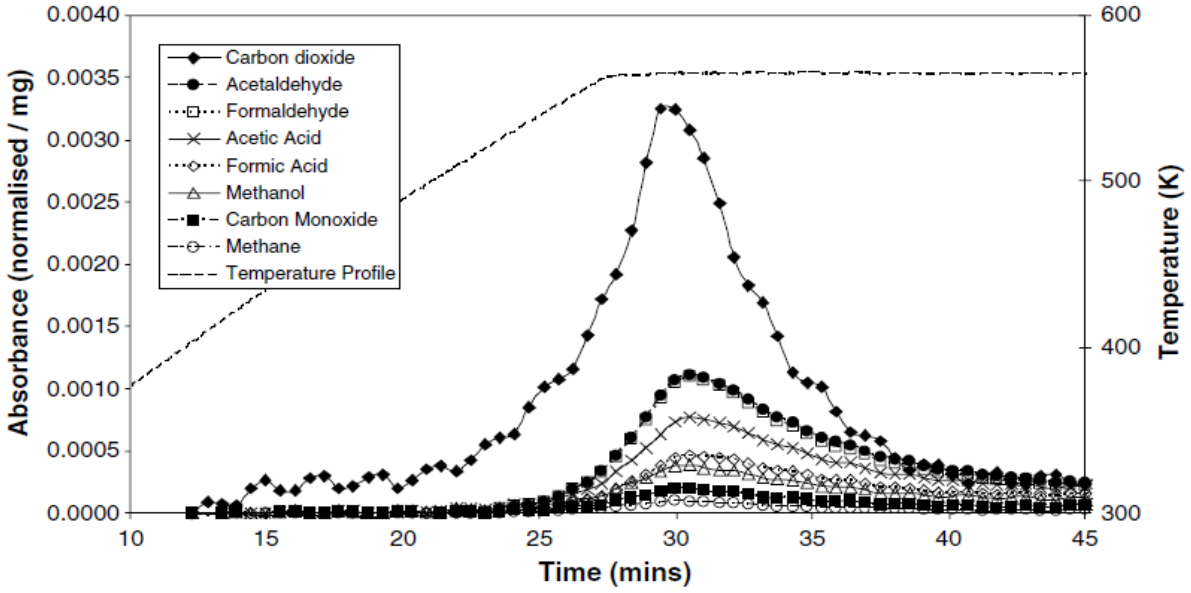

Figure 3.25. Evolution of volatile products during the torrefaction of reed canary grass at 290°C as detected in the FTIR (Bridgeman *et al*., 2008).

Chen *et al* (2011) torrefied wood blocks of Lauan at three temperatures (220, 250 and 280ºC) and as soon as the volatiles left the torrefaction reactor, they were condensed and collected in

the provided collection unit as shown in Figure 1.27. The colours of the liquid from different treatments were observed, which were bright yellow and then brown and darker brown with increased temperature. They explained that this could be due to the sensitive behaviour of volatiles released during torrefaction. The liquid products were analysed using the GC-MS, where species with molecular weight less than 45 were not detected and most of the identified components were found to be aromatics. Water, formic acid, lactic acid and methanol as well as gaseous products were not measured in this study.

The results from GC-MS showed that most of the species found in the condensed liquid were monoaromatics for example phenol, eugenol and vanillin as illustrated accordingly in Figure 3.26. Increasing the temperature triggered the formation of heavier products such as 7,9-dihydroxy-3-methoxy-1-methyl-6H-dibenzo[b,d]pyrane-6-one.

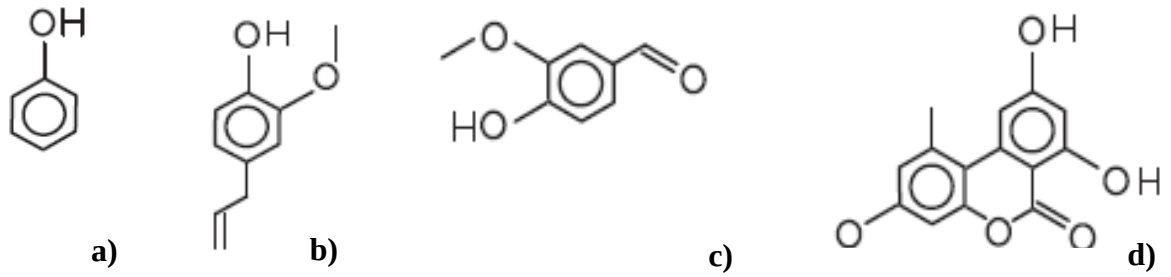

Figure 3.26. Main components contained in condensed liquid, namely a) phenol, b) eugenol, c) vanillin and d) 7,9-dihydroxy-3-methoxy-1-methyl-6H-dibenzo[b,d]pyrane-6-one (Chen *et al*., 2011).

3.11 The use of FG-Biomass model to predict torrefaction

As briefly described in 1.17.3, one of the main sources of inaccuracies and difficulties experienced when modelling the emission behaviour of biomass thermal conversion processes is the lack of data and diversity of biomass (Solomon *et al*., 1991). There are only few accessible kinetic data available on the evolution of individual products during biomass pyrolysis (de Jong *et al*., 2003).

de Jong *et al* (2003) studied slow pyrolysis experiments for two types of biomass, namely pelletised *Miscanthus Gigantheus* and wood using TGA-FTIR. Samples were heated in helium at 10°C min^{-1}. The temperature profile started with a drying period at 80°C for 20 min, followed by pyrolysis up to 900°C, at which was held for 3 min upon reaching the temperature and immediately cooled down to 250°C for 20 min. After cooling, oxygen was

added to the helium and the temperature was raised again to 900°C at 30°C min^{-1} to carry out the char combustion. This profile was repeated at pyrolysis heating rates of 30 and 100°C min^{-1}. Concentrations of volatiles could be obtained from the infra-red spectrum based on calibration runs with pure compounds (which were not mentioned in the article), while yields of tar were determined by taking the differences using the sum of gases quantified by FTIR and the balance curve obtained by the TGA (de Jong *et al*., 2003). In this study, kinetic rates for species evolution were also determined and used as input files for (FG–DVC) biomass pyrolysis model.

The results showed that yields of condensables increased while those of CO_2, CO and acetaldehyde (CH_3CHO) decreased with increased heating rates. There were 12 other volatile species studied, that is methane (CH_4), ethylene (C_2H_4), hydrogen cyanide (HCN), ammonia (NH_3), isocyanic acid (HNCO), carbonyl sulphide (COS), sulphur dioxide (SO_2), formaldehyde (CH_2O), methanol (CH_3OH), formic acid (HCOOH), acetic acid (CH_3COOH), phenol (C_6H_5OH) and acetone (CH_3OCH_3).

With regards to FG-DVC model, it was originally developed by AFR to describe coal thermal decomposition by predicting the product distribution, extract yields, cross-link density, molecular weight distribution and fluidity as a function of coal rank, heating rate and pressure (de Jong *et al*., 2003). FG describes the gas evolution, compositions of the subject in terms of elemental and functional groups while DVC determines the amount and molecular weight of macromolecular fragments (de Jong *et al*., 2003). The DVC is de-emphasised when dealing with biomass because tar is treated just like any other volatile species in the biomass model. Figure 3.27 compares the evolution rates and yields of products from pyrolysis of wood between those obtained in TG-FTIR and those predicted by the FG-DVC model. It shows that the model correctly simulates the results for species such as water, methane, carbon dioxide and carbon monoxide while other species were difficult to fit with the experimental data.

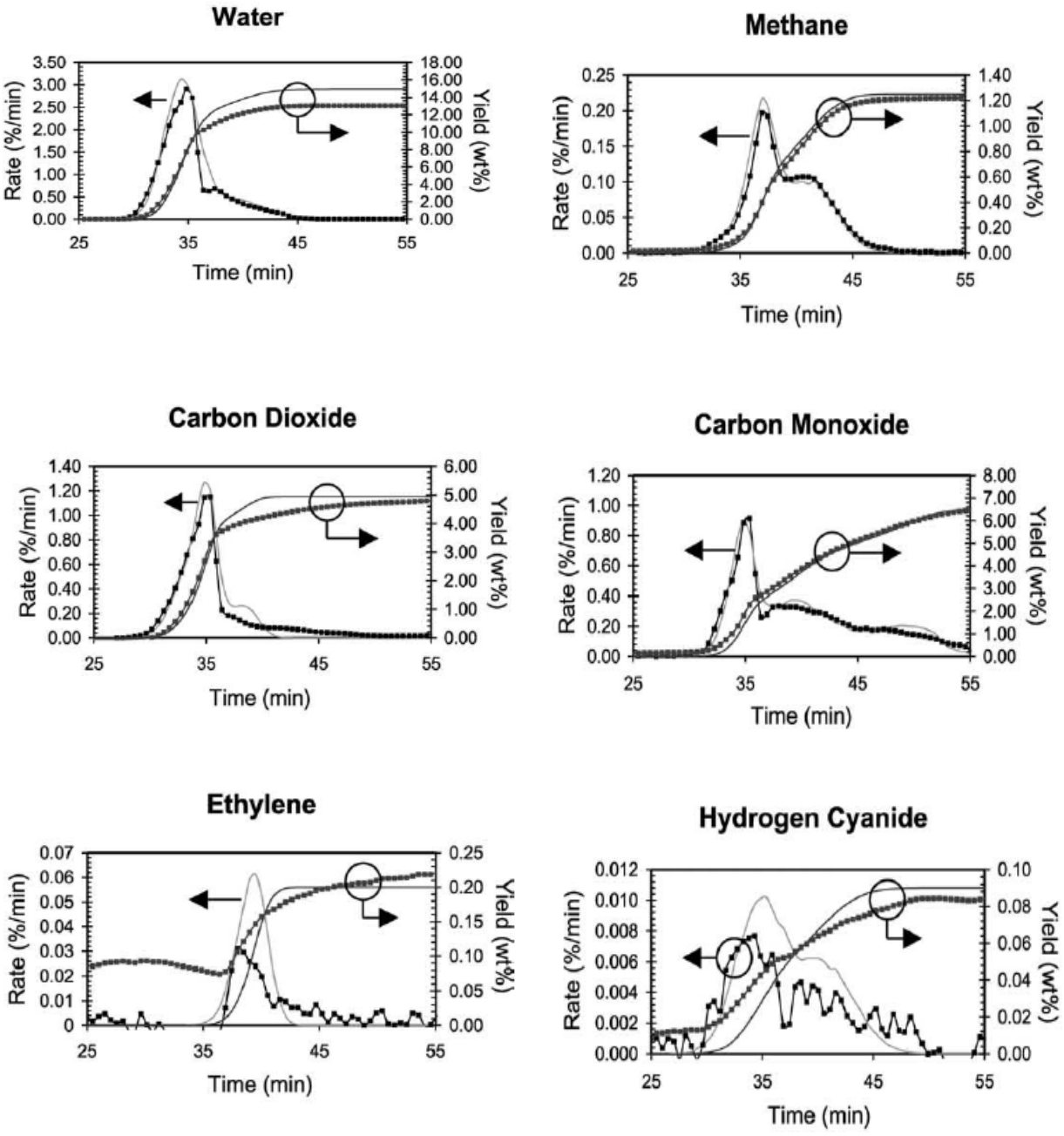

Figure 3.27. Comparison between the results of TG-FTIR and FG-DVC model for evolution rates and yields obtained from pyrolysis of wood pellets (de Jong *et al*., 2003).

3.12 Conclusions

Past literature reviews suggest that torrefaction is indeed a promising technique that can improve the performance of biomass fuels for future energy utilisation. This chapter highlights possible areas that require further research as there are noticeable gaps and remains of information that has not been studied in sufficient detail.

When this project began in the late 2010, most literatures focussed on the solid torrefied biomass. Standard characteristics of the torrefied fuel such as the colour, shape, size, moisture content, heating value and main elemental compositions were some of the common investigations that were carried out. Less attention was paid towards the change in its morphology composition and in depth look at its physical and chemical characteristics. Therefore, spectroscopic instruments, for example, Fourier Transform Infrared Spectroscopy and X-ray Photoelectron Spectroscopy and microscopies, namely, Scanning Electron Microscopy and Transmission Electron Microscopy as well as Brunauer-Emmett-Teller Surface Area Analysis were used thoroughly in this study.

Grindability behaviour of torrefied biomass in comparison to the untreated biomass was also of great interest in this project. The performance of grindability behaviour of a biomass fuel is crucial in power stations and pellet production for energy saving and maintenance costs especially in entrained-flow gasification and co-firing. Apart from that, great understanding of optimum torrefaction conditions is important to produce a torrefied biomass fuel that contains energy yield/density that is suitable for an efficient energy use. There has been increasing interests in designing a matrix approach that involves torrefaction parameters such as temperature, residence time and particle size. In this project, a continued research was developed, where the implication of Hardgrove Grindability Index was applied through correlations between the HGI_{equiv} and carbon content, mass yields and energy yields.

There is also a limited research on the analysis of volatile products. There are studies that have successfully identified the gaseous and liquid products using GC-MS and TGA-FTIR, where samples were in powdered form, particles with less than 5 mm and some were in blocks. Many pyrolysis studies of biomass found the existence of mass and heat transfer limitations in bigger particle sizes upon higher temperature pyrolysis. Few studies have examined the influence of particle sizes on torrefaction. The primary focus of one of the researches was to determine the influence of particle sizes in terms of mass and energy yields. Some aimed to develop a kinetic model for torrefaction. In this project, the impact of different particle sizes on torrefaction with respect to the evolution of main volatiles as well as the properties of the torrefied biomass was investigated. This project develops method for the TGA-FTIR, where calibrations of FTIR for main gases were conducted.

Collection of liquid products involved condensation upon release from torrefaction reactor but not many literature reviews have described how it was done. In this project, laboratory methods for collection of liquids were developed, where few cold traps will be utilised. Characterisation of liquid products was investigated quite thoroughly, in which literatures are lacking. Liquids were separated into two phases: tar (organic) and water phase, where each phase was analysed differently.

Torrefaction modelling was implemented in this project through a software program, FG-Biomass to simulate the decomposition of biomass fuels during thermal treatment. It is able to predict the yields and rates of evolution of char, moisture, gases and other condensable organics with calculations. The output allows the comparison between the results obtained experimentally using the reactor and TGA-FTIR.

Finally, a short investigation on the combustion behaviour of torrefied biomass fuels was carried out for this thesis. To date, there are still gaps on how these torrefied biomass fuels respond to combustion. Similar experiments were carried out as those conducted by Bridgeman *et al* (2010), where they used a Meker burner flame. The approximate heating rate of the flame experienced by the biomass particles was determined with the use of FG-Biomass model. The rate of char combustion was predicted using the kinetic parameters determined by Jones *et al* (2012).

CHAPTER 4

EXPERIMENTAL PROCEDURES

4.1 Samples

Figure 4.1 displays the fuels studied, which consists of willow, eucalyptus, a mixture of hardwoods (oak and birch) and a mixture of softwoods (spruce, pine and larch). The samples were sourced from farms around Yorkshire, UK in the form of chips in the size range of 10 mm to 50 mm.

a) Willow

b) Eucalyptus

c) Hardwood (Oak and birch)

d) Softwood (Spruce, pine and larch)

Figure 4.1. Woody biomass samples used in this study.

4.2 Sample preparation for torrefaction using TGA-FTIR

Willow (*Salix spp*.) and eucalyptus (*Eucalyptus Gunnii*) were the samples used for the study of the influence of particle sizes on torrefaction of woody biomass (Chapter 6). The barks were removed and the resultant white woods were cut into cubes and cuboids of different sizes (sorted in an ascending order): 5x5x5 mm, 6x6x6 mm, 5x5x10 mm, 7x7x7 mm, 6x6x10 mm, 7x7x10 mm and 8x8x8 mm.

4.3 Torrefaction procedures

4.3.1 Torrefaction using the bench scale reactor

The bench scale reactor was used for torrefaction experiments in Chapter 5. Four biomass fuels shown in Figure 4.1 were treated in a three zone tube furnace as displayed in Figure 4.2. It has an internal diameter of 75 mm and is 750 mm long and contained a reactor tube, with an internal diameter of 60 mm and 800 mm in length. Approximately 100 g of biomass was packed inside the reactor tube and placed in position between two glass wool plugs as shown in Figure 4.3. Figure 4.4 displays the positions of three thermocouples at about 20 cm intervals inside the reactor tube with a purpose to record the inlet gas temperature, bed temperature and outlet gas temperatures. Nitrogen, with a flow rate of 1.2 mL min^{-1}, was supplied to the reactor to ensure a continuous inert atmosphere throughout the experiment. Samples were initially dried at 150ºC for 60 min, followed by further heating at a rate of 10ºC min^{-1} to the final temperature. The final temperatures and residence times used are listed in Table 4.1. Here, the residence time is taken as the time at which the treatment dwells at the maximum reaction temperature, after which the samples were rapidly quenched under nitrogen flow to prevent further reaction. However, it was noted that the cooling stage exhibited a sample dependency, and cooling to below 200ºC could be of significant duration. Therefore, strictly speaking the residence times were between 10-20 min longer than intended. The final temperature in the centre of the bed was also noted to be higher than the set point (up to 20°C higher), indicating the torrefaction process can be exothermic. The resulted torrefied product was weighed and the mass yield, η_m was calculated as percentage of the original mass sample, as follows

$$\eta_m = \frac{(m_{treated})}{m_{raw}} \times 100 \qquad (4.1)$$

where $m_{treated}$ is the mass of the torrefied product and m_{raw} is the mass of the untreated biomass (Bridgeman *et al.*, 2010).

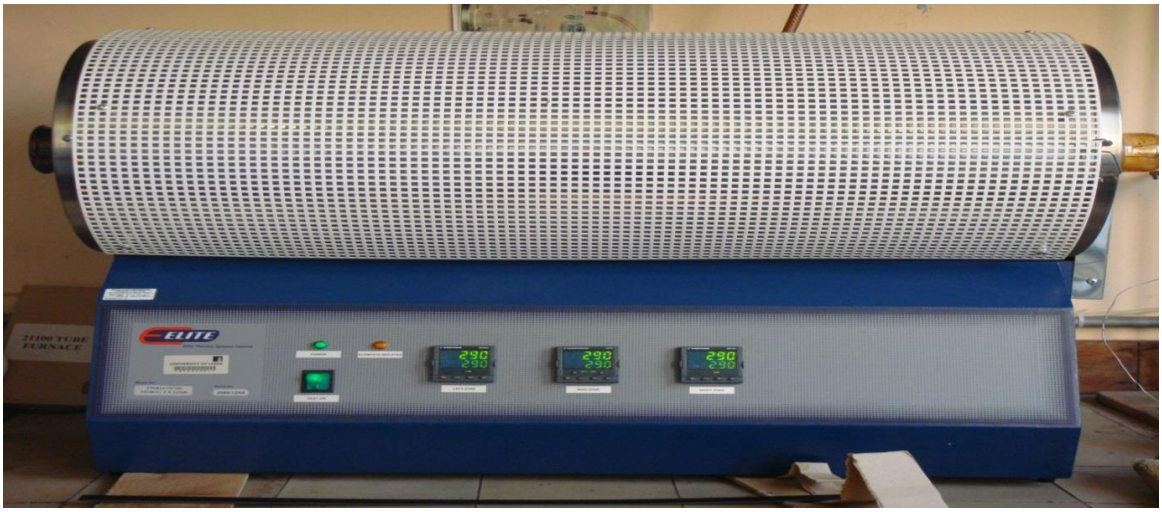

Figure 4.2. A longitudinal rig furnace that is equipped with three temperature zones to allow maximum temperature control used for torrefaction.

Figure 4.3. How biomass fuels are positioned inside the reactor tube. The biomass shown in the above picture is eucalyptus.

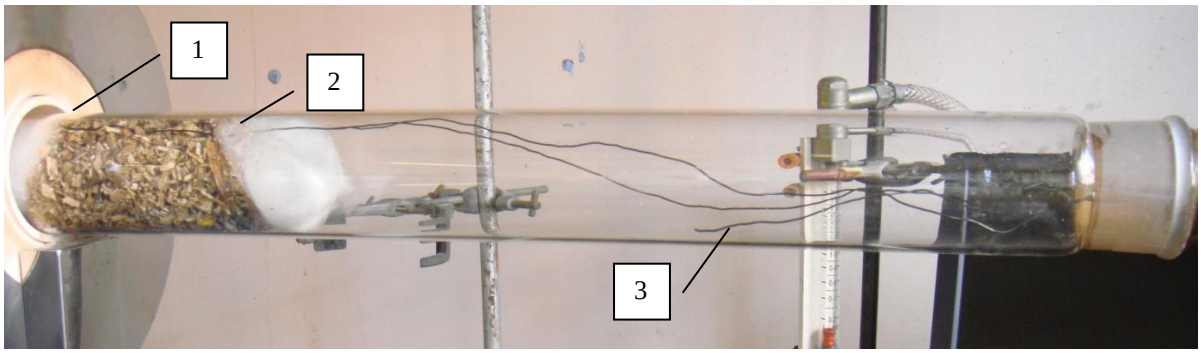

Figure 4.4. How thermocouples are arranged in the tube. The longest (1) thermocouple is located near to the glass wool on the left. The second (2) goes to the other wool and the last (3) one is 20 cm away from the second as pointed out in the figure.

Table 4.1. Conditions used in this study.

Condition	Temperature/ºC	Residence time/min
A	270	30
B	270	60
C	290	30

In this research, the overall mass balances for the torrefaction of the investigated biomass fuels were investigated. Figure 4.5 illustrates the traps used to collect liquid products and how the last trap was connected to a gas chromatography (Perkin Elmer Autosystem XL GC) as shown in Figure 4.6, where methane, carbon dioxide and carbon monoxide were detected (unfortunately, it is important to note that these gaseous products were unsuccessfully quantified due to technical errors). The condenser that was connected to the other end of the reactor tube was also connected to a chiller (that was set to 0°C), where it was then attached to three types of traps. Traps were filled as described in Figure 4.6 to trap tars and volatiles that could cause blockage to the GC. The GC was connected to this last trap and was set to operate 5 min before the drying period ended.

Each of the collecting round bottom flasks for the first, second and third traps were weighed, together with their respective stoppers before and after torrefaction. For health and safety reasons, the next steps were all done in the fume cupboard. After weighing, liquid contents were poured into a 100 mL separating funnel. Any leftover liquids in the flasks were washed with 10 mL of dichloromethane (DCM) and poured into the funnel. Added volume of DCM was used to wash the condenser as some tars were seen stuck on the sides and later poured into the same funnel. These mixtures were shaken for a few seconds and left to stand to allow the separation of two layers. The bottom layer represents the organic phase while the top represents the aqueous fraction. A 100 mL of beaker was weighed and filled with the bottom layer of the mixture. The top layer was transferred into a weighed glass vial. Both the beaker and the vial were left in the fume cupboard for evaporation to ensure that no DCM was contained in these liquids. It took about three to four days for the evaporation to complete. Light-weighted volatiles may also be lost at this stage. Beakers and vials were weighed every day until the weights appeared constant. Analysis of these liquids will be revisited in Section 4.6.

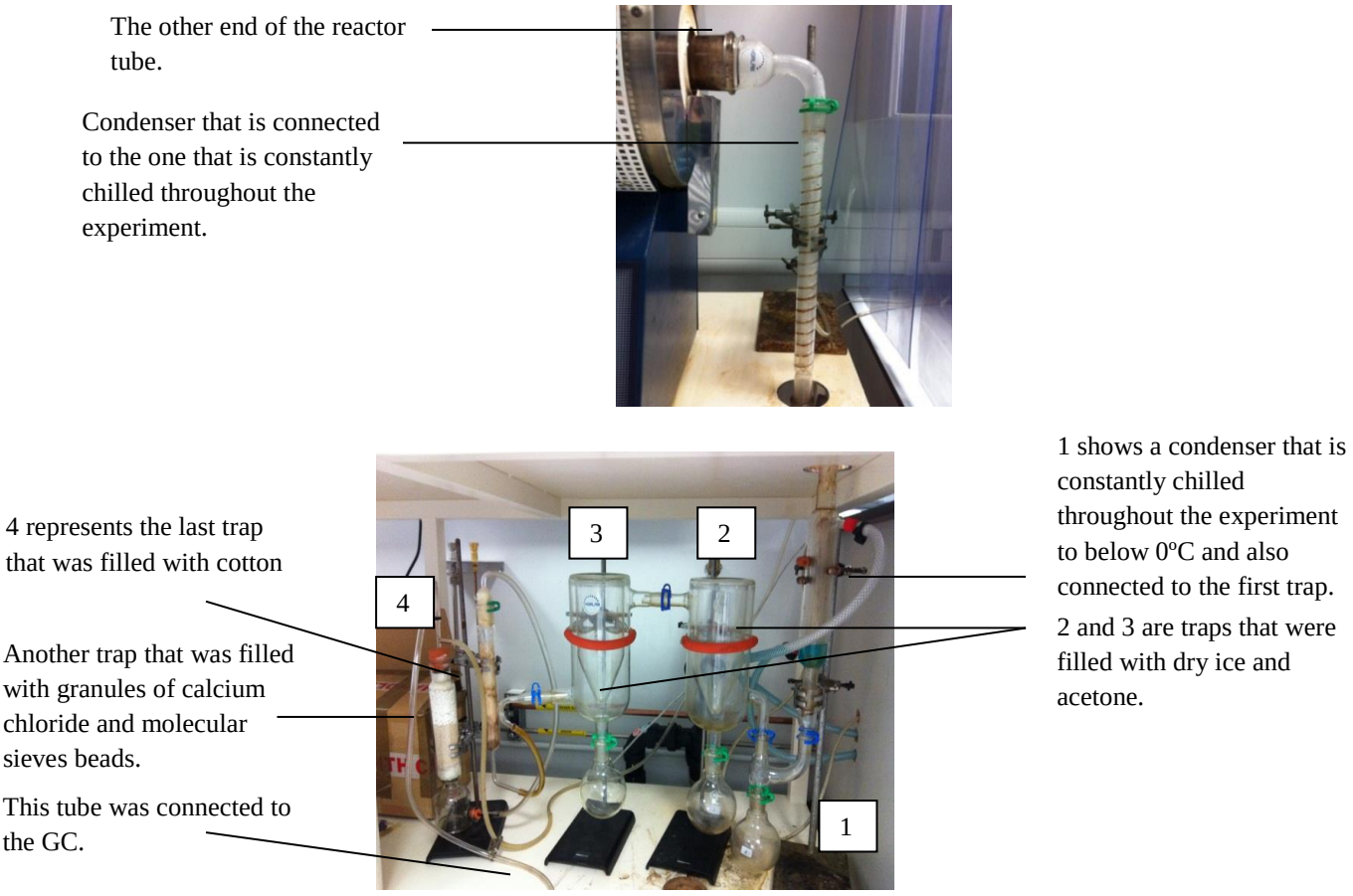

Figure 4.5. Apparatus used for the collection of liquid products.

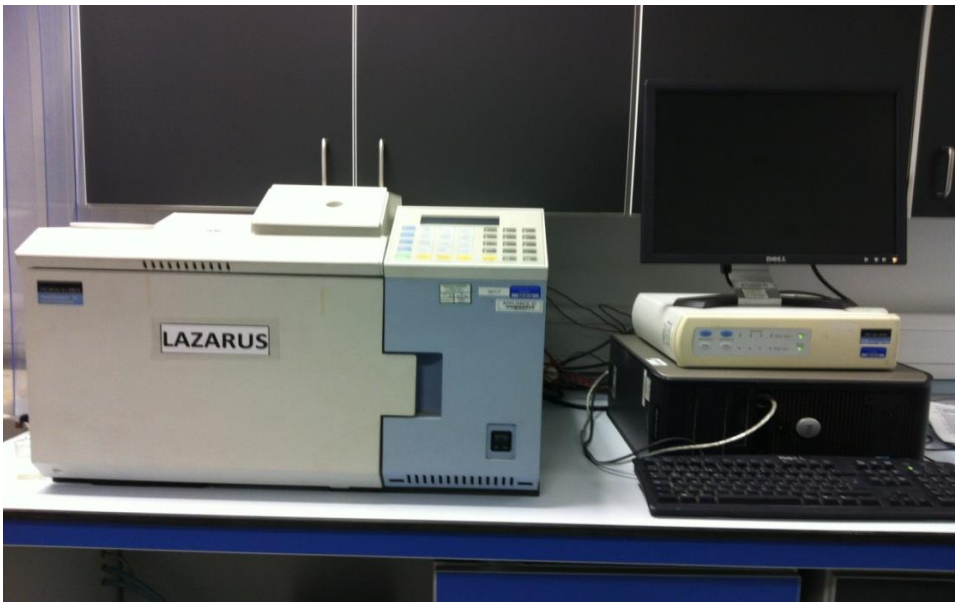

Figure 4.6. Perkin Elmer Autosystem XL Gas chromatograph that was used to detect the permanent gases (CH_4, CO_2 and CO).

4.4 Fuel characterisation

The yields of products of torrefaction (solid, liquid and gases) of willow, a mixture of softwoods and a mixture of hardwoods obtained from using the bench scale reactor were collectively analysed to produce overall mass balances for each biomass fuels. The treatment applied for this study was condition C.

For torrefaction of eucalyptus in a bench scale reactor, the torrefied solids were the only products that were collected due to sample availability. Most of the eucalyptus samples were used for the investigation of the 'Physicochemical Properties of Solid Torrefied Biomass' in Chapter 5.

Figure 4.7 illustrates a flow diagram of the different types of analysis that were carried out to determine the characterisation of products of torrefaction in this study.

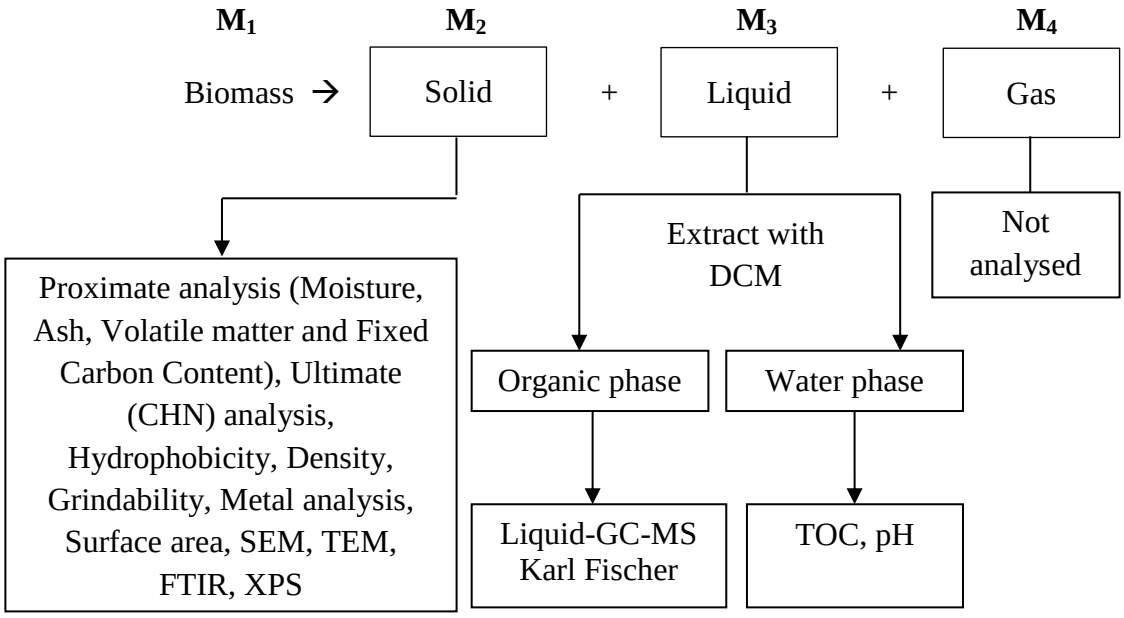

Figure 4.7. Flow diagram of different types of analysis carried out for characterisation of torrefied products, where M_1, M_2, M_3 and M_4 represent the masses of biomass before torrefaction and its respective products.

In order to determine the overall mass balances of torrefaction of biomass, mass yields of the torrefied products are calculated as:

$$\text{Solid yield (as received)} = \frac{M_2}{M_1} \times 100 \qquad (4.2)$$

where M_1 is the mass of biomass before torrefaction and M_2 is the mass of torrefied biomass. Both are as received.

$$\text{Liquid yield (total)} = \frac{M_3}{M_1} \times 100 \quad (4.3)$$

where M_3 is the total mass of organic phase, M_o and water phase, M_w that comprised the contents of the liquid.

The mass yields of organic and water phases can be expressed as follows:

$$M_o = \frac{M_{3a}}{M_1} \times 100 \qquad M_w = \frac{M_{3b}}{M_1} \times 100$$

where M_{3a} and M_{3b} are masses of collected organic and water phases respectively.

$$\text{Gas yield} = \frac{M_1 - M_2 - M_3}{M_1} \times 100 \quad (4.4)$$

4.4.1 Proximate analysis using British Standard methods

Determination of moisture, ash and volatile matter content were carried out based on the methods laid out in the British standards DD CEN/TS 14775:2004, DD CEN/TS 15148:2005 and DD CEN/TS 14774-2:2004 respectively. These determinations were carried out in duplicates and the mean values were taken for further analysis. These determinations were done for samples studied in Chapter 5 only.

4.4.1.1 Moisture content, M_{ad}

A minimum of 1 g of the ground sample was added into a flat dish in an even layer and this was weighed together with its lid on to the nearest 0.0001 g. The uncovered dish and lid was heated separately in the oven at (105±2)ºC for two to three hours. After drying, the lid was replaced while the dish was still in the oven. They were allowed to cool at the room temperature in a desiccator and reweighed.

M_{ad} is expressed as percentage by mass and calculated using the formula equated below:

$$M_{ad} = \frac{(m_2 - m_3)}{(m_2 - m_1)} \times 100 \quad (4.5)$$

where,

m_1 is the mass of the empty dish plus lid,

m_2 is the mass of the dish plus lid and sample before drying and

m_3 is the mass of the dish plus lid and sample after drying.

4.4.1.2 Ash content, A_d

A minimum of 1 g of ground sample was added into a crucible in an even layer and this was weighed to the nearest 0.0001 g. The crucible was then heated into a furnace at 250ºC for 60 min and raised to (550±10)ºC for another two to three hours. In the end, the crucible was allowed to cool and then weighed.

$\boldsymbol{A_d}$ is expressed as percentage by mass on a dry basis and calculated using the formula equated below:

$$\boldsymbol{A_d} = \left[\frac{(m_3 - m_1)}{(m_2 - m_1)}\right] \text{ x } 100 \text{ x } \left[\frac{100}{(100 - M_{ad})}\right] \quad (4.6)$$

where,

m_1 is the mass of the empty crucible,

m_2 is the mass of the crucible and sample before ashing,

m_3 is the mass of the crucible and sample after ashing and

M_{ad} is the moisture content (%) of the test sample used for determination.

4.4.1.3 Volatile matter content, V_d

A minimum of 1 g of ground sample was added into a crucible in an even layer and this was weighed together with its lid to the nearest 0.0001 g. The covered crucible was heated in the furnace at (900±10)ºC for seven minutes. Then the crucible was left to cool to room temperature and reweighed.

$\boldsymbol{V_d}$ is expressed as percentage by mass on a dry basis and calculated using the formula equated below:

$$\boldsymbol{V_d} = \left[\frac{100\ (m_2 - m_3) - M_{ad}}{(m_2 - m_1)}\right] \text{ x } \left[\frac{100}{(100 - M_{ad})}\right] \quad (4.7)$$

where,

m_1 is the mass of the empty crucible and lid,

m_2 is the mass of the crucible and lid plus sample before heating,

m_3 is the mass of the crucible and lid plus sample after heating and

M_{ad} is the moisture content (%) of the test sample used for determination.

4.4.1.4 Fixed carbon content, *FCC*

Fixed carbon content (dry basis) can be determined using the following equation by difference:

$$\boldsymbol{FCC} = 100 - \%\, M_{ad} - \%\, A_d - \%\, V_d \qquad (4.8)$$

4.4.2 Proximate analysis using the Thermogravimetric Analyser (TGA)

Proximate analysis can also be determined by pyrolysis tests using a TGA Q5000 analyser (Figure 4.8) by heating to a final temperature of 900ºC at 10ºC min^{-1} under nitrogen with a holding time of 10 min. After this time, the gas was switched to air in order to obtain the ash content. Figure 1.16 illustrates the data obtained from these tests which includes the moisture, volatile, fixed carbon and ash contents of biomass samples. These determinations were carried out for samples studied in Chapter 6 that were involved in the investigation of the influence of particle sizes.

Figure 4.8. TGA Q5000 analyser.

4.4.3 Ultimate analysis

The elemental composition, C, H and N contents were measured using CE Instruments Flash EA 1112 Series elemental analyser as pictured in Figure 4.9. Samples were ground and sieved to particle sizes of less than 1 mm in accordance with the requirements to do an ultimate analysis. Each was then weighed to 3-4 mg, wrapped in tin capsules and dropped into the chamber inside the analyser. Each sample was carried out in duplicates.

Carbon dioxide, water vapour and nitrogen dioxide were produced and separated into a chromatography column. Each quantity was detected using a thermal conductivity detector and compared with standards to determine the percentage of carbon, hydrogen and nitrogen.

Standards used in this project were 2, 5 – (Bis (5-tert-butyl-2-benzo-oxazol-2-yl) thiophene (BBOT) and Oatmeal. Since all measurements were done in duplicates, the mean values were calculated. The O content was also taken into consideration in the determination of this type of analysis. It was measured by difference (dry ash free basis), provided that all the contents of C, H and N were also corrected to dry ash free.

$$\text{wt \% O} = 100 - \text{wt \% C} - \text{wt \% H} - \text{wt \% N} \quad (4.9)$$

Figure 4.9. CE Instruments Flash EA 1112 Series elemental analyser.

4.4.4 Calorific value determination

Friedl *et al* (2005) selected a data of 154 biomass samples (a subset of 122 samples) to investigate the correlation between heating values of biomass and elemental composition. Samples were grouped according to the type of biomass. The determination of C, H, N, S, Cl, ash and high heating values (HHV) were carried out as detailed in Friedl *et al* (2005).

A method using two equations to calculate HHV (dry basis) based on C, H and N contents were then resulted: an ordinary least squares regression (OLS) and a particle least squares regression (PLS) method as displayed in (10) and (11) respectively:

$$\text{HHV (OLS)} = 1.87C^2 - 144C - 2802H + 63.8CH + 129N + 20147 \quad (4.10)$$

$$\text{HHV (PLS)} = 5.22C^2 - 319C - 1647H + 38.6CH + 133N + 21028 \quad (4.11)$$

C, H and N contents were expressed on a dry basis in terms of percentage and the units were in kJ kg^{-1}. The results showed that the application of both models to the data of all 122 samples for HHV gave almost the same performance. Therefore, the average of both HHV was used to form a final model for the determination of the calorific value of a biomass, as equated in Equation (4.12):

$$HHV = 3.55C^2 – 232C – 2230H + 51.2CH + 131N + 20600 \quad (4.12)$$

The model gave a standard error of calibration of 337 kJ kg^{-1} and a R^2 of 0.943. Bridgeman *et al* (2010) tested this correlation for torrefied willow and found that inaccuracies may be resulted due to the high carbon content of the torrefied fuel. Therefore, in their study, calorific values were further determined using the Bomb calorimetry analysis to validate the calculated values. Those with carbon contents that were greater than 50.5% (dry basis) were further validated and the authors discovered that the measurements were comparable with differences that ranged from 300 to 600 kJ kg^{-1} (Table 4.2).

Table 4.2. Calculated and measured HHV of different conditions of torrefied willow (Bridgeman *et al*., 2010).

Sample	**Condition**		**% Carbon content**	**HHV kJ kg^{-1} (dry basis)**		
	T (°C)	**t (min)**	**(daf basis)**	**Calculated**	**Measured**	**Differences**
Willow A	290	10	56.5	22400	21800	600
Willow B	230-250	60	54.3	21400	21000	400
Willow D	290	60	60.3	23900	23600	300

In this research, high heating values (HHV) of raw and torrefied biomass fuels were calculated using the formula suggested by Friedl *et al* (2005) as equated in Equation (4.12). Since the findings in Bridgeman et al showed comparable results between those calculated using Friedl *et al*'s equation and those obtained from the bomb calorimeter, comparisons between the two methods were not carried out in this thesis.

4.4.5 Energy yield, η_E

Energy yields of studied fuels were determined based on the formula as equated by Bergman *et al* (2005):

$$\eta_E = \eta_m \times \frac{HHV_{treated}}{HHV_{raw}} \quad (4.13)$$

where η_m is the mass yield of the torrefied biomass, HHV_{raw} is the high heating value of the raw biomass and $HHV_{treated}$ is that of the torrefied biomass.

4.4.6 Hydrophobicity

To compare the hydrophobicity of the fuels, approximately 0.5 g of biomass (particle size < 1 mm) were immersed in deionised water at room temperature in a sintered glass filter for two hours, followed by air drying for an hour, prior to the determination of its moisture content. Figure 4.10 illustrates how the apparatus were assembled for hydrophobicity.

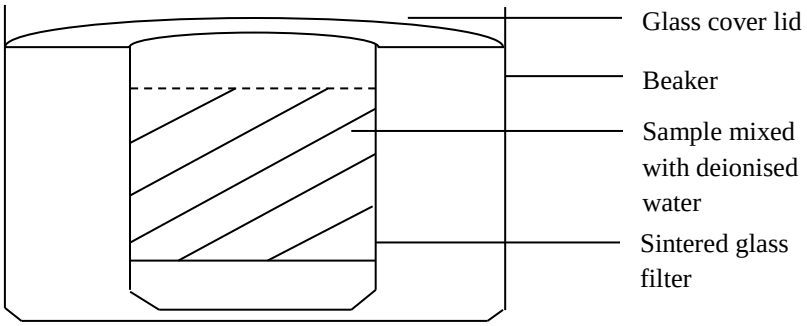

Figure 4.10. The set up to test the hydrophobicity of the biomass fuels.

4.4.7 Density

Measurements to determine the density of the biomass samples were attempted using the water displacement method in accordance to the wood density protocol by Osazuwa-Peters & Zanne (2011). Wood chips were oven-dried overnight and weighed prior to this experiment. Each wood chip was attached to a needle and taped onto a stick and rod as shown in Figure 4.11. The beaker was filled with deionised water and placed on a balance. The balance was tared and the wood was then immersed into the water, making sure that the top of the wood was below the meniscus and not touching the sides of the beaker. According to the protocol (2011), the mass of water displaced by the wood is equivalent to the fresh volume of the wood, assuming that the density of water is equal to 1 g cm^{-3}. The mass of wood was taken right after the immersion.

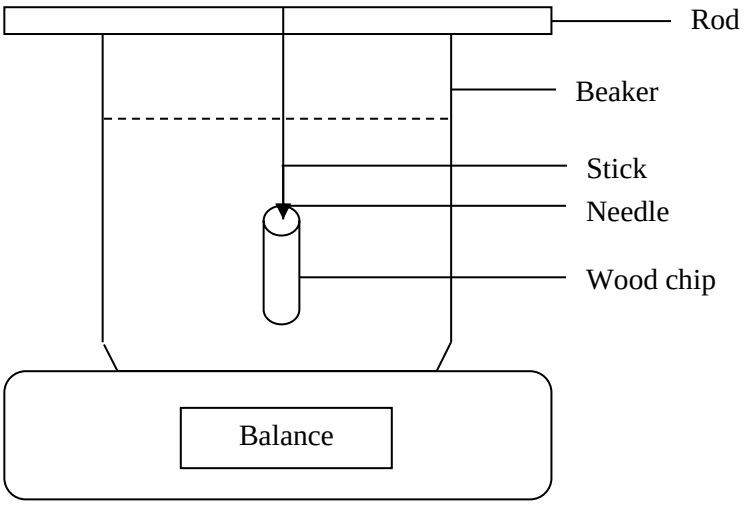

Figure 4.11. The set up to determine the density of each biomass fuel.

4.4.8 Grindability tests

4.4.8.1 Calibration of Retsch PM 100 ball mill

To compare the grindability properties of the fuels, a modified version of the Hardgrove Grindability Index (HGI) was used, as detailed in Bridgeman *et al* (2010). In this approach, the same fixed volume (50 cm^3) for each coal and biomass samples was used (Agus and Waters, 1971; Joshi, 1979) instead of a fixed weight. Additionally, a bigger mill size (500 mL) was used than the one originally stated in the method (i.e. 250 mL).

For this purpose, a Retsch PM 100 ball mill (Figure 4.12 c) was re-calibrated with coals of known HGI values (32, 49, 66 and 92), as described in Bridgeman *et al* (2010). Each standard reference coal was milled using a Retsch cutting mill SM 100 (Figure 4.12 a), using a 4 mm screen mesh. The coal was then sieved using a stack of 1.18 mm and 600 µm sieves using a Retsch Sieve Shaker AS 200 Basic (Figure 4.12 b) at amplitude of 80 for 5 min. A volume of 50 cm^3 of the coal collected on the 600 µm sieve was measured using a measuring cylinder and transferred to a 500 mL milling cup and further ground in the ball mill. The coal was sieved again using a 75 µm sieve and shaken at the same amplitude as before for 5 min using the sieve shaker as shown in Figure 4.12 b). The speed and time taken to sieve at this stage were the same as the rest of the coal and studied biomass fuels for comparison purposes. The mass, *m* that passed through 75 µm sieve can be calculated using the formula equated below:

$$m = m_v - m_1 \qquad (4.14)$$

where m_v is the mass of coal or biomass fuel that was measured up to 50 cm^3 and m_1 is the mass of coal or biomass fuel that was collected on the 75 µm sieve.

This process was carried out three to four times, depending on the consistency of the results and an average from those results could be calculated. If the mass loss was greater than 0.5 g, the procedure has to be repeated. Figure 4.13 shows the plot of the percentage of sample that passed through a 75 µm sieve against the HGI values for the four coals used to calibrate the 500 mL ball mill. The linear fit was then used to determine the equivalent HGI of the biomass tested as shown in equation (4.15).

$$HGI_{equiv} = \frac{(m_{\%} + 11.205)}{0.4955} \qquad (4.15)$$

where $m_{\%}$ is the percentage mass of sample that passed through the 75 µm sieve.

a)

b)

c)

Figure 4.12. a) Retsch cutting mill SM 100, b) Stack of sieves of 600, 355, 212, 150, 75 and 53 µm on an Retsch Mechanical Sieve Shaker AS 200 Basic for particle size distribution experiment and c) Retsch PM 100 ball mill, that is equipped with 20 steel balls and 500 mL milling cup.

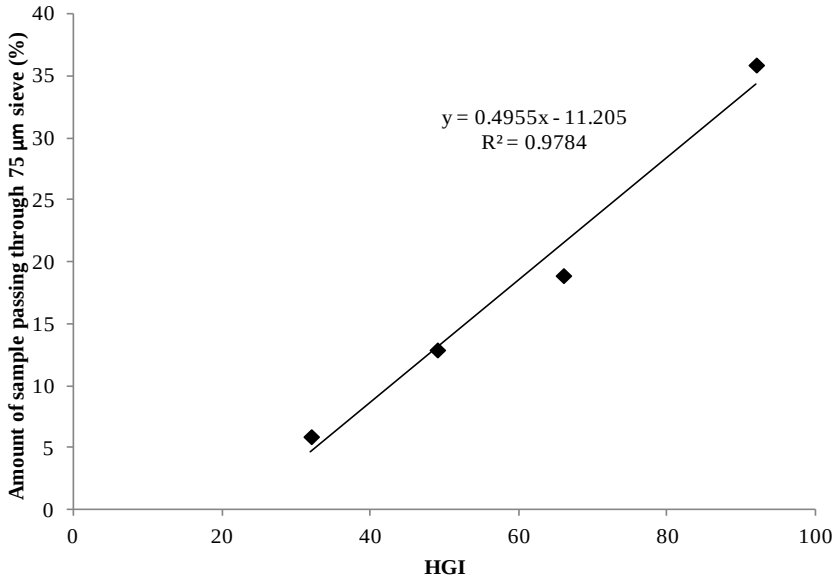

Figure 4.13. Calibration curve of the Retsch PM100 mill (500 mL) using four standard coals of known HGI values of 32, 49, 66 and 92.

4.4.8.2 Particle size distribution

The particle size distribution profiles for the raw and torrefied fuels in comparison to coals were assessed to give a greater insight into their grindability behaviour, using the method described in Bridgeman *et al* (2010). After the sample was shaken on a series of 1.18 nm and 600 µm sieves using the sieve shaker at amplitude of 80 for 5 min, the sample collected on the 600 µm sieve was measured up to 50 cm^3 of measuring cylinder and weighed. Then, it was further ground in the ball mill and sieved using a series of sieves of mesh sizes 600, 355, 212, 150, 75 and 53 µm as stacked in Figure 4.12 b). The mass of sample collected on each sieve was measured and recorded as a percentage of the original mass sample.

4.4.9 Ash metal analysis

Ash metal analysis was carried out at TES Bretby Ltd. Ashes were prepared according to the British Standard, as described in 4.4.1.2. 0.25 g of the ash was dissolved in nitric acid in a digestion tube, which was whirlmixed and kept at room temperature for two hours before being placed in a heating block and incubated overnight. 5 mL of 25% of hydrochloric acid was then added and the sample was heated to 80ºC before analysing it using inductively coupled plasma spectrometry (ICP) with mass spectrometric detection.

4.5 Morphology of raw and torrefied biomass

4.5.1 Determination of surface area (BET method)

The Brunauer-Emmett-Teller (BET) method was used to determine the surface area and porosity of solid torrefied biomass using the Quantachrome Instruments NOVA 2200 Multi-station Any-gas Sorption Analyser Standard Model v10.03 (see Figure 4.14.). Powdered samples were oven-dried overnight prior to this experiment. This is to remove most of the moisture as it would cause condensation and blockage. On the day of the experiment, samples were weighed between 0.1000-0.1800 g to two elongated glass tubes. These tubes were then screwed into the analyser and evacuated at 150ºC for an hour. While evacuating, a volume of liquid nitrogen was poured into a cylindrical container and placed inside the analyser. After evacuation has complete, the tubes were removed, cooled at room temperature and re-weighed. Then, the tubes were put back into analyser and left to run overnight for the determination of surface areas and porosity.

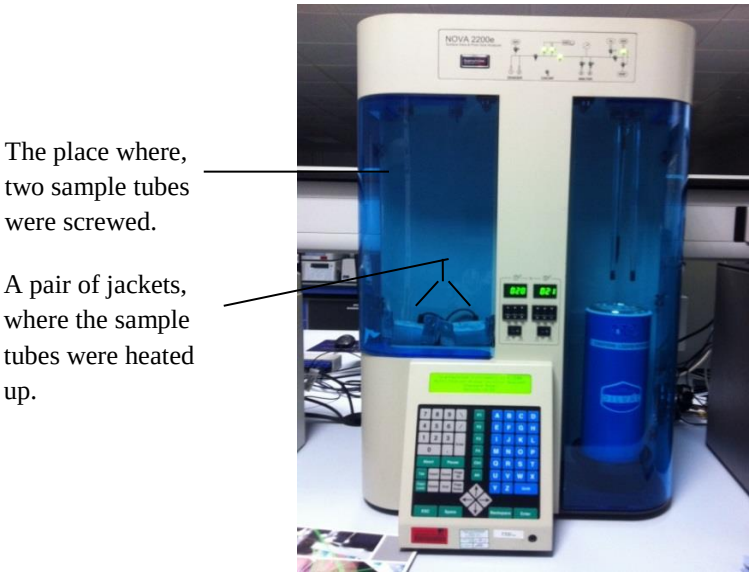

Figure 4.14. Quantachrome Instruments NOVA 2200 Multi-station Any-gas Sorption Analyser Standard Model v10.03, where sample tubes were warmed in the pair of jackets as shown in the figure.

4.5.2 Scanning Electron Microscopy and Energy Dispersive X-ray Detection (SEM-EDX)

Scanning Electron Microscopy (SEM) and Energy Dispersive X-ray Detection (EDX) analysis were carried out to study the changes in structure and chemical composition of the samples due to the treatments respectively. Samples were sieved through 600 µm and freeze-dried overnight prior to this experiment. Samples were then stuck onto a stub, carbon coated and placed inside the analyser for analysis. Figure 4.15 presents the instruments used were

Camscan 4 SEM with Oxford Instruments INCA 250 EDX system and HKL automated electron backscattered diffraction (EBSD).

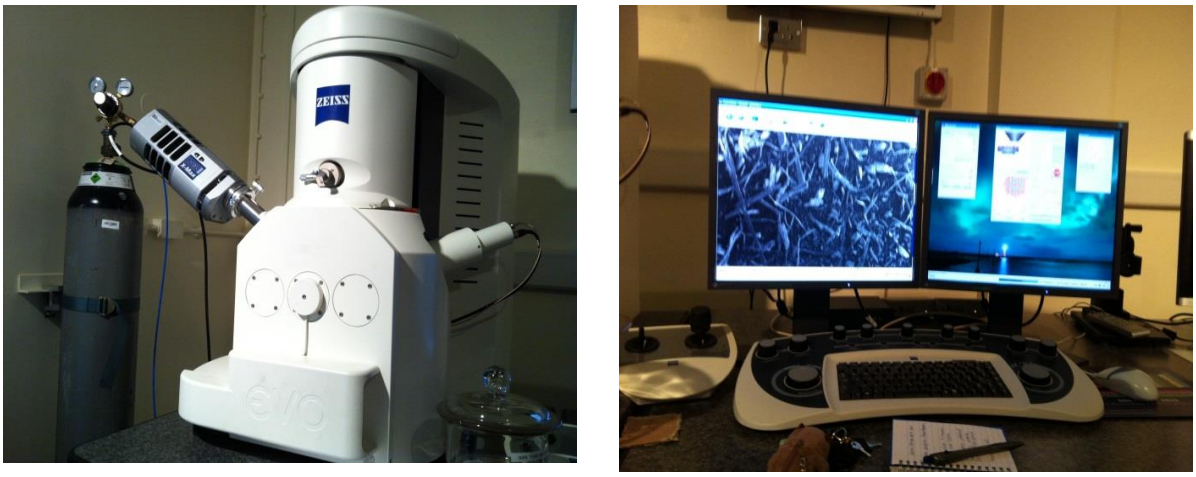

Figure 4.15. Camscan 4 SEM with Oxford Instruments INCA 250 EDX system and HKL automated electron backscattered diffraction (EBSD) that were used to take SEM images.

4.5.3 Transmission Electron Microscopy (TEM)

The structure of torrefied samples was investigated using a Philips F20 Tecnai Transmission Electron Microscopy (TEM) analyser (see Figure 4.16). Powdered samples were mixed with a volume of acetone prior to this experiment. Three drops of the mixture were added onto carbon-coated copper grids and allowed to dry. Then the grids were placed inside the analyser. This microscope uses a high energy electron beam transmitted through these samples to create images and able to see the structure of the samples at high resolution.

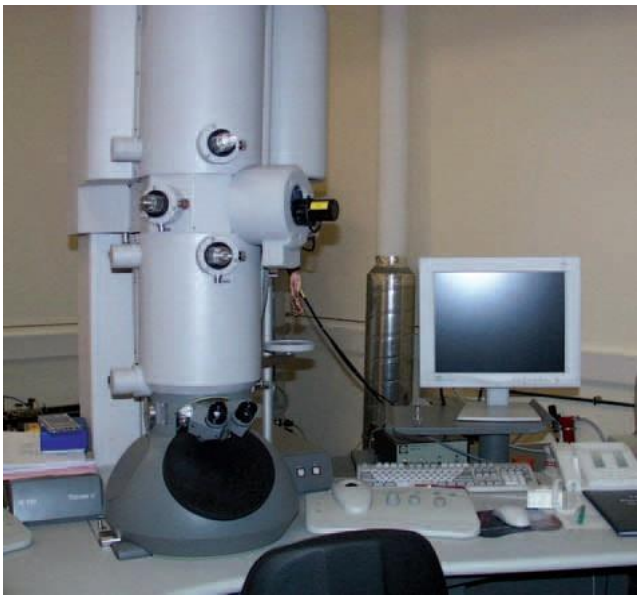

Figure 4.16. Transmission Electron Microscopy (TEM) analyser.

4.5.4 Transmission Fourier Transform Infra-Red (FTIR)

Transmission Fourier Transform Infra-Red (FTIR) was conducted to study the changes in the functional groups of the fuels using a Thermo Scientific Nicolet iS10 FT-IR Spectrometer, and data was collected using the OMNIC software. Prior to this analysis, samples were prepared in KBr wafers, by compressing 3 mg of dried sample with KBr (300 mg).

4.5.4.1 Preparation of KBr pellets

Potassium bromide (KBr) was dried in the oven for an hour and then was left to cool in a desiccator, filled with brown indicator gels (silica gel). To make a blank KBr pellet, 300 mg of KBr was measured in a small beaker. Then, it was poured into a SPECAC dye for pellet making and pressed using a hydraulic press (see Figure 4.17), which was connected to a vacuum and pump. The pressure was increased up to 10 bar. A similar procedure was followed in order to make pellets of KBr-sample mixture, where 3 mg of dried and milled sample was weighed into a beaker and mixed with 300 mg of powdered KBr.

4.5.4.2 Running the samples

The KBr (Blank) pellet was placed onto a sample holder and placed in the sample compartment of the FTIR spectrometer. After the background (blank) spectrum was recorded, the pellet of KBr-sample mixture was next to being placed onto the holder and the IR spectrum collected. It was important for the blank to be run for every sample.

4.5.5 X-ray Photoelectron Spectrometer (XPS)

XPS was used to probe the surface chemistry of the thermal treated woods to detect any changes in the components of the torrefied biomass. A Thermo Scientific ESCALAB 250 X-ray Photoelectron Spectrometer (see Figure 4.18) with a monochromated Al Kα source. Powdered samples were oven-dried overnight prior to this experiment. Samples were pressed onto an adhesive carbon tape. These biomass samples behave as non-conducting materials, therefore, a charge neutraliser was applied. XPS spectra were analysed using the CasaXPS software, where the binding energies were calibrated by setting the C 1s peak (C - graphite) to 284.5 eV to compensate for charging and act as an internal reference. A Shirley background was fitted to them and the peaks were fitted using mixed Gaussian−Lorentzian fits.

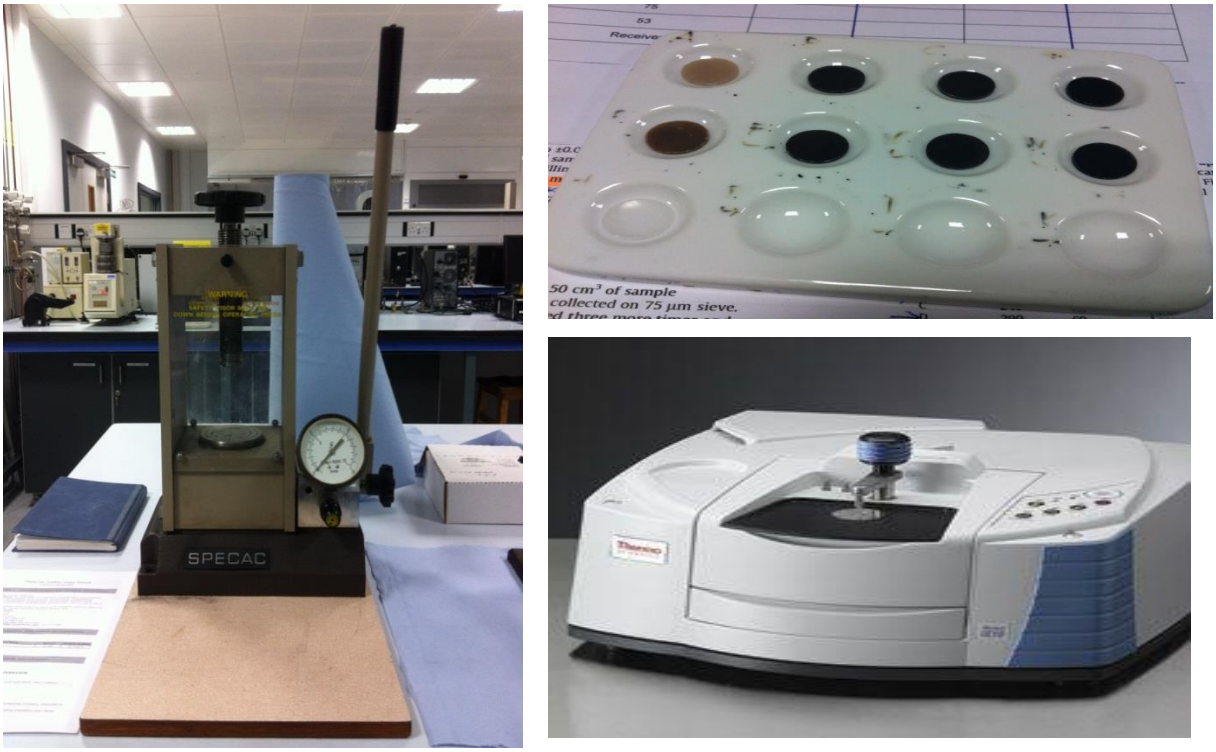

Figure 4.17. SPECAC instrument that was used to make pellets. The top right shows the KBr discs of raw and torrefied willow and eucalyptus of different treatment conditions. While the bottom right is the spectrometer where pellets are placed.

Figure 4.18. Thermo Scientific ESCALAB 250 X-ray Photoelectron Spectrometer.

4.6 Analysis of liquid products

At the end of torrefaction, liquid products were collected for further analysis. The required tests for the aqueous fraction were Total Organic and Total Inorganic Carbon content (TOC) and pH, while those for the tar fraction comprised of Karl Fischer titration, ultimate analysis and liquid-GC-MS. If the tar was more than 5 mL, viscosity and density of this liquid could have been determined. This could be suggested for future work.

4.6.1 Aqueous fraction

4.6.1.1 Total organic carbon content (TOC)

A 550 Total Organic Carbon (TOC) Analyser as pictured in Figure 4.19 was used to study the organic carbon content in the aqueous solution collected from torrefaction. This was conducted when studying the overall mass balance for willow, hardwood and softwood torrefied at condition C (290ºC with a residence time of 30 min). Solutions obtained from this treatment went through 100 times dilution in order to be within the calibration range for concentration determination. These solutions were transferred to opened glass vials, each filled with a magnetic stirrer and well-stirred prior to analysis.

Figure 4.19. TOC analyser.

4.6.1.2 pH

The pH indicator paper was used to test the acidity of the aqueous solutions.

4.6.2 Organic fraction

4.6.2.1 Karl Fischer titration

A Mettler Toledo Titrator Karl Fischer V20 (see Figure 4.20) was used to measure the water content in tars. A 1 mL plastic syringe filled with 0.3 mL of the tar was weighed on a balance pan and then, three drops of it was injected into the vortex. The syringe was re-weighed and the mass of tar injected was recorded into the Karl Fischer titrator, where the water concentration will be then displayed. This experiment was carried out in triplicates and an average of the two nearest results was taken.

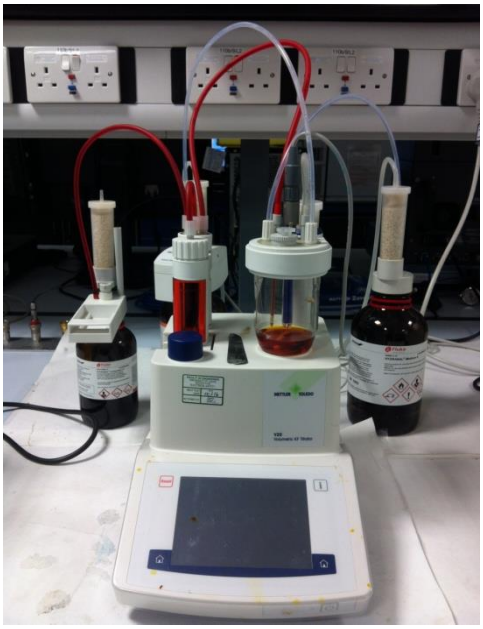

Figure 4.20. Mettler Toledo Titrator Karl Fischer V20 for measuring the water content in tars.

4.6.2.2 Liquid-GC-MS

Investigation of the components in the organic liquids (condensed from torrefaction) used Agilent 7683 series autosampler connected to an Agilent Technologies 6890N GC with an Agilent Technologies 5975B Inert XL Mass Selective Detector as shown in Figure 4.21. Approximately 0.2000 g of each organic liquid was transferred in vials and mixed with DCM that is twice the volume.

Figure 4.21. Equipments used to detect components in liquid products from torrefaction.

4.7 Torrefaction using the TGA-FTIR

Torrefaction runs were performed using a TG-FTIR instrument, which comprised of a Netzsch STA 449C Jupiter simultaneous analyser, coupled to a Nicolet Magma-IR 560 Spectrometer via a heated gas transfer line, for the determination of the rate of mass loss and quantification of the evolved gases and light volatile compounds.

Samples were prepared as described in Section 4.2 and each initially weighted cube/cuboid was placed inside the sample crucible as shown in Figure 4.22. The whole system was then vacuumed three times to remove any unwanted air/oxygen and later filled with helium at a flow rate of 80 mL min^{-1}. The temperature programme began with a drying period, heating at 10ºC min^{-1} to 150ºC and held for 30 min to remove most of the moisture in the biomass. Then the temperature was ramped to the desired torrefaction temperature at the same heating rate under helium flowing at 80 mL min^{-1}. Each sample size was treated at conditions as tabulated in Table 4.1 and the typical temperature profiles for each condition can be illustrated in Figure 4.23.

Before TGA starts running, FTIR has to be programmed or set up as well so that the absorbance from evolution of volatiles could be detected and recorded in the form of IR spectra. Spectra of the gas mixture were measured every 30 s at 4 cm^{-1} resolution.

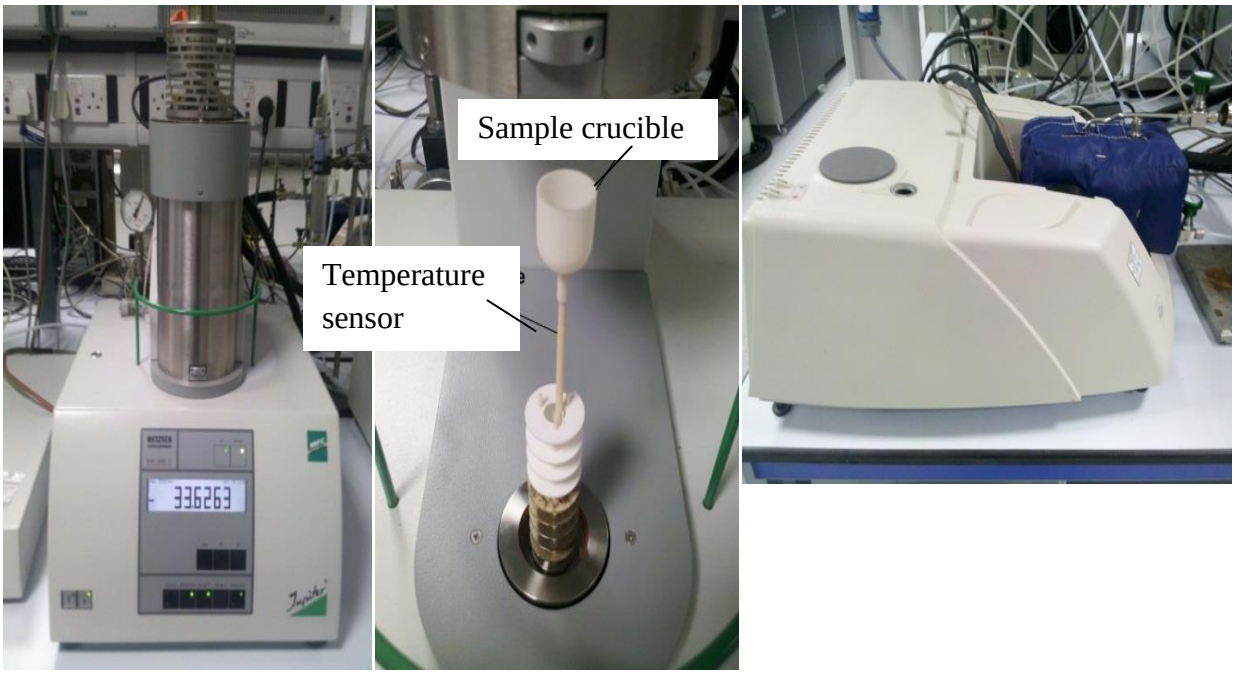

Figure 4.22. Netzsch STA 449C Jupiter simultaneous analyser (as shown on the left), coupled to a Nicolet Magma-IR 560 Spectrometer (as shown on the far right) via a heated gas transfer line. The middle picture shows how big the crucible is to allow a particle as big as 8x8x8 mm to fit in.

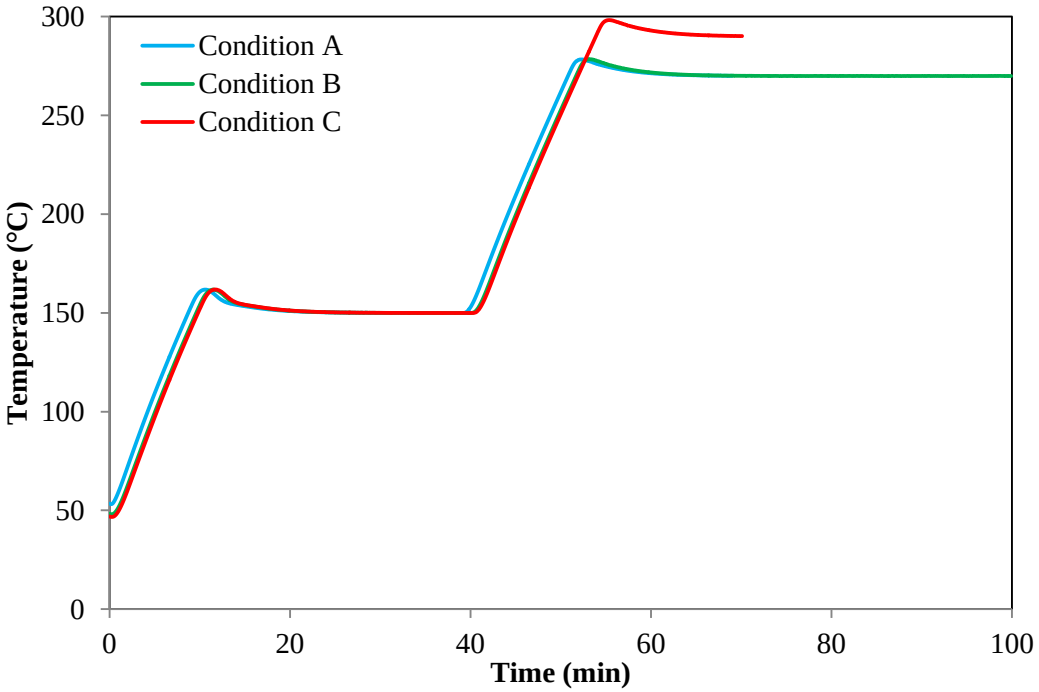

Figure 4.23. Typical temperature profile that is programmed for torrefaction of biomass at three conditions A, B (both at 270°C with a residence time of 30 and 60 min respectively) and C (at 290°C with a residence time of 30 min).

4.8 Analysis of volatile products (Permanent gases and low molecular weight volatiles)

As previously described, the evolution of volatiles from torrefaction of woody biomass from TGA was recorded by FTIR. For this project, 14 species were identified as listed below:

1. Water
2. Carbon dioxide
3. Carbon monoxide
4. Acetaldehyde
5. Formaldehyde
6. Acetic acid
7. Formic acid
8. Methane
9. Methanol
10. Acetone
11. Phenol
12. Hydrogen cyanide
13. Ammonia
14. Ethylene

These species were chosen for comparison purposes to the findings as determined in Wöjtowicz *et al* (2011), who worked on the similar sample (willow) using smaller particle sizes ($d_p < 180$ μm, where d_p is the diameter of the particle).

.

The FTIR was calibrated for permanent gases, that is, water, carbon dioxide and carbon monoxide. Thermal decompositions of calcium oxalate were carried out using TGA-FTIR, where the temperature was ramped up to 900°C at a heating rate of 10°C min^{-1}. The release of water, carbon dioxide and carbon monoxide during the reaction could be captured in the FTIR spectra. Peak areas of each gas were taken and graphs against the masses of calcium oxalate were plotted. The three plots displayed in Figure 4.24 show the equations used for the determination of the amount of the three principal products, which can be represented as *x* and *y* is the area under the peak that can be automatically obtained from the FTIR.

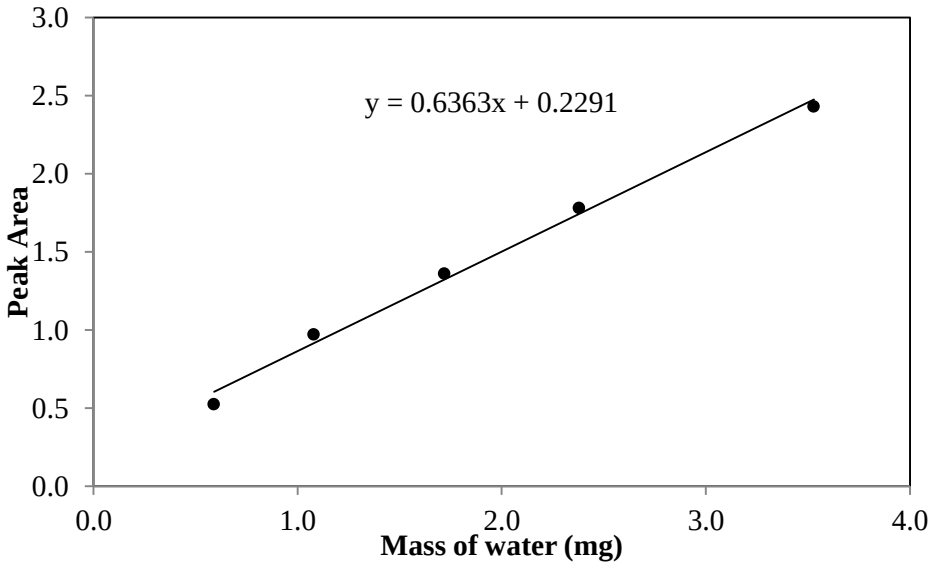

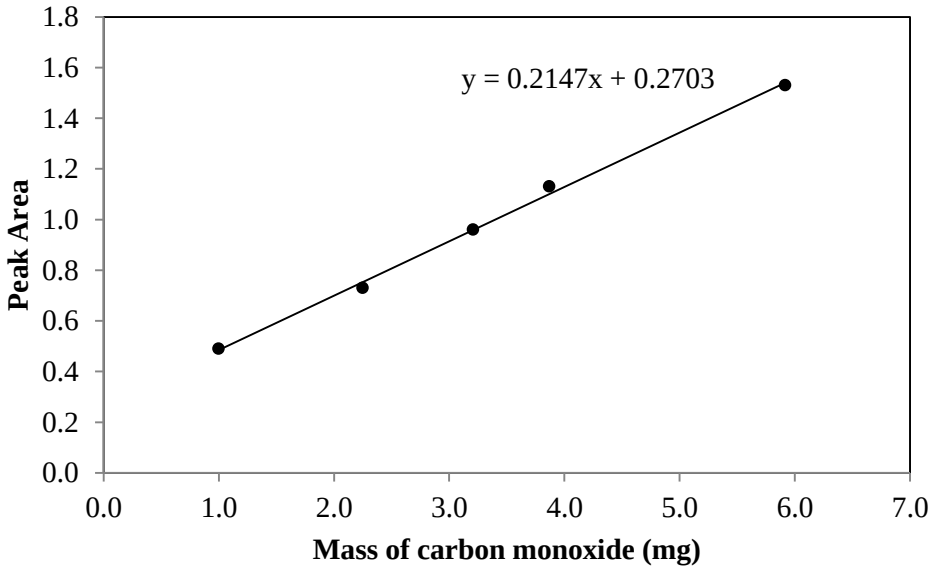

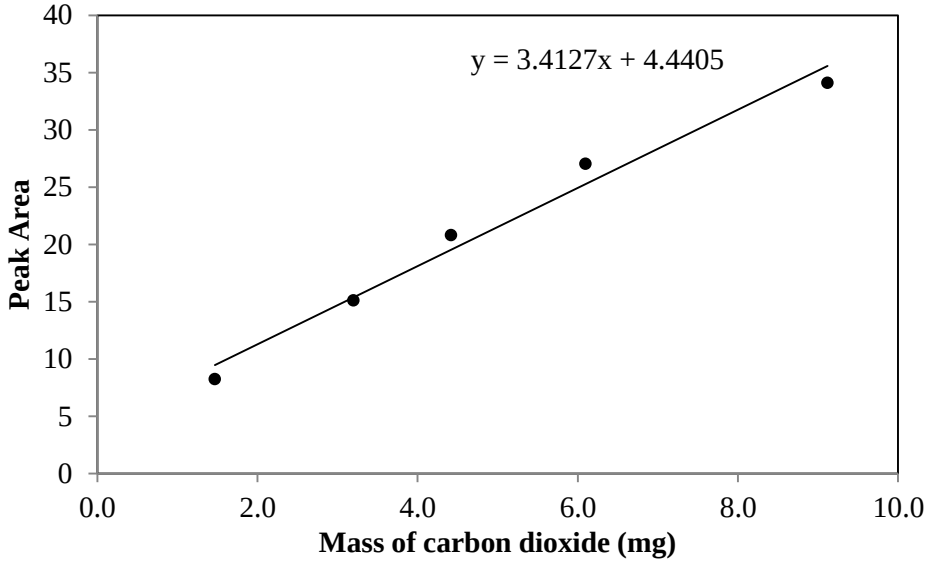

Figure 4.24. Calibration plots of water, carbon monoxide and carbon dioxide for FTIR.

4.9 Single Particle Combustion of woody biomass

Cubes of willow and eucalyptus of 2 mm were used for the investigation of this part of the study. Torrefied samples were prepared using the TGA and they were treated at conditions A and C (at 270 and 290ºC respectively with a residence time of 30 min). Figure 4.25 shows the instruments used to carry out combustion tests. Prior to combustion, each particle was weighed and held in place on a steel needle adjacent to an R-type thermocouple in a ceramic housing. A water-cooled probe surrounded the particle and thermocouple before being introduced to the flame. A Meker burner was used and the probe was positioned so that the particle and thermocouple were about central above the burner. When the flame was lit, the water-cooled sleeve was retracted, exposing the particle to the flame. As soon as the combustion has completed, the sleeve was slid back and the unit was removed from the flame. A video camera, Photron FastCam SA5 and the software, PFV 3.0 (Photron Fastcam Viewer) were used to record the images of the combusting particles at a speed of 125 frames per second (fps). Those images were then used to study the combustion behaviour and determine the duration of different combustion stages.

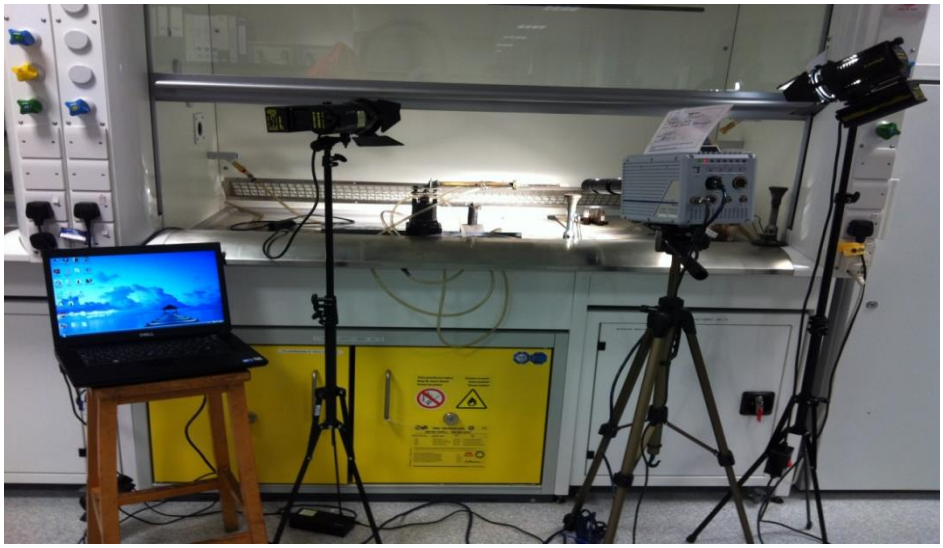

Figure 4.25. Instruments used in conducting the single particle combustion of biomass.

4.10 Functional-Group (FG) Biomass model

FG Biomass model is a software that is programmed by the Advanced Fuel Research (AFR), Hartford, USA. This model was used to simulate the decomposition of biomass (in this project, willow and eucalyptus) during torrefaction and predict the yields as well as the composition of the products. It also provides information about the changes in the chemical

composition of the torrefied solid in a form of Van Krevelen diagram and displays the volatiles evolved from torrefaction. Few data from the biomass fuels such as their chemical composition and heating regime will be required for this program to work. The same torrefaction temperature programme was set as displayed in Table 4.1. This allowed the comparison between the results produced from the torrefaction using TGA-FTIR and the furnace to be made in terms of the products yield and the chemical composition of the torrefied solid.

The following figures (Figure 4.26-4.31) display some parts of the user interface, input requirements, configuration settings heating program and some of the calculated results produced during FG Biomass model.

The following is the input requirements and configuration settings for willow and eucalyptus as provided by the AFR.

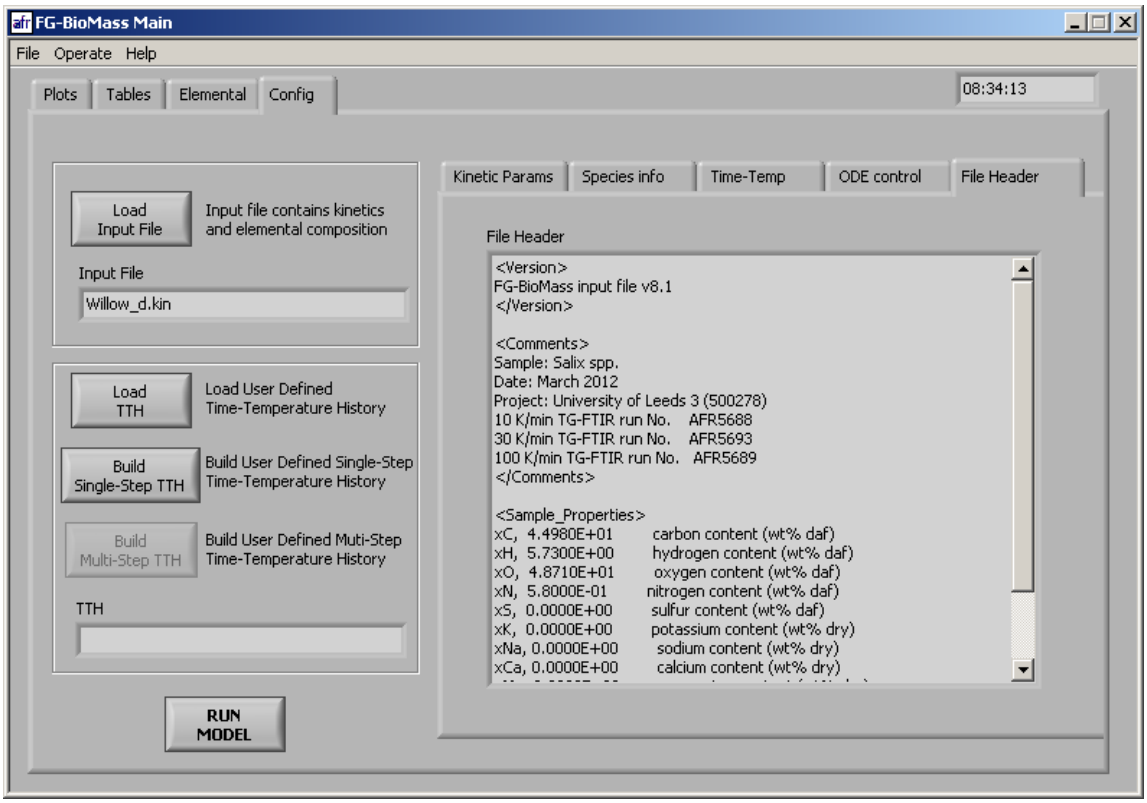

Figure 4.26. Input requirements for willow as provided by the AFR.

The properties of willow are listed as follows:

C, 40.50	carbon content (wt% daf)
H, 5.73	hydrogen content (wt% daf)
O, 40.87	oxygen content (wt% daf)
N, 0.58	nitrogen content (wt% daf)
S, 0.00	sulphur content (wt% daf)
K, 0.00	potassium content (wt% dry)
Na, 0.00	sodium content (wt% dry)
Ca, 0.00	calcium content (wt% dry)
Mg, 0.00	magnesium content (wt% dry)
a, 0.90	ash content (wt%, dry) – 30K/min
VM, 80.82	volatile matter (wt%, daf) – 30K/min

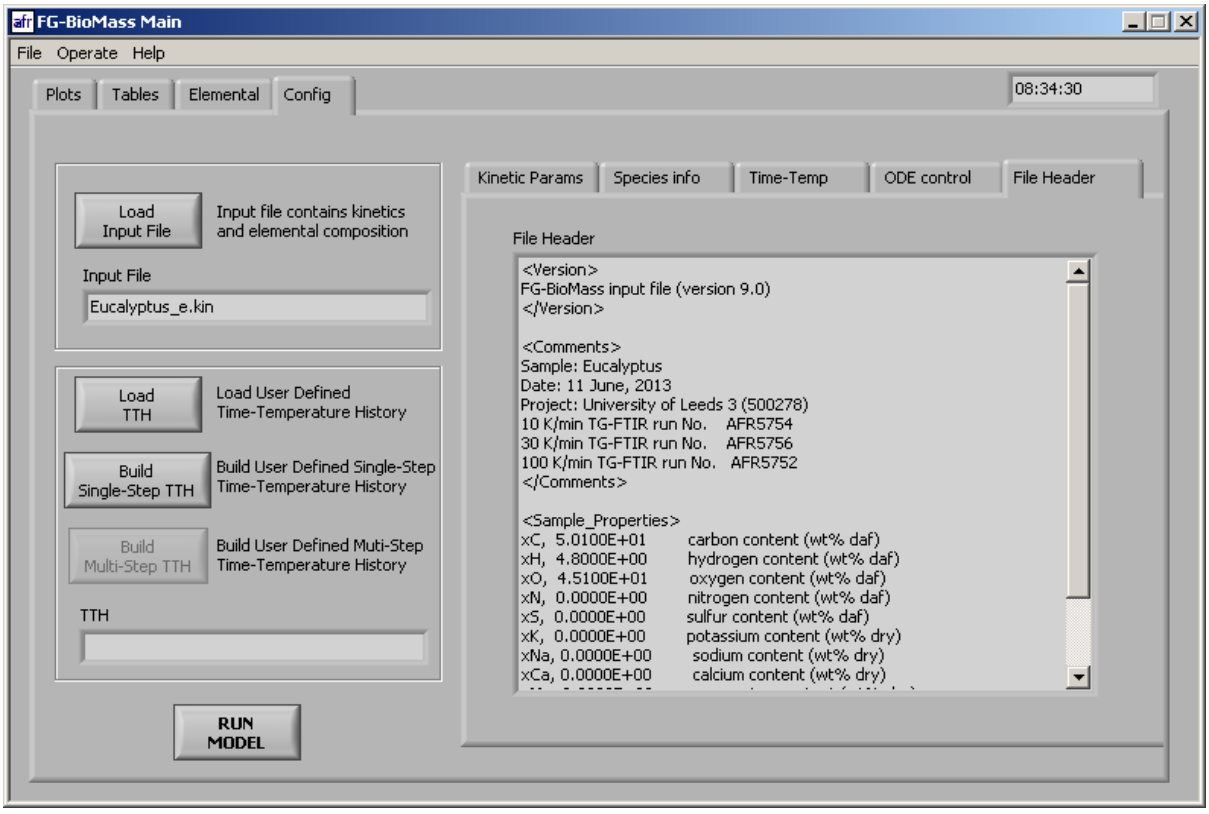

Figure 4.27. Input requirements of eucalyptus as provided by the AFR.

The properties of eucalyptus are listed as follows:

C, 50.01	carbon content (wt% daf)
H, 4.80	hydrogen content (wt% daf)
O, 40.51	oxygen content (wt% daf)
N, 0.00	nitrogen content (wt% daf)
S, 0.00	sulfur content (wt% daf)
K, 0.00	potassium content (wt% dry)
Na, 0.00	sodium content (wt% dry)
Ca, 0.00	calcium content (wt% dry)
Mg, 0.00	magnesium content (wt% dry)
a, 0.90	ash content (wt%, dry) - 30K/min
VM, 80.37	volatile matter (wt%, daf) - 30K/min

The following figures illustrate the setting of the temperature and heating regime as well as the temperature profile. To set up, one has to go to 'Build Single-Step TTH', shown in Figure 4.28 (a) and another window, as shown in Figure 4.28 (b) will be displayed. The hold time is the residence time at the final temperature. For example, if the reaction time (T>200°C) is 30 min, the hold time will be 23 min since it takes 7 min for the temperature to raise from 200 to the desired temperature, for example, 270°C. The heating rate is in °C s^{-1}, so if the heating rate used in the big reactor and TGA-FTIR is 10°C min^{-1}, the conversion of unit for FG-Biomass model will be 0.1667°C s^{-1} (~0.17°C s^{-1}). After the set-up is completed, one can click 'Run model' as displayed in Figure 4.28 (a).

Results will be as displayed in the following figures. The figures represent the results for willow. Similar displays are resulted for eucalyptus. In the 'Plots' section, yields of char and other volatile products will be illustrated and Figure 4.29 a) shows the plot of the char yield, where it decreases during the heating process. FG-Biomass model also displays evolution rates of torrefaction products as displayed in Figure 4.29 b), which shows that of char. The rate of char dropped after the 1000^{th} s, which represents the degradation of char.

In the 'Tables' section (Figure 4.30) lists the yields and evolution rates of torrefied products in terms of dry ash free basis, recorded at 1°C per second. Those of 14 species were recorded and they are as listed in Section 4.7.

a)

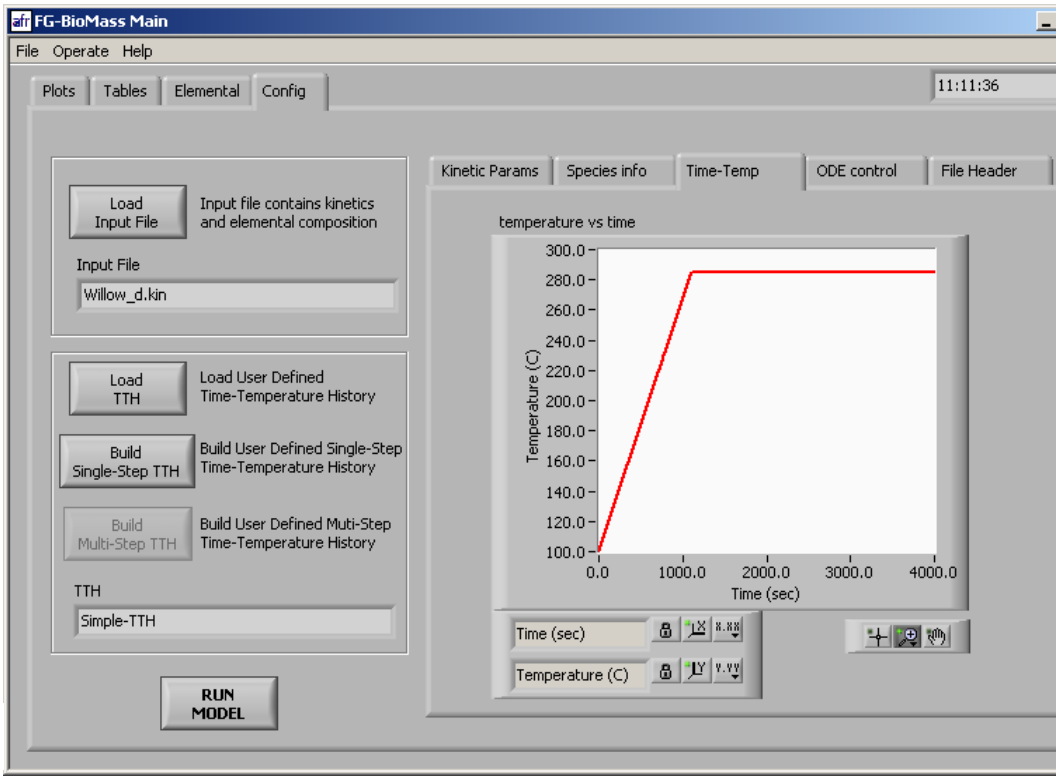

b)

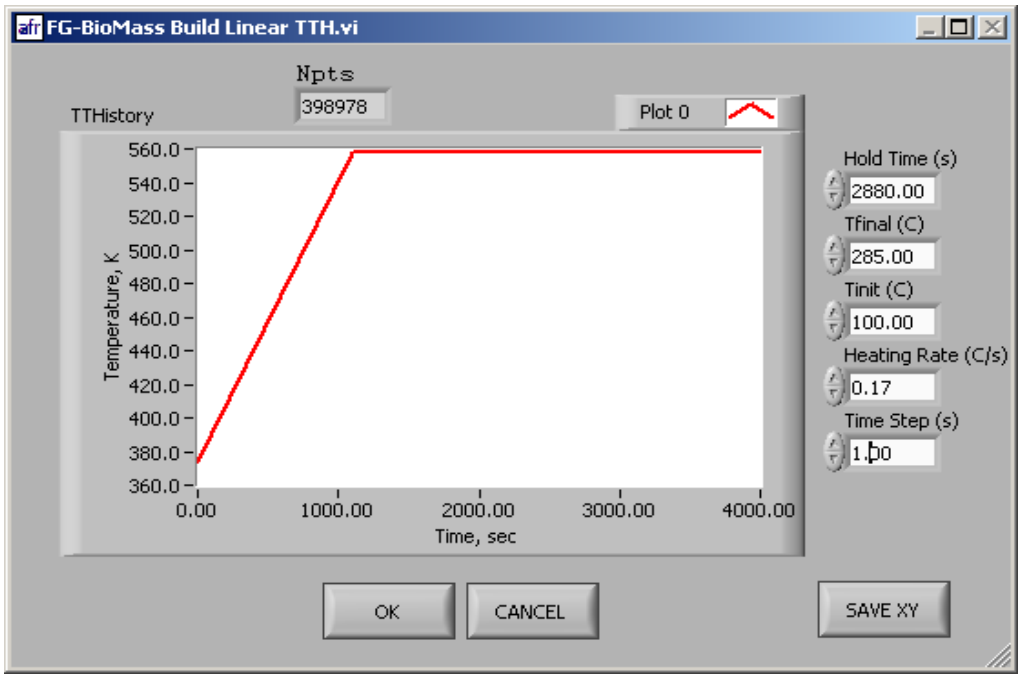

Figure 4.28. a) The setting of the heating regime and b) the temperature profile as resulted from the set up.

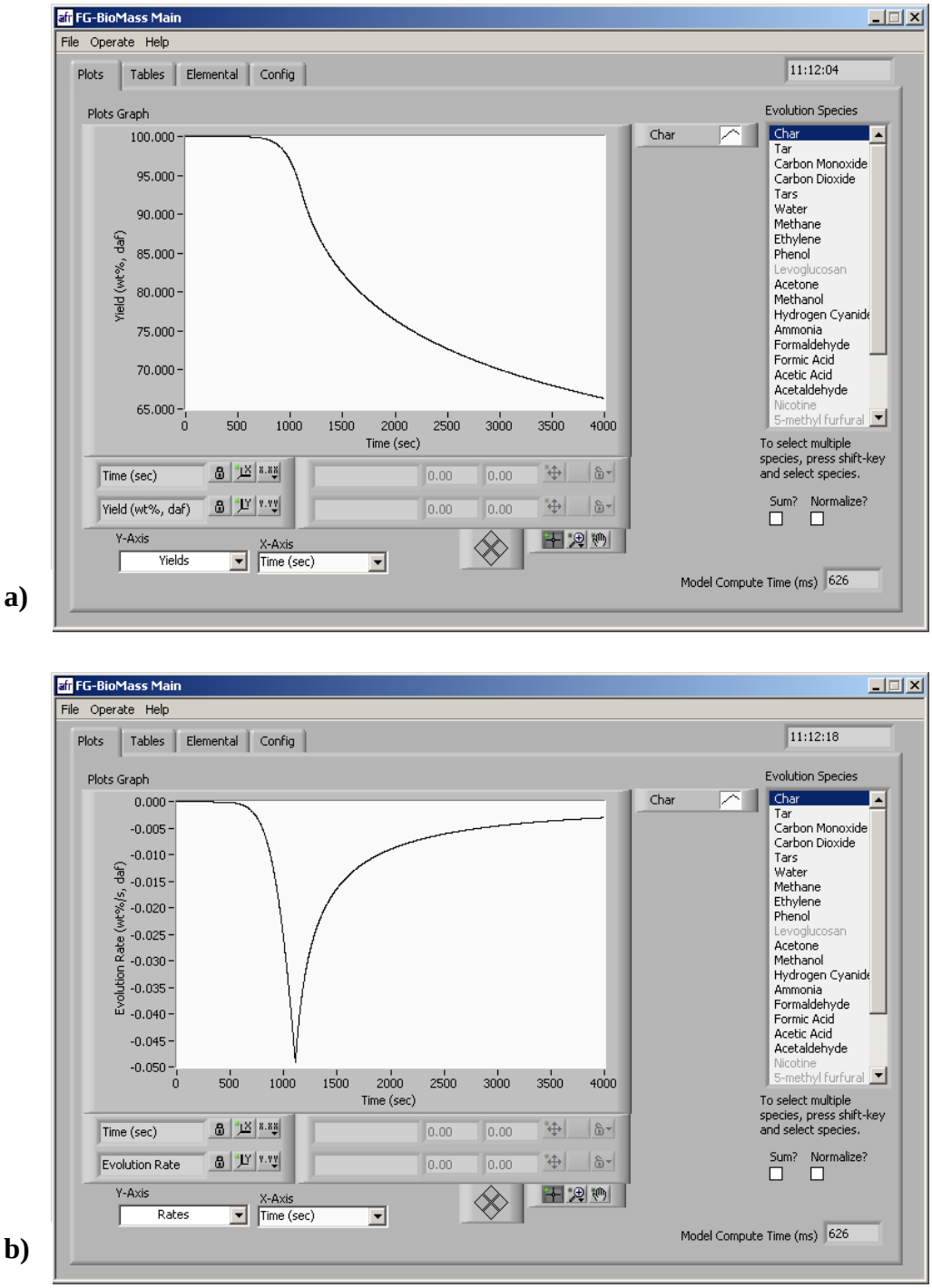

Figure 4.29. a) Predicted char yield as simulated by the FG-Biomass as a result of torrefaction of willow and b) the evolution rate of char during the torrefaction.

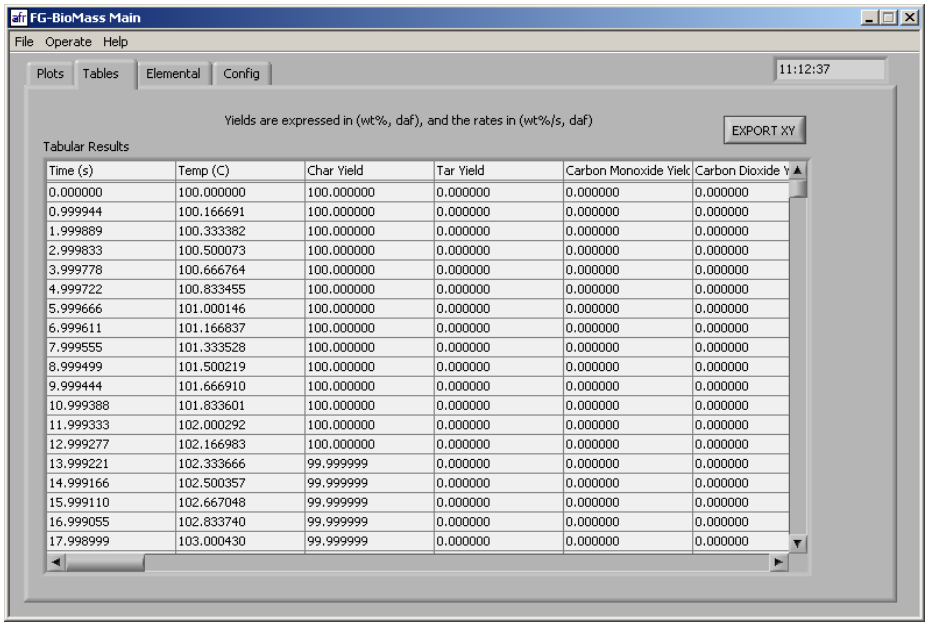

Time (s)	Temp (C)	Char Yield	Tar Yield	Carbon Monoxide Yiel	Carbon Dioxide Y
0.000000	100.000000	100.000000	0.000000	0.000000	0.000000
0.999944	100.166691	100.000000	0.000000	0.000000	0.000000
1.999889	100.333382	100.000000	0.000000	0.000000	0.000000
2.999833	100.500073	100.000000	0.000000	0.000000	0.000000
3.999778	100.666764	100.000000	0.000000	0.000000	0.000000
4.999722	100.833455	100.000000	0.000000	0.000000	0.000000
5.999666	101.000146	100.000000	0.000000	0.000000	0.000000
6.999611	101.166837	100.000000	0.000000	0.000000	0.000000
7.999555	101.333528	100.000000	0.000000	0.000000	0.000000
8.999499	101.500219	100.000000	0.000000	0.000000	0.000000
9.999444	101.666910	100.000000	0.000000	0.000000	0.000000
10.999388	101.833601	100.000000	0.000000	0.000000	0.000000
11.999333	102.000292	100.000000	0.000000	0.000000	0.000000
12.999277	102.166983	100.000000	0.000000	0.000000	0.000000
13.999221	102.333666	99.999999	0.000000	0.000000	0.000000
14.999166	102.500357	99.999999	0.000000	0.000000	0.000000
15.999110	102.667048	99.999999	0.000000	0.000000	0.000000
16.999055	102.833740	99.999999	0.000000	0.000000	0.000000
17.998999	103.000430	99.999999	0.000000	0.000000	0.000000

Figure 4.30. Lists of yields and evolution rates of torrefied products as predicted from the simulated torrefaction of willow.

In the ‘Elemental’ section (Figure 4.31) illustrates the change in the main elemental composition (C, H, O, N and S) after torrefaction (pyrolysis) in terms of wt% against time.

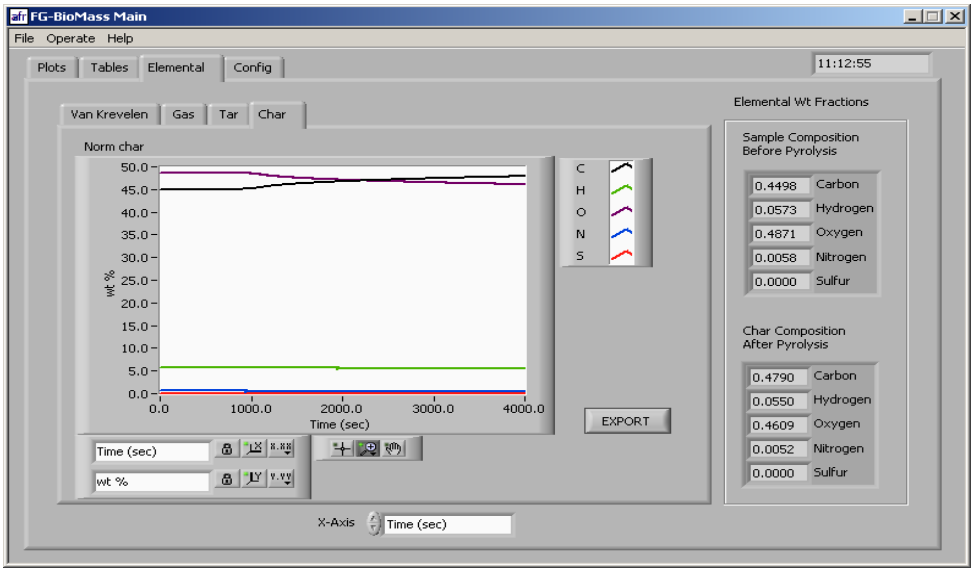

Figure 4.31. Evolution rate of elements of torrefied char.

CHAPTER 5

TORREFACTION STUDIES AND AN INVESTIGATION OF THE PROPERTIES AND CHARACTERISATION OF PRODUCTS OF TORREFACTION

5.1 Introduction

Problems associated with the properties and characterisation of biomass fuels have long been identified ever since they are put into energy use. There is no doubt that the biomass as a renewable source of energy can provide positive contributions to reach the EU target. However, high maintenance costs, loss of financial support and loss of jobs can be part of the reasons for its decline in the future if the issues continue. Several pre-treatments have been practiced and they are previously discussed in Chapter 1. One of the pre-treatments of biomass that now has increasing interest is torrefaction. This thermochemical treatment has been studied for its ability to upgrade the chemical and physical properties of a biomass.

Several studies, as thoroughly described in Chapter 3, have been conducted using different final temperatures within the range of 200-300ºC and residence times, that is mainly 30-60 min (Prins *et al*., 2006b; Rodrigues and Rousset, 2009; Bridgeman *et al*., 2008; 2010; Chen *et al*., 2011; Phanphanich and Mani, 2011; Medic *et al*., 2012). A few studies extended the residence time to three to five hours (Arias *et al*., 2008; van der Stelt *et al*., 2011). In general, all results showed that the more severe the torrefaction conditions are, the more improved the solid end-product is such as the ease of grinding and the greater amount of milling energy that can be saved (Melkior *et al*., 2012). However, the mass loss of the solid torrefied product must be kept as low as possible to attain a reasonably high energy yield (Melkior *et al*., 2012).

Basu (2013) mentioned that the product motivation of torrefaction of biomass, as opposed to pyrolysis and carbonization, is the production of torrefied biomass, containing the maximum energy and mass yields with reduction in the O:C and H:C ratios. Therefore, choosing an optimum operating condition is crucial, as different types of biomass give different outcomes. Section 3.1 explains how different biomass thermally behaves differently due to the difference in lignocellulosic contents particularly hemicellulose. What is required and acceptable is that this approach is able to retain approximately 70% of the initial biomass dry weight, and about 80-90% of the biomass's original energy content (Lipinsky *et al*., 2002).

With regards to the solid torrefied biomass, there has been a great deal of research considering the standard fuel analysis, mass yield and energy yield (Chen *et al*., 2011; Bridgeman *et al*., 2008; Prins *et al*., 2006; van der Stelt *et al*., 2011; Pentananunt *et al*., 1990; Pimchuai *et al*., 2010; Rousset *et al*., 2011). While a few studies have reported the improvement of their grindability properties (Chen *et al*., 2011; Arias *et al*., 2008). However, very little research has given a thorough look into the structure and physicochemical properties of the solid product (Chen *et al*., 2011). This chapter focuses on the investigation of not only the morphology and composition of the solid torrefied biomass (several woody biomass including short rotation willow coppice (SRC) and eucalyptus) but also, their physical and chemical characteristics. Torrefaction of these biomass fuels were carried out in the reactor as detailed in Section 4.3.1 and their standard fuel analysis were studied as described in Section 4.4.1 and 4.4.2. A range of characterisation methods were used, including Transmission Electron Microscope (TEM) and Scanning Electron Microscope (SEM) for morphology examination, X-ray Photoelectron Spectroscopy (XPS), which was used to study the changes in the O:C ratio and components in the biomass, and Fourier Transform Infrared spectroscopy (FTIR), that was aimed to follow changes in the chemical structure. The surface area and pore size distribution were also investigated using the Brunauer Emmett Teller (BET) method. Furthermore, the density, hydrophobicity and grindability of the torrefied products were also studied. All these methods are described in Section 4.4 and 4.5.

5.2 Results and discussion

5.2.1 Temperature profile

Plots in Figure 5.1 are temperature profiles of torrefaction of softwood that was treated at different conditions (A, B and C). Table 4.1 displays these sets of conditions. Torrefaction experiments were carried out in a big scale reactor as presented in Figure 4.2 and described in Section 4.3.1. Figure 5.1 also represents the typical temperature profiles of torrefaction of other biomass fuels. The process started off with a drying period at 150°C and was held for 3600 s (60 min), followed by a final desired temperature (270°C and 290°C) and held for another 1800-3600 s (30-60 min). Thermocouples were used to monitor the temperature zones in the reactor and biomass, where thermocouple 3 is positioned at the furthest away from the biomass. Thermocouple 1 is located where the biomass is while thermocouple 2 is positioned in between the two thermocouples. These positions are clearly pointed out in Figure 4.4. Temperature profiles of torrefaction of the rest of the biomass can be obtained in the Appendix section (**Appendix 5.1**).

Notice that the temperature detected by thermocouple 1 in Figure 5.1 is higher than the other two. There have been a number of reviews that commented on this effect, where the temperature detected in the biomass (core temperature) is higher than the temperature of the reactor. The biomass fuels used in this study consist of large particle sizes, hence, torrefaction mainly takes place within its interior (Peng *et al*., 2012; Basu, 2013). The heat transfer from the hot gas to the surface of the particle by convection and then into the interior (core) by conduction, creating a temperature gradient (Peng *et al*., 2012). Section 3.5 explains how the core temperature increases steadily while receiving heat from the reactor until it approaches above that of the reactor, where it was suggested that torrefaction has become net exothermic (Basu, 2013). This, in effect, greatly influenced the rate of torrefaction, rather than the temperature of the reactor. The next chapter further investigates the effect of particle sizes of biomass fuels on torrefaction, in terms of mass yield, energy yield and evolution of volatile products as well as the overall mass balance.

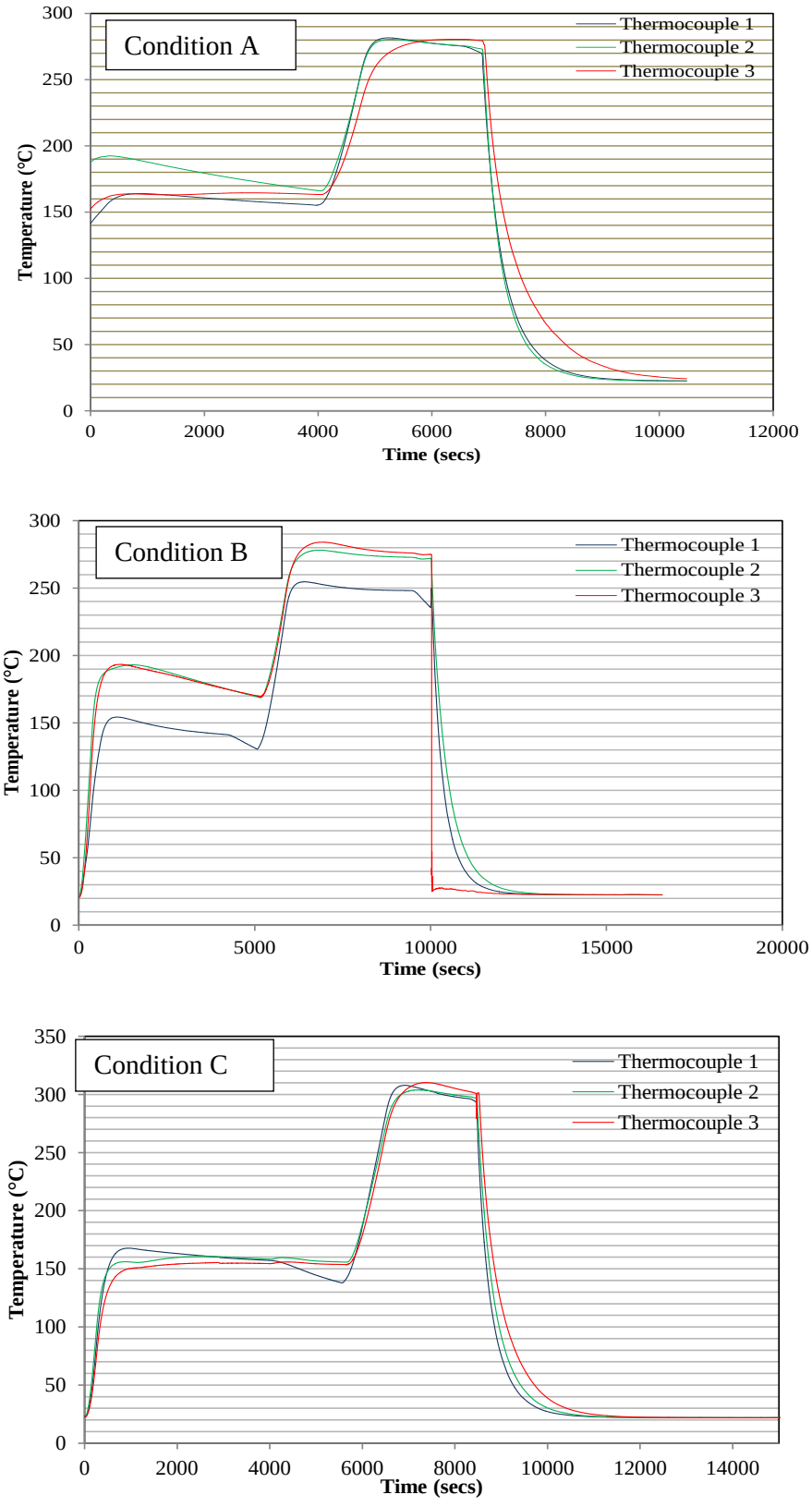

Figure 5.1. Temperature profiles of torrefaction of softwood at conditions A, B (270°C with a residence time of 30 and 60 min respectively) and C (290°C with a residence time of 30 min).

5.2.2 Mass balances

A mass balance compares what comes out with what goes in. In a mass balance, yields of torrefied solid biomass, permanent gases and condensables are important. Here, the condensables include aqueous and organic liquids. However, it is important to note that the mass yields of solid torrefied biomass listed in Section 5.2.2.1 are different than those displayed in Section 5.2.2.2. This chapter investigates the properties of solid torrefied biomass fuels and only the mass yields of the solids after torrefaction were taken (Table 5.1). The yields of the other products (gases and liquids) were not considered. This chapter also seeks into taking the overall mass balance but for this section, fuels were only treated at the most severe condition, C (290°C with a residence time of 30 min). The results can be seen in Figure 5.2.

5.2.2.1 Mass yields

The resultant mass yields of biomass fuels and the changes in mass yields with response to temperature, T and residence time, t are listed in Table 5.1. In general, the results show that temperature plays a more important role in torrefaction than the residence time. For example, the change in mass yield received a greater impact with a change in T than t, which was about 16-19% mass loss extra. This effect has previously been observed by Bridgeman *et al* (2010), who investigated process variables with a factorial method using a three-factor methodology (temperature, residence time and particle size). They concluded that temperature had the greatest influence on the change in both mass yields of willow and *Miscanthus*, followed by residence time and particle size. With regards to eucalyptus, the changes of mass yields due to both changes seem to show a bigger impact in comparison to the other biomass fuels. Particle sizes of eucalyptus used in this experiment were half of the other fuels so this could contribute to this effect. Again, the next chapter will emphasise more on the effect of particle sizes of biomass on torrefaction.

Table 5.1. Mass yields of biomass fuels that were treated at different conditions, A, B and C as tabulated in Table 4.1 (dry basis).

Sample	Mass yield (% dry)			Change of mass yield between torrefied biomass (A and B) due to a change in residence time, t[a]	Change of mass yield between torrefied biomass (A and C) due to a change in temperature, T[b]
	A	B	C		
Willow	68.76	67.53	56.21	1.23	12.55
Eucalyptus	67.62	56.66	50.61	10.96	17.01
Hardwood	73.00	71.60	59.15	1.40	13.85
Softwood	79.53	74.61	66.50	4.92	13.03

[a] Difference between yield for sample A (t=30 min) and sample B (t=60 min), both torrefied at T=270ºC.
[b] Difference between yield for sample A (T=270ºC) and sample C (T=290ºC), both t=30 min.

5.2.2.2 Overall mass balance

Figure 5.2 illustrates the overall mass balance of willow, hardwood and softwood torrefied at 290ºC with a residence time of 30 min obtained from the reactor. Unfortunately, that of eucalyptus cannot be determined due to sample availability. The data was expressed as received and the percentages were calculated with respect to the mass of willow prior to torrefaction as formulated in equations (4.1)-(4.4) in Chapter 4. Figure 5.2 shows that most of the mass comes from the torrefied wood, followed by the gases and other condensables (comprised of aqueous and organic liquids). Here, the gases and volatiles represent the permanent gases, which include carbon dioxide and carbon monoxide, lower molecular weights of organic volatile compounds such as acetone and formaldehyde and other heavier (aromatic) compounds such as phenol and benzaldehyde. Some materials (condensed volatiles) were lost during torrefaction due to evaporation or spillage, which means experimental errors in weighing them were larger than for the solid.

5.2.3 Standard fuel analysis

The standard fuel analysis listed in Table 5.2 and 5.3 are based on solids obtained from torrefaction (Table 5.1). Solids obtained for Section 5.2.2.2 were not analysed. Table 5.2, on one hand, presents the influence of different torrefaction conditions on the proximate analysis of the biomass samples in comparison to when they are untreated. It can be seen that pre-treated fuels have lower moisture contents than the untreated fuels. This is because water is the major product of torrefaction (Bridgeman *et al*., 2008; Prins *et al*., 2006; Medic *et al*., 2012).

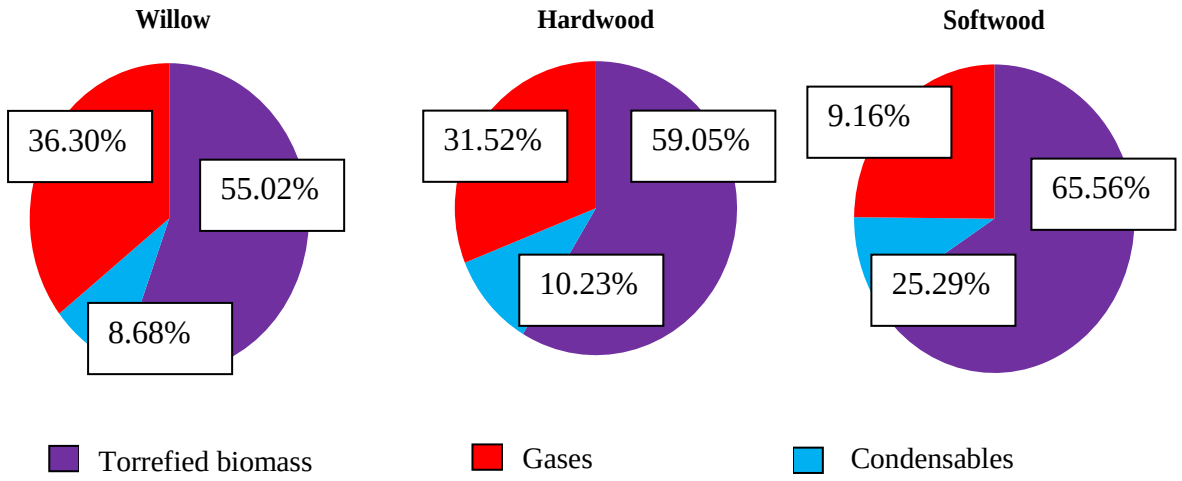

Figure 5.2. Overall mass balance of torrefaction of willow, hardwood and softwood, treated at 290ºC with a residence time of 30 min.

In other words, a significant amount of water has lost during the thermal treatment and this effect usually takes place in two mechanisms: during the drying period (prior to torrefaction) and during dehydration reactions between organic constituents upon torrefaction (Bridgeman *et al*., 2008). Table 5.2 also shows the general trend of decreasing volatile matter and increasing fixed carbon content as the torrefaction conditions become more severe. This suggests that more volatiles have evolved with increased severity of torrefaction conditions. The ash content also increased, which is related to the loss of mass of organic matter during torrefaction (Phanphanich and Mani, 2011). The ashes usually contain elements such as potassium, sodium, chlorine, sulphur and silica, in which if they are present in high concentrations, can lead to slagging and fouling. The results of metal analysis of raw biomass fuels can be found available in **Appendix 5.2**.

Table 5.2. Proximate analysis of raw and torrefied biomass samples.

Sample	Moisture (% ar[a])	Volatile (% daf[b])	Ash (% dry)	Fixed carbon (% daf[b])
Raw Willow	6.0	84.8	0.5	15.2
Willow A	3.9	73.8	0.5	26.2
Willow B	3.8	72.4	0.7	27.6
Willow C	3.6	63.2	1.1	36.8
Raw Eucalyptus	8.0	80.4	1.6	19.6
Eucalyptus A	4.3	67.9	1.6	32.1
Eucalyptus B	4.3	71.2	2.0	28.8
Eucalyptus C	4.2	60.3	2.2	39.7
Raw Hardwood	6.7	83.2	0.7	16.9
Hardwood A	5.0	72.2	1.0	27.8
Hardwood B	3.8	72.0	1.6	28.0
Hardwood C	3.7	64.6	2.1	35.4
Raw Softwood	7.0	83.0	0.1	17.0
Softwood A	4.7	79.7	0.1	20.3
Softwood B	4.0	78.3	0.3	21.7
Softwood C	3.9	71.8	0.4	28.2

[a]ar – as received
[b]daf – dry as free

Table 5.3, on the other hand, demonstrates the alterations in the chemical composition of the torrefied biomass. As expected, there is an increasing trend in the carbon content, whilst the oxygen and hydrogen contents have gone down. These observations agreed with literature reviews as discussed in Section 3.3.5. It is important to note that the contents of hydrogen and oxygen in the ultimate analysis do not include the hydrogen and oxygen in the moisture (Basu, 2013). Rather, the significant loss of such contents are the water vapour lost from the dehydration reactions between organic constituents and evolution of volatiles (that are rich in hydrogen and oxygen). A consequence of the changing C, H and O content is the increase in higher heating values. The sulphur contents were below the detection limit, and the nitrogen was closed to the detection limits, hence, there are no significant changes reported.

Table 5.3. Ultimate analysis of raw and torrefied biomass samples (daf basis).

Sample	**C (%)**	**H (%)**	**N (%)**	**O* (%)**	**HHV (MJ kg^{-1})**
Raw Willow	49.5	6.1	0.2	44.4	19.4
Willow A	55.6	6.0	0.0	38.4	22.2
Willow B	56.9	5.9	0.0	37.3	22.8
Willow C	60.1	5.8	0.0	34.2	24.2
Raw Eucalyptus	49.3	6.5	0.0	44.3	20.5
Eucalyptus A	57.8	6.0	0.0	36.2	22.8
Eucalyptus B	61.9	5.8	0.0	32.3	24.3
Eucalyptus C	69.4	5.3	0.0	25.1	27.3
Raw Hardwood	46.8	5.9	0.1	47.2	18.3
Hardwood A	57.7	6.1	0.0	36.2	23.2
Hardwood B	58.4	5.7	0.0	35.8	23.0
Hardwood C	61.4	5.7	0.0	32.9	24.3
Raw Softwood	46.7	5.9	0.0	47.4	18.4
Softwood A	54.6	6.3	0.0	39.1	22.1
Softwood B	55.7	6.1	0.0	38.2	22.4
Softwood C	58.7	6.0	0.0	35.3	23.7

* Calculated by difference. S was not detected.

Further illustration to the changes in the chemical composition of torrefied biomass can be observed on the Van Krevelen diagram, shown in Figure 5.3. The figure also illustrates the typical data points of lignite and anthracite. Changes resulted in fuels moving along the coalification series towards the composition of lignite can be observed. These observations are in agreement with those studies discussed in Section 3.3.5 as illustrated in Figure 3.14 by Bridgeman *et al* (2008). This change is particularly noticeable for the hardwood samples, including eucalyptus and willow.

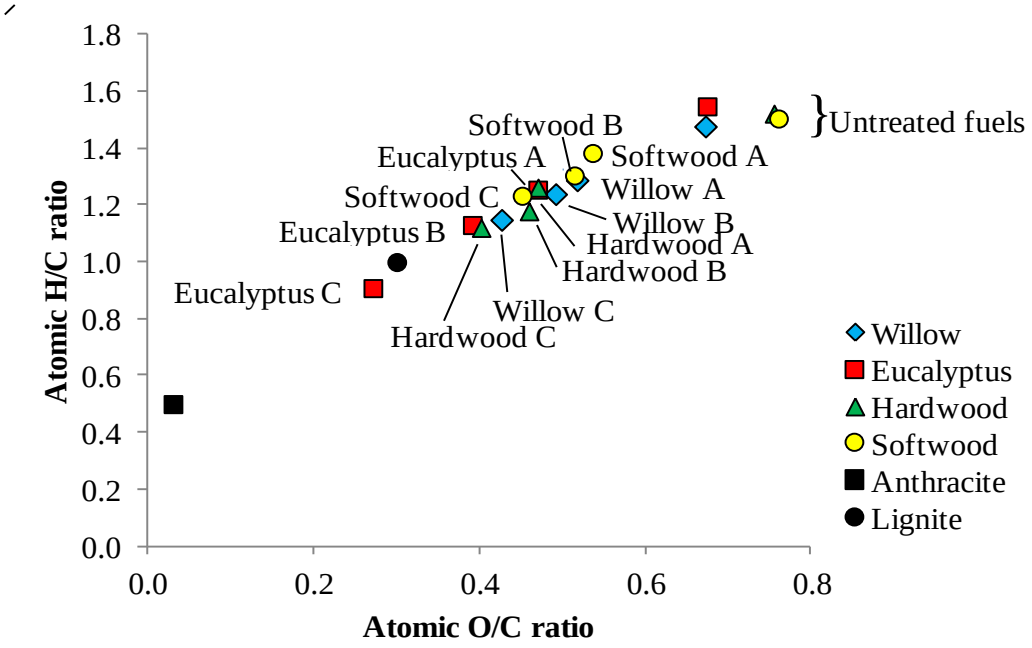

Figure 5.3. Van Krevelen plot of raw and torrefied biomass alongside anthracite and lignite.

Next, Figure 5.4 shows the relationship between mass yield and energy yield, where the slope gives the average energy ratio. Of the fuels and conditions studied, all of the torrefied softwood samples have attractive mass and energy yields (61-76% and 82-95% respectively). A mass yield of 70% and energy yield of 80-90% is highly recommended and sounds reasonable for energy utilisation (Bergman, 2005c). Other fuels that were produced at condition C have mass and energy yields that would be unattractive for a commercial process. Eucalyptus is the most reactive fuel, and as such, only that produced at condition A has a respectable mass and energy yield. It is interesting that different woody biomass appear to produce a single relationship between mass yield and energy yield, which can also be observed in Saddawi *et al* (2012) and this implies that optimisation for new woody biomass may be easier than originally anticipated. It can be concluded that the optimisation for torrefaction condition is species dependent due to differences in lignocellulosic composition.

The line shown in Figure 5.4 provides an indication and a boundary as to how well the biomass fuels performed. Equation 4.13 is used to determine the energy yield of torrefied biomass. The point of reference is when the energy yield equals to the mass yield, where the ratio of HHV is 1. If the ratio is greater than 1, it gives a good indication that the fuels can perform well when put into energy use. Figure 5.4 shows that all the torrefied biomass fuels are above the line, which can also mean that the ratios of all the fuels were greater than 1.

Moreover, the distance of the location of each point in the figure also provides how these fuels can be beneficial. If the point is further from the line, it shows that the fuel can be benefitted more than the others. For example, Softwood A benefitted more than Hardwood A, more than Willow A, and more than Eucalyptus A. It is however, important to note that due to difference in hemicellulose contents, Softwood A may not experience much change upon torrefaction as can be seen in its standard fuel analysis and grindability behaviour in comparison to the other biomass fuels that were torrefied at the same condition.

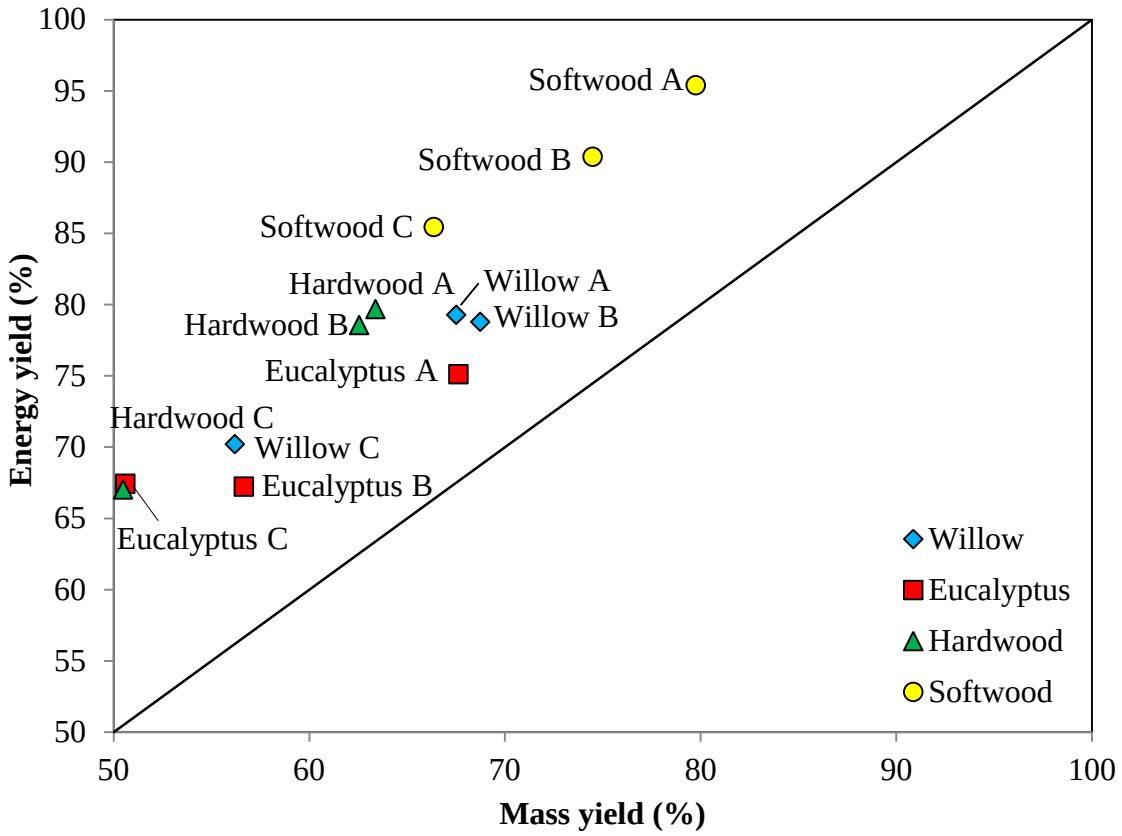

Figure 5.4. Energy yield against mass yield for all torrefied biomass (dry basis), where the line represents an indication of the performance index (ratio) of the fuels.

5.2.4 Physical characterisation

5.2.4.1 Hydrophobicity

Figure 5.5 represents a relationship between the mass yields of biomass fuels and moisture uptake after an immersion test. There is a general trend for the reduction of absorbed moisture content with mass yield as the torrefaction temperature and residence time increased. Figure 5.5 shows that both raw willow and eucalyptus experienced the greatest uptake of water during the two-hours of immersion (66.7% and 62.6% respectively), while

willow C and eucalyptus C absorbed the least amount (15.1% and 18.1% respectively). These findings revealed the capability of torrefaction that is proven to improve the physical property of a biomass by increasing its hydrophobicity. This is in agreement with Pimchuai *et al* (2010) where the hydrophobicity of one of the agricultural residues used, such as rice husks, torrefied at different temperatures (250, 270, 300ºC) was investigated and a decrease in absorbed moisture was observed as the torrefaction temperature increased (4.0, 2.6, 2.3% respectively), compared to the rice husks when it was raw (36.9%). These results suggest that it is apparent that the more severe torrefaction conditions yield a dryer solid, which is less hydrophilic.

Section 3.8 described the susceptibility of an untreated biomass to moisture absorption due to the presence of hydroxyl groups (O-H) in which water binds well with these groups (Yan *et al*., 2009). Yan *et al* (2009) stated that the breakage of hydroxyl groups during thermal treatment explained the reduction of moisture uptake, hence resulted a hydrophobic solid. Although both properties are desirable in a fuel (hydrophobicity and low moisture content), the process conditions required to achieve these favourable changes can also have a detrimental effect on the energy yields. This could be explained further in Figure 5.6.

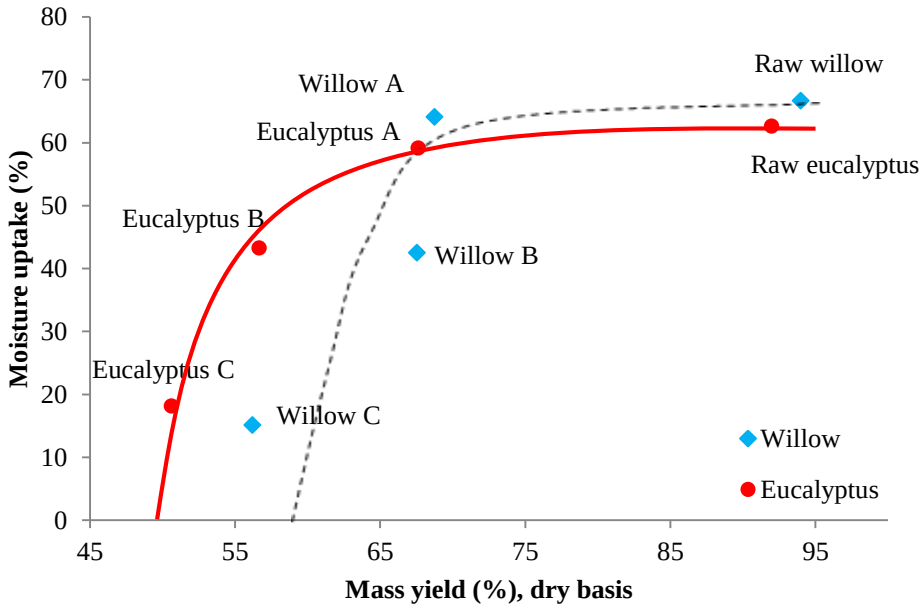

Figure 5.5. Variation in moisture uptake (as measured by the water immersion test) with the mass yield of the raw and torrefied willow and eucalyptus samples (treatments A, B, and C).

Both plots in Figure 5.6 illustrate the relationship between the moisture content and the energy yield and higher heating value respectively. It is clear that the highest process

temperature, treatment C, yielded the driest fuel (15-18% moisture) with the highest hydrophobicity, and also with the highest heating value (Figure 5.6 b), however this treatment also resulted in the lowest energy yields (70.2% for willow and 67.4% for eucalyptus), as presented in Figure 5.6 a. These results highlight the need for optimisation of the torrefaction conditions used in order to improve the fuel quality without sacrificing energy yields. Moreover, Figure 5.6 b) clearly shows that at some point in the torrefaction process, there is an abrupt change in the characteristics of the solid product. For both fuels, this change happened below ~68-73% mass yield. For lower mass yields than this, the HHV of the solid and the hydrophobicity increased very sharply.

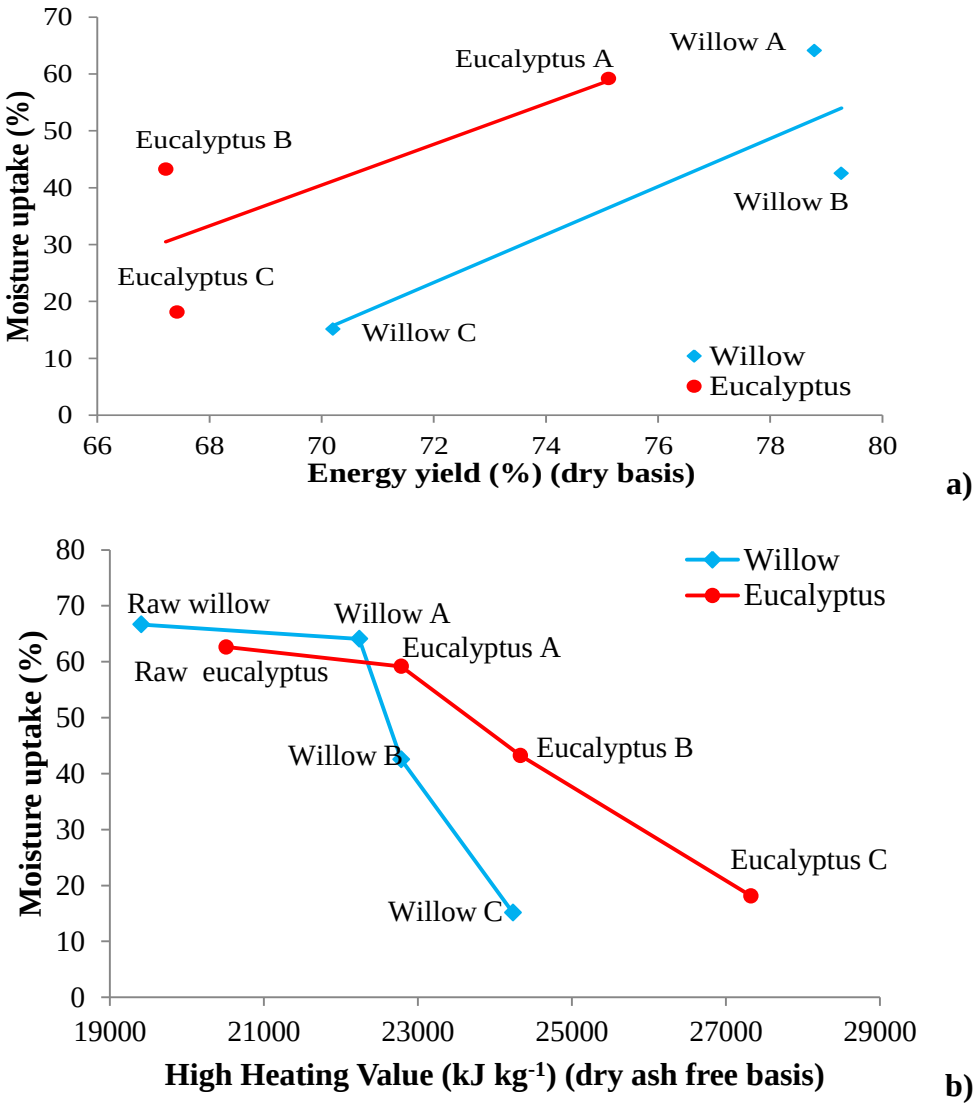

Figure 5.6. Relationship between moisture uptake (as measured by the water immersion test) and a) energy yield; b) high heating value; of raw, and torrefied willow and eucalyptus (treatments A, B, and C).

It is important to note that the increased hydrophobicity of a torrefied biomass is also due to the change in its chemical structures. Reviews such as in Stelte *et al* (2011) and Shang *et al* (2012) have discovered the formation of non-polar, unsaturated compounds in the biomass after torrefaction. Further investigation to observe such formation will be discussed in the later section.

5.2.4.2 Grindability of torrefied biomass

This following section discussed about the grindability performance of the increasing torrefied biomass fuels, in comparison with their raw counterparts and four reference coals of known Hardgrove Grindability Index values (32, 49, 66, 92). The HGI_{equiv} values of the tested biomass were determined according to the calibration curve shown in Figure 4.13 and are listed in Table 5.4. All the raw biomass samples resulted in an HGI_{equiv} value of less than 32, which indicates their poor grindability behaviour. The low friability properties of the untreated biomass samples are more clearly illustrated in Figure 5.7. Raw eucalyptus seemed to have the best grindability behaviour amongst the rest of the fuels.

Furthermore, it can be seen in Table 5.4 that the HGI_{equiv} values of treated biomass have improved with severity of the torrefaction conditions. As the process conditions became more severe, the torrefied biomass became more grindable and brittle, resulted in a greater fraction of the biomass passing through the 75 µm sieve. The table also shows that the hardwood mixture sample was, in general, less affected by the increasingly aggressive torrefaction treatments, compared to the other treated biomass fuels. Technical and human errors may be one of the reasons that can explain such effect as this experiment involved mechanical grinding and shaking. Some particles may get stuck onto the sieves and probably some may have lost during the weighing of each sieve.

Table 5.4. Calculated HGI_{equiv} values of raw and torrefied biomass samples, where the m (%) represents the value of mass that passed through the 75µm sieve as displayed in Equation 5.1.

Sample	m (%)	HGI_{equiv} value	Sample	m (%)	HGI_{equiv} value
Raw willow	0.2	< 32	Raw softwood	0.0	< 32
Willow A	10.5	64.6	Softwood A	7.7	41.5
Willow C	28.1	86.4	Softwood B	9.9	46.4
			Softwood C	20.3	69.2
Raw eucalyptus	1.7	< 32	Raw hardwood	0.3	< 32
Eucalyptus A	6.5	38.9	Hardwood A	8.5	43.3
Eucalyptus B	10.1	46.8	Hardwood B	7.8	41.8
Eucalyptus C	25.0	79.6	Hardwood C	17.6	63.3

$$m\% = (m/m_v) \times 100 \quad (5.1)$$

where m% is the percentage of mass that passed through the 75 µm sieve, m is the mass that passed through the 75 µm sieve mv is the mass of original biomass fuel that was measured up to 50 cm^3.

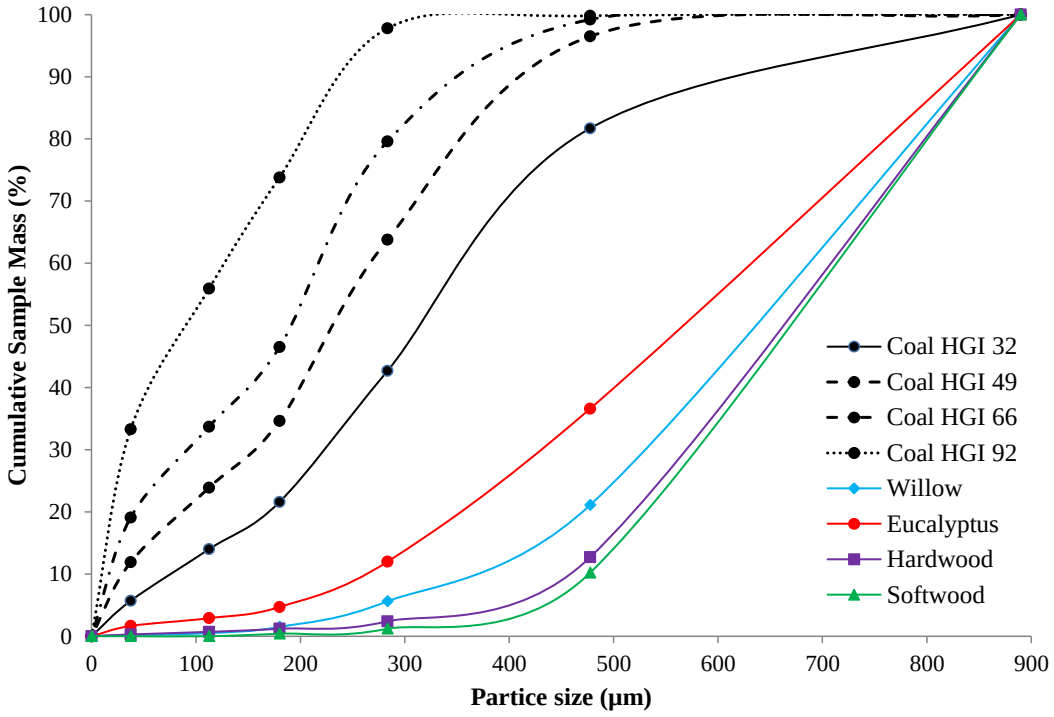

Figure 5.7. Cumulative particle size distributions resulting from milling tests of the raw biomass samples compared with standard reference coals of HGI 32, 49, 66 and 92.

Figure 5.8 illustrates the plot of the particle size distribution of the raw eucalyptus and its torrefied counterparts after milling. The particle size distribution curves of the four reference coals are also shown in the figure for comparison purposes. It is noted that there is a marked improvement on the grindability behaviour of the eucalyptus samples when torrefied at increasingly more severe conditions, with eucalyptus C showing comparable behaviour to coal of HGI 49. This trend was also observed in the other samples, which can be found in the **Appendix 5.3**. Similar results were observed in Bridgeman *et al* (2010) who have tested this approach with willow and *Miscanthus*. Figure 3.20 illustrates the similarity even though the behaviour observed in the study was lower than that in this investigation due to different volume of milling cup used. The milling cup used in this thesis was larger (500 cm^3), while that in Bridgeman *et al*'s study was 250 cm^3. Therefore, there were more spaces for the biomass fuels and coals to be ground and to have more interactions with the balls and walls of the cup at a given time. In their study, the Miscanthus treated at conditions A and D (at 290°C with a residence time of 10 and 60 min) has HGI values that are close to those of standard reference coals (49 and 92 respectively). The HGI values of the biomass fuels treated at the same temperature with a residence time of 30 min as presented in Table 5.4 were lower than 92. They were in the range of ~ 63 to 80.

Figure 5.9 probes the correlations of the HGI_{equiv} values and a) the carbon content, b) the mass yield and c) the energy yield. In brief, the HGI_{equiv} values increased with increasing carbon content, and decreased with increasing mass yield and energy yield.

Similar to hydrophobicity, there seems to be an abrupt change in the slopes for all of the plots in Figure 5.9, where the HGI_{equiv} value increased significantly when the torrefaction temperature changes from 270°C to 290°C. The point at which the change in slope happens is different for different fuels. For these fuels, the change in slopes are at approximately 55-60% carbon content in the solid, but this condition is met over a wide range of mass yields, from 75% for softwoods to 55% for eucalyptus. Similar responses on the energy yields are also observed. This illustrates how sensitive the biomass is to changes in temperature. At the higher temperatures, the hemicellulose decomposition will become very aggressive, and in the case of treatment C, reviews discovered that during the torrefaction above 280°C, the decomposition of cellulose will become appreciable (Chen *et al*., 2011; Shang *et al*., 2012; Basu, 2013). Cellulose decomposition has been studied extensively. FTIR studies indicate a

rapid change in the chemical functional groups once the temperature is approaching 300°C (Shang *et al*., 2012; Morterra and Low, 1983). At this point, the O-H groups are reduced rapidly due to dehydration and cross-linking reactions, creating more C=O groups compounds. Coupling of these two factors will mean that the fibres become easier to separate (through degradation of hemicellulose) and the solid become more hydrophobic. The large mass loss observed for treatment C is further evidence that cellulose decomposition has become very important.

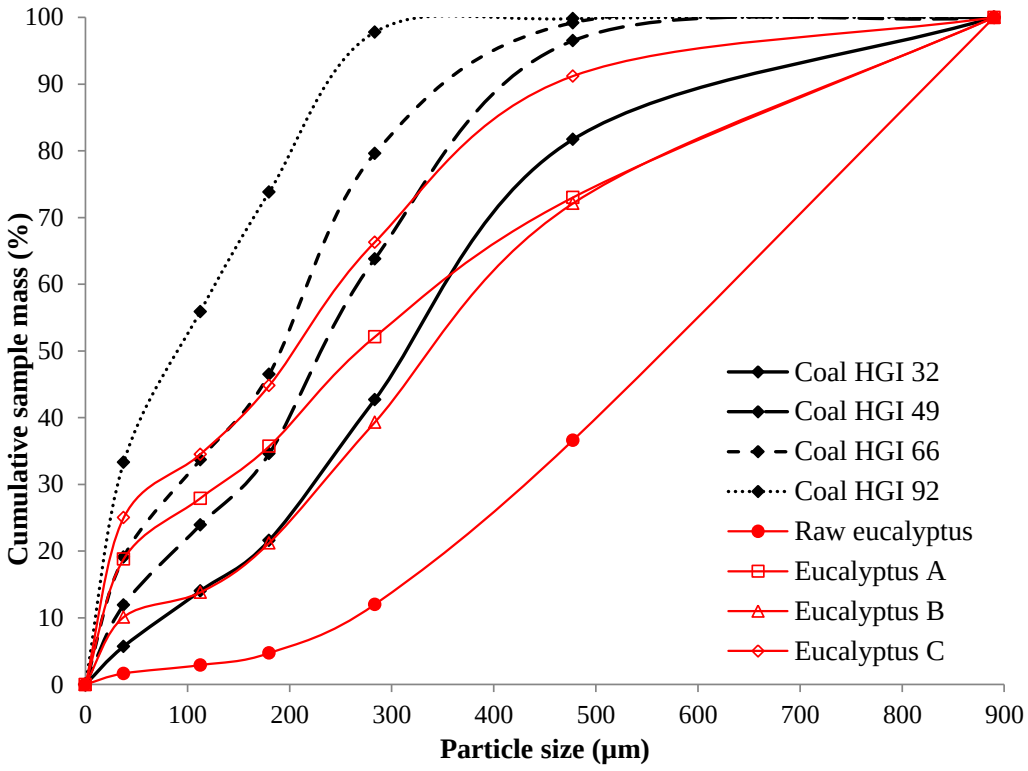

Figure 5.8. Cumulative particle size distributions resulting from milling tests of raw and torrefied eucalyptus under conditions A, B and C and compared with standard reference coals of known HGI values.

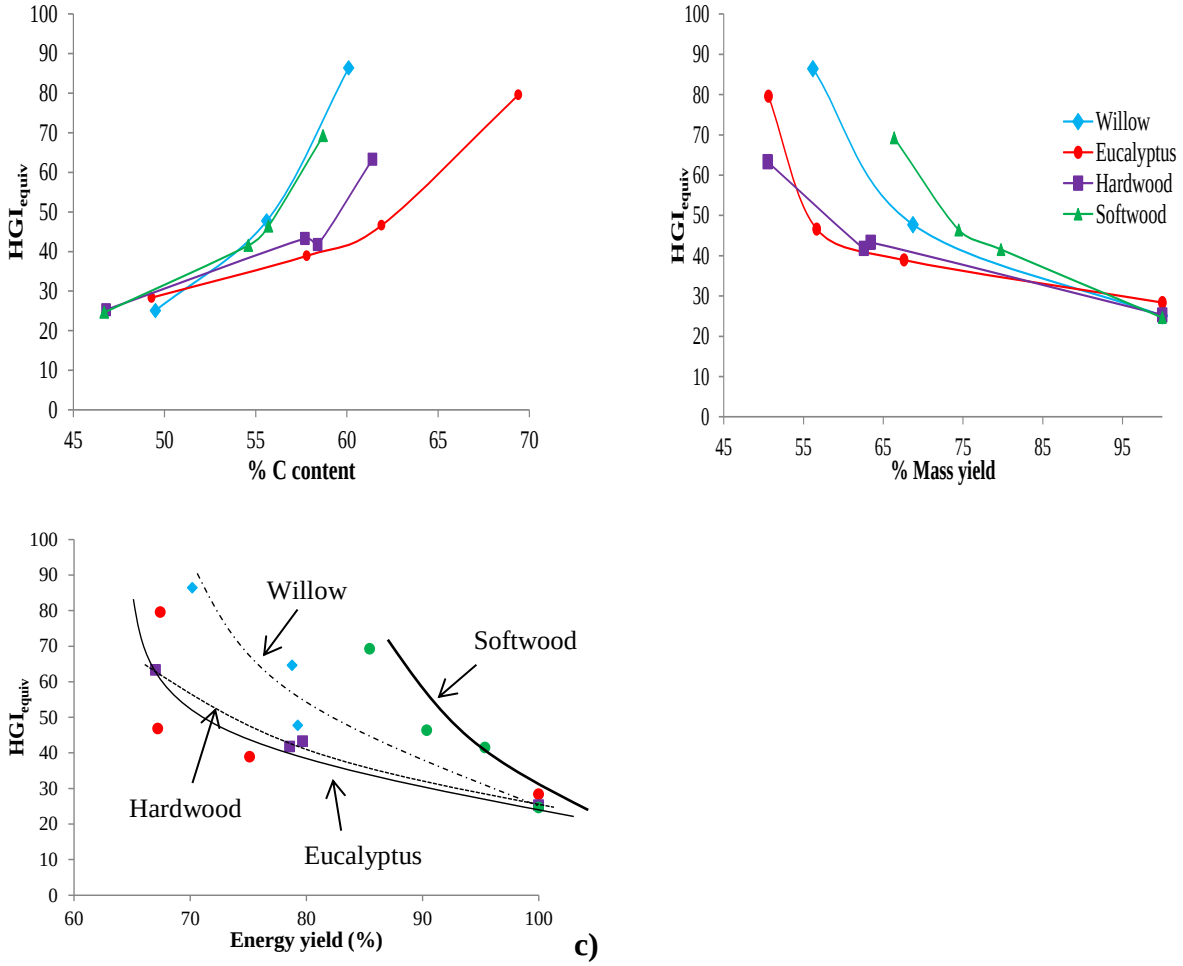

Figure 5.9. Relationships of HGI_{equiv} against a) the C content (dry ash free basis), b) the mass yield, (dry basis) and c) the energy yield (dry basis) of the raw and torrefied biomass fuels.

5.2.4.3 Density

Information on the effect of torrefaction on density of biomass is quite important for the design of a torrefaction plant (Basu, 2013). This experiment shows that the torrefaction treatment did not appear to have a noticeable effect on the density of biomass, as measured by the immersion method as described in 4.4.7. The dry masses and volumes recorded in this experiment yielded densities of approximately 1 g cm^{-3} for all the samples tested. This method may not be sensitive enough to detect changes in density in this experiment. Rodrigues and Rousset (2009) conducted similar experiment on *Eucalyptus grandis* and also did not observed any significant changes to the density at 220ºC (they only differed by 0.02 g cm^{-3} compared to the raw eucalyptus) but they found out that when the temperature increased (at 250 and 280ºC, both treated with a residence time of 60 min), there was a decrease in the property, primarily due to the loss of mass.

5.2.5 Morphological changes to the structure of solid torrefied biomass fuels

5.2.5.1 Surface area

The surface areas of investigated samples using the BET method did not indicate any significant pore development upon torrefaction, as shown in Table 5.5 for the willow and eucalyptus fuels. Surface areas fall within the range of 1.1-3.8 m^2 g^{-1} and duplicate measurements on some fuels indicate a relative error of approximately 10% of the measurement. In this study, TEM was applied to look into the porosity of raw and torrefied eucalyptus but the resulted images did not looked promising and not inserted into this thesis.

Table 5.5. BET Total surface areas of raw and torrefied biomass samples (size fraction of < 0.25 mm).

Sample	Surface area (m^2 g^{-1})
Raw willow	3.8 ± 0.4
Willow A	3.4
Willow B	3.1 ± 0.6
Willow C	1.9
Raw eucalyptus	1.1 ± 0.1
Eucalyptus A	ND
Eucalyptus B	2.7
Eucalyptus C	ND

ND – Not Determined

5.2.5.2 Electron microscopy

Figure 5.10 shows the SEM images of raw and torrefied willow and eucalyptus at increasing treatment temperatures (270ºC and 290ºC, both treated with a residence time of 30 min). It can be seen that the raw biomass looked compact, hard and contains very strong, bulky xylem tissues. Upon torrefaction, the biomass began to lose its bound fibrous structure and cracks and fissures became more obvious in the particles. This is particularly evident in the samples torrefied at 290ºC. These images are in agreement with Arias *et al* (2008), who torrefied eucalyptus at increased temperatures and observed similar structural changes as displayed in Figure 3.9 and discussed in Section 3.3.2. Torrefied eucalyptus in the study became more spherical in shape and less fibrous. This section provides a better insight for the improved grindability behaviour of biomass fuels after torrefaction.

a)

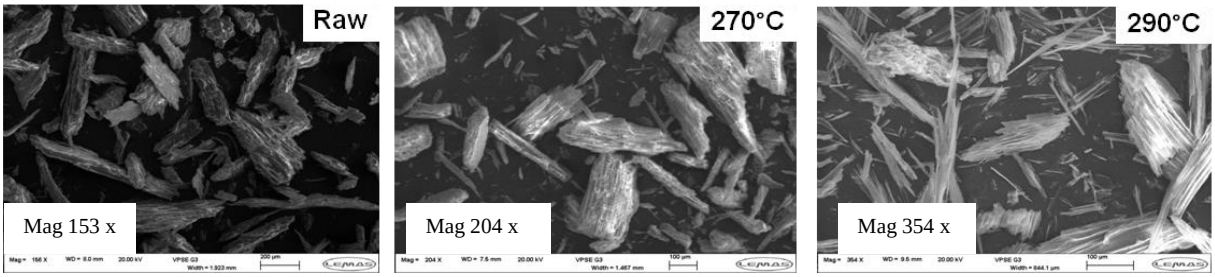

b)

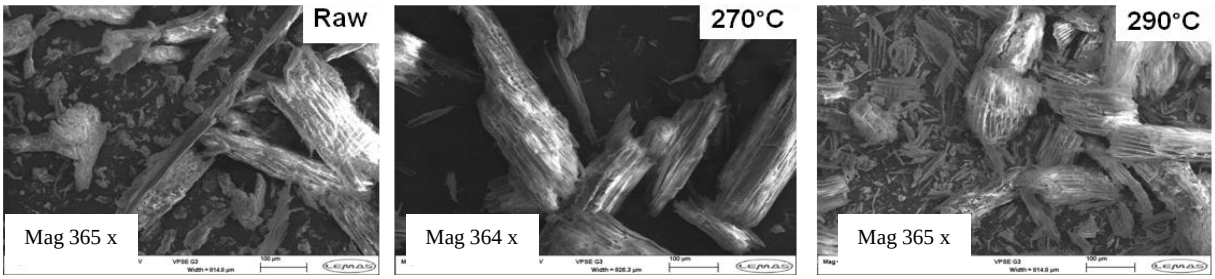

Figure 5.10. SEM images of raw and torrefied a) willow and b) eucalyptus.

5.2.6 Chemical properties of solid torrefied biomass

5.2.6.1 FTIR analysis

Fourier Transform Infrared Spectroscopy was used to investigate the changes in the chemical structure of the solid torrefied biomass as shown in Figure 5.11. Changes were largely due to the degradation of hemicellulose in the biomass. Functional groups of interest were those in the regions where most of the transformation could be seen, namely, in the O–H, C=O, C=C, C–H and C–O–C groups. Similar changes have been observed in Rousset *et al*'s study (2011). They torrefied bamboo at 220-280°C and saw the shifts of two major bands due to stretching vibrations in the C=O and C–O–C groups. Moreover, a significant shift in wavenumbers could also be observed in the C=C group vibrations. In brief, the study showed that the most severely treated biomass had its functional group vibrations shifted towards the lower wavenumbers and noticeable changes in the intensity can be observed.

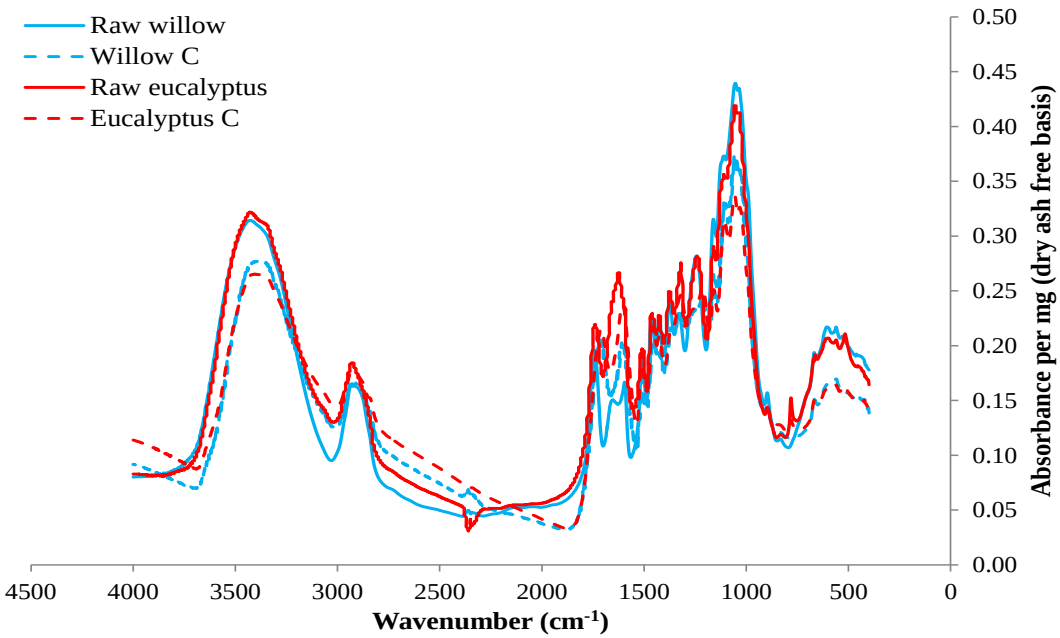

Figure 5.11. FTIR spectra of raw and torrefied willow and eucalyptus.

In this research, Figure 5.11 demonstrates the decrease in intensity of the O–H band around 3600-3100 cm^{-1}, in comparison between the raw eucalyptus and eucalyptus C, as well as those for the analogous willow samples. The FTIR spectra of their other torrefied counterparts (those that were treated with condition A and B) can be displayed in the **Appendix 5.4**.

The loss of O–H group explains the improved hydrophobicity of torrefied biomass and this result is in agreement with those observed in Shang *et al* (2012) and Rousset *et al* (2011) and Stelte *et al*., 2011). This loss of O-H group is also in agreement with the loss of oxygen and hydrogen content determined in ultimate analysis, where most of these loss were due to the release of water vapour from dehydration reactions and formation of volatiles that are rich in hydrogen and oxygen. Next, the C=O group that is located at about 1740-1710 cm^{-1} is shown in Figure 5.12, where the vibration is largely due to the stretching vibrations of the carboxylic acids in hemicellulose of raw eucalyptus (Shang *et al*., 2012; Stelte *et al*., 2011). These include xyloglucan, arabinoglucuronoxylan and galactoglucomannan, as discussed by Stelte *et al* (2011). Previous work suggested that torrefaction eliminates this signal by decreasing the amount of carboxylic acid groups, leading to the formation of new products, which appeared at wavenumbers lower than those acid groups (1700 cm^{-1}) (Zawadzki, 1989). In other words, the C=O groups are still present but not solely due to the presence of carboxylic

acid groups. Figure 5.12 clearly showed these changes in both torrefied willow and eucalyptus. Moreover, the C=C stretch bands from both samples have moved to the lower wavenumber and they have increased in intensity upon torrefaction. The degradation of hemicellulose results in an increase of unsaturation, which explains the observed trends. Torrefaction leads to the formation of more non-polar and unsaturated compounds in the samples. Such formation also explains the improved hydrophobicity of the biomass fuels. The C–O–C vibrations in cellulose appeared in the 1250-1220 cm^{-1} region and the intensity of bands in this region tends to decrease by half its original state for the torrefied samples. The decrease in the intensity of this band has become more extensive with increased severity of torrefaction conditions. With regards to lignin, the vibrations at 1300 cm^{-1} could be due to the aromatic C–O stretching of methoxyl and phenyl-propane units while those at 1516 cm^{-1} and 1508 cm^{-1} could be due to the C=C aromatic ring vibrations (Stelte *et al*., 2011). Rousset *et al* (2011) suggested that the wavenumbers between 900 and 1000 cm^{-1} determine the hemicellulose and cellulose content in a biomass. Figure 5.12 shows changes in this range, where the torrefied biomass fuels now have reduced amount of those two components compared to when they were raw.

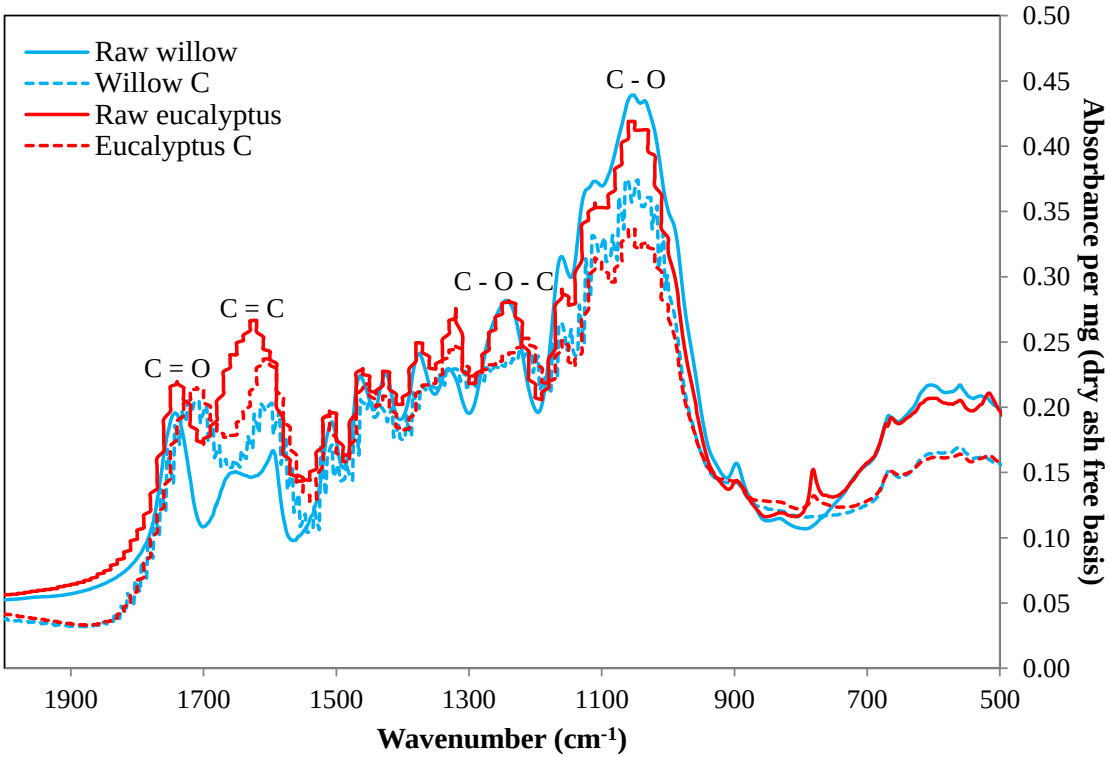

Figure 5.12. Zoom on spectra between 2000 and 500 cm^{-1}.

5.2.6.2 XPS measurements

The XPS technique has been used to investigate the chemical transformations on the surface of carbon fibres and more recently, of thermally treated biomass samples (Bradley *et al*., 1993; Inari *et al*., 2006). For this purpose, the C 1s signal is usually deconvoluted into four components that correspond to four types of carbon atoms bonded to either other elements or functional groups, as follows (Bradley *et al*., 1993; Inari *et al*., 2006). Firstly, the signal for C_1 at binding energy (BE) of 284.6 eV, has been attributed in the literature to carbon atoms bonded with carbon (C-C) or hydrogen (C-H) atoms only (Inari *et al*., 2006). Secondly, the signal for C_2 is typically found at a slightly higher BE compared to C_1 (ΔBE= +1.5±0.2 eV) and this corresponds to a carbon atom bonded with one oxygen atom, which could be ether (C-O-C) or hydroxyl (C-O-H) groups. Thirdly, the signal for C_3 corresponds to carbon atoms bonded to a carbonyl (C-C=O) or two non-carbonyl oxygen atoms (-C-COO) (ΔBE= +2.8±0.2 eV). Finally, a C_4 has been linked to carbon atoms bonded to a carbonyl and a non-carbonyl oxygen atom or carboxylic functionalities (ΔBE= +3.75±0.2 eV) (Bradley *et al*., 1993; Inari *et al*., 2006). In contrast, data for the BE of the O 1s signal are scarce and the assignment of the oxygenated functional groups are still a matter of debate. However, the O_1 peak at BE of 531.4-532.3 eV has been tentatively assigned to carbonyl groups, while the signal for C-O-R groups are expected at 533.0-534.0 eV, where R is an alkyl group (Inari *et al*., 2006). It is important to note that the signal for moisture in wood is also expected to fall within the BE range for C-O- functionalities, at 533.0-533.5 eV (Inari *et al*., 2006).

The survey XPS spectra of the raw and torrefied eucalyptus (shown in the **Appendix 5.5**) indicate the presence of carbon, oxygen and a small proportion of nitrogen. High resolution scans of the XPS spectra of C 1s and O 1s levels for the analysis of raw and torrefied eucalyptus samples are shown with the deconvolutions of their peak envelopes in Figures 5.13 a) - d). The deconvolution of the XPS spectra of the C 1s signal of the raw eucalyptus, shown in Fig. 5.13 a), results in a large peak (at BE 284.6 eV) due to both carbon-carbon bonds and carbon-hydrogen bonds (C_1), which accounts for approximately 90% of the XPS signal. A smaller peak (10%) can also be found at BE of 287.5 eV, that has been tentatively attributed in the literature to ether/hydroxyl groups (C_2). In contrast, the C 1s spectrum of the torrefied eucalyptus C in Fig. 5.13 b) shows the disappearance of the ether/hydroxyl groups and a noticeable decrease of the C_1 from 90% to 47%, upon torrefaction. Additionally, the presence of carbonyl groups (C_3) are also detected, which were absent from the raw sample. Figure 5.13 c) shows the O 1s spectrum of raw eucalyptus, where a peak for oxygen can be

observed at BE of 533.1 eV, which could be attributed to ether groups (C-O-C), hydroxyl groups (C-OH) and possibly moisture (Inari *et al*., 2006). In the case of the torrefied sample C (Figure 5.13 d)), the O 1s spectrum shows two peaks, where in addition to the large peak assigned to C-O-C or C–OH groups (533.3 eV), there is also a peak at 531.5 eV, which could be due to the formation of carbonyl groups.

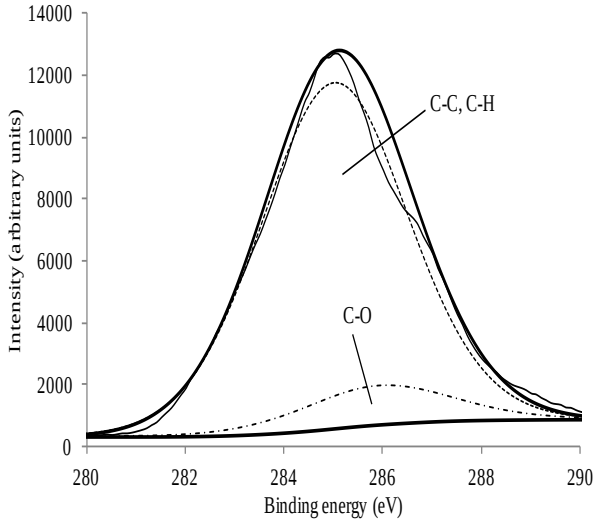

a) C 1s XPS spectra of raw eucalyptus

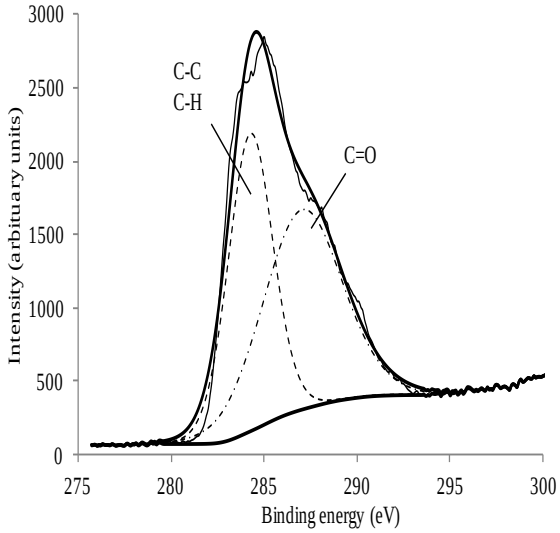

b) C 1s XPS spectra of torrefied eucalyptus

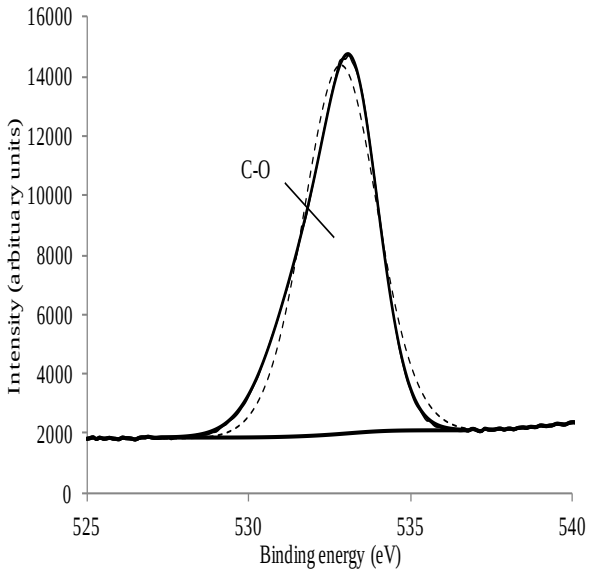

c) O 1s XPS spectra of raw eucalyptus

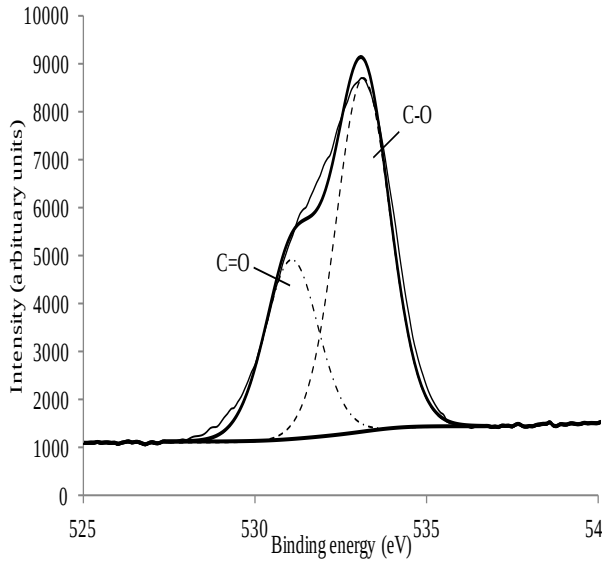

d) O 1s XPS spectra of torrefied eucalyptus

Figure 5.13. XPS spectra of untreated eucalyptus and torrefied eucalyptus sample C, where a) and c) are the C 1s and O 1s XPS spectra of raw eucalyptus; b) and d) are the C 1s and O1s XPS spectra of torrefied eucalyptus.

The results of the XPS data agree with the observations from the FTIR spectroscopy investigations, which show that the heat treatment results in loss of O-H groups and formation of C=O groups consistent with dehydration reactions and cross-linking. The result is a solid with a lower capability to hydrogen bond with water, and hence more hydrophobic.

5.2.7 Analysis of liquid products

The Total Organic Carbon content of the aqueous fraction of torrefied willow is 1460 ppm and its acidity reads a pH 3. The water content present in organic condensables is 1.14±0.04%, which is equivalent to 0.21±0.02 mL. The TOC contents of hardwood and softwood are 1392 and 1238 ppm respectively. Softwood has a higher acidity than hardwood and willow. Ferro *et al* (2004) studied the acidity of the liquid products from the torrefaction of pine and the results showed an increase acidity of the liquid from 2 to 3 with increased temperature from 230ºC to 280ºC. They suggested that acetic acid was responsible for the lower pH at the lowest temperature. The water content present in organic condensables in torrefied hardwood and softwood are 1.33±0.01% and 1.24±0.04%, which are equivalent to 0.25±0.01% and 0.21±0.01% respectively.

The chromatogram obtained from the liquid-GC-MS identified the main components in the organic fraction (Figure 5.14). Most of the components were monoaromatics and are listed in Table 5.6. **Appendix 5.6** lists the components found in the organic fraction of torrefied hardwood and softwood.

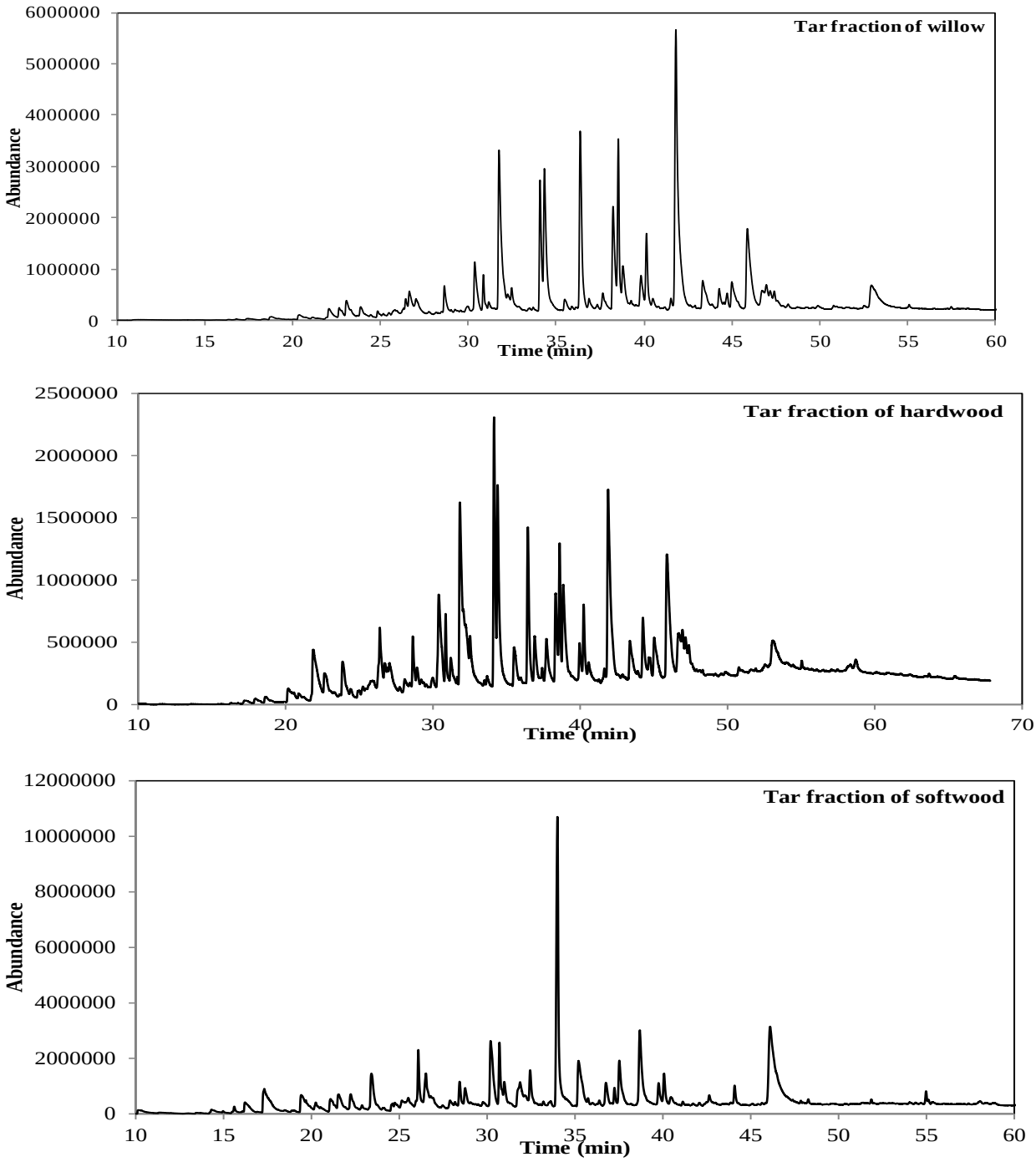

Figure 5.14. Chromatogram of tar produced from the torrefaction of willow, hardwood and softwood.

Table 5.6. Identified components in the tar fraction from torrefied willow.

RT (min)	Identification
28.6042	Phenol, 4-ethyl-2-methoxy-
30.332	2-Methoxy-4-vinylphenol
31.7122	Phenol, 2,6-dimethoxy-
34.047	Phenol, 2-methoxy-4-(1-propenyl)-, (Z)-
34.3013	1,2,3-Trimethoxybenzene
36.3352	Hydroquinone mono-trimethylsilyl ether
38.2083	2,3,5,6-Tetrafluoroanisole
38.5041	Phenol, 2,6-dimethoxy-4-(2-propenyl)-
38.7687	Homovanillyl alcohol
39.8012	2(3H)-Naphthalenone,4,4a,5,6,7,8-hexahydro-4a-methyl-
40.1074	Phenol, 2,6-dimethoxy-4-(2-propenyl)-
41.7833	Phenol, 2,6-dimethoxy-4-(2-propenyl)-
43.3139	Benzaldehyde, 4-hydroxy-3,5-dimethoxy-
44.9691	Ethanone, 1-(4-hydroxy-3,5-dimethoxyphenyl)-
45.8512	2-Pentanone, 1-(2,4,6-trihydroxyphenyl)
52.9285	3,5-Dimethoxy-4-hydroxycinnamaldehyde

RT – Retention time

5.3 Conclusions

The physical and chemical characteristics of some torrefied woods have been investigated. Willow, eucalyptus, a mixture of hardwoods (oak and birch), and a mixture of softwoods (pine, spruce and larch) were torrefied at three conditions: A, at 270ºC with a residence time of 30 min; B, at 270ºC with a longer residence time, 60 min and C, at 290ºC with a residence time of 30 min. Particular emphasis was given to the determination of coal-like grindability behaviour and to any changes in their morphological structure, as observed by microscopic and spectrometric methods. Eucalyptus was observed to experience the greatest mass loss, and although the resultant solid had the highest HHV and changes physically and chemically, it nevertheless had the lowest energy yield. The next reactive fuel in terms of mass loss was the mixture of hardwoods, followed by willow, and finally the mixture of softwoods. The properties of solid torrefied biomass increasingly improved with increased severity of torrefaction. But attaining an optimum operating condition is crucial, without sacrificing energy yields. In this study, treatment at 270ºC with a residence time of 30 min resulted in a

fuel with a mass yield of ~70% of and an energy content ~80–90%, which could be the best condition for the fuels used. Investigations of the torrefied solid indicate that the decrease in the O:C and H:C ratios upon torrefaction is accompanied by the loss of hydroxyl (O-H) groups and an increase in C=O groups relative to C-O groups. The result is a more hydrophobic solid, since its hydrogen-bonding capacity is decreased. In addition, the solid becomes easier to grind to small particle size, as measured by an equivalent Hardgrove Grindability Index test. For these conditions, no obvious change in porosity or surface area was observed, at least with the techniques used. The energy yield of the torrefied solid appeared to vary monotonically with mass yield, but other properties did not. Rather, there was a sudden change in properties such as grindability and hydrophobicity after a certain mass yield and the point at which this abrupt change happens differed for the different samples. The liquid analysis showed that the aqueous phase was acidic and that the principal components in the tar were monoaromatics.

CHAPTER 6

THE INVESTIGATION OF THE INFLUENCE OF PARTICLE SIZES ON PRODUCTS FROM TORREFACTION OF BIOMASS

6. 1 Introduction

In Chapter 5, it was shown that torrefaction has significantly improved the physical and chemical properties of the woody biomass fuels (willow, eucalyptus, a mixture of hardwoods (oak and birch), and a mixture of softwoods (pine, spruce and larch)) that were studied. Operating parameters such as temperature and residence time influenced torrefaction and it was also concluded that through investigations on the solid torrefied biomass using microscopic and spectroscopic methods, temperature has a greater effect on the process in comparison to residence time. In addition to that, heating rate, together with fuel physical characteristics such as the particle size and composition of the original biomass itself also have effect on the end-products of torrefaction. The degree of the thermal degradation of biomass and difference in the hemicellulose contents in a biomass fuel are two of the factors that decide which parameter might influence the overall torrefaction process.

This chapter investigates the extent of the influence of particle size on how far it could affect the yields of torrefaction. Section 3.5 discussed some publications with regards to this parameter in relation to torrefaction. A particular research by Peng *et al* (2012) studied the effect of particle size of pine chips on torrefaction (0.23, 0.67 and 0.81 mm) using a fixed bed reactor. The results showed the influence of this parameter on the mass loss during torrefaction, where the particle size is indirectly proportional to the rate of mass loss; smaller particles have faster mass loss than bigger particles. They concluded that the rate of torrefaction of bigger particles could be hindered by the influence of interparticle heat and mass transfer. The authors also developed a kinetic model of pyrolysis of wood based on the model defined by Di Blasi and Lanzetta (1997) which are laid out in the same section.

The thermal degradation of a biomass takes place by means of a series of chemical reactions of mass and heat transfer (Basu *et al*, 2013). Heat transfer is important and need to be understood, especially for thick biomass particles. The process of torrefaction involves three pathways, namely, 1) the convective heat transfer from the reactor to the biomass surface, 2)

conduction of heat into the biomass interior and 3) the reaction within it. The Biot number (Bi) and Pyrolysis number (Py), as already described in Section 3.2.2, are parameters that can influence the torrefaction process. They also serve an indication to achieve a desired kinetic control.

In general, detailed studies of pyrolysis and in particular, torrefaction of larger particles are very scarce. Biomass fuels come in different shapes and if they are torrefied prior to industrial uses, great amount of milling energy can be saved especially when pulverised biomass fuels are required in co-firing and gasification. Therefore, the understanding of the behaviour of larger particle sizes upon torrefaction is important. In this chapter, willow and eucalyptus were treated in a thermogravimetric analyser, coupled to an FTIR (TGA-FTIR) as detailed in Section 4.3.2. The first part of this chapter examines the influence of two important parameters of torrefaction: temperature and residence time, where the rate of mass loss was studied to get a better insight of the understanding of torrefaction. The next part is the investigation of large particle sizes of biomass on torrefaction, where the sizes consisted of cubes and cuboids that were ≥ cubes of 5 mm as prepared in Section 4.2. Here, results were analysed and compared in terms of mass yield, energy yield, properties of the resultant solid and evolution of volatile products.

At the end of this chapter, the use of a biomass pyrolysis model, FG-Biomass will be discussed. It is designed to be able to simulate torrefaction and predict the yields of products as listed in Section 4.7 as well as the elemental composition of the torrefied solid product. Furthermore, the AFR has developed this model to work together with another program known as Sphere that will be discussed in the next paragraph. This combination allows one to predict the behaviour of a biomass resulting from torrefaction due to difference in particle sizes. Conditions as presented in Table 4.1 were applied, which were similar to those treated in the reactor and TGA. The aim of this part of the study is to compare and analyse the results of torrefaction work that were conducted experimentally using TGA and the large reactor with those simulated by the model.

The Sphere program is designed for sphere particles. It is important to note that the samples torrefied in the TGA were prepared in cubes (5, 6, 7 and 8 mm). So for comparison purposes, these cubes were treated as spheres with the same volumes. It can be shown that the cubes with dimensions L x L x L correspond to the following sphere radii (R) as listed in Table 6.1.

Table 6.1. Cubes and their respective radii.

L (mm)	R (mm)	R (m)
5	3.10	0.00310
6	3.72	0.00372
7	4.34	0.00434
8	4.96	0.00496

The following shows how the above sphere radii were obtained. For example, when L is 5 mm, the calculated volume, V is 125 mm^3. Since the volume of a cube is treated having the same volume as a sphere, the radius, R can be calculated, where the volume of a sphere, $V = 4/3 \times \Pi \times R^3$. When the equation is rearranged, the value of R, 3.10 mm is obtained.

The Sphere program has to be executed first in order to calculate the mean temperature of the particle as a function of time. This time-temperature profile will then be used with the FG-Biomass model to perform torrefaction simulations for a given type of biomass. Apart from that, Sphere can be used to calculate the temperature distribution and the average temperature. Here, the initial temperature, t_o, is uniform while the temperature of the surrounding medium changes in a step-wise fashion from t_o t_o t_{cz}, where t_{cz} refers to the surrounding-medium temperature after a step-wise change. The mean temperature within the sphere is T_{sr}. The temperature at all locations within the sphere is recorded as a function of time. The subroutine shell divides a sphere into a number of shells, ns, in such a way that each shell has an identical volume. The program then calculates temperature as a function of time for all shells and for each of the shells, generates a time-temperature input file for the FG-Biomass model. This part of the code assumes that the number of shells is five.

Before the Sphere program runs, an input file, 'sphere.in' has to be created at the same folder as the program. This is where the particle radius is defined for FG-Biomass calculations. The structure of the input file, 'sphere.in', can be explained below.

Line 1: ne ns

Line 2: t_o t_{cz} r_z a

Line 3: λ α tt tstep, where

ne is number of roots of the characteristic equation x*cot(x)=1-Bi (Bi stands for Biot), which is 6,

ns is number of shells into which the sphere is subdivided, which is 5,

t_o is initial sphere and surrounding-medium temperature (°C), which is set at 20°C,

t_{cz} is surrounding-medium temperature after a step-wise change, which in this case, can also be referred to as the final or desired torrefaction temperature (°C),

r_z is outer radius of the sphere (m),

a is thermal diffusivity of the surrounding medium (m^2/s), where $a = \lambda/(\rho * c_p)$, 0.00000023 m^2/s,

λ is thermal conductivity of the surrounding medium [W/(mK)], 0.12 W/(mK),

ρ is density of the surrounding medium (kg/m^3), where the density of willow is assumed to be 520 kg/m^3 and eucalyptus is 700 kg/m^3 (Francescato *et al*., 2008),

c_p is specific heat capacity at constant pressure for the surrounding medium, [J/(kg*K)],

α is convective heat-transfer coefficient for the heat exchanged between the sphere and the surrounding medium, [$W/(m^2K)$], that is 9 $W/(m^2K)$,

tt is total time, which can also be referred to as the reaction time [s],

tstep is time step for temperature evaluation [s], and this is 5 s.

An example of the input file is given below for willow that is to be torrefied at 290°C with a reaction time of 3600 s and the size of the radius is 0.00496 m, which corresponds to 8 mm cube.

6 5

20 290 0.00496 0.00000023

0.12 9.0 3600 5

When the Sphere's input file is created, another input file of the desired biomass is selected in the FG-Biomass model. The detailed procedure is provided by the AFR and can be found in **Appendix 6.1**. Seven resulted files will appear at the end of the run. 'sphere.out' will present a list of time-temperature profiles when r=0 (the radius of the innermost shell) and $r=r_z$ (the radius of the outermost shell) as shown in Figure 6.1. Five text files (tth1.txt, tth2.txt, tth3.txt, tth4.txt, and tth5.txt) show the time-temperature profiles for the specific five shells. This gives the temperature distribution within the spherical particle. Another file containing values

of the mean sphere temperature as a function of time is called tthm.txt. Each of the above six text files can be used directly as a time-temperature input file for the FG-Biomass model.

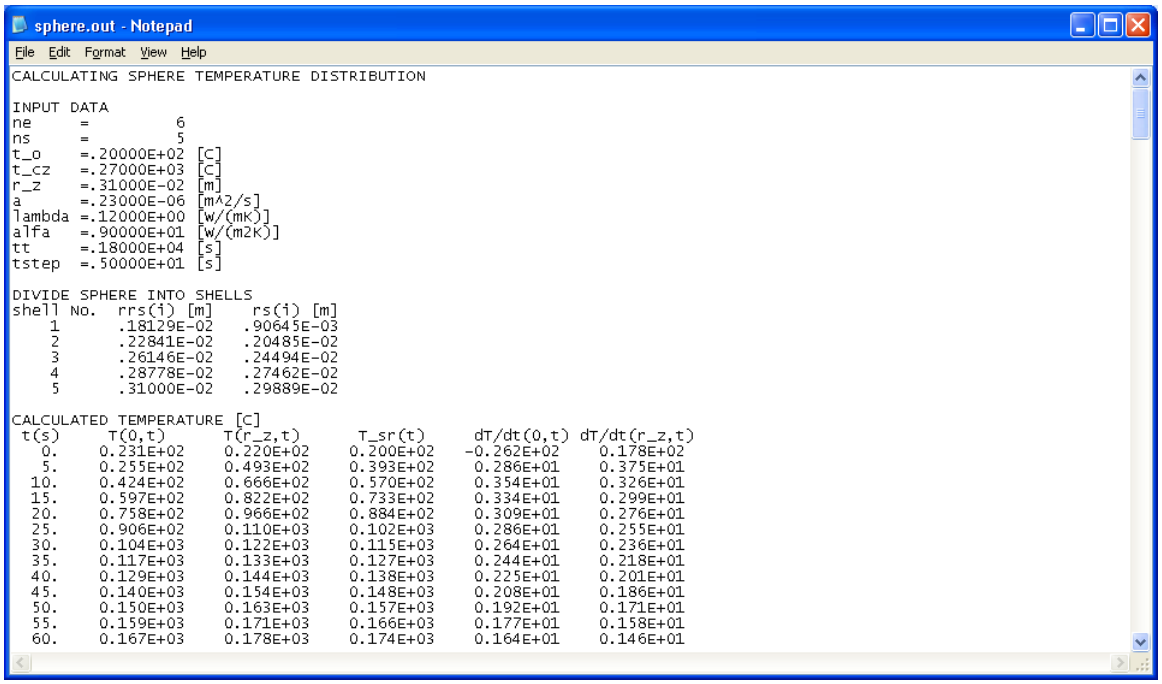

sphere.out - Notepad

File Edit Format View Help

```
CALCULATING SPHERE TEMPERATURE DISTRIBUTION

INPUT DATA
ne      =          6
ns      =          5
t_o     =.20000E+02 [C]
t_cz    =.27000E+03 [C]
r_z     =.31000E-02 [m]
a       =.23000E-06 [m^2/s]
lambda  =.12000E+00 [W/(mK)]
alfa    =.90000E+01 [W/(m2K)]
tt      =.18000E+04 [s]
tstep   =.50000E+01 [s]

DIVIDE SPHERE INTO SHELLS
shell No.   rrs(i) [m]     rs(i) [m]
    1       .18129E-02    .90645E-03
    2       .22841E-02    .20485E-02
    3       .26146E-02    .24494E-02
    4       .28778E-02    .27462E-02
    5       .31000E-02    .29889E-02

CALCULATED TEMPERATURE [C]
 t(s)      T(0,t)       T(r_z,t)       T_sr(t)      dT/dt(0,t) dT/dt(r_z,t)
   0.     0.231E+02     0.220E+02     0.200E+02    -0.262E+02     0.178E+02
   5.     0.255E+02     0.493E+02     0.393E+02     0.286E+01     0.375E+01
  10.     0.424E+02     0.666E+02     0.570E+02     0.354E+01     0.326E+01
  15.     0.597E+02     0.822E+02     0.733E+02     0.334E+01     0.299E+01
  20.     0.758E+02     0.966E+02     0.884E+02     0.309E+01     0.276E+01
  25.     0.906E+02     0.110E+03     0.102E+03     0.286E+01     0.255E+01
  30.     0.104E+03     0.122E+03     0.115E+03     0.264E+01     0.236E+01
  35.     0.117E+03     0.133E+03     0.127E+03     0.244E+01     0.218E+01
  40.     0.129E+03     0.144E+03     0.138E+03     0.225E+01     0.201E+01
  45.     0.140E+03     0.154E+03     0.148E+03     0.208E+01     0.186E+01
  50.     0.150E+03     0.163E+03     0.157E+03     0.192E+01     0.171E+01
  55.     0.159E+03     0.171E+03     0.166E+03     0.177E+01     0.158E+01
  60.     0.167E+03     0.178E+03     0.174E+03     0.164E+01     0.146E+01
```

Figure 6.1. Data in the 'sphere.out' after running the Sphere program.

In the 'sphere.out', there is also a list of radii (Table 6.2) that corresponds to the data in the five text files. For example, the time-temperature profile found in tth1.txt corresponds to the mean radius, rs(i) of each shell, 1.45 mm, data found in tth2.txt corresponds to the rs(i), 3.28 mm and so on.

Table 6.2. Radius and the mean radius of each specific shell.

Shell No.	**rrs(i), (m)**	**rs(i), (m)**
1	0.029	0.014503
2	0.037	0.032776
3	0.042	0.039190
4	0.046	0.043939
5	0.050	0.047822

To study the effect of particle size on torrefaction temperature, the value of r_z will have to be substituted (in metres) as listed in Table 6.1. The results can be analysed when temperatures recorded from the FG-Biomass software were plotted against the time taken.

6.2 Results and Discussion

6.2.1 Fuel analyses of raw willow and eucalyptus (*E.Gunnii*)

The proximate and ultimate analysis, and calculated heating values of the raw willow and eucalyptus samples studied are shown in Table 6.3. The table also lists the particle sizes and their dimensions used in this study. Volumes were calculated according to the measured mass and given densities of the biomass. It is important to note that each particle sizes that were treated at different conditions have different calculated volumes due to their different measured masses. It is also noted that **A**, **B** and **C** are referred to the conditions applied for the treatment as tabulated in Table 4.1 in Chapter 4. The density of willow used is 520 kg m^{-3} while that of *E.Gunnii* is 700 kg m^{-3} (Francescato *et al*., 2008). It can be seen that the raw willow has higher volatile and ash contents than eucalyptus. Moreover, the raw willow has higher hydrogen and oxygen contents as well as a lower carbon content, which results in a lower HHV than the other fuel.

Table 6.3. Fuel characteristics of raw willow and eucalyptus (*E.Gunnii*).

	Willow			***E.Gunnii***		
Particle sizes (mm x mm x mm)	**A** (mm^3)[a]	**B** (mm^3)[a]	**C** (mm^3)[a]	**A** (mm^3)[a]	**B** (mm^3)[a]	**C** (mm^3)[a]
5 x 5 x 5	150.4	133.7	156.8	96.9	72.9	94.7
6 x 6 x 6	251.6	284.3	293.1	159.4	157.1	168.5
5 x 5 x 10	315.6	209.1	360.3	197.7	NA	189.1
7 x 7 x 7	412.5	342.2	335.2	244.2	212.5	255.3
6 x 6 x 10	277.8	416.2	422.3	249.4	NA	255.9
7 x 7 x 10	625.5	466.1	491.9	356.9	NA	348.8
8 x 8 x 8	519.4	534.8	436.4	315.4	340.1	366.0
Proximate analysis (wt %)						
Moisture[b]		3.3			4.2	
Volatile matter[c]		85.4			83.5	
Fixed carbon[c]		13.2			16.3	
Ash[c]		1.4			0.2	
Ultimate analysis (wt %)						
C		46.8			50.1	
H		5.8			4.8	
O[d]		47.4			45.1	
N		0.0			0.0	
S		ND			ND	
HHV (MJ kg^{-1})		18.5			19.5	

[a]Volumes were calculated from the mass and density of the samples as tabulated in **Appendix 6.2**.
[b]As received. NA Not Applicable.
[c]Dry basis. ND Not Detected.
[d]Calculated by difference.

6.2.2 Thermogravimetric analysis (TGA-FTIR)

6.2.2.1 Mass loss and temperature profile

A typical plot of the mass loss curve for the torrefaction process is shown in Figure 6.2, where two stages of mass loss can be observed. To see if there is any influence of particle size, plots of mass loss curve of torrefaction processes for cubes of willow samples, treated with condition B (270°C with a reaction time of 60 min) and the rest of the investigated samples can be found in Figure 6.3 and **Appendix 6.3)** respectively. The decrease of mass at the first stage at a temperature of approximately 150ºC is due to water evaporation, while another distinct mass loss can be seen at temperatures higher than 200ºC, that is largely due to hemicellulose degradation. These observations have also been studied in several publications: Bergman *et al* (2005a), Bridgeman *et al* (2008), Medic *et al* (2012) and Chen *et al* (2011) and Prins *et al* (2006a) to name a few. Interestingly, Figure 6.3 shows that samples of different sizes started off at different moisture contents, which seemed to have an effect, even though small (even by 1-2%, dry basis) on the rate of mass loss during torrefaction. For example, those that experienced a greater loss of moisture content during the drying period experienced a further mass loss during torrefaction, regardless of the sample size.

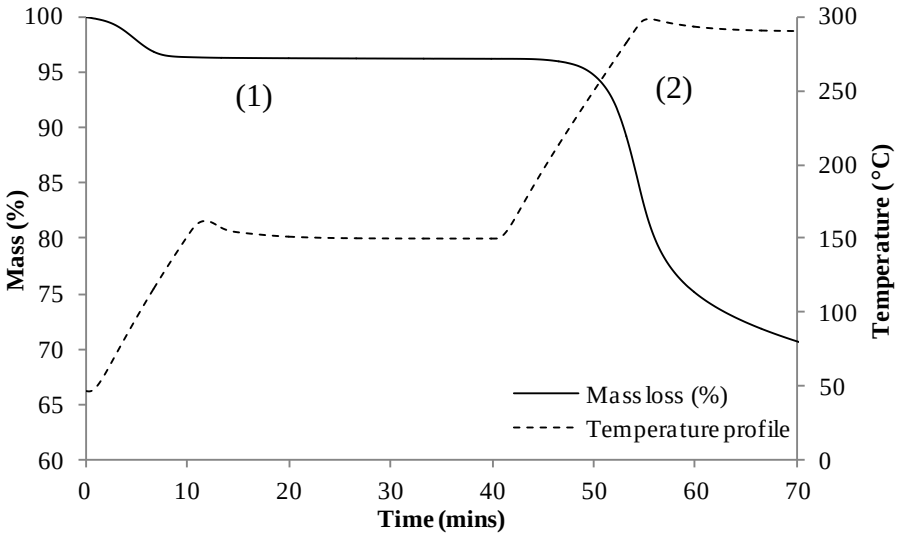

Figure 6.2. Typical mass loss and temperature profile during torrefaction of willow and eucalyptus. Two stages of mass loss and change in temperature can be seen, labelled (1) and (2).

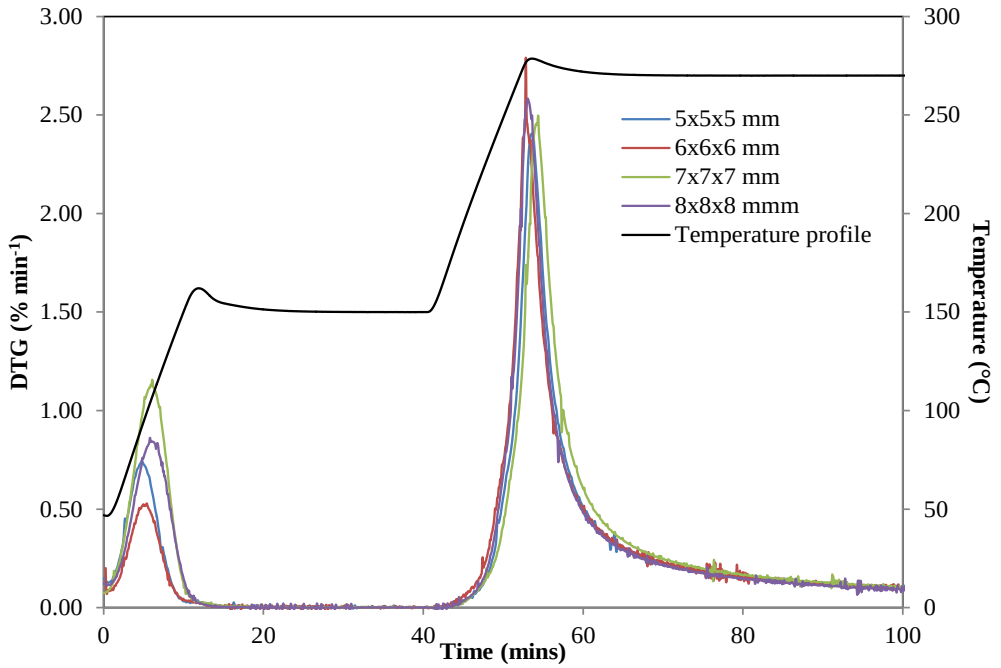

Figure 6.3. Rates of mass loss and temperature profile as recorded by the software during torrefaction of willow of different sizes (cubes) at condition B, when the final temperature was set to 270ºC with a reaction time of 60 min.

However, despite the inconsistent results shown in Figure 6.3, the next plot (Figure 6.4) illustrates the general view of the changes in mass yield where the trends became clear. An increase in mass yield was observed with increased in size. It shows the overall mass yields of willow and *E.Gunnii* of different particle sizes for torrefaction with treatment A, B and C (270°C, 30 min, 270°C, 60 min and 290°C, 30 min respectively).

Peng *et al* (2012) stated that the weight loss can be influenced by differences in particle size. Interparticle heat and mass transfer could influence torrefaction. Smaller particles will give rise to a faster heat transfer (Oyedun *et al*., 2012). This resulted in a positive correlation between the particle size and mass yield. Beaumont and Schwob (1984) and Heo *et al* (2010) discussed how larger particle sizes would yield more char and that they can influence the heating rate. These authors stated that larger particles require more time to heat by conduction. Therefore, when there is a slower torrefaction rate, there will be less decomposition taking place at a given reaction time, which leads to a little mass loss at the end of the torrefaction process.

6.2.2.2 Influence of temperature and residence time on torrefaction using a TGA in terms of rate of mass loss

Figure 6.5 shows a typical curve of the first derivative for the mass loss with time (DTG) during the torrefaction of willow and *E.Gunnii* samples. Note that the time was corrected to zero instead of the 40th min as previously used in Figure 6.2 and 6.3. The large peak observed in each torrefaction run is from the decomposition of the thermally reactive component, hemicellulose (Haykiri-Acma, 2006). This is in agreement with Chen *et al* (2011) who discovered that the degradation of hemicellulose started at temperatures as low as 230°C, while that of cellulose only appeared to degrade significantly at a higher temperature (290°C). These observations are shown in Figure 3.2.

Figure 6.5 a) refers to willow samples of a particle size of 7x7x7 mm. There was only a small difference between the intensity of the DTG peaks when willow was treated at conditions A and B (0.24% min^{-1}), while the difference between the DTG peak intensities for treatments A and C was bigger (1.76% min^{-1}). Conditions A and B differ by the change in residence time (30 and 60 min respectively), while A and C differ by the change in temperature (270°C and 290°C respectively). This shows that temperature has a greater effect on torrefaction than the residence time. This effect has been widely studied and many have agreed to the statement (Bridgeman *et al*., 2010; Pimchuai *et al*., 2010; Felfli *et al*., 2005). Similar trends could also be seen in eucalyptus (Figure 6.5 b)). The rates of mass loss of *E.Gunnii* for treatments A and B were almost the same. The difference between the peaks for treatments A and C was much more significant (1.39% min^{-1}). In terms of biomass types, eucalyptus samples have faster rates of mass loss upon torrefaction than those of willow (~0.5% min^{-1}). To see if shapes may have impact on torrefaction, DTG curves of cubes and cuboids of willow and eucalyptus at condition C treatments were displayed in Figure 6.5 c) and d). However, no obvious trend can be seen between those two shapes.

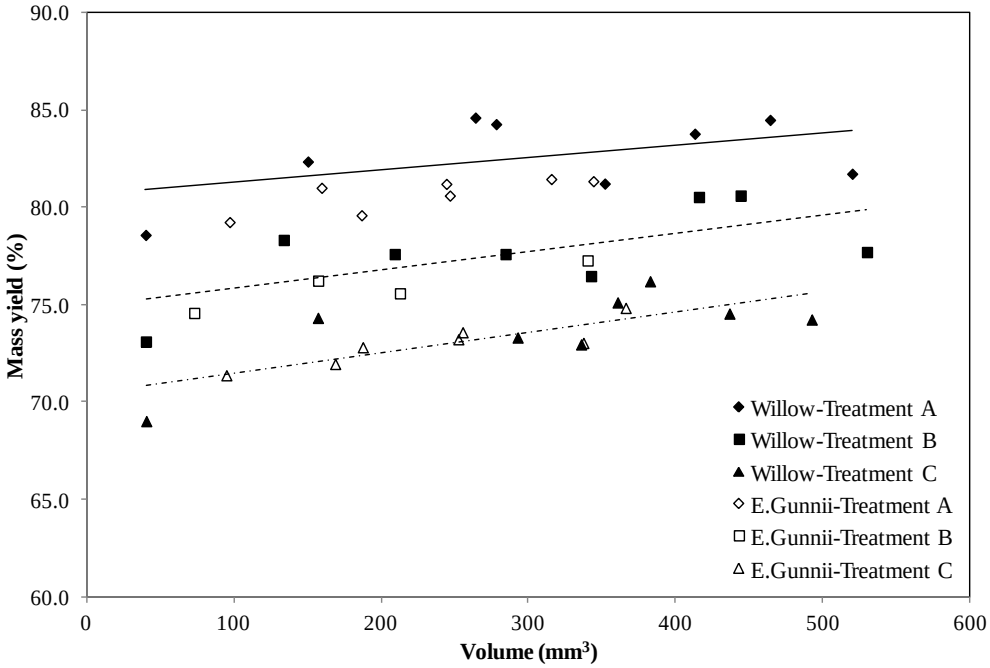

Figure 6.4. Mass yield (dry basis) of willow and *E.Gunnii* of different particle sizes for torrefaction at treatments A, B and C (270°C, 30 min, 270°C, 60 min and 290ºC, 30 min respectively).

However, Basu *et al* (2013) saw changes when they studied the effect of shapes and found that the mass yields decreased with increased diameter (fixed length) while the mass yields increased with increased length (fixed diameter) of the particle. The greater wall thickness of a larger diameter particle leads to a higher thermal resistance. When heat is generated by exothermic reactions, it caused the core temperature of the particle to rise. As a result, more thermal degradation of the biomass occurred, which resulted in lower mass yields. On the other hand, the core temperature did not seem to be influenced by the increase in length. The heat from exothermic reaction is able to escape and leads to no increase in the the core temperature of the biomass. As a result, not much of decomposition takes place in longer particles.

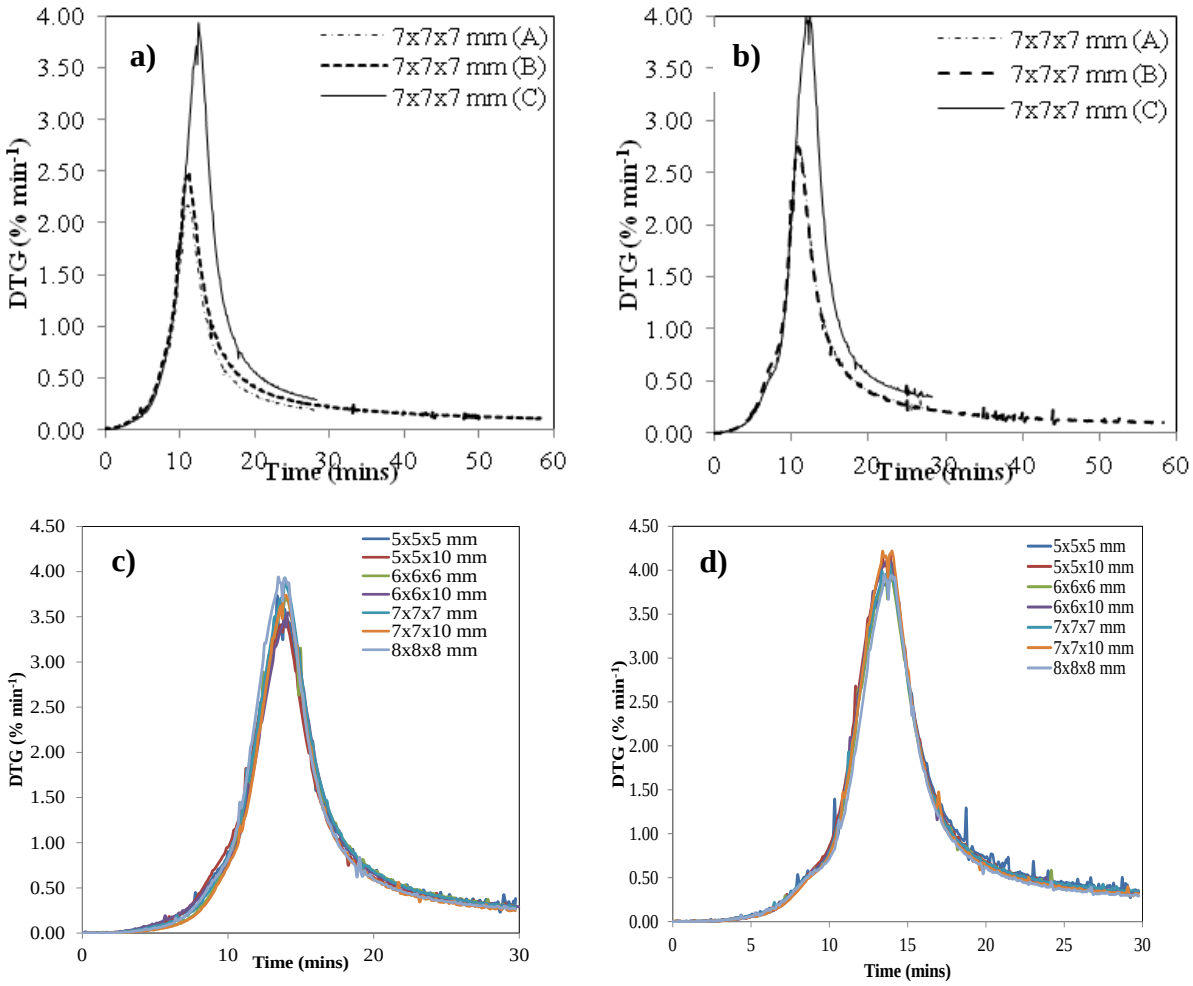

Figure 6.5. DTG of the decomposition of a) willow and b) *E.Gunnii* of particle size 7x7x7 mm for treatments A, B and C (at 270ºC with residence times 30 and 60 min and at 290ºC with residence time 30 min respectively), c) cubes and cuboids of willow and d) those of eucalyptus treated at condition C in helium at 10ºC min^{-1}.

6.2.2.3 Influence of particle sizes on the pyrolysis of torrefied biomass

The TGA curves for the pyrolysis of the cubes of willow and *E.Gunnii* from treatment C are shown in Figures 6.6 a) and b) in comparison with their raw counterparts. Figures 6.6 c) and d) illustrate the corresponding typical DTG curves for the pyrolysis of torrefied willow and *E.Gunnii* respectively. The peaks and shoulders shown in these figures can be attributed to the decomposition of the major components of biomass (hemicellulose, cellulose and lignin). In these figures, there are obvious distinctions between the raw and torrefied biomass. The shoulder in the DTG curves of the two raw biomass (observed in the range 200<T<325ºC) had disappeared upon torrefaction. Chen *et al* (2011) have seen similar plots when they studied the pyrolysis of torrefied willow, bamboo and banyan. They discussed that the

shoulder represents the presence of hemicellulose and most of the cellulose does not react during torrefaction but as the treatment becomes severe, the peaks of cellulose decreased resulting in an increase of the amount of lignin retained in the torrefied biomass. This was also observed in a number of studies such as Bridgeman *et al* (2008) and Kim *et al* (2012). In terms of particle sizes, there seemed to be very little changes in the lignocellulosic contents upon torrefaction. This conclusion explains the plateau observed in the proximate analysis that will be presented in the next section.

6.2.2.4 Properties of torrefied solid product

6.2.2.4.1 Proximate analysis (Moisture, ash, volatile and char contents)

In general, the volatile contents of torrefied fuels in this study were lower and the char and ash contents were higher than those of raw fuels (as shown in Table 6.3) due to the partial devolatisation suffered during torrefaction. With respect to different particle sizes, Figure 6.7 a) shows the influence of treatment conditions on the proximate analysis of the torrefied eucalyptus at 290°C with a reaction time of 30 min. The figure represents an overall decrease in ash and FCC, with a corresponding increase in the volatile content as the particle sizes increased from 5x5x5 mm (with a calculated volume of 94.7 mm^3) to 8x8x8 mm (366.0 mm^3). This change of behaviour could be attributed to the hemicellulose decomposition mechanism that took place during torrefaction. Smaller particle sizes are very reactive, which promotes a greater loss of volatile during the thermal treatment and in turn have their ash and FCC improved. But mass and heat transfer seemed to play their parts appreciably with increased particle size (Wei *et al*., 2006; Yin *et al*., 2012). Despite this, there seemed to be no obvious trend when looking at the overall picture for the response of these fuels with increased particle sizes on this type of analysis (Table 6.4).

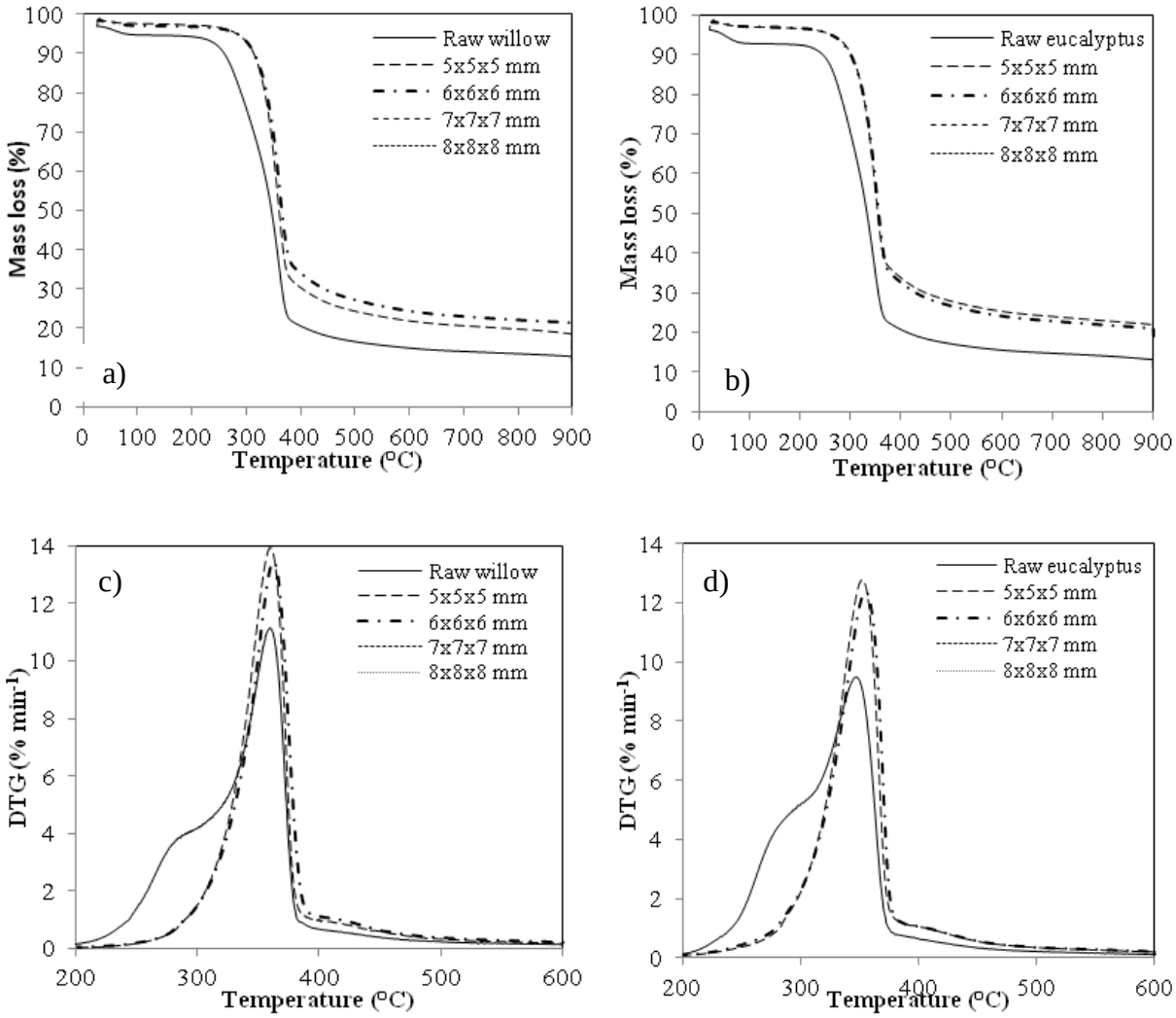

Figure 6.6. TGA and DTG curves for the pyrolysis of raw and torrefied willow and eucalyptus of different particle sizes from treatment C, in helium at 10°C min^{-1}.

Figure 6.7 b) shows the proximate analysis of torrefied willow, where the volatile contents and FCC seemed to level off at almost a plateau (differed by only ±2.0%) and the scattered plots of ash with increased particle size. Similar outcomes can also be observed for the rest of the willow samples. The following section may explain these effects. Unfortunately, there is not much in the literatures that consider the changes in the proximate analysis that could support nor challenge these results. Kim *et al* (2012) observed the decreasing trend of ash content in torrefied yellow poplar as well as Mani *et al* (2010) in pyrolysis of wheat straw but no comments were presented on the reason behind these observations.

Table 6.4. Proximate analysis of torrefied willow and eucalyptus obtained from pyrolysis.

Willow					
Sample	**Condition**	**Moisture (%)**	**Volatile (%)[a]**	**Ash (%)[a]**	**FCC (%)[a]**
5x5x5 mm	C	0.9	79.6	0.8	19.6
6x6x6 mm	A	1.5	81.0	0.5	18.4
6x6x6 mm	B	3.0	79.3	1.5	19.2
6x6x6 mm	C	4.8	76.8	0.9	22.3
5x5x10 mm	A	2.5	81.5	0.8	17.7
5x5x10 mm	B	3.8	79.5	0.7	19.8
5x5x10 mm	C	1.5	77.9	0.7	21.4
7x7x7 mm	A	1.8	81.9	0.4	17.7
7x7x7 mm	B	1.3	80.9	0.7	18.5
7x7x7 mm	C	1.6	78.8	0.5	20.8
6x6x10 mm	A	1.7	81.6	0.4	18.0
6x6x10 mm	B	1.6	77.7	ND	ND
6x6x10 mm	C	1.6	78.0	1.0	21.0
7x7x10 mm	A	3.8	83.1	0.4	16.5
7x7x10 mm	B	3.6	82.8	0.7	16.5
7x7x10 mm	C	4.1	80.6	0.7	18.7
8x8x8 mm	A	1.9	78.9	0.7	20.4
8x8x8 mm	B	1.6	77.4	0.8	21.8
8x8x8 mm	C	1.2	77.8	0.6	21.6

[a]dry basis
ND Not Determined
FCC Fixed Carbon Content

6.2.2.4.2 Ultimate analysis (C, H, N contents) and calorific values

The ultimate analysis of biomass investigated the change in the chemical composition of different particle sizes of biomass when they are torrefied. This study showed that the carbon content increased while oxygen and hydrogen contents decreased from raw to torrefied fuels. The nitrogen content remained almost constant. However, particle sizes did not seemed to have any significant effect on the chemical composition of both types of fuels and hence, no effect could be observed on the energy yields for willow and *E.Gunnii* (Table 6.5).

Table 6.4. *Continued*

Eucalyptus					
Sample	**Condition**	**Moisture (%)**	**Volatile (%)[a]**	**Ash (%)[a]**	**FCC (%)[a]**
5x5x5 mm	B	1.6	76.9	0.6	22.5
5x5x5 mm	C	1.3	76.0	1.1	22.9
6x6x6 mm	A	1.2	86.7	0.7	12.6
6x6x6 mm	B	1.6	80.9	0.8	18.3
6x6x6 mm	C	1.9	77.1	0.7	22.2
5x5x10 mm	A	3.9	80.7	0.5	18.8
5x5x10 mm	C	4.1	78.1	0.5	21.4
7x7x7 mm	A	1.7	77.1	0.7	22.2
7x7x7 mm	B	1.8	75.6	0.8	23.6
7x7x7 mm	C	2.1	79.6	0.6	19.8
6x6x10 mm	A	4.2	80.1	0.6	19.3
7x7x10 mm	A	4.1	80.0	0.5	19.4
7x7x10 mm	C	3.6	79.7	0.4	19.9
8x8x8 mm	A	1.9	79.0	0.6	20.4
8x8x8 mm	B	6.0	78.1	1.1	20.8
8x8x8 mm	C	1.9	75.7	0.4	23.8

6.2.2.5 Gas evolution profile

Figure 6.8 was obtained from the FTIR and it corresponds to the spectral analysis of the volatiles produced in the TGA during torrefaction of willow. The identification of each volatile was determined at different wavenumbers as displayed in Table 6.6. There were 14 species of interest identified in the torrefaction of willow and eucalyptus. Bridgeman *et al* (2008) stated that the peak observed in Figure 6.6 indicate the point at which torrefaction takes place at its maximum and it is corresponded with the mass loss curve shown in Figure 6.2. One of the main condensable liquids produced during this process was acetic acid and other condensable organics were acetaldehyde, formaldehyde, methanol, acetone, formic acid and small amounts of furfural and phenol. Water was also produced during this process due to dehydration reactions of organic molecules (Bridgeman *et al*., 2008; Medic *et al*., 2012). Permanent gases were carbon dioxide, methane and smaller quantities of ethane, ammonia and carbon monoxide. This list of products has been identified previously in Ferro *et al* (2004), Bridgeman *et al* (2010) and Medic *et al* (2012) during the torrefaction of agricultural residues like sugar cane bagasse, willow and corn stover respectively and these products were

mainly resulted from the decomposition of hemicellulose. Interestingly, it could be observed in the figure below that carbon dioxide, methanol, water, methane and carbon monoxide appeared earlier than other volatiles during the torrefaction process. This shows that low molecular weight volatiles/gases are emitted during the drying period, where the temperature was still below 200°C. Minor decomposition of the hemicellulose may occur and moisture as

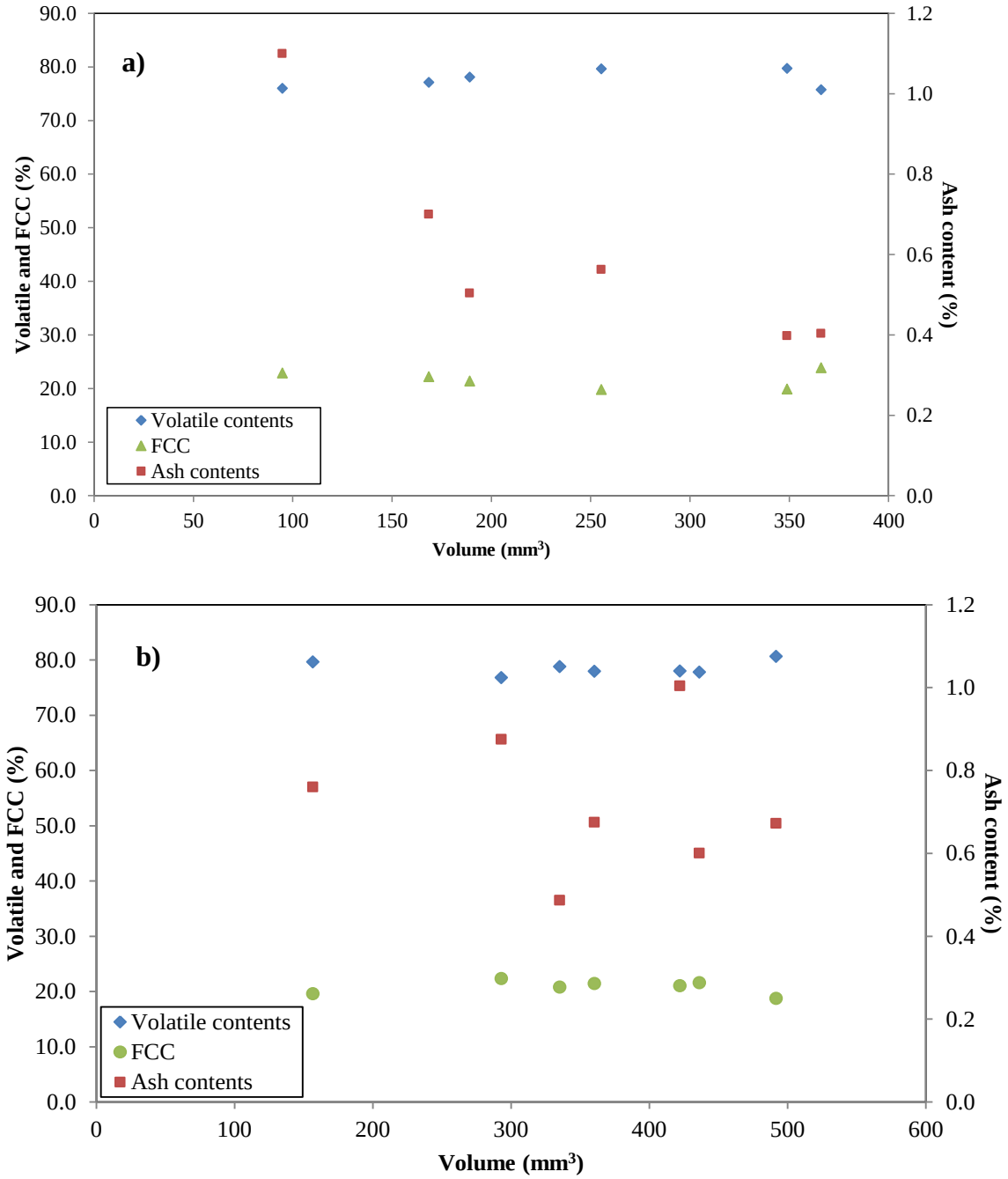

Figure 6.7. Plots of volatile, fixed carbon and ash contents of different particle sizes of torrefied a) *E.Gunnii* and b) willow (treatment C) against particle volume. Note that the volumes were calculated according to the density of the biomass fuels as tabulated in **Appendix 6.2**.

well as reaction water may have released at this stage. Bound water may have been released as a result of chemical reactions, releasing hydrates (Lu *et al*., 2008).

Table 6.5. Energy yields of torrefied willow and *E.Gunnii* (dry ash free basis).

Willow	
Condition A	**Energy yield (%)**
6x6x6mm	86.8
5x5x10mm	91.9
7x7x7mm	94.7
6x6x10mm	92.4
7x7x10mm	84.1
8x8x8mm	88.7
Condition B	
6x6x6 mm	93.3
5x5x10 mm	91.9
7x7x7 mm	87.0
7x7x10mm	94.9
8x8x8mm	90.5
Condition C	
5x5x5 mm	80.5
6x6x6 mm	87.9
5x5x10 mm	85.5
7x7x7 mm	88.5
6x6x10 mm	95.2
7x7x10 mm	81.7
8x8x8 mm	84.4

E.Gunnii	
Condition A	**Energy yield (%)**
6x6x6 mm	76.5
5x5x10 mm	90.4
7x7x7 mm	85.1
6x6x10 mm	97.8
8x8x8 mm	89.8
Condition B	
5x5x5 mm	78.6
6x6x6 mm	80.2
7x7x7 mm	77.0
8x8x8 mm	91.6
Condition C	
5x5x5mm	74.3
6x6x6mm	75.3
5x5x10mm	70.7
7x7x7mm	70.6
7x7x10mm	71.0
8x8x8mm	83.3

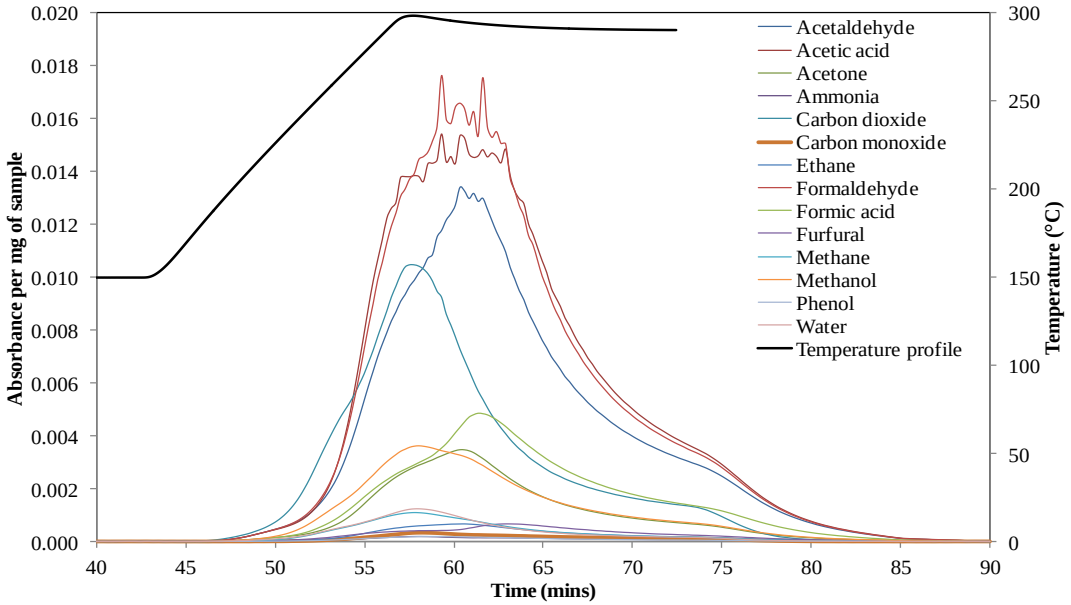

Figure 6.8. Typical evolution profile of volatile products during torrefaction of willow and eucalyptus of treatment C. This plot was taken from the torrefaction of willow (7x7x7 mm).

Table 6.6. Characteristic wavenumbers of evolved volatiles during torrefaction of biomass.

Compound	Wavenumber (cm^{-1})	Compound	Wavenumber (cm^{-1})
Acetaldehyde	1760	Formaldehyde	1783
Acetic acid	1798	Formic acid	1121
Acetone	1369	Furfural	752
Ammonia	929	Methane	3011
Carbon dioxide	2362	Methanol	1059
Carbon monoxide	2175	Phenol	1601
Ethane	947	Water	3739

The intensities of each volatile increased with more severe torrefaction condition for example, willow of 7x7x7 mm as shown in Figure 6.9. Carbon dioxide obtained from conditions A and B reached the same maximum peak and when condition C was used, the intensity increased. Studies have been reported that temperature plays the most important role in torrefaction (Bridgeman *et al*., 2010; Pimchuai *et al*., 2010; Feifli *et al*., 2005; Medic *et al*., 2012). Figure 6.10 further illustrates that this parameter has a more significant effect on the process than the residence time. This effect is in agreement with the derivative mass loss shown in Figure 6.5 a) and b), where the mass loss of torrefaction at increasing the

temperature in condition C showed a more remarkable rate than lengthening the time in condition B.

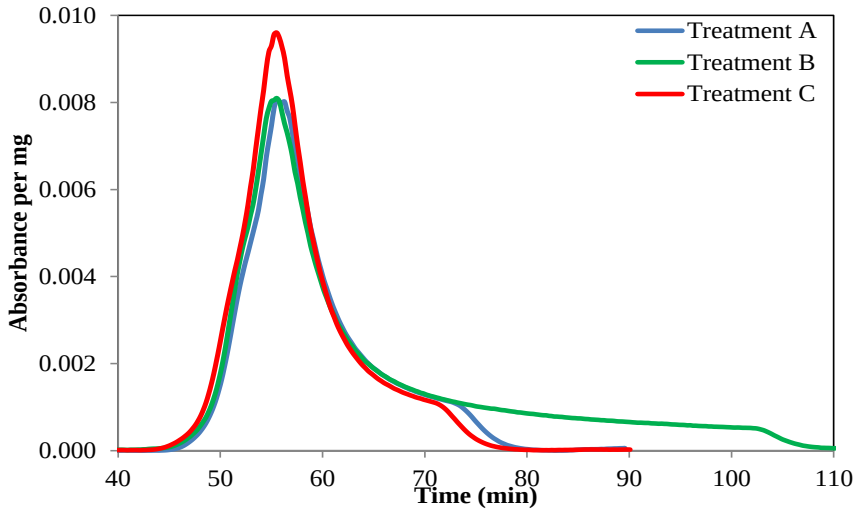

Figure 6.9. Evolution profiles of carbon dioxide obtained from torrefaction of willow (7x7x7 mm) at increasing torrefaction conditions (A, B and C).

With respect to particle size, Figure 6.10 illustrates how different particle sizes may have influence the amount of volatiles evolved during the thermal process. It shows that the size is indirectly proportional to the amount of volatiles evolved. Note that the figures were plotted against normalised absorbance (as per mg of the sample used). According to Figure 6.10, as the particle becomes bigger, the amount of carbon dioxide produced is smaller. This can be attributed to the increase mass and heat transfer limitations with increase particle size as explained in literatures as discussed in Section 3.5. This, in effect, hinders the heating rate during torrefaction and hence, affecting the evolution of products. More plots on other volatiles can be found in Figure 6.10.

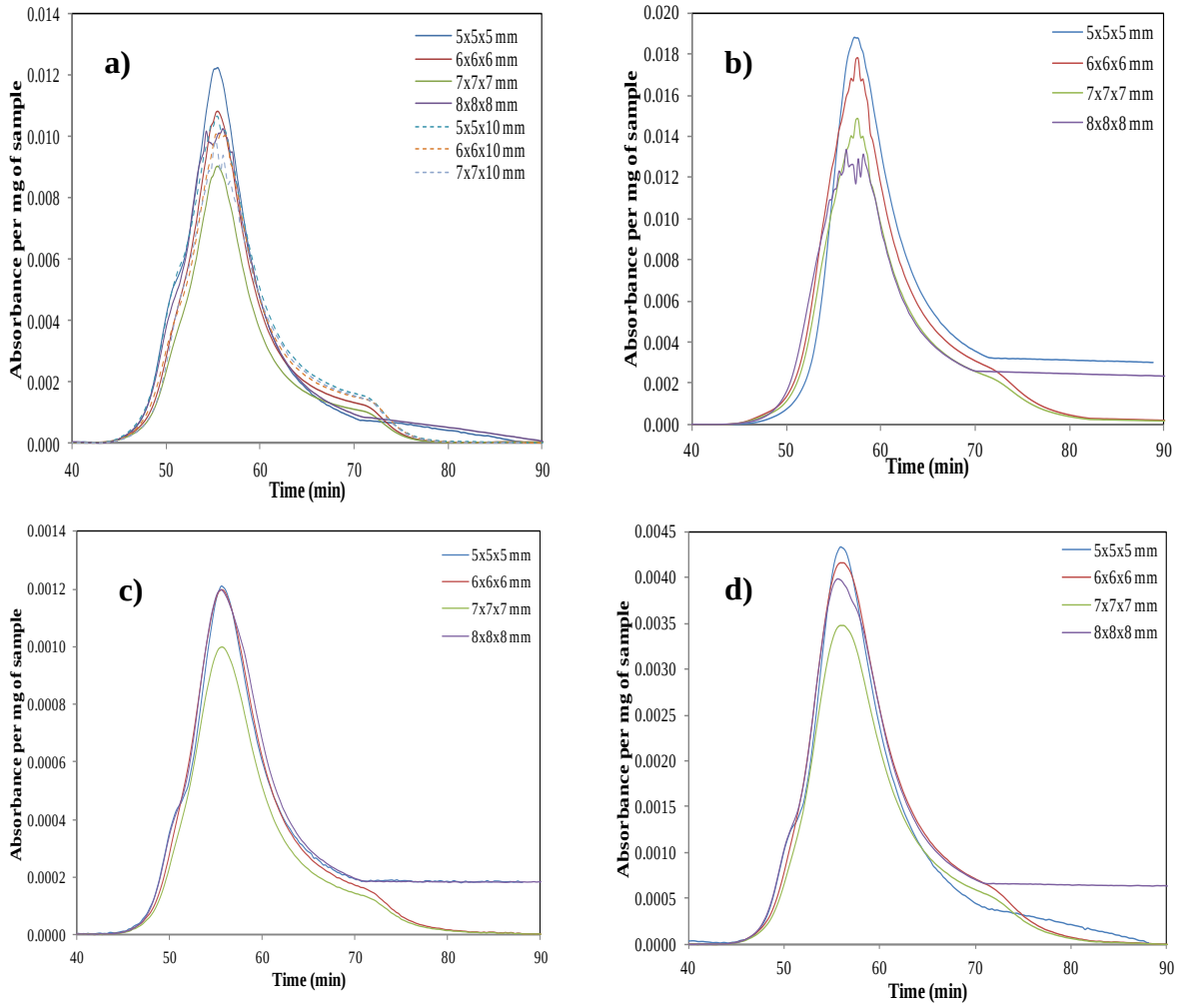

Figure 6.10. Evolution profiles of a) carbon dioxide, b) acetaldehyde, c) methane and d) methanol obtained from torrefaction of cubes of willow at condition C.

Figure 6.11 represents the plots of the permanent gases (water, carbon dioxide and carbon monoxide) based on the equations displayed in Figure 4.25.In general, there seemed to be a turning point where there may be a limiting factor that causes the volatiles not to evolve increasingly further as the particle size increases. Each graph shows either a decreasing trend after a maximum point is reached or reaching a plateau but not increasing. These particles produced different amount of volatiles at different conditions therefore, it is difficult to determine a point where the limitation factor starts for a specific particle size. Mass and heat transfer limitation may explain the change in behaviour; when the size becomes bigger, the limitation effect becomes more noticeable.

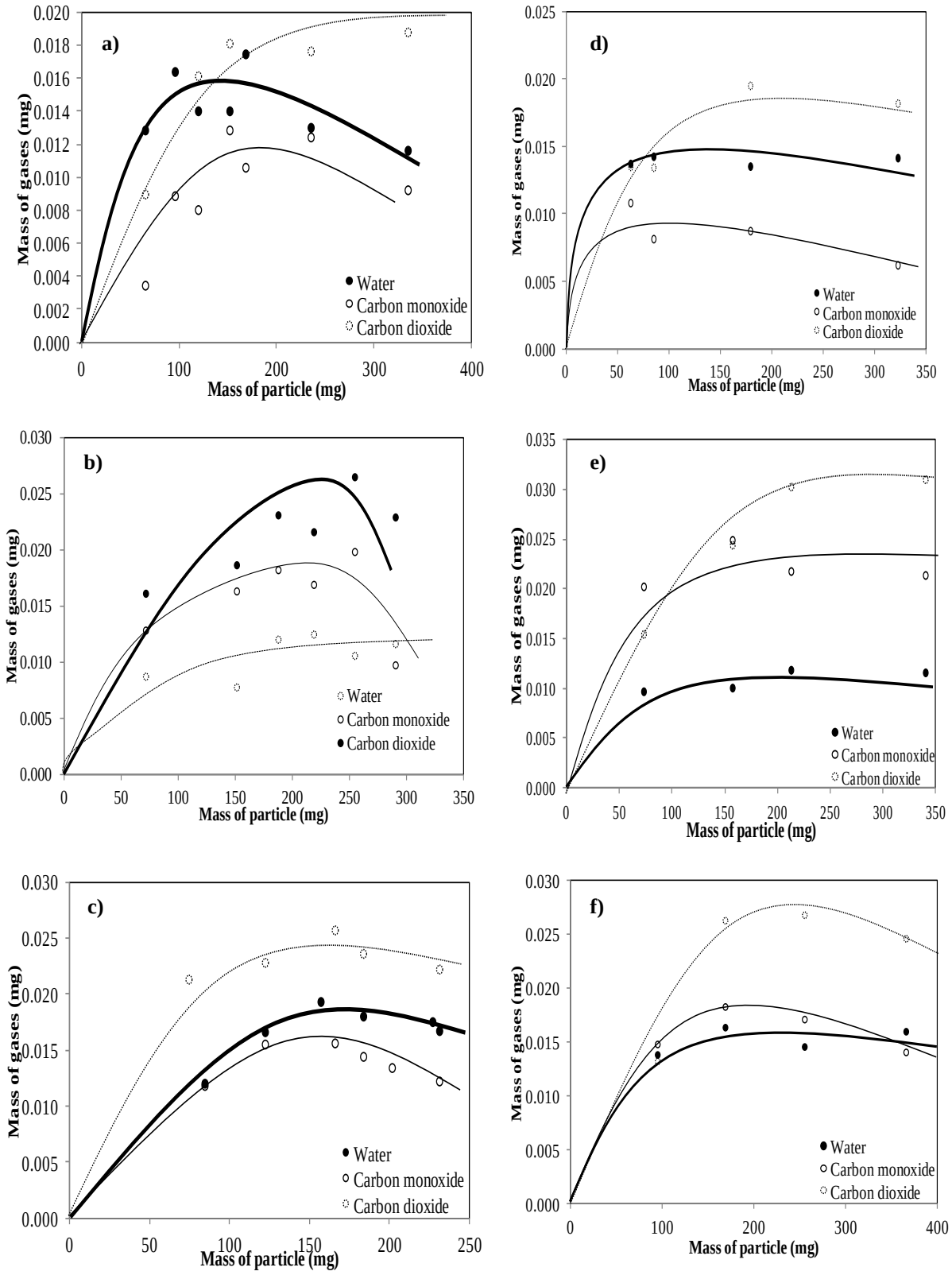

Figure 6.11. Plots of water, carbon monoxide and carbon dioxide from torrefaction of willow (a-c) and eucalyptus (d-f) at conditions A, B and C.

6.2.3 Comparison between the product distributions obtained experimentally and as predicted in FG-Biomass model

6.2.3.1 Overall mass balance

Overall mass balances of torrefaction of willow and eucalyptus (5 mm) treated at condition A as simulated by the FG-Biomass model can be illustrated in Figure 6.12. This showed that the product distribution is dominated by torrefied biomass, followed by tars, condensable organics (ethylene, phenol, acetone, methanol, hydrogen cyanide, ammonia, formaldehyde, formic acid, acetic acid and acetaldehyde), water and finally permanent gases (carbon dioxide, carbon monoxide and methane). Moreover, the model predicted that the yields of torrefied biomass were expected to decrease with increased temperature and longer residence time. This is shown in Table 6.7. This is followed by an increase of the remaining products shown in Table 6.8. These results were in agreement with those observed experimentally using the reactor and TGA-FTIR as displayed in Figure 5.2 and Figure 6.4 respectively. In general, the results obtained showed that the yields collected from torrefaction using the reactor were the lowest in comparison to those obtained in TGA-FTIR and FG-Biomass model. Further explanations will be discussed in the next section.

The yields were observed to be species-dependent. Figure 6.12 showed that the char yields of eucalyptus were predicted to be lower than those of willow. For example, those of the respective biomass fuels (5 mm at condition A) were 76.90% and 83.15%. These findings can be explained by the more reactive devolatisation that took place during the torrefaction of eucalyptus that produced more volatiles and tars than willow (Figure 6.12). With regards to tars and water, the yields obtained from both biomass fuels increased with increased condition (**Appendix 6.4**). The table shown in **Appendix 6.4** also showed that the yields of permanent gases, which include carbon monoxide and carbon dioxide, as well as methane, increased with increased severity of the condition. The yields of carbon dioxide were the highest, followed by carbon monoxide and methane. The yields of methane were minute and they ranged from 0.01-0.02% for both fuels.

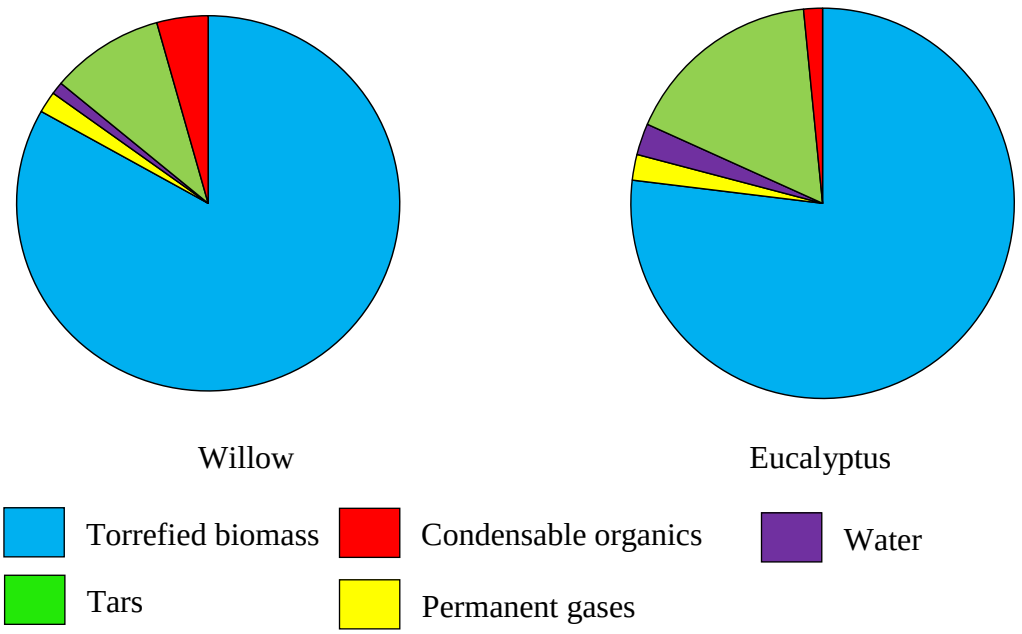

Figure 6.12. Simulated overall mass balances of willow and eucalyptus upon torrefaction at condition A.

Table 6.7. Distribution of products (daf) in terms of % mass obtained from the torrefaction of willow and eucalyptus as simulated by FG-Biomass model.

Willow					
Sample	**Torrefied willow (%)**	**Permanent gases (%)**	**Water (%)**	**Tars (%)**	**Condensables (%)**
5 mm	83.15	1.84	1.06	9.63	4.33
6 mm	83.52	1.81	1.03	9.42	4.22
7 mm	83.91	1.77	1.00	9.21	4.10
8 mm	84.33	1.74	0.97	8.98	3.98

Eucalyptus					
Sample	**Torrefied Eucalyptus (%)**	**Permanent gases (%)**	**Water (%)**	**Tars (%)**	**Condensables (%)**
5 mm	76.90	2.13	2.61	16.77	1.59
6 mm	77.42	2.10	2.56	16.38	1.54
7 mm	78.00	2.06	2.51	15.95	1.49
8 mm	78.64	2.01	2.45	15.46	1.43

With respect to particle size, graphs in Figure 6.13 a)-d) show the yields of char, tars and permanent gases from torrefaction of willow of different particle sizes plotted against time.

These samples were torrefied with treatment A. Similar results are observed with the other two treatments (B and C) but with increasing char yields and decreasing tars and permanent gases as shown in Table 6.8. These trends are also observed in eucalyptus samples (see Table 6.8). The FG-Biomass model is able to predict the change in behaviour, where the char yield increased and tars as well as permanent gases decreased with increased particle size. These observations agreed with those carried out by the AFR, who have tested with sizes of range 0.180 and 5 mm.

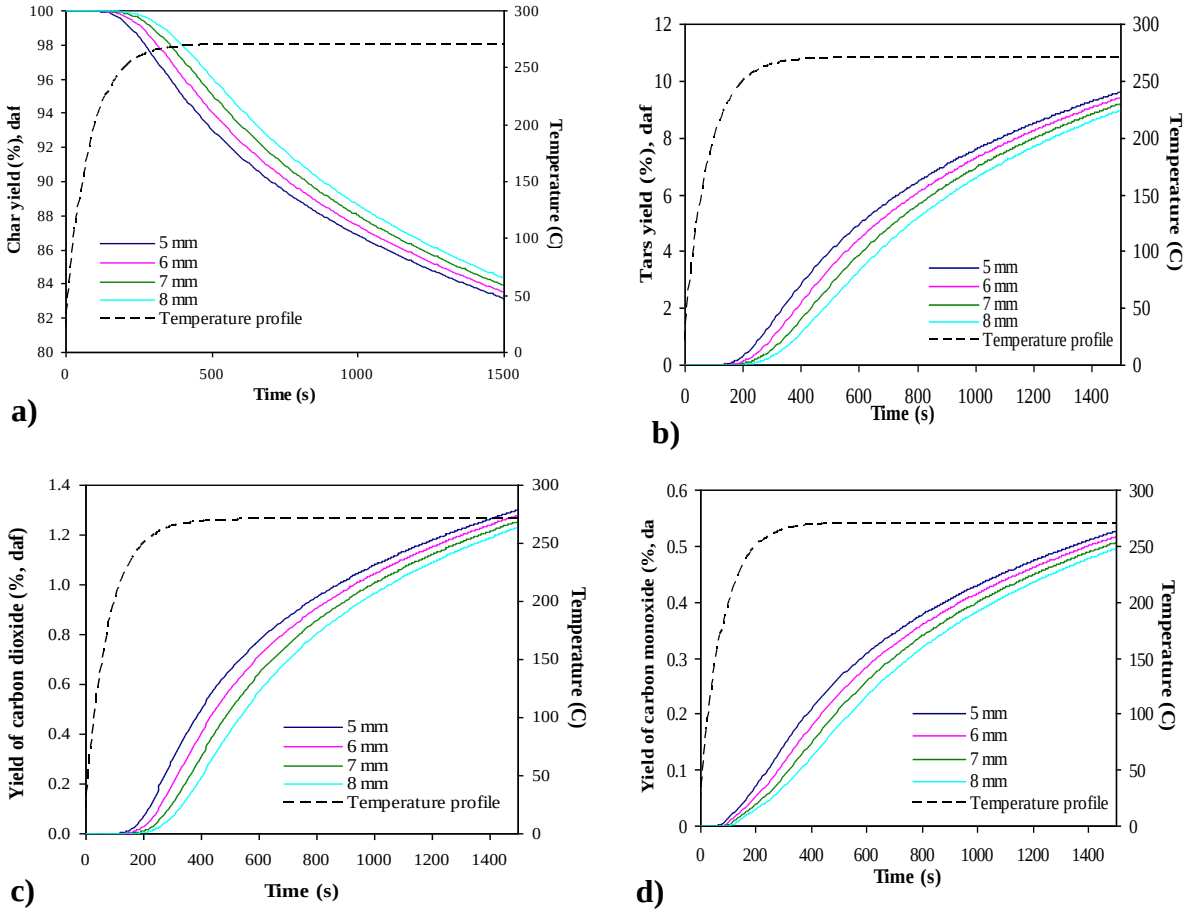

Figure 6.13. a) Yields of torrefied biomass of different particle sizes against time, b) tar yields, c) and d) yields of permanent gases (carbon dioxide and carbon monoxide respectively) obtained from the torrefaction of willow of increasing particle sizes (5, 6, 7 and 8 mm).

Table 6.8. Yields of torrefied biomass fuels, tars and permanent gases against radius of particle size of willow and eucalyptus after torrefaction at conditions A, B and C.

Willow

Size	Condition	TW[a]	Tar	H_2O	CO	CO_2	CH_4
3.10 mm	A	81.13	10.72	1.22	0.58	1.42	0.012
3.72 mm	A	81.37	10.59	1.20	0.57	1.40	0.012
4.34 mm	A	81.61	10.46	1.18	0.57	1.39	0.012
4.96 mm	A	81.86	10.33	1.16	0.56	1.38	0.012
3.10 mm	B	74.75	14.09	1.76	0.75	1.77	0.019
3.72 mm	B	74.87	14.02	1.75	0.75	1.77	0.019
4.34 mm	B	74.99	13.96	1.74	0.75	1.76	0.019
4.96 mm	B	75.12	13.89	1.73	0.74	1.75	0.018
3.10 mm	C	68.96	17.10	2.35	0.92	2.09	0.027
3.72 mm	C	69.23	16.96	2.32	0.91	2.08	0.026
4.34 mm	C	69.52	16.81	2.29	0.91	2.06	0.026
4.96 mm	C	69.82	16.66	2.26	0.90	2.05	0.025

[a] TW Torrefied willow

Eucalyptus

Size	Condition	TE[b]	Tars	H_2O	CO	CO_2	CH_4
3.10 mm	A	74.46	18.56	2.84	0.52	1.78	0.012
3.72 mm	A	74.67	18.41	2.82	0.51	1.77	0.011
4.34 mm	A	74.88	18.26	2.80	0.51	1.76	0.011
4.96 mm	A	75.11	18.09	2.78	0.50	1.75	0.011
3.10 mm	B	69.16	22.27	3.41	0.69	2.05	0.018
3.72 mm	B	69.25	22.20	3.40	0.68	2.04	0.018
4.34 mm	B	69.35	22.13	3.39	0.68	2.04	0.018
4.96 mm	B	69.46	22.07	3.37	0.68	2.03	0.017
3.10 mm	C	64.01	25.72	4.01	0.87	2.35	0.026
3.72 mm	C	64.27	25.55	3.98	0.86	2.33	0.025
4.34 mm	C	64.53	25.37	3.95	0.85	2.32	0.025
4.96 mm	C	64.81	25.18	3.91	0.84	2.30	0.024

[b] TE Torrefied eucalyptus

As shown in Table 6.9, there were three products of willow that were below 0.02%, namely ethylene, hydrogen cyanide (HCN) and ammonia. Due to the low nitrogen content of eucalyptus, the presence of HCN and ammonia were not detected upon torrefaction. The most abundant product was acetic acid, followed by acetaldehyde, acetone and formaldehyde. Of the rest were traces of phenol, formic acid and methanol that were below 1.00% at all conditions. In comparison with those products obtained from torrefaction using TGA-FTIR, Table 6.8 shows that acetic acid, acetaldehyde, formaldehyde were amongst those that dominated the product distribution of condensable organics. With regards to permanent gases, similar results were observed, where carbon dioxide was the highest, followed by carbon monoxide and methane.

Table 6.9. Percentage yields (daf) of the remaining products of torrefaction (condensable organics), obtained from the torrefaction of willow and eucalyptus at conditions A. **Appendix 6.4** displays the yields obtained from that of those biomass fuels at conditions B and C.

Willow	**5 mm**	**6 mm**	**7 mm**	**8 mm**
Ethylene	0.000025	0.000023	0.000022	0.000021
Phenol	0.41	0.40	0.39	0.37
Acetone	0.53	0.52	0.50	0.49
Methanol	0.55	0.55	0.54	0.53
Hydrogen cyanide	0.013	0.014	0.013	0.013
Ammonia	0.0094	0.0093	0.0092	0.0091
Formaldehyde	0.51	0.49	0.48	0.47
Formic acid	0.29	0.28	0.27	0.26
Acetic acid	1.3	1.3	1.28	1.3
Acetaldehyde	0.67	0.64	0.62	0.59

Table 6.9. *Continued*

Eucalyptus	**5 mm**	**6 mm**	**7 mm**	**8 mm**
Ethylene	0.000037	0.000034	0.000031	0.000028
Phenol	0.17	0.16	0.16	0.15
Acetone	0.083	0.080	0.076	0.073
Methanol	0.46	0.45	0.44	0.43
Hydrogen cyanide	ND	ND	ND	ND
Ammonia	ND	ND	ND	ND
Formaldehyde	0.62	0.60	0.57	0.55
Formic acid	0.086	0.084	0.082	0.079
Acetic acid	0.15	0.15	0.15	0.14
Acetaldehyde	0.018	0.017	0.015	0.014

ND Not Detected

6.2.3.2 Mass yields of torrefied biomass

The yields in FG-Biomass model were all calculated on a dry ash free basis. Therefore, the mass yields obtained from the reactor and TGA-FTIR studies of willow and eucalyptus were corrected for comparison purposes as illustrated in Figure 6.14 and 6.15 respectively. The results showed that those obtained from FG-Biomass have mass yields that increased with particle size but for TGA-FTIR, there seemed to be inconsistencies with the results, mainly due to their different moisture contents. In FG-Biomass, the moisture content was assumed to be constant for all the particles. But as for TGA-FTIR, the particles were prepared at different times and it is possible that moisture may have absorbed prior to the experiment. Apparently, moisture content affects the overall performance of the torrefaction in the TGA-FTIR. The higher the moisture, the lower the mass yields as most of the masses were lost during the drying period.

In comparison between the yields collected from the three procedures, it can be seen that the results obtained experimentally from TGA-FTIR have almost similar mass yields with those predicted by the model even though they may differed by 3-6%. However, as can be observed in Figure 6.14 and 6.15, experimental results collected from the reactor gave a significant greater mass loss than those from TGA-FTIR and FG-Biomass by about 10% and even more at the most severe condition, C, which was by about 20%. Since the particle sizes used in the reactor were larger (40 x 20 x 10 mm), exothermic reaction may have taken place during torrefaction, hence, increasing the internal temperature of the particles. This phenomenon has

been clarified in the previous chapters. Overall, the software predicts that between willow and eucalyptus, the former biomass fuel retained a higher solid yield. For example, for treatment at 290°C, the solid yield of willow is 67.34% while eucalyptus could only retain 62.45%. These results were in line with those obtained from the reactor and TGA in terms of rate of mass loss where the decomposition of willow is slower, hence, resulted a higher mass yield than that of eucalyptus.

6.2.3.3 Ultimate analysis

The FG-Biomass model is also able to provide information on its chemical composition of the torrefied biomass fuel as previously shown in Figure 4.31. The ultimate analysis of raw willow and eucalyptus are provided in Table 6.3. Upon torrefaction, Table 6.10 presents the results for willow and eucalyptus under a number of conditions, at which the program predicts that the carbon content increased and a reduction in hydrogen and oxygen contents; these would lead to an increase in the HHV with increased severity of the treatments. The changes in elemental composition became more significant in the torrefied biomass fuels prepared experimentally, for example, in the reactor (Table 5.3). The differences between raw and torrefied willow and eucalyptus at treatment C (290°C with a residence time of 30 min) were 20%, 1% and 10% for carbon, hydrogen and oxygen respectively.

Table 6.10 also lists the ultimate analysis of biomass fuels for different particle sizes. It can be seen that the values were almost similar especially hydrogen and nitrogen contents (differed by only 1%). Figure 6.16 illustrates the changes in the carbon and oxygen contents with increase in particle size of willow and eucalyptus at condition A. The bar charts showed slight changes, where the carbon contents decreased and oxygen contents increased with increase in particle size of willow. The same trend could be observed in eucalyptus but only to a very minor extent (by ±0.0001-0.0002% for conditions A and B). Considerable changes could only be seen at the most severe condition (condition C). In summary, the FG-Biomass model predicted that the HHV decreased slightly (not reported in this thesis) with increase in particle sizes.

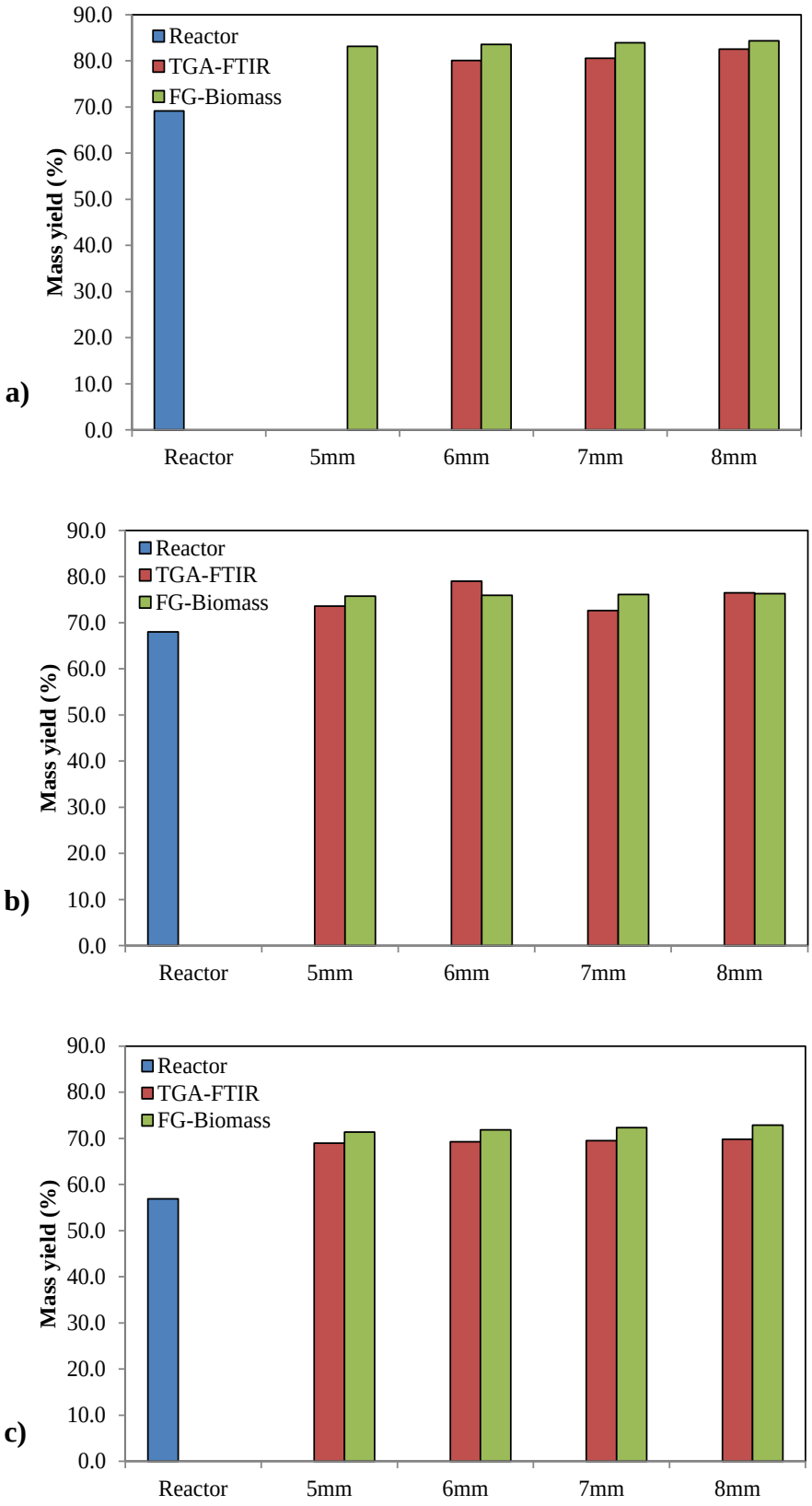

Figure 6.14. Mass yields (dry ash free basis) determined from torrefaction of willow by the reactor, TGA-FTIR and FG-Biomass model at increasing conditions: a) A, b) B and c) C. It is important to note that the sample size torrefied in the reactor was 40 x 20 x 10 mm, while those in the other two were cubes of 5 mm, 6 mm, 7 mm and 8 mm.

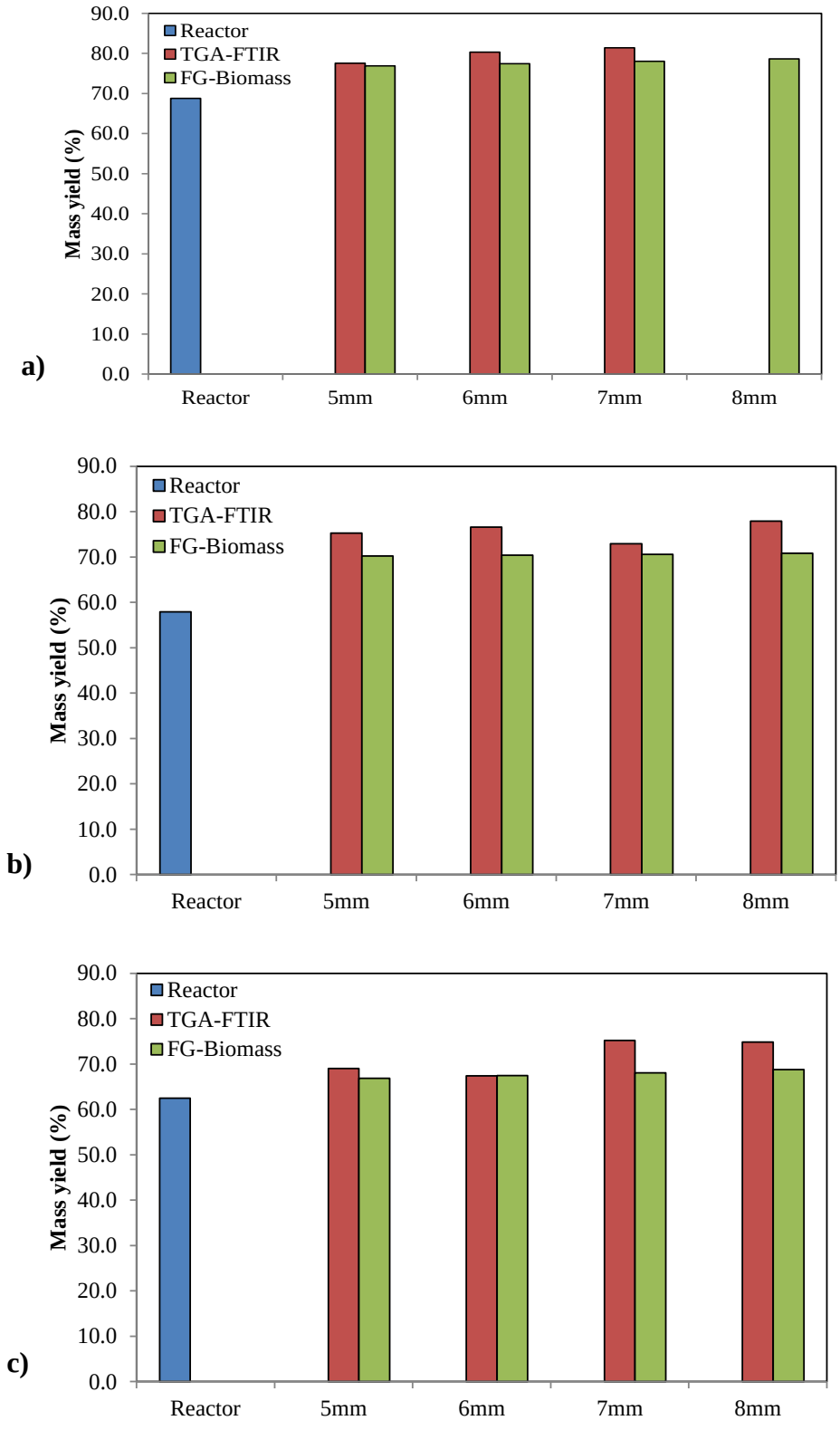

Figure 6.15. Mass yields (dry ash free basis) determined from torrefaction of eucalyptus by the reactor, TGA-FTIR of different particle sizes and FG-Biomass model at increasing conditions: a) A, b) B and c) C. It is important to note that the sample size torrefied in the reactor was 40 x 20 x 10 mm, while those in the other two were cubes of 5 mm, 6 mm, 7 mm and 8 mm

6.2.4 Influence of particle size on temperature distribution as predicted by the FG-Biomass model

AFR has developed a model with the capability to predict torrefaction of large particle biomass. It has been tested for particle sizes that have diameter in the range of less than 0.180 and 5 mm. Results from AFR have been made available to the project and results showed that the larger the particle size, the greater the mass yields and the lower the yields of tars and permanent gases but it was also reported that other gaseous products did not exhibit a well-defined trend. Plots in Figure 6.17 a) and b) illustrate similar results to those obtained by AFR, where the torrefaction temperature was reduced with increase in particle sizes. This could be due to the presence of heat transfer limitations in larger particles as explained in Section 3.5. The reduction of the torrefaction temperature could explain the higher yields of bigger particle sizes, where torrefaction may not have taken place as efficiently as when the sample is smaller. However, the changes were not large, which could explain the minor change in the char yields.

The following figures (Figure 6.18 a-d) illustrate the temperature distribution within a spherical particle of willow when the reaction condition was at 270°C with a residence time of 30 min. Curves for the five shells r1 to r5 are plotted in each case. Figure 6.18 (e) presents data for willow (8 mm) with increasing temperature of torrefaction (condition A and C). The first four plots in Figure 6.18 show that the distribution became increasingly broadened with increase in particle size from 5 mm to 8 mm. The wider range of distribution in the larger particles demonstrates the slower torrefaction rate, which leads to lower mass loss (higher mass yield) than those of smaller particles. Another interesting observation was that the gradients in each figure became lower with increase in size. This, again, demonstrated the wider distribution of temperature during torrefaction process. With regards to change in temperature of torrefaction (A and C), there seemed to be not much of a difference in the temperature distribution within the spherical of 8 mm.

Table 6.10. Ultimate analysis (daf basis) in terms of torrefied willow and eucalyptus (cubes) as predicted by the FG-Biomass model.

	Sample (mm)	Condition	C	H	O	N
WILLOW	5	A	46.2	5.67	47.6	0.54
	6	A	46.2	5.67	47.6	0.54
	7	A	46.1	5.67	47.6	0.54
	8	A	46.1	5.68	47.7	0.54
	5	B	46.9	5.61	47.0	0.0053
	6	B	46.8	5.61	47.0	0.0053
	7	B	46.8	5.61	47.0	0.0053
	8	B	46.8	5.61	47.1	0.0053
	5	C	47.5	5.56	46.6	0.0052
	6	C	47.3	5.56	46.7	0.0052
	7	C	47.2	5.57	46.7	0.0053
	8	C	47.2	5.57	46.8	0.0053
EUCALYPTUS	5	A	50.7	4.85	44.4	ND
	6	A	50.7	4.85	44.4	ND
	7	A	50.7	4.85	44.4	ND
	8	A	50.7	4.85	44.4	ND
	5	B	50.7	4.87	44.3	ND
	6	B	50.7	4.87	44.3	ND
	7	B	50.7	4.86	44.3	ND
	8	B	50.7	4.86	44.3	ND
	5	C	50.9	4.87	44.1	ND
	6	C	50.9	4.87	44.2	ND
	7	C	50.9	4.87	44.2	ND
	8	C	50.8	4.87	44.2	ND

ND Not Detected

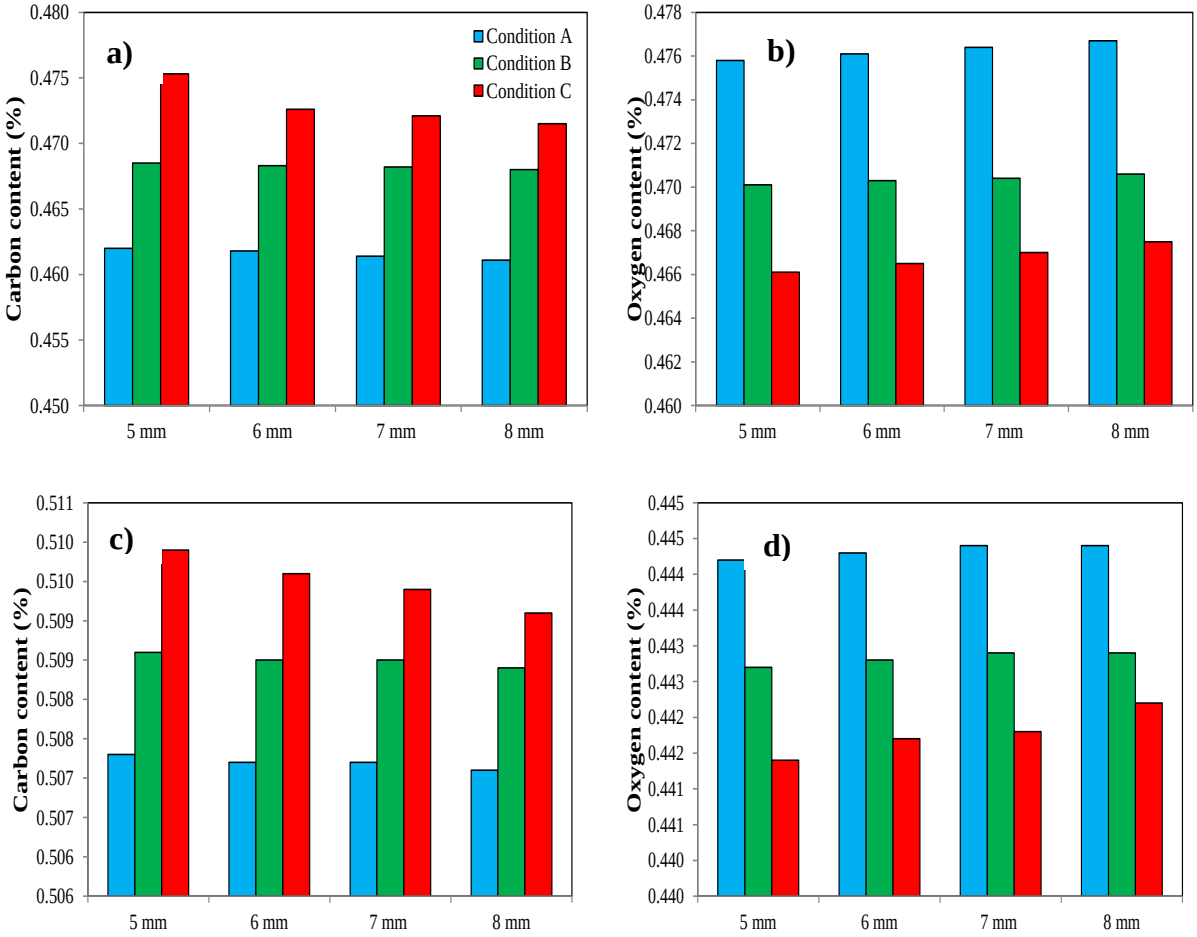

Figure 6.16. Carbon and oxygen contents of torrefied willow (a and b) and eucalyptus (c and d) at conditions A, B and C.

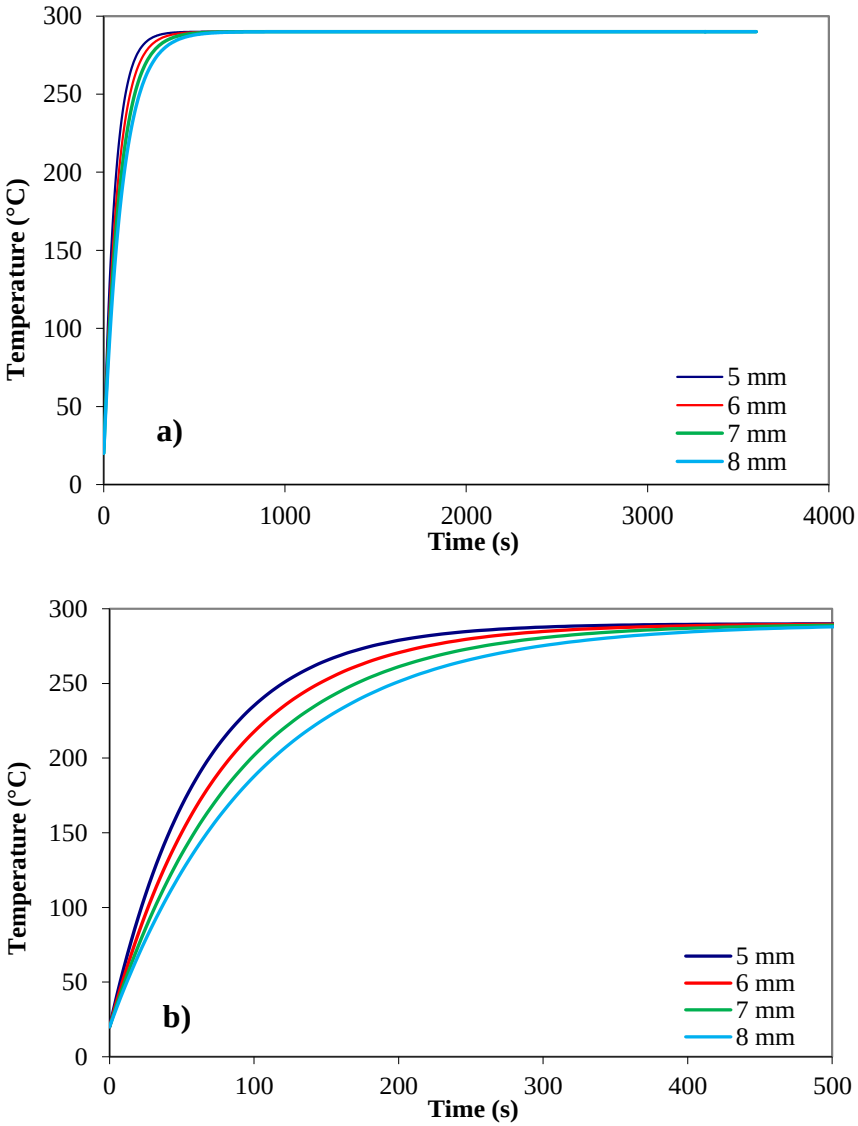

Figure 6.17. a) The effect of particle size on the temperature of torrefaction of willow and b) The zoom version of the plot in a) from 0-500 s. The condition applied was 270°C with a reaction time of 60 min.

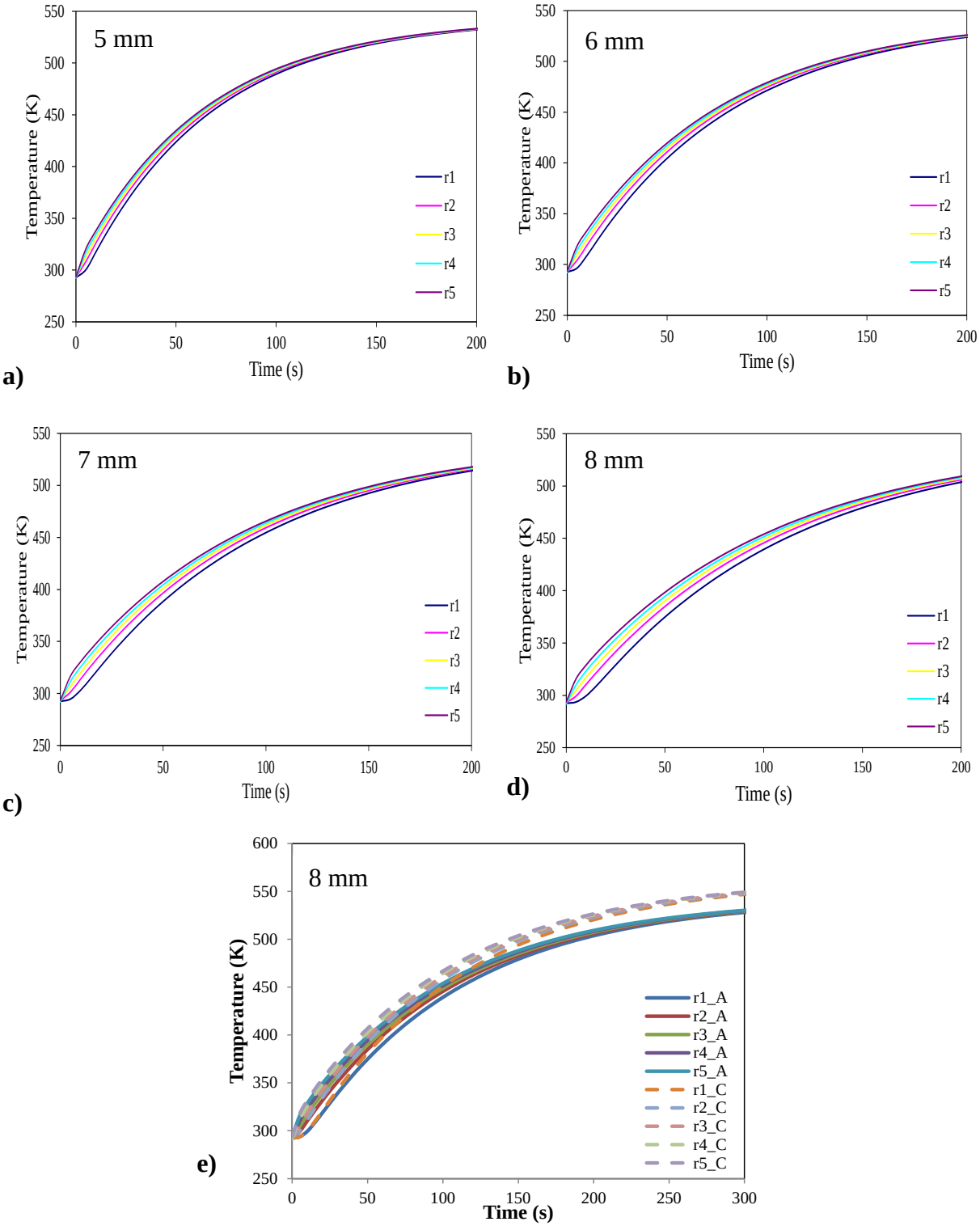

Figure 6.18. Temperature-time distribution within a spherical particle of a)-d) different cubes of willow treated at condition A and e) that of 8 mm treated at condition A and C.

6.3. Conclusions

The influence of particle sizes of biomass on torrefaction of willow and eucalyptus was studied. Four particle sizes of cubes of 5, 6, 7 and 8 mm as well as cuboids of 5x5x10, 6x6x10 and 7x7x10 mm were torrefied in an STA coupled to a mass spectrometer to allow for the analysis of the evolved gases and volatiles. These samples were torrefied at 270 and 290ºC with residence times of 30 and 60 min. Results showed that for larger particle sizes, the solid mass yields increased due to the presence of heat transfer limitations. However, the effect of particle size on the fuel properties of the solid chars was small. In terms of volatile products, 14 species (H_2O, CO_2, CO, CH_4, CH_3OH, acetaldehyde, formaldehyde, acetone, acetic acid, formic acid and small amounts of ethane, furfural, phenol and ammonia) were identified. In general, it was found that the amount of each of the volatile products studied increased with particle size to a maximum then decreases for the largest particles. These results indicate that mass transfer limitations are becoming important at larger particles. Comparison between the yields of products (torrefied biomass, liquids and gases) obtained from the reactor, TGA-FTIR and as predicted by FG-Biomass model was also carried out. The results showed that the program gave similar trends to those obtained experimentally even though the actual yields may be somewhat different. Yields obtained experimentally especially from the reactor shows a greater mass loss of torrefied biomass fuels (10-20%) whilst yields of permanent gases and condensables were also greater than predicted. Furthermore, the influence of particle size on the core temperature was investigated using the program. The results showed that it took longer for bigger particle sizes to reach a desired temperature than for smaller sizes, at which the plots displayed gradients that became gentler with increasing sizes. Moreover, when the temperature distribution within a spherical particle was plotted against time, a wider distribution of temperature was observed in the bigger particles. These findings demonstrated that particle sizes have an effect on the heating rate especially torrefaction.

CHAPTER 7

THE STUDY OF A SINGLE PARTICLE COMBUSTION OF WILLOW (*Salix spp.*) AND EUCALYPTUS (*Eucalyptus Gunnii*)

7.1 Introduction

While most authors were interested working on the physical and chemical characteristics of the thermally treated biomass such as grindability (Arias *et al*., 2008; Bridgeman *et al*., 2010) and hydrophobicity (Pimchuai *et al*., 2010) and also chemical changes using the Infra-Red Microscopy and X-ray Photoelectron Spectroscopy (Stelte *et al*., 2011; Shang *et al*., 2012; Ibrahim *et al*., 2012), there are only a few publications related to the combustion behaviour of torrefied biomass in comparison to the untreated biomass (Pentananunt *et al*, 1990; Bridgeman *et al*., 2008; Pimchuai *et al*., 2010; Wannapeera and Worasuwannarak, 2012; Jones *et al*., 2012). Raw biomass produces smoke during combustion and can have a low combustion efficiency (Pimchuai *et al*., 2010). Understanding the combustion behaviour is an important matter as it reflects the performance of the biomass and environmental issues when considering biomass as a potential source of energy.

In this study, torrefied cubes of 2 mm of willow (*Salix spp.*) and eucalyptus (*Eucalyptus Gunnii*) were prepared using TGA-FTIR, as detailed in Section 4.3.2. They were then studied for their combustion behaviours, where the durations of each stage that involved throughout the experiment (ignition delay, duration of volatile combustion and duration of char combustion), were examined and compared to their raw counterparts. The rates of devolatisation and char combustion were also studied to get a better understanding on the mechanism of combustion of raw and torrefied biomass fuels. However, it is important to note that this is just a short investigation of the combustion of torrefied biomass fuels.

7.2 Combustion of biomass

The combustion of biomass fuels is considered in this chapter and the investigation of the behaviour of these fuels provides an insight into the design and performance of furnaces and boilers (Borman and Ragland, 1998). A complete combustion of biomass involves a rapid oxidation of the biomass and oxygen, releasing an amount of energy and leads to the formation of products that is mainly consist of carbon dioxide and water (Basu, 2013).

7.2.1 The chemistry of combustion of solid biomass fuels

The mechanism in the combustion of a solid biomass fuel involves a series of chemical reactions, where the carbon is oxidised to carbon dioxide and hydrogen to water.

Lu *et al* (2008) studied the behaviour of poplar in a single particle reactor and they described the processes involved as the biomass enters the reactor with air as the carrier gas. The following processes are heating and drying, devolatisation, volatiles and char combustion. These processes occur depending on the properties of the particle such as the particle size. For pulverised fuel particles, Borman and Ragland (1998) described drying, devolatisation and char burn take place sequentially, at which the char burn period lasts much longer than the devolatisation and drying stages. While for larger particles, the processes occur simultaneously (Borman and Ragland, 1998).

Figure 1.13 illustrates the stages involved in the solid fuel combustion. The mechanisms at each stage based on biomass fuels are described in the following sections.

7.2.1.1 Heating and drying

The heating and drying stage is normally not accompanied by chemical reaction, where moisture is driven off (Brown, 2003). This stage is an endothermic process, where the biomass fuels are heated from the ambient condition to that temperature where pyrolysis can occur (Tillman *et al*., 1981). Lu *et al* (2008) explained that moisture in biomass exists in two forms: moisture (free water) and bound water. Free water is present in a liquid form in pores and cells while bound water exists as moisture that is physically or chemically bound to surface sites or as hydrated species. When the biomass is exposed to the reactor, the heat is convected and radiated to the particle surface and conducted into the particle. For small particles, the water is vapourised and forced out of the particle very rapidly before volatiles are released. For larger particles, temperature gradients are present within the particle, where moisture evolves from inside the particle and volatiles driven off from near the outer shell of the particle. High pressure is created and forces some moisture towards the centre of the particle until the pressure continues to build up throughout the particle. A pyrolysis layer starts at the outer edge of the particle and gradually moves inwards, releasing volatiles and forming char.

7.2.1.2 Devolatisation

When the drying stage is completed, the temperature rises and this is when the biomass fuel starts to decompose, producing volatiles. The release of volatiles through the biomass pores inhibits the entrance of external oxygen into the particle. In other words, there is a large gaseous outflow of volatiles from the surface of the particles that oxygen is excluded (Brown, 2003). Lu *et al* (2008) described the movement of volatiles as mass transfer of the devolatisation products by advection and diffusion. This stage is also known as the pyrolysis stage. Lu *et al* (2008) also added that some authors differentiate devolatisation and pyrolysis, where the former occurs in an oxidising environment, while the latter occurs in a neutral or reducing environment. They explained that "*most particles thermally decompose within a volatile cloud (reducing environment) when the overall environment is oxidising*", making the distinction unclear. Figure 7.1 presents the model of a wood pyrolysis, where the wood undergoes thermal degradation according to primary reactions (K_1, K_2 and K_3) and the tar undergoes further degradation (secondary reaction), producing more light gas and char (K_4 and K_5). Di Blasi (2008) suggested that upon fast heating rates and high temperatures, the majority of kinetic mechanisms consist of this one component mechanism. The primary reactions are assumed to be first-order in the mass of the pyrolysed wood and having an Arrhenius type of temperature dependence (Di Blasi, 1996), as equated in (7.1). The secondary reactions are assumed to take place only in the gas/vapour phase within the pores of the wood and their rates are proportional to the concentration of the tar (Di Blasi, 1996). This model is used to predict the product yields and distribution that vary with temperature and heating rate.

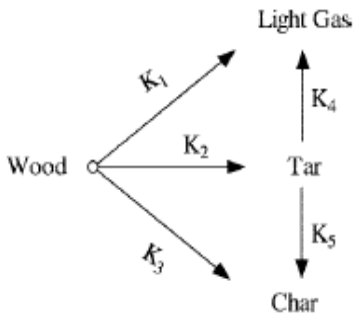

Figure 7.1. Wood pyrolysis model (Lu *et al*., 2008).

The products of pyrolysis mainly consist of CO, CO_2, H_2O, H_2, light and heavy hydrocarbons (Lu *et al*., 2008). The products of pyrolysis ignite and form an attached flame around the particle as oxygen starts to react with these products. The flame in turn heats the particle,

causing enhanced devolatisation. While the water vapour escapes through the pores, the flame temperature surrounding the particle will be low and the flame looks weak. But once all the moisture content is driven off, the flame will be hotter. As earlier mentioned, the rate of devolatisation of a solid fuel may be represented approximately as a first order reaction with an Arrhenius rate constant:

$$\frac{dm_v}{dt} = -m_v k_{pyr} \qquad (7.1)$$

where $k_{pyr} = - k_{0,pyr} \exp(-E_{pyr} / RT_p)$. pyr refers to pyrolysis. m_v (mass of volatiles) = $m_p - m_c - m_a$, where m_p is the mass of the dry particle and m_c and m_a are the masses of char and ash respectively. The values of $k_{0,pyr}$ and E_{pyr} must be determined experimentally (Borman and Ragland, 1998). The mass of char can be estimated from the proximate analysis.

Ignition of solid fuels occurs in two ways: by ignition of fixed carbon (char) on the surface of the fuel, or by ignition of the volatiles in the boundary layer around the particle (Borman and Ragland, 1998). This depends on the rate of convective and radiative heat transfer to the particle. Borman and Ragland (1998) stated that if the convective heat transfer is high so that the surface rapidly heats but the volatiles escape before a combustible mixture starts to accumulate or if the radiative heat transfer is high so that the surface will heat up quickly to the ignition temperature of the carbon, the ignition will occur at the surface. If the surface heating is low, volatiles may ignite first since they have a lower ignition temperature than carbon.

Ignition delay is the time interval between the start of injection and the start of combustion (Borman and Ragland, 1998). The authors mentioned that ignition time delay depends upon particle size, thermal diffusivity, heating rate and pyrolysis rate. Smaller particle sized fuels have ignition time of a few milliseconds, while for 10 mm particles can go longer to seconds. If the temperature is barely above the ignition temperature, then the ignition delay can be many minutes for large particles. Moreover, moisture lengthens the ignition delay. Ignition delay can be an important consideration in designing burners for pulverised fuels.

7.2.1.3 Char combustion

When devolatisation completes, char combustion occurs and that will be the final step in the solid fuel combustion. This is the stage, where char and ash remain. When there are no

volatiles escaping from the char and, since the char is highly porous, oxygen can easily diffuse through the external boundary layer and into the char particles (Borman and Ragland, 1998). Biomass char is reported to have higher reactivity than that of coal (Jones *et al*., 2012).

The burning rate of the char depends on both the chemical rate of the carbon-oxygen reaction at the surfaces and the rate of boundary layer and internal diffusion of oxygen. Borman and Ragland (1998) stated that the surface reaction generates carbon monoxide. This gas is oxidised outside the particle and form carbon dioxide. As a result, the temperature of the char increases 100-200°C above the gas temperature. The burning rate also depends on the oxygen concentration, gas temperature, char size and porosity. The authors suggested that it is appropriate to use a global reaction rate for the determination of the burning rate. The global reaction rate is defined in terms of rate of reaction of the char mass per unit external surface area and per unit oxygen concentration outside the particle boundary layer.

During the burning stage, it was reported that the temperature of the particle increases to a peak value and then declines dramatically (Lu *et al*., 2008). Brown (2003) mentioned that depending on the porosity and reactivity of the char and the temperature of combustion, the oxygen may react with the char at the surface of the particle or it may penetrate into the pores before oxidising char inside the particle. If the former situation takes place, it results in a steadily shrinking core of char. The latter situation will still produce the same diameter of the particle but increased porosity.

The following equations are the reaction that mainly takes place during char combustion. The carbon char reacts with oxygen and form carbon dioxide and carbon monoxide as displayed in Equations 7.2 and 7.3 respectively:

$$C + O_2 \rightarrow CO_2 \quad (7.2)$$

$$C + \tfrac{1}{2} O_2 \rightarrow CO \quad (7.3)$$

The carbon also reacts with carbon dioxide and water vapour:

$$C + CO_2 \rightarrow 2CO \quad (7.4)$$

$$C + H_2O \rightarrow CO + H_2 \quad (7.5)$$

The rate of reactions for equations (7.4) and (7.5) are slower than that for equation (7.3). For combustion, reaction (7.3) is the only one that needs to be considered but if the oxygen is depleted, then reactions (7.4) and (7.5) are important.

Arrhenius equation is used to determine the kinetic rate constant of char combustion

$$k = A_e (-E_a/RT) \quad (7.5)$$

where

k is the kinetic rate constant,

T is the temperature (K),

A_e is the pre-exponential factor,

E_a is the activation energy and

R is the universal gas constant.

Provided that the oxygen reacts with the char on the surface of the particle, Lu *et al* (2008) stated that the rates of oxidiser diffusion control the rates of char combustion. When the char particle oxidation front reaches the centre of the particle, the particle size shrinks with ash builds up in the outer layer of the particle. The rate of combustion and temperature increase and later, decrease with size due to changes in the radiation losses, convection and diffusion. Once the char is completely consumed, the resultant ash cools rapidly to near the convection gas temperature, depending on the radiative environment.

7.2.1.4 Char burnout

The reactivity of the char, its porosity and particle size are important for the determination of the degree of char burnout (Jones *et al*., 2012). Char burning rate can be either diffusionally controlled or kinetically controlled (Turns, 2000). The burning rate is said to be diffusionally controlled if the value of k as shown in equation (5) is very large, which indicates a very fast surface reaction (Turns, 2000). This type of controlled combustion usually occurs in large particles or with the presence of a high pressure (Turns, 2000). Turns (2000) stated that when the burning being diffusionally controlled, the oxygen concentration at the surface approaches zero. On the other hand, if the burning rate is said to be kinetically controlled, the value of k is small. The concentration of oxygen at the surface is large. Turns (2000) explained that the mass transfer parameters are less important now that the chemical kinetic parameters control the burning rate. This type of controlled combustion occurs when particle sizes are small and at low pressure and temperature.

7.3 Single Particle Combustion Studies

In this part of the research, raw and torrefied willow and eucalyptus were studied to test their combustion behaviour in an air flame as detailed in Section 4.8. Willow and eucalyptus were treated at two conditions: A and C (270°C and 290°C with a residence time of 30 min respectively). Temperature has already been shown to have a significant impact on torrefaction (Bridgeman *et al*., 2010; Pimchuai *et al*., 2010; Feifli *et al*., 2005; Medic *et al*., 2012) so this study focused on this parameter on how it can affect the combustion behaviour of the torrefied biomass fuels in comparison to their raw counterparts. The flame temperature was about 1500 K and the oxygen content at this location was 2.75 mol%. The analysis was carried out by selecting frame numbers as to when changes happened during the combustion. Recorded frame numbers were then divided by the frame speed (fps), 125 in order to get the time taken.

Four stages of single particle combustion were looked into as described below:

1) The time at which the particle is exposed to the flame.
2) The time at which the particle starts to ignite. The duration between 1) and 2) is known as the ignition delay.
3) The beginning of the char burnout. The duration at which the particle started to ignite until devolatisation ended as seen by the extinguishing of the volatile combustion flame is known as the duration of volatile combustion.
4) The time at which the char burnout ends. The duration at which the shrinkage starts to appear until the particle was no longer change in shape is known as the duration of char combustion. It is important to note that the char combustion is marked by radiation from the particle and also a reduction in particle size.

7.3.1 Determination of rate of devolatisation

The rate of devolatisation depends on the temperature and type of fuel (Borman and Ragland, 1998). In this study, FG-Biomass model (see Section 4.10) was used to simulate pyrolysis of raw willow and eucalyptus from the room temperature (20°C) ramped up to temperature of 1227°C, which is equivalent to 1500 K (Jones *et al*., 2012). That was the measured flame temperature used in the single particle combustion experiment). Different heating rates were tested (ranged from 100 K s^{-1} to 1000 K s^{-1}). The outcome will be related to the duration of volatile combustion that was obtained experimentally using the Meker burner. The time at which the duration of devolatisation took place experimentally was in the range of 3-5 s.

Therefore, the aim of simulating pyrolysis using the program was to determine the approximate heating rate experienced by the biomass fuels in the flame. Plots of char yield and its curves of evolution rates with time of the raw fuels were plotted.

7.3.2 Determination of rate of char combustion

Equation (7.5) is used to calculate the rate of char combustion. Jones *et al* (2012) studied the mechanism of char combustion of willow that was torrefied at 290°C with a reaction time of 60 min. Oxidative reactivity of the chars was assumed to be in the first order. They used the reaction rate constant method to determine the kinetic parameters calculated for the torrefied willow which occurred in the combustion. The E_a was 93.8 kJ mol^{-1} and A_e was 5336 s^{-1}. The oxygen content during which this study was carried out was 12.5 mol%. These values are used to determine the rate constant, k of char combustion of willow and eucalyptus for this present study. The oxygen content used in the single particle combustion experiment was 2.75 mol% similar to that in Jones *et al* (2007).

Assuming that the temperature of the particle is constant during char combustion,

$$\alpha = e^{-kt} \tag{7.6}$$

If t is zero, the value of α is 1, which indicates that it is not converted but if it is operated for a long time, the value of α is zero, which indicates that it is fully converted. In this study, the value of k is determined from the model at a certain temperature and from here, the value of α is calculated.

7.4 Results and discussion

7.4.1 Four stages of single particle combustion

Figure 7.2 (a) to (f) are images of each stage during the combustion of willow that was torrefied at condition C. Figure 7.2 (a) shows the exposure of the particle, at which the time was taken at this moment. The time of ignition was noted down when a white appeared as can be observed in Figure 7.2 (b). Figure 7.2 (c) illustrated the disappearance of the white flame and this indicated the end of devolatisation. As soon as that occurred, char combustion took place, where the glowing of the char at the bottom started to show even though it might not be seen clearly in Figure 7.2 (d). During the char combustion, the particle started to shrink and the time at which the end of the char burnout was recorded when the particle no longer changed in shape as can be seen in Figure 7.2 (e) and (f).

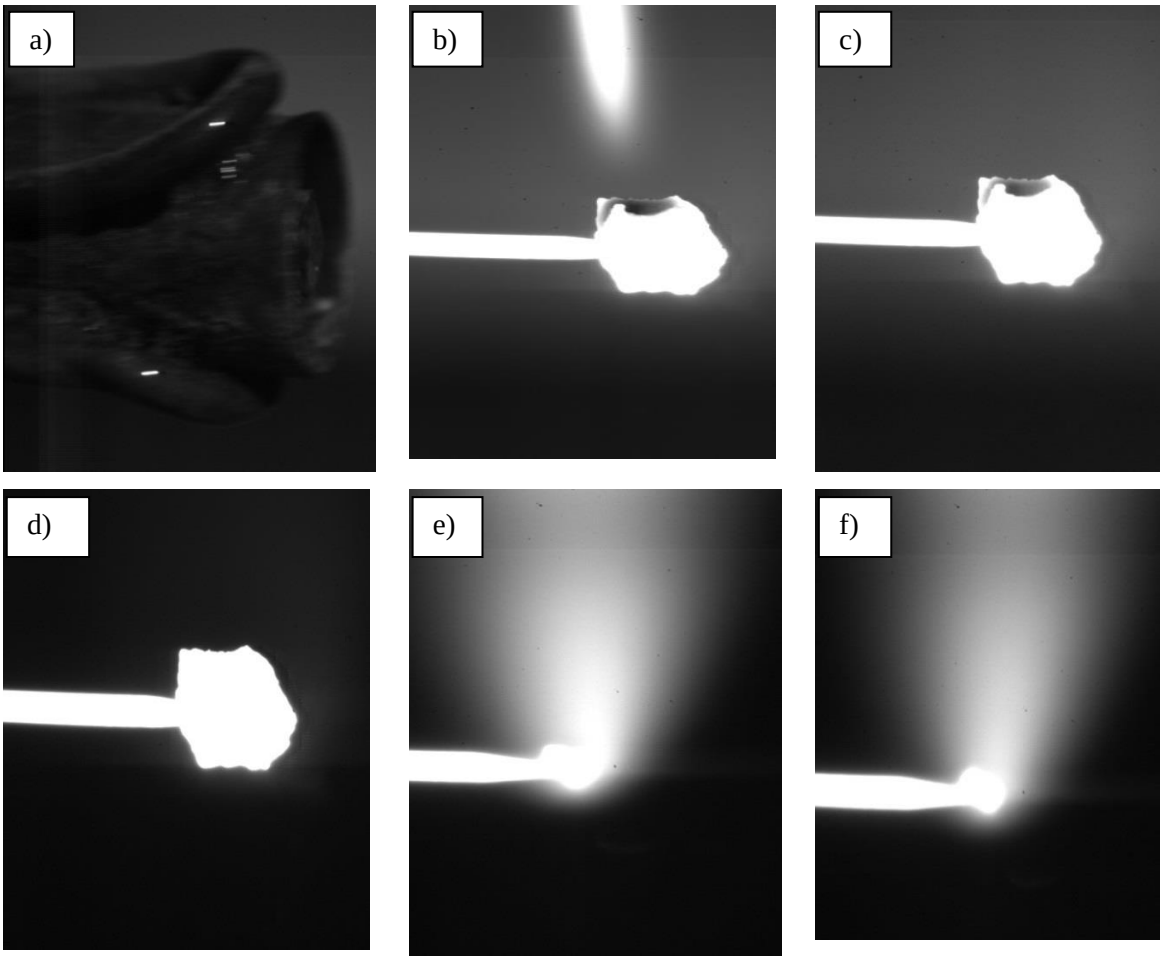

Figure 7.2. (a – f) Images taken during the combustion of willow C.

11-15 replicates per sample were tested and Table 7.2 a) – f). Durations of ignition delay, volatile and char combustion were plotted against the masses of particle for further analysis.

7.4.2 Combustion behaviour with respect to torrefaction

The durations of ignition delay, volatile combustion and combustion of raw and torrefied willow and eucalyptus were plotted and compared in Figure 7.3. The results showed clear distinction between the raw and torrefied samples.

7.4.2.1 Ignition delay

Figure 7.3 a) illustrates that there is a linear relationship between the ignition delay and the mass of willows. It shows that the ignition delays of raw willow are longer than those of torrefied ones (A and C). Borman and Ragland (1998) stated that moisture contents delay the ignition. The moisture content of raw willow is higher than those of torrefied willow A and C

(respectively). Furthermore, it can be seen that the ignition delay has also a positive correlation with the mass of the particle. The result indicates that the bigger the particle size, the higher the moisture content, hence the longer the ignition delay. This effect is seen clearly in raw willow, but not much in the torrefied fuels. However, the trend is not observed in eucalyptus samples (see Figure 7.3 b)). The plots looked scattered and indistinguishable. As the main factor that influence the ignition delay is moisture content, it can be assumed that the raw and torrefied eucalyptus have similar moisture contents at the point when this experiment was conducted.

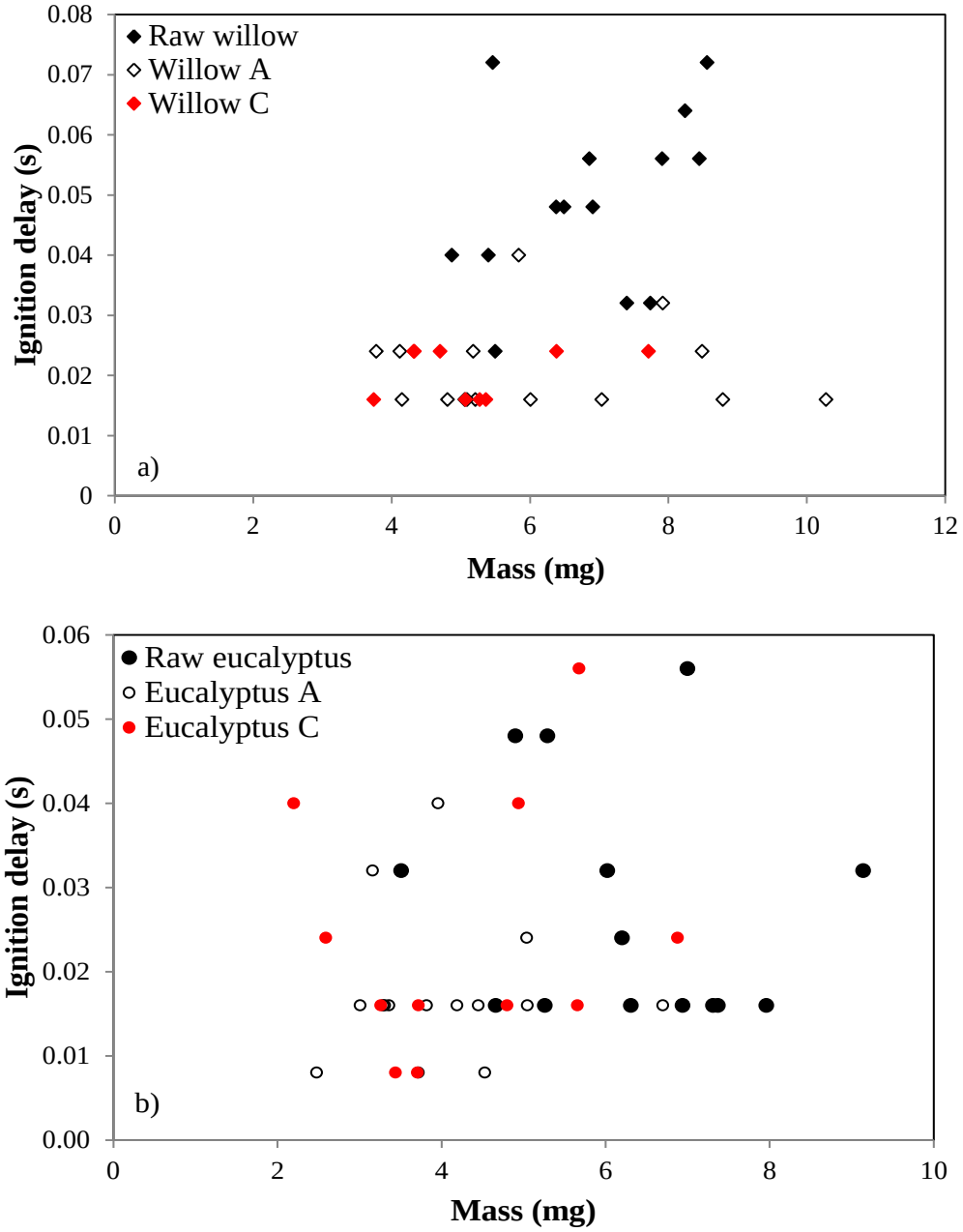

Figure 7.3. Ignition delays of raw and torrefied a) willow and b) eucalyptus, where the mass refers to the masses of each fuel before the combustion experiment.

7.4.2.2 Volatile combustion

Raw willow and eucalyptus seemed to have longer durations of volatile combustion than their torrefied counterparts (Figure 7.4 a) and b)). Between torrefied willow of increasing treatment, willow A and C, in general, shows that willow A performed similarly to willow C that is almost indistinguishable at most of the times as shown in Figure 7.4 (a). But there was a distinctive differentiation between two eucalyptus samples of different torrefaction conditions at which eucalyptus C has a shorter duration of volatile combustion than eucalyptus A (Figure 7.4 (b)). Longer duration of volatile combustion suggest that the rate of devolatisation that occurred in the sample was slower because it contains a greater amount of volatiles. Willow and eucalyptus A and C have short durations because most of the volatiles were already lost during torrefaction, so they have low volatile contents. Further investigations on the rate of devolatisation can be discussed in the later section.

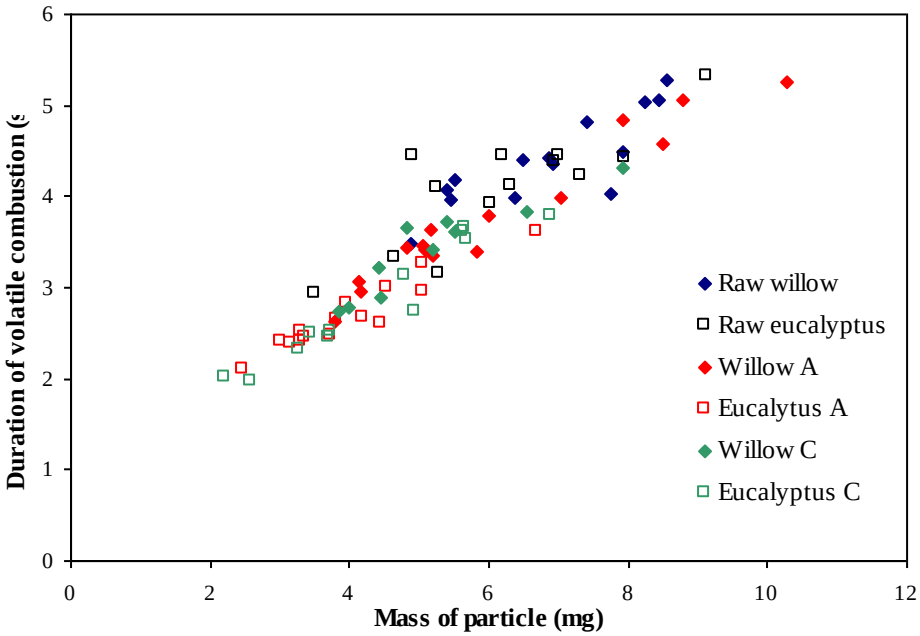

Figure 7.4. Durations of volatile combustion of raw and torrefied willow and eucalyptus.

7.4.2.3 Char combustion

Figure 7.5 a) and b) show plots of duration of char combustion against theoretical mass of the char. The theoretical mass of char was calculated using the percentage fixed carbon content (FCC), which was expressed in dry ash free basis (see Equation 7.7). The values of FCC were obtained from Table 5.2.

$$\text{Theoretical mass of char (daf basis)} = (\text{FCC}/100) \times m_s \qquad (7.7)$$

where m_s is the mass of 2 mm cubes of willow and eucalyptus before combustion (mg).

It can be seen that raw willow and eucalyptus have shorter times of char combustion than those that were torrefied (A and C). The slower duration of char combustion (burnout) in raw willow and eucalyptus leads to the production of lower mass of char. Raw eucalyptus has a faster duration than raw willow. Similar to those observed in the volatile combustion, torrefied willow samples also have indistinguishable trend in the duration of char combustion but not with eucalyptus samples. Eucalyptus C has a longer duration of char combustion than eucalyptus A. Longer duration of the char combustion gives more time for combustion to take place inside the particle and leads to the production of more mass of char. Longer duration of char combustion of a sample also suggests that it has a high char (fixed carbon) (Bridgeman *et al*., 2008). Upon treatment, studies have shown that torrefied biomass have increased carbon content and decreased hydrogen and oxygen contents, which results in an increased higher heating value and energy yield (see Table 5.3). This, in other words, supports the increased duration of the char combustion stage.

In addition to that, as previously stated, the rate of combustion depends on the oxygen concentration, gas temperature, char size and porosity (Borman and Ragland., 1998). Tillman *et al* (1981) stated that the char produced from pyrolysis is porous. Jones *et al* (2012) studied the surface areas and porosity of chars that were prepared from torrefied willow. They discovered an increase in the surface areas and developments of porosity in the chars. Theoretically, there is a rapid escape of volatiles from the biomass through its pores during char formation. Therefore, the more porous the biomass is, the faster the volatiles can escape, which can speeds up the char formation. However, this study showed that the more torrefied eucalyptus (C) has a shorter volatile combustion but it took a longer time to burn than the less torrefied fuel (A). The porosity of these fuels were not investigated but in Jones *et al*'s study (2012), it was stated that even though they have found a development of porosity, they discovered the reactivity of torrefied biomass char was lower than that of raw biomass, hence, it was concluded that the porosity and surface area have no influence on the reactivity. The duration of char combustion of torrefied willow in Jones *et al* (2012) is in agreement to those of torrefied biomass fuels analysed in this present study. The torrefied biomass fuels burned slower than those raw fuels. Further work has been done to determine the rate of char combustion of these fuels and will be discussed in the later section.

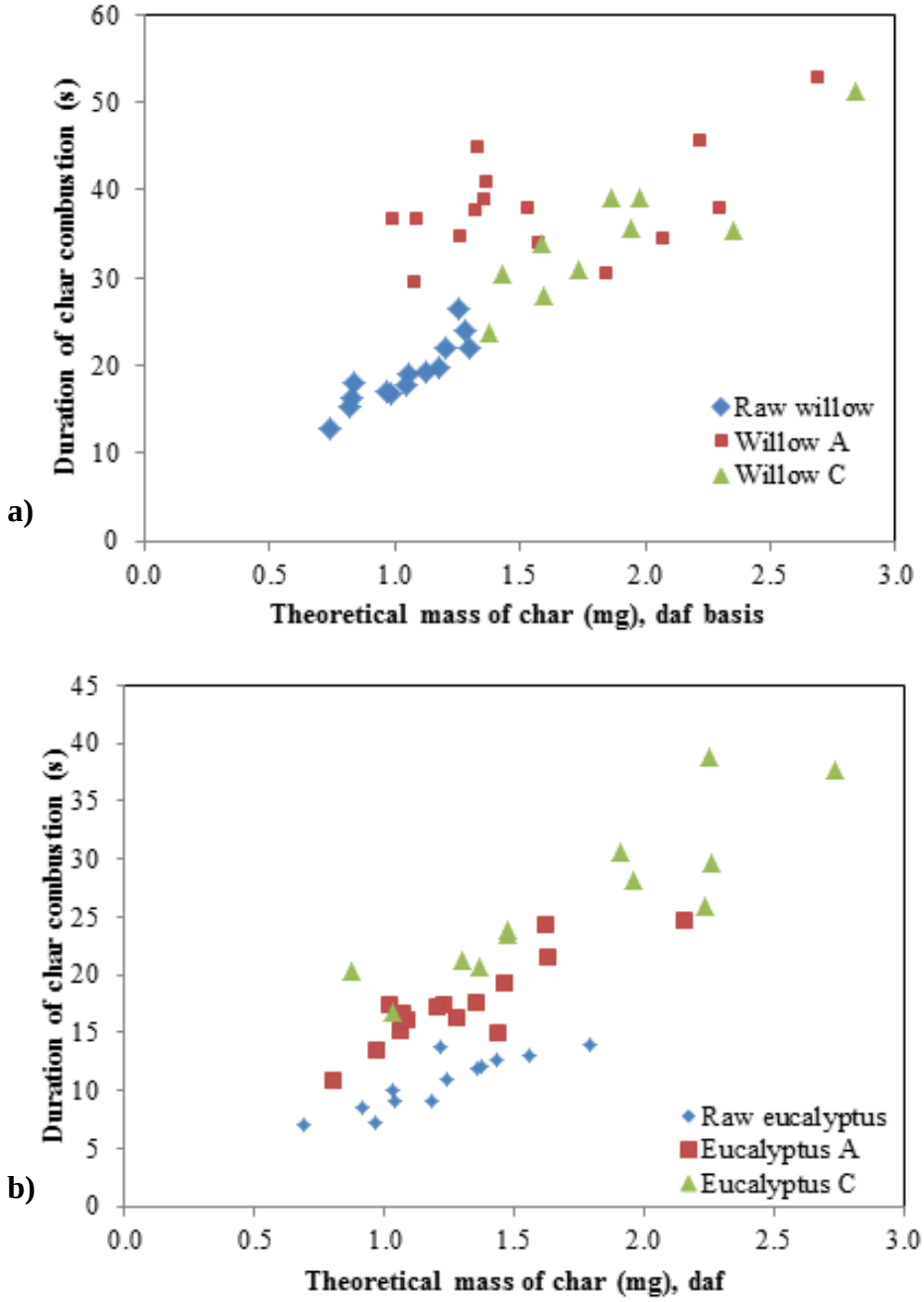

Figure 7.5. Durations of char combustion of raw and torrefied a) willow and b) eucalyptus.

7.4.3 Rate of devolatisation and char combustion

This section discusses the rate of devolatisation of raw willow and eucalyptus. In the single particle combustion experiment, the durations of devolatisation of both raw fuels were in the range of 3-6 s. The FG-Biomass model was used to simulate the pyrolysis of raw willow and eucalyptus at parameters mentioned earlier in 7.3.1. Figure 7.6 a) and b) and Figure 7.7 a) and b) illustrate the char yields of the raw fuels and their DTG curves plotted with time during pyrolysis respectively.

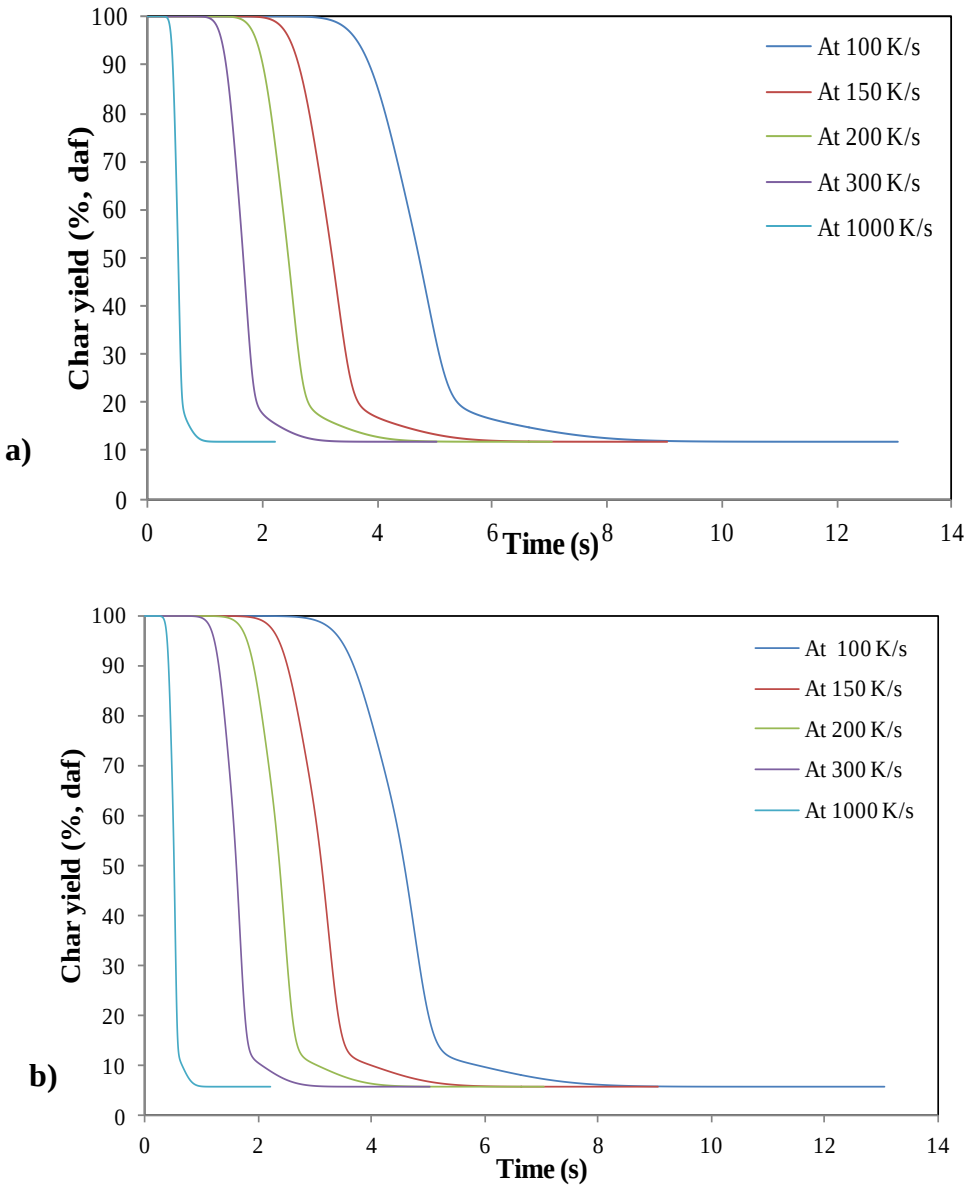

Figure 7.6. Char yields of raw a) willow and b) eucalyptus that upon pyrolysis treatment at different heating rates that ranged from 100 to 1000 K s^{-1}.

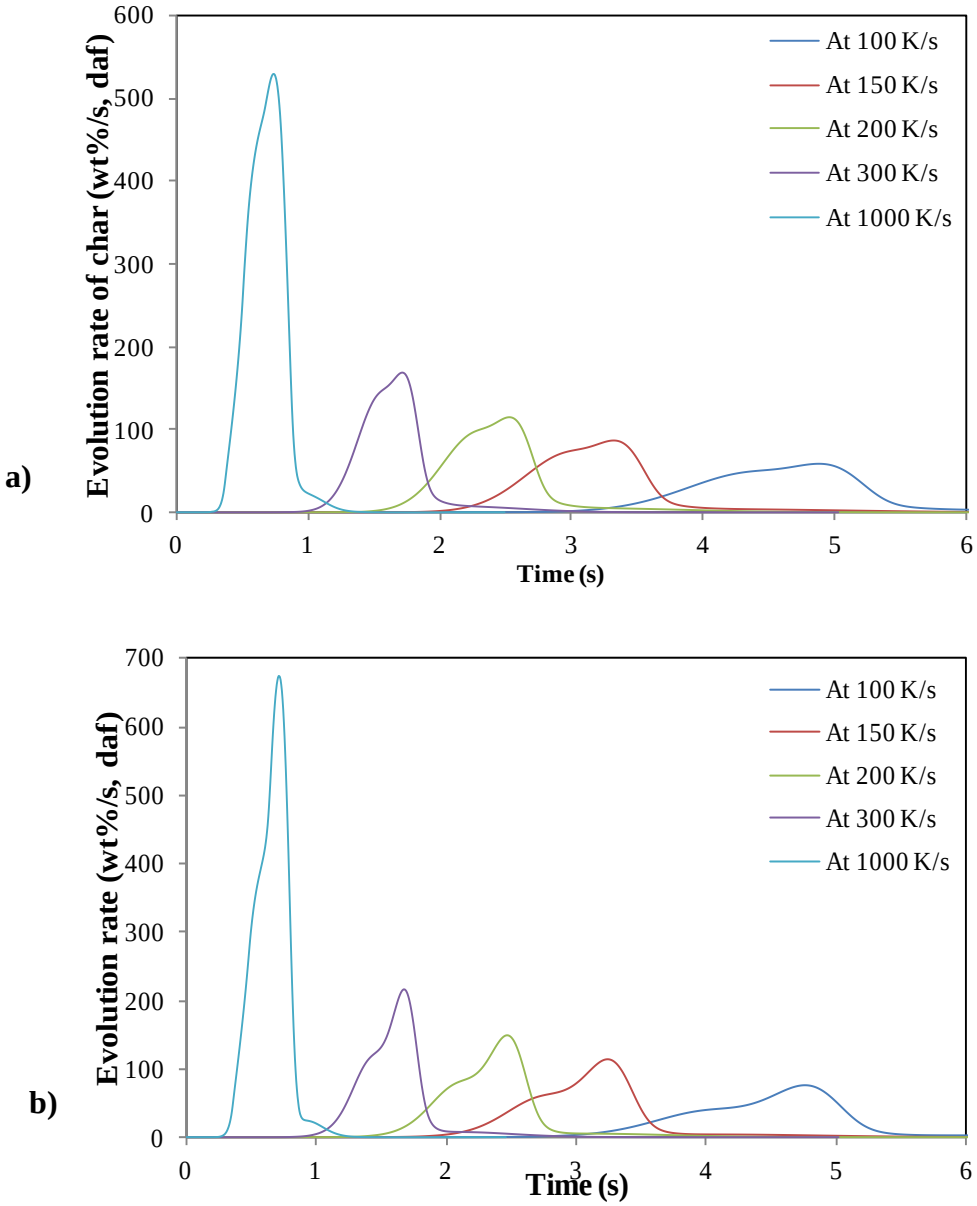

Figure 7.7. The evolution rates of char of raw a) willow and b) eucalyptus (wt% s^{-1}, daf) plotted with time upon pyrolysis at different heating rates.

As mentioned earlier, different heating rates were tested to determine the heating rate that produced similar rates to those observed in the Meker burner. Figure 7.4 shows that the duration of devolatisation of both raw samples was in the range of 3-6 s. Figure 7.6 shows that most of the devolatisation for both fuels that took place between 3-6 s is when the heating rate is 100-200 Ks^{-1}. Figure 7.7 gives a clearer view of the heating rate at which most of devolatisation takes place and that is 100 K s^{-1}, regardless whether it is willow or eucalyptus. Therefore, it can be concluded that the heating rate during which this stage took place experimentally was about 100 K s^{-1}. With regards to the type of fuel, eucalyptus tends

to decompose more and faster than willow. This effect is due to the difference of lignocellulosic contents, where it has been studied that eucalyptus has more hemicellulose content than willow. The char yield of willow was predicted to be 11.95% (daf) and that of eucalyptus was 5.81% (daf). Moreover, the highest char rate of willow was about 59.14 wt% s^{-1}, while that of eucalyptus was about 77.04wt% s^{-1}. These values were based on the heating rate of 100 K s^{-1}.

As displayed in equation (7.5) and with the given parameters as determined in Jones *et al* (2012), the value of rate of constant of char combustion, k is 2.89 s^{-1}. The value of k is reduced to 0.636 s^{-1} when the oxygen content was 2.75%, assuming the reaction rate is first order with respect to $[O_2]$. These two values of k are used to determine the value of α as shown in equation (6), hence, results in Figure 7.8. It clearly shows that the conversion factor decreases steadily with time. The actual observed rate is slower than this as shown in Figure 7.5. Furthermore, the video observation showed that the char combustion via a shrinking core mechanism, indicating diffusion limitations on this chemical reaction rate. With reference to Table 7.1, the predicted duration of char combustion is 4.7 s for 95% burnout and 3.6 s for 90% burnout.

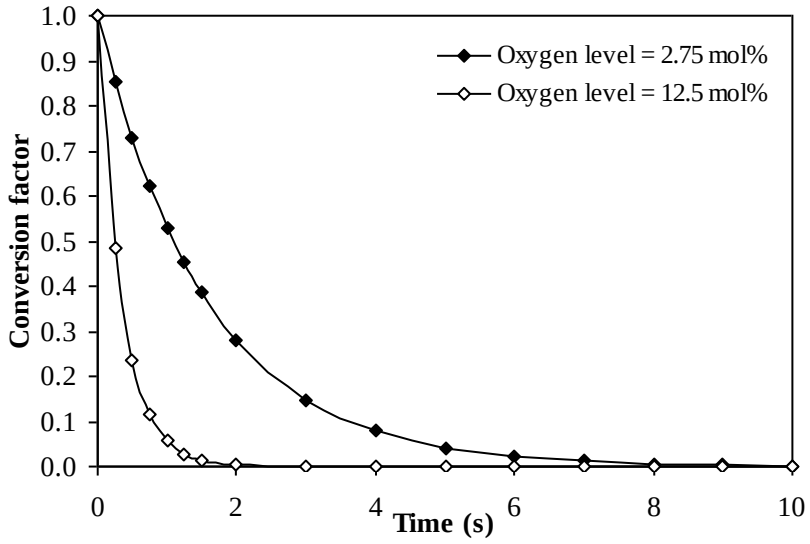

Figure 7.8. Conversion factor as a function of time upon pyrolysis of torrefied willow.

Table 7.1. Predicted char burnout of torrefied willow.

Burnout (%)	**Time (s)**
90	3.6
95	4.7
99	7.2

7.5 Conclusion

Combustion behaviours of raw and torrefied willow and eucalyptus were examined in a methane air flame using a high speed camera. The observations showed that torrefaction has changed the combustion properties of biomass. Torrefied willow samples have improved ignition delay due to their lower moisture content than the raw willow but the results could not be observed in eucalyptus samples. Moreover, even though this study shows that torrefaction seemed to not affect the duration of volatile combustion, it produced significant changes to the duration of char combustion, where the time taken is longer in comparison to the raw materials. This could be due to their increasing fixed carbon content as a result of torrefaction. These behavioural changes were more pronouncedly observed in eucalyptus samples of increasing severity of treatment than in willow. With regards to the type of biomass' response to combustion behaviour, lignocellulose composition may have an impact to such changes in the durations of volatile and char combustion. Rate of devolatisation and char combustion were also investigated. FG-Biomass model was used to simulate pyrolysis of raw willow and eucalyptus and the results are compared with the duration of volatile combustion obtained experimentally in order to estimate the heating rate experienced by the particles in the Meker burner. The results showed that the approximate heating rate was 100 K s^{-1}. The rate of char combustion of torrefied willow was obtained using the parameters determined in Jones *et al* (2012), as 0.636 s^{-1} when the oxygen content used in the present study was taken into consideration. Plots of the conversion factor with time for both rate constants were illustrated and gave a maximum predicted burnout time of 88.73 s for 95% burnout. Since the actual burnout durations were in the range of 30-65 s, diffusion appears to also contribute to the char combustion rate, that is, the combustion is taking place in zone II.

CHAPTER 8

ENVIRONMENTAL IMPACT ASSESSMENT OF TORREFACTION OF BIOMASS

8.1 Introduction

To date, biomass contributes a small proportion (10%) of the global energy supply (IEA, 2013). Approximately two thirds are used in the developing countries for heating and cooking, while the rest are utilised in industrialised countries to generate heat, power and also used in road transportation sectors (IEA, 2013). When considering biomass in future energy systems, it is important that information on the environmental effects is available (Rupar and Sanati, 2003; Ravindranath and Hall, 1995). Biomass is one of the renewable energy sources that has the potential to compete against fossil fuels (IEA, 2012b). In terms of capital cost, biomass-based power plant is one of the most economical of all renewable technologies to construct, even though the raw materials would require more earnings in comparison to all the fossil fuels. The use of biomass for large-scale electricity is contentious. Some major producers for example, Drax are lobbying for energy policies in the UK to "*continue to recognise the true potential of biomass as a cost-effective, renewable technology, which can play an important role in the future energy mix of the UK and in helping to meet the country's 2020 targets especially in terms of carbon dioxide emission reductions*" (Drax, 2011).

One significant driver for the use of biomass is that the carbon dioxide released during its thermal conversion to energy is removed from the atmosphere via photosynthesis. Theoretically, its basic cycle is carbon neutral, where there is no net increase in the atmospheric carbon dioxide, provided that the biomass is sustainably managed (Thornley, 2006). Lifecycle assessment (LCA) is "*a technique to assess the environmental aspects that are associated with products and services*" (SAIC, 2006). When the entire lifecycle of carbon dioxide is assessed, external activities are found to negate some of the greenhouse gases (GHG) savings. Such activities as listed in Thornley (2006) are as follows:

- Fossil fuel energy content is utilised in the agricultural production and results in more emission of CO_2.

- Biomass residues degrade upon long storage, hence, it releases GHG particularly methane.
- Interactions between the soil and root system, with regards to carbon balance, for example, some of the carbon content of the biomass may have been adsorbed from the soil rather than from the atmospheric CO_2.
- The techniques involved, for example, the emissions of N_2O from fertilisers.
- Storage and transportation of the biomass feedstock also emit CO_2.
- Fossil fuel energy may be used in construction and operation of the power plant, adding CO_2 to the atmosphere.

Thornley (2006) also reported about the necessity to consider environmental impacts other than the GHG balance, which include "*emissions from vehicle movements, environmental effects of the usage of agricultural chemicals (pesticides, herbicides and fungicides) used during cultivation, changes in the soil fertility, mineral and carbon balance and ecological impacts on natural and semi-natural habitats and the biodiversity supported*".

Table 8.1 lists some of the environmental, social and economic benefits and consequences that could rise from UK bioenergy implementation. Thornley (2006) mentioned that little information is available to quantify their impact or importance for future uses in the UK.

The first part of this chapter describes an overview of the lifecycle assessment, biomass sustainability and environmental impacts of biomass production and energy. Following that, the basic concept and structure of an environmental impact assessment (EIA) are discussed. The later part of this chapter provides a preliminary study of the hazards and EIA of torrefaction of biomass fuels. The assessment covers the following areas: the torrefaction process, the biomass materials used, the products after torrefaction and their potential impacts to the environment. A proposed environmental risk assessment profile is also included towards the end of this chapter. As seen in Table 8.1, socio-economic impacts, for example changes in the schedule for labour, where the preferred harvesting period for biomass are usually happens later than those conventional crops, are also factors that can influence bioenergy implementation in the UK (Thornley, 2006). But these issues are beyond the scope of this chapter.

8.2 Biomass and air quality

Biomass conversion to charcoal was the first large-scale application of biomass conversion processes especially in countries like India and China. Then coal was discovered and replaced charcoal. Major attraction towards gasification came into play as this process is able to convert biomass to more useful products that can be burned to release energy (Basu, 2013). Apart from that, combustion has also gained industries' interests for energy supply.

Table 8.1. Potential benefits and consequences of different aspects of bioenergy development (Thornley, 2006).

Aspects	**Benefits**	**Consequences**
Environmental	Increased biodiversity Reduced GHG emissions Possible improved soil fertility Uptake/removal of heavy metals from soil Minimal use of agricultural chemicals	Impacts on particular native species Loss of existing natural habitats Visual impact of crop growth and conversion plant Associated traffic noise and pollution Environmental emissions associated with thermal conversion plant Uptake of significant amounts of water from below ground Potential soil erosion with poor management practices
Social	Diversification of rural economics Opportunities for farm labourers in winter months Local employment at conversion plant and associated activities Potential for low cost heat supply Potentially improved security of supply	Actual and perceived impact of conversion plant on quality of life Potential impacts on tourism and leisure opportunities
Economics	Potential income stream for farmers Local economic activity related to employment opportunities Development of UK manufacturing and export potential	Requirement for financial/policy support in addition to existing RO

Unfortunately, over the years, there have been increasing concerns about the inappropriate use of biomass that have caused adverse effects on the air quality. For example, biomass is commonly burned in boilers but the process of combustion is often incomplete. Such process leads to the emission of particulate matters (PM) and airborne pollutant such as methane and volatile organic compounds, nitrogen oxides, sulphur oxides, hydrogen chloride, polyaromatic hydrocarbons (PAH), furans and dioxins, as well as organic and inorganic aerosols (Williams *et al*., 2012). Not only that, other issues can also be related to the malodorous gases and smoke formation resulted from inadequate combustion. According to the Environmental Protection Unit (EPU) (2009), the overall emissions depend on three factors: "*the design of the combustion plant, the chemical and physical qualities of the fuel and the presence of any emissions abatement equipment fitted to the plant*". The National Air Quality Standard was first introduced in March 1997 in response to the Environmental Act 1995 for improving the air quality for health and environmental protection. The Strategy sets out standards for eight main health-threatening air pollutants in the UK (benzene, 1,3-butadiene, carbon monoxide, lead, nitrogen dioxide, particles, sulphur dioxide and ozone.

8.3 Lifecycle assessment (LCA)

The increase of environmental awareness has encouraged biomass-related industries and businesses to assess their activities on how they might affect the environment (SAIC, 2006). The society has also raised its concerns about the issues of natural resource depletion and environmental degradation (SAIC, 2006). One tool that is able to assess the environmental performances of products and processes is lifecycle assessment (LCA). LCA uses a "cradle-to-grave" approach, where it considers the entire lifecycle of the product's life. SAIC (2006) describes the term "cradle-to-grave", at which it begins with the gathering of the raw materials from the earth to create products and ends at the point where all materials are returned to the earth. LCA can also be used to quantify GHG emission savings of bioenergy by comparing the bioenergy system with a reference energy system.

Bird *et al* (2011) discussed the LCAs based on the IEA Bioenergy Task 38 case studies, where the GHG balances of biomass and bioenergy systems were assessed and the potential of other impacts were acknowledged. Six areas were covered and listed as follows:

a) Choice of reference system (fossil-derived or the best available fossil energy technology such as natural gas).

b) System boundary that includes all stages in the life cycle, significant energy uses, materials flows and GHG emissions in both the study and reference systems.
c) Comparing systems with different products as the bioenergy systems are usually characterised by multiple products.
d) Units for comparison known as functional unit (input-related and output-related).
e) Changes in land management and use, which can be direct or indirect.
f) Timing of emissions and removals.

Figure 8.1 shows the main stages involved in the lifecycle of a bioenergy system that can be used to carry out LCA. Detailed description of the LCA is important to attain the sustainability of biomass fuels but will not be discussed in this chapter.

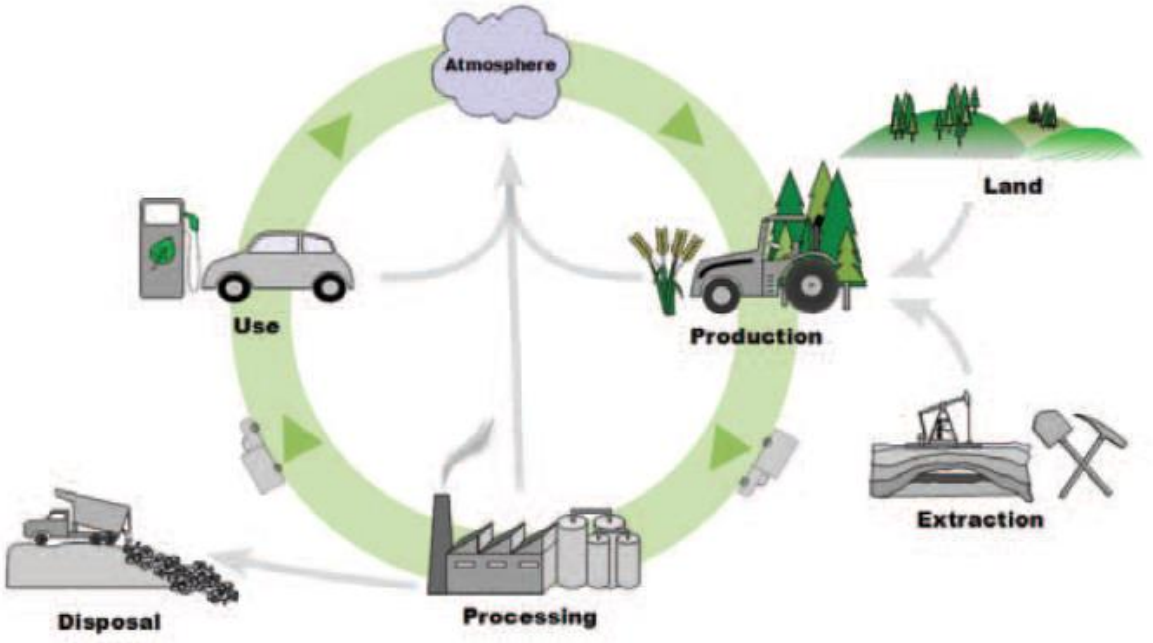

Figure 8.1. An illustration of the main lifecycle stages for a bioenergy system (Bird *et al*., 2006). The green circle represents the carbon cycle, while the grey arrows demonstrate the input and outputs from the bioenergy system.

8.4 Environmental impacts of biomass production

Biomass production results in either positive or negative impacts on the environment depending on how it is practiced (Brown, 2003). Figure 8.2 illustrates potential environmental impacts of biomass production as results of unsustainable biomass practices.

8.4.1 Soil quality

The fertility of a soil depends on the content of organic carbon and inorganic nutrients, that is, nitrogen, phosphorus and potassium in the soil. Organic carbon is a natural by-product of the decay of plant material in anaerobic environments (Brown, 2003). The amount of organic carbon depends on the tillage practices. Ploughing the soil will expose the carbon to oxidation and leads to the loss in the fertility of the soil. Other than that, the uptake of the inorganic nutrients by standing biomass that is subsequently removed can speed up the depletion of these nutrients from the soil than the wind- and water-transport processes can replace (Brown, 2003). Therefore, these nutrients must be quickly replaced by applying fertilisers into the soil and the application differs depending on the cropping system. For example, corn requires more nitrogen on the order of 135 kg/ha/yr compared to 50-60 kg/ha/yr for herbaceous energy crops (Brown, 2003). However, fertilisers are expensive and this process is labour-energy intensive. If they are not properly managed, water pollution can arise, which will be discussed in the next section.

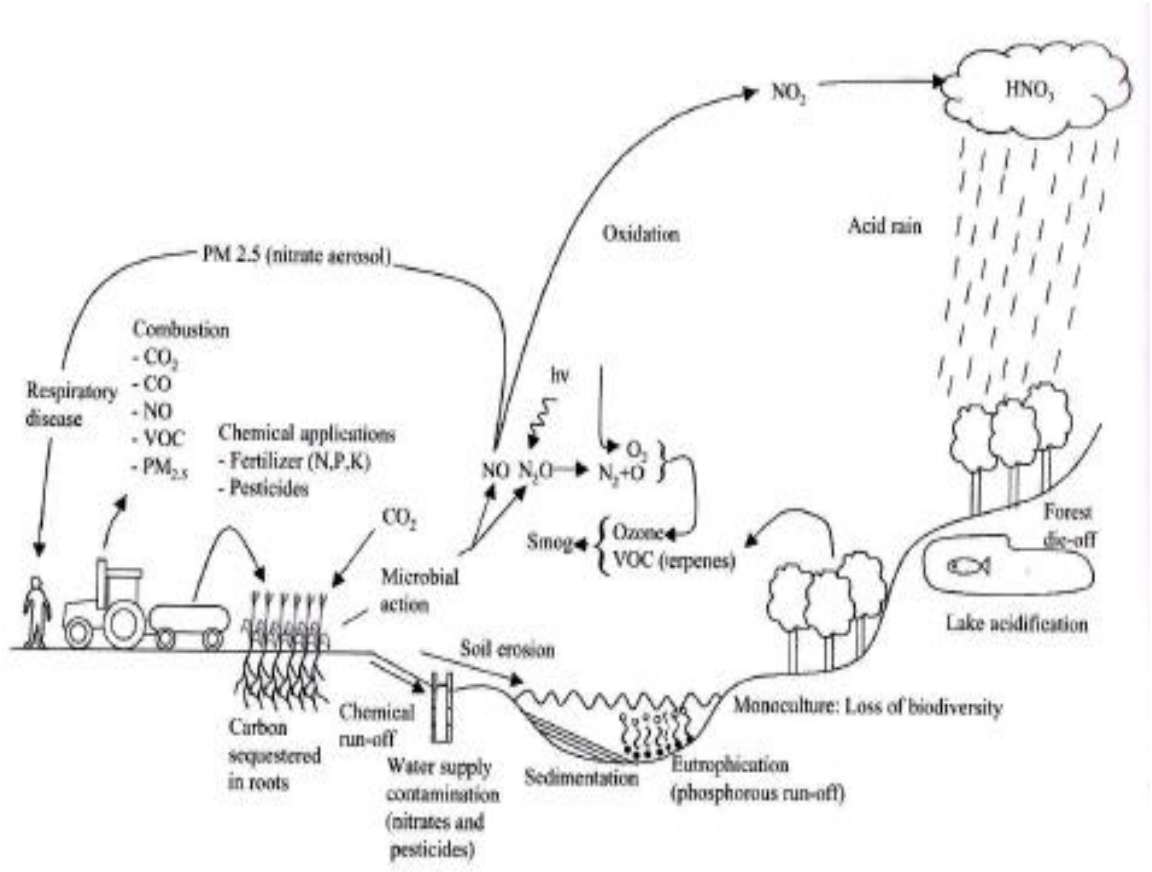

Figure 8.2. Potential impacts of biomass production due to non-sustainability of biomass practices (Brown, 2003).

8.4.2 Water pollution

Two of the sources of water pollution are soil erosion and leaching of chemicals from soils. Soil erosion can lead to the loss of organic carbon and inorganic nutrients and in turn, reduces the crop productivity (Brown, 2003). Moreover, it distributes soil and nutrients to unwanted locations, making them pollutants. Soils can eventually get washed into reservoirs and lakes and form sediments and interfere both animal and human activities (Brown, 2003). Apart from that, nitrates, formed from oxidation of ammonia in fertilisers upon exposure to air, readily leach from soils and can appear in well water and river water at concentrations above the human health standard. Even though phosphorus binds tightly to soil particles, it gets easily washed from fields as a result of erosion. It poses threat to aquatic ecosystem in a process called eutrophication. Moreover, herbicides and insecticides can directly leached from soil and most problems associated with this matter usually comes from the point-source emissions such as accidental spills or improper disposal of chemical containers, or non-point-source such as heavy rainfalls (Brown, 2003).

8.4.3 Air pollution

Soil tillage helps to reduce soil erosion. However, it can lead to air pollution, which generates both particulates and gaseous pollutants. The soil nitrogen that comes from either nitrogen-fixing bacteria or fertilisers is converted to nitric oxide (NO) and nitrous oxide (N_2O) by microbial processes in wet, anaerobic soils (Brown, 2003). Nitric oxide can further oxidise to nitrogen dioxide and results in acid rain and can lead to the formation of photochemical smog (Brown, 2003). Even though nitrous oxide is relatively stable to chemical reaction compared to NO, it is a strong GHG because of its optical properties. Methane is also produced by microbial processes in tilled soils. Moreover, volatile organic compounds are produced from growing plants and they are able to react with nitrogen oxides and produce haze (Brown, 2003).

Towards expanding biomass use for energy, it is important to consider the potential impact of the air quality and pollutants on public health. The UK Biomass Strategy aims to ensure that the appliances installed in the UK are modern and low in pollutant emissions. There are currently 140 models of biomass boilers, which meet the requirements of the Clean Air Act 1993 and have been exempt for use in UK smoke control areas (DEFRA, 2007). Air pollution impacts of biomass combustion was analysed and compared to those of coal, oil and gas combustion for the Scottish Executive in 2006 (EPU, 2009). The results showed significant

reductions in sulphur dioxide particulate matters, carbon monoxide, oxides of nitrogen and non-methane volatile organic compound emissions. As to date, the Government, led by DEFRA, is working "*to increase the level of reliable emissions data and to quantify the impact of the implementation of this strategy on non-greenhouse emissions, air quality and the UK's ability to comply with mandatory air quality limit values*" (DEFRA, 2007).

8.4.4 Biodiversity

In India, for example, the soil is exposed to tropical monsoon rains. Excessive removal of vegetation and damage to ground vegetation during removal of biomass for fuel could affect plant diversity (Ravindranath and Hall, 1995). However, dedicated feedstock supply systems actually provide advantages to a certain degree of biodiversity (Brown, 2003). For example, multi-species production systems are able to reduce the risks associated with pests and adding nitrogen-fixing plants could reduce fertiliser applications. Furthermore, other plants might provide erosion control during establishment (Brown, 2003).

8.4.5 Greenhouse gases

One of the principal GHG is carbon dioxide. Brown (2003) mentioned that with dedicated feedstock supply systems, they have the ability to sequester carbon from the atmosphere. As the plants grow, they absorb the atmospheric carbon dioxide and convert it into carbohydrates, oils or proteins. If the plants are harvested and used for bioenergy or fuels, the gas is returned to the atmosphere. GHG is also an issue in the industrial uses of biomass energy and it will be discussed again in the later section.

8.5 Brief summary of the environmental impacts of biomass use in industries for energy

The utilisation of biomass energy for heat and power has become a political demand in many countries all over the world (Hustad *et al*., 1995). The IEA Bioernergy Task 40 in IEA (2013a) reported that Brazil, India and United States are the top three countries that used biomass for energy purposes in the industrial sector in 2009 (see Table 1.2). They mainly use primary solid biomass and in total, the countries listed in the table use 5.9 EJ of biomass a year, which is 80% of the global biomass use in the industrial sector (IEA, 2013a). This section provides a brief overview of the environmental impacts of industrial uses of biomass energy from combustion, gasification and others (fuel ethanol distilleries, iron and steel plants and paper and pulp mills).

As illustrated in Figure 1.15, combustion of biomass consists of four steps, that is heating and drying, devolatisation, volatile combustion and char combustion. Recently, Williams *et al* (2012) provided an extensive review on pollutants from combustion of solid biomass fuels and it was stated that large combustion units that are carefully monitored generally form low levels of pollutants, while small units with poor operations leads to the production of high levels of pollutants. Figure 8.3 illustrates the pathways leading to the formation of pollutants as displayed in Williams *et al* (2012).

Smoke is a result of secondary reactions from unburned volatiles. Smoke consists of soot, aerosols (inorganic, organic and aqueous), CO, VOC and PAH (Williams *et al*., 2012). Carbon monoxide leads to cardiovascular diseases while VOC plays a role in smog formation. In addition to that, nitrogen compounds are partially emitted with the volatiles. Some form a C-N matrix in the char and later released during the combustion of char stage, forming NO_x and NO_x precursors, HCN and HNCO (Williams *et al*., 2012). Biomass that contains sufficient sulphur will release SO_2 during both volatile and char combustion. Sulphur dioxide can further react in the atmosphere to form sulphuric acid, which eventually contributes to acid rain (Brown, 2003). Furthermore, Williams *et al* (2012) reported that KCl and KOH and other metal containing compounds together with the sulphur compounds form a range of gas phase species, which can be released as aerosols. They can also form deposits in combustion chambers. Chlorine is converted to hydrogen chloride (HCl) and forms hydrochloric acid upon reaction with water. Heavy metals usually form oxides or chlorides upon combustion and exist as particulate matter. Brown (2003) stated that even though heavy metals are present in small quantities, they are highly toxic and can be bioaccumulators like mercury. Bioaccumulators are taken up by plant or animal tissue and can move through the food chain where they build up to toxic concentrations. The operation of heat and power production can result in water pollution if it is not managed properly (Brown, 2003). Wastewater is produced when the biomass is cleaned before it is burned or if spray towers are used to scrub out dust, tar or other pollutant from producer or flue gas.

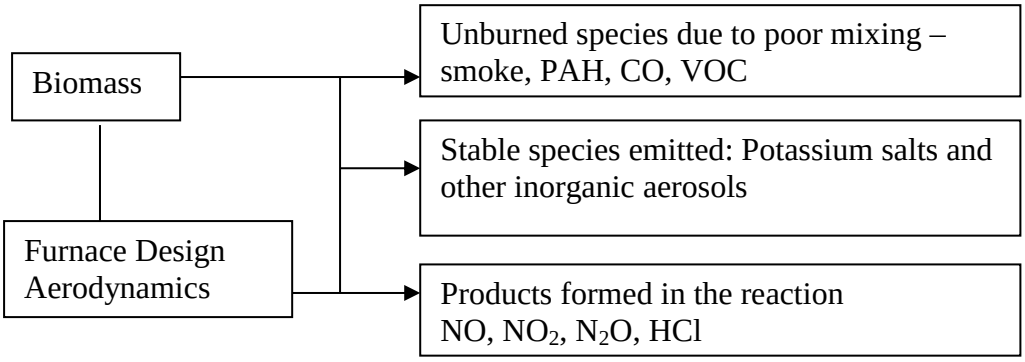

Figure 8.3. Products formed during the combustion of biomass (Williams *et al*., 2012).

Products of combustion depend on the composition of the biomass, the design of the combustion device and the operation of the system (Hustad *et al*., 1995). Klass (1998) suggested that the operation of biomass combustion systems should be designed to promote complete combustion under controlled conditions as closely as possible to produce a maximum amount of thermal energy, minimize undesirable emissions (volatiles) and meet environmental regulations/standards. Williams *et al* (2012) reviewed the pollutants emitted from small-scale plants to large combustors. Small combustion units that practiced poor mixing of fuel and air tend to be the major source of particulates. Unfortunately, no common international standards for emission control from these units are available at present (Williams *et al*., 2012). On the other hand, large combustion units are equipped with pollution control units with bag filters or electrostatic precipitators and offer the best route to clean combustion.

Table 8.2 presents a list of the pollutants emitted and their origins that are sourced from incomplete combustion.

Table 8.2. Emissions and their origin when treated with combustion (Hustad *et al*., 1995).

Pollutants	**Origin**
Unburned pollutants (CO, HC, tar, PAH and VOC) and oxidised pollutants (NO_x, CO_2 and in certain cases, N_2O)	All types of biomass
Acid gases (HCl, SO_2) and salts (NH_4Cl etc)	Biomass containing Cl and S, demolition wood and short rotation crops (straw, grass, miscanthus, etc)
Ash particles	All types of biomass
Heavy metals (Pb, Zn, Cd, Cu, Cr, etc)	Biomass containing heavy metals
Dioxins Low concentration (Low Cl content) High concentration (High Cl content)	 Native biomass Urban waste wood and demolition wood

Figure 8.4 illustrates the potential environmental impacts of processing bio-renewable resources into heat and power.

During gasification, flammable gas mixtures are produced from solid, carbonaceous fuels, which are collectively known as producer gas. Such gases are carbon monoxide, methane, nitrogen, carbon dioxide and smaller quantities of higher hydrocarbons. These gases can be burned to produce heat and steam or used in gas turbines to produce electricity (Demirbas, 2005). Unfortunately, higher hydrocarbons condense to form tars, which can cause blockage in the system. Furthermore, the presence of tars can contaminate producer gas and this usually occurs in many downstream applications (Brown, 2003). Gas scrubbing is one approach for removing tars from product gas but this can lead to the production of a toxic stream of tar, which can complicate waste disposal (Brown, 2003).

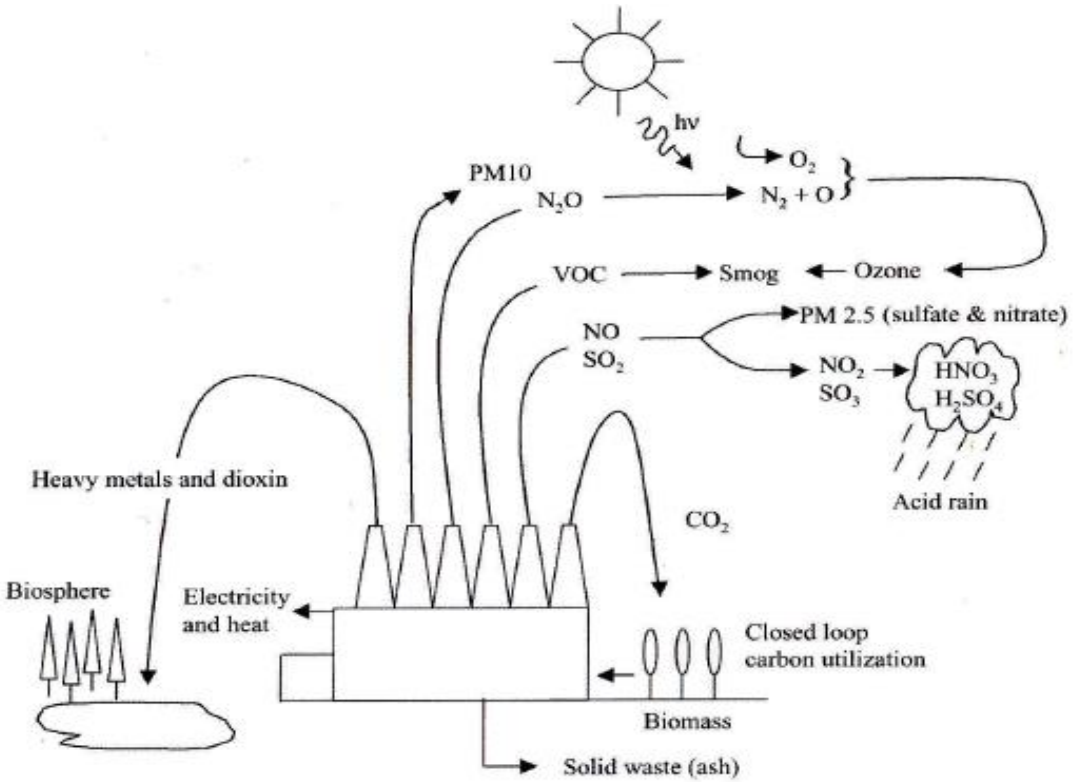

Figure 8.4. Potential environmental impacts of converting bio-renewable resources into heat and power (Brown, 2003).

Biomass contains trace elements that are of great environmental importance but heavy metals such as Pb, Cd and Hg are harmful to some plants (Demirbas, 2005). It was reported that the extensive information on the metal contents in many biomass species is not available, hence it is difficult to assess due to the limited knowledge on their chemical forms (Demirbas, 2005).

In Brazil, for example, there are three energy-intensive industrial sectors that depend largely on biomass, both as raw material and for energy supply, namely fuel ethanol distilleries, iron and steel plants and paper and pulp mills (Rosillo-Calle *et al*., 2000). Since 1975, Brazil has produced anhydrous alcohol from sugarcane to blend it with gasoline in car engines. The use of sugar cane as an energy source makes Brazil responsible for one of the most important renewable energy programmes in the world (Rosillo-Calle *et al*., 2000). It contributes to improving the air quality in urban areas, for example the elimination of lead emissions and able to reduce greenhouse gases, where the CO_2 emissions during combustion are compensated by photosynthesis (Rosillo-Calle *et al*., 2000). Charcoal is used in iron and steel plants and considered to be more environmentally friendly than coal. For example, it is estimated that for each tonne of charcoal consumed, 0.4-1.2 t of CO_2 are fixed compared to

1.86 t released from coke (Rosillo-Calle *et al*., 2000). The Brazilian pulp industry uses wood derived exclusively from forest plantations. Replanting and reforestation programmes are actively operated by companies in this sector. Black liquor is a by-product of pulp production and it is consumed as a fuel in steam generators of pulp plants.

8.6 Emission controls

This section discusses the emission control for combustion of biomass since most of the bioenergy production is sourced from this process. Williams *et al* (2012) mentioned that the emissions of pollutants are difficult to control in small combustion units. The authors commented that large combustion units are more efficient to use as they incorporate with emission control equipment. Moreover, sustainability issues are better handled in large plants. In order to reach a perfect combustion of biomass, a wide range of parameters were taken into consideration. As suggested by Klass (1998), the best condition is that a solid biomass fuel should consist of small, uniform particles, low in moisture and ash contents and zero to very low chlorine, nitrogen and sulphur contents. In addition to that, power plants should always be controlled with the objective of maximising boiler efficiency and minimizing stack gas emissions (Klass, 1998). Emissions from biomass-fueled boilers can be controlled by a variety of methods. Klass (1998) stated that an efficient removal of particulate matter in the flue gases can be achieved by various combinations of cyclonic separation, electrostatic precipitation, agglomeration and filtration. Williams *et al* (2012) reported that electrostatic precipitators however, do not remove all of the submicron or ultra-fine materials. Removal of acid gas emissions can be achieved by flue gas scrubbing and treatment with lime. Furthermore, Williams *et al* (2012) mentioned about the attempts of improving the small combustion units in developing countries.

8.7 Biomass sustainability

The European Union policy urges the use of renewable sources to generate energy. Biomass is seen as a source that has the ability to meet those targets set by the EU as discussed in Chapter 1. However, there have been issues on the environmental impact of the use of biomass (Ares, 2013). Therefore, the European Commission (2010a) has prepared a report from the Commission to the Council and the European Parliament on “Sustainability requirements for the use of solid and gaseous biomass sources in electricity, heating and cooling” in 2010. This was in response to the Renewable Energy Directive to include a sustainability scheme for biofuels for transport and bioliquids used in other sectors

(electricity, heating and cooling). The main sustainability issues were addressed in the report, as listed below:

a) Sustainability in production (land management, cultivation and harvesting)

b) Land use, land use change and forestry accounting

c) Lifecycle greenhouse gas performance

d) Energy conversion efficiency

The impact assessment of the listed concerns is reported in "Commission staff working document: Impact Assessment" (EC, 2010b). The Environment Agency supports the use of biomass but they pointed out two challenges:

a) "*Biomass energy should be developed in a way that provides the greatest reductions in greenhouse gas emissions possible at an acceptable financial cost, and*

b) *Biomass should be produced sustainably in order that negative environmental impacts, such as on soils, groundwater, air quality, forests and water resources, are reduced as far as possible*" (Ares, 2013).

DECC (2012) provided a document, which discussed about consultation on proposals to enhance the sustainability criteria and to ensure affordability for the use of biomass feedstocks under the Renewable Obligation (RO). Details on the recommended sustainability criteria are not discussed in this thesis. Very recently, a press release documented by the Department of Energy and Climate Change in August 2013 stated that it will be a necessity for the biomass industry to demonstrate their fuels to sustainable or they will lose the financial support (DECC, 2013b). This is required from April 2015. Furthermore, it was quoted by Gregory Barker, Minister of State for Energy and Climate Change, "*The new sustainability criteria will provide the necessary investor certainty and crucially ensure that the biomass is delivered in a transparent and sustainable way*". The new criteria for sustainable forest management will be based on issues such as "*sustainable harvesting rates, biodiversity protection and land use rights for indigenous populations*" (DECC, 2013b).

8.8 Potential of biomass energy in the future

At present, the most common biomass feedstocks for the production of heat and power are forestry and agricultural residues and various organic wastes (Bauen *et al*., 2009). Others such as vegetable oil crops are used for biofuels. Energy crops have the potential to provide the bulk of the resource in the longer term. Interestingly, algae also have the potential but are

yet to be explored. The availability of biomass feedstocks is mainly determined by future developments in agricultural and forestry production. This is because the production of biomass primarily depends on the availability of land and the weather condition (Basu, 2013). According to Bauen *et al* (2009), the main factors that could determine the availability of feedstocks are the modernisation and development of the technology in agriculture, the efficiency of feedstocks logistics, the sustainability constraints imposed on energy crop production and population growth and food and feed demand. Other key factors that will arise in the future are the costs of production, the availability of suitable infrastructure, competing fossil fuels costs and the levels of policy incentives in support of bioenergy. Lastly, the development of aquatic species, such as algae is another key factor. The world energy demand can be estimated to be in the range of 600-1000 EJ/year and biomass energy could contribute up to 250 EJ/year, in competition with other sources.

As listed in Table 8.1, the impacts of biomass energy production can be both positive and negative. "*The best practice and appropriate regulation should be used to maximise benefits and minimise negative impacts*" (Bauen *et al*., 2009).

8.9 Overview of environmental impact assessment (EIA)

Environmental impact assessment (EIA) is "*an evaluation of the impacts that may arise due to some action or operation and that has a significant effect on the natural and man-made environment*" (Nurminen, 2012). In other words, the purpose of having an EIA is to investigate and mitigate any potential effects of a development/operation on the natural, physical and human environment. In an EIA, potential impacts on factors such as local communities, biodiversity, soil quality, water, air, climate are studied and where necessary, mitigation measures to eliminate or at least reduce such impacts are identified well in advance of the operation. Therefore, an EIA is a management-intensive process and offers an aid to decision-making. It also plays a role to achieve a sustainable development

Figure 8.5 illustrates the important steps involved in the EIA process and is described in Table 8.3. The figure shows that scoping is the critical part of the process initiated at the early stage. This stage identifies possible hazards and a further study will examine the hazards in various categories. It is important to note that scoping is generally carried out in discussions between the developer, the competent authority, other relevant agencies and ideally, the public (Glasson *et al*., 2005). Scoping often involves negotiations and consultations between

a developer and other interested parties. Some developers may start informal consultations as part of their project development planning (EA, 2002). This approach prevents misunderstanding between parties concerned about the information required in an Environment Impact Statement (EIS). Environmental Agency (2002) provides a list of potential stakeholders including statutory and non-statutory consultees that can provide information to investigate particular environmental issues (see **Appendix 8.1**). According to Glasson *et al* (2005), scoping should begin with the identification of individuals, communities, local authorities and statutory consultees that are likely to be affected by the project. Other countries such as in Canada and The Netherlands have a formal scoping stage, in which the developer agrees with the competent authority and sometimes after public consultation (Glasson *et al*., 2005).

DEFRA (2011) demonstrates an analysis that includes consequences and probabilities of the identified hazards as shown in Figure 8.6. The low-consequence/low-probability risks are perceived as acceptable and would only require monitoring. The high-consequence/high-probability risks are perceived as unacceptable and mitigation measures or better alternatives are required to manage the risk.

Generally, during the course of project planning, decisions are made that concerns with the type and scale of the project proposed, the location, the layout of the site, the processes involved and operating conditions (Glasson *et al*., 2005). After risks are assessed, mitigation measures and alternative options will be considered. Mitigation measures comprise some of the following forms that is, to terminate the hazard or reduce the effects by improving the engineered systems (DEFRA, 2011). It was pointed out that the alternatives must be reasonable, where it is technically possible and legal. If these alternatives are to be discussed with local residents, statutory consultees and special interest groups, some may eliminate some alternatives from consideration and suggest others. Also, it is unlikely that one alternative will emerge as being most acceptable to most of the parties concerned (Glasson *et al*., 2005). Factors that can affect the choice of alternatives are technical, economic, environmental, social issues and organisational capabilities (DEFRA, 2011).

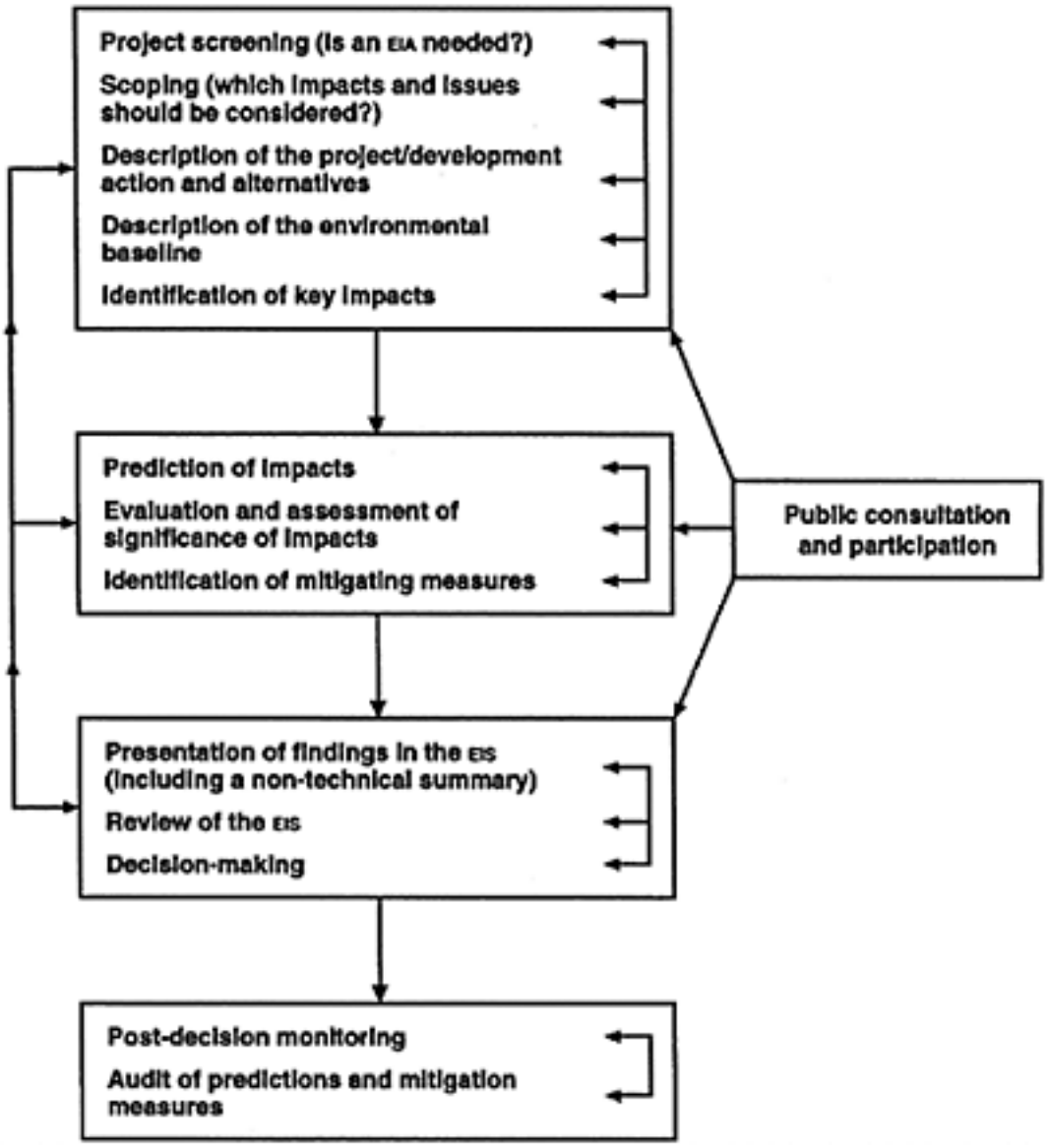

Figure 8.5. Key steps in the Environmental Impact Assessment process (Glasson *et al.*, 2005).

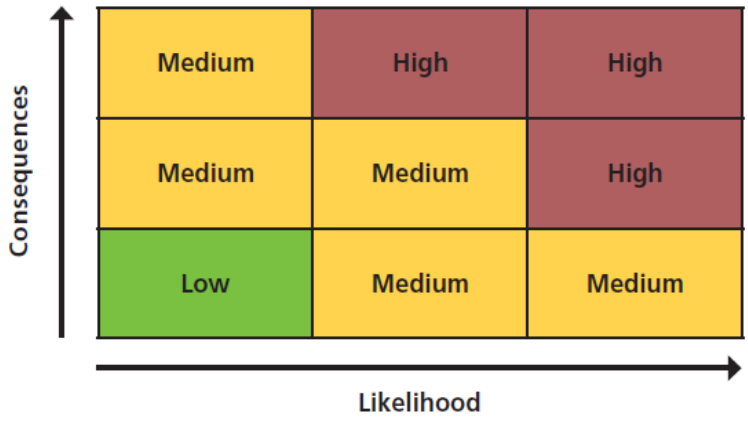

Figure 8.6. An example of an environment risk assessment profile that consists of probabilities and consequences of the identified environmental hazards (DEFRA, 2011).

The EIA report will have a comprehensive information about the potential environmental impacts of the project proposal and suggest any measures to mitigate such impacts. This report must be prepared by a registered EIA consultant. Once the EIA report is ready, an EIA review consultant will be appointed to give reviews to ensure its adequacy. If it is approved, the impacts of the proposal will be monitored.

8.10Environmental impact assessment of torrefaction of biomass

To date, there has been a great deal of research (laboratory-scale and large-scale demonstration plants) and technology developments that has been designed and improved especially in northern Europe and North America, but only a few of commercial scale torrefaction plants are yet in operation. Section 1.19.3 discusses the overview of project initiatives and status of torrefaction. Most research examined parameters and how they might affect torrefaction in terms of mass and energy yields of the torrefied solid. Few studies have identified the components of the other products of interest, volatiles (tars, gases and other condensable organic products). The determined components can be considered as pollutants if they are produced in an uncontrolled manner. These volatiles have the potential to cause adverse impacts on the environment and will be discussed in this section.

Apart from that, there is still a lack of information with regards to the environmental considerations of operation of the plant and the handling of biomass materials. Nurminen (2012) stated that many torrefaction organizations are still developing their processes. Therefore, data of environmental impacts of plants is mainly confidential and only some general limit levels could be shared (Nurminen, 2012). Nurminen (2012) examined the environmental impacts of two torrefaction power plants that are located in Pursiala (torrefaction pilot plant) and Risolog (commericial-scale torrefaction plant), Finland. Pursiala and Risolog torrefaction plants are still at the initial stage. Not all the details of the equipment and suppliers are finalised yet. Therefore, not all process details or environmental impacts can be known in advance. Some of the information from his report will be reviewed for the development of this EIA. Other literature that particularly investigated the products of torrefaction will also be referenced. Their environmental impacts will be assessed in this chapter. Even though the information is quite general, it is obvious that torrefaction of biomass fuels falls into the category, where environmental impact assessment (EIA) is required.

Table 8.3. Description of each step involved in the EIA process (Glasson *et al*., 2005).

Steps	**Description**
Screening	This step narrows down the application of EIA. If the operation has few or no impact to the environment, it can proceed to the normal planning permission and administrative processes.
Scoping	This step is the critical stage early in the EIA process, where the key environmental impacts and issues of concern are identified and assessed. It also helps to identify the mitigation measures.
Consideration of other alternatives	This step seeks to ensure that the proponent has considered other approaches such as locations, scales, processes, lay outs and operating conditions.
The description of the project/development action	This step provides clarification of the project and requires an understanding of its characteristics for example, stages of development, location and processes.
The description of the environmental baseline	This step includes the establishment of both the present and future state of the environment, in the absence of the project.
The identification of the main impacts	This step ensures that all the potentially significant environmental impacts are identified in the process.
The prediction of impacts	This step aims to identify the magnitude and other dimensions of identified change in the environment with the project, by comparison with the situation without that project.
The evaluation and assessment of significance	This step assesses the relative significance of the predicted impacts to allow a focus on the main adverse impacts.
Mitigation	This step involves the introduction of measures to avoid, reduce any significant adverse impacts.

In a wider context of EIA, after the environmental impacts have been identified, mitigation measures and alternative options will have to be determined. This may be a challenge and rather difficult to estimate due to the lack of information available and in particular, alternative options, may not be thoroughly discussed in this chapter.

8.10.1 Screening

Screening helps to focus on projects that potentially has adverse environmental impacts or those that are not fully known (Glasson *et al*., 2005). As stated earlier, with the available information regarding the impacts of torrefaction, this operation is eligible to be "screened in" and requires full assessment.

8.10.2 Scoping

Scoping is the critical stage in the EIA process. The report of the assessment largely depends on the identification of the environmental impacts. A collective review of the environmental impacts of torrefaction will be pointed out and discussed in this section. Areas of interests are listed as follows:

i) Raw materials, in terms of the availability of biomass, fuel flexibility, harvesting, preparation prior to storage (chipping), storage and transportation.
ii) The torrefaction plant, in terms of its location, operation and maintenance.
iii) Torrefaction processes that involve before, during and after torrefaction process.
iv) Torrefied biomass materials, in terms of handling, storage, grinding, transportation, pelletisation and ashes
v) Environmental fates of volatiles (tars and gases) produced from torrefaction.
vi) Environmental risk assessments (biomass materials, plant equipment, process, activities of the plant, torrefied wood and other products, external factors).

8.10.2.1 Raw materials

Technically, all biomass resources are suitable for torrefaction. Exploratory studies have found that the properties of woody, herbaceous biomass and agricultural residues significantly improved after torrefaction (Ibrahim *et al*., 2012; Chen *et al.*, 2011; Bridgeman *et al.*, 2008). However, not all of these fuels will be viable for commercial plants especially agricultural residues such as straw. The wheat straw studied in Bridgeman *et al* (2008) contained a higher ash content (6.3%) than willow (1.7%). This is of great concern because high content of ash can lead to fouling and corrosion. Section 1.11.1 discusses the impact of ash in thermochemical conversion reactors. For commercial purposes, torrefaction suppliers would prefer woody biomass as feedstock to minimise technical challenges and maintenance costs. One drawback to such limited fuel flexibility is the required demand for woody biomass fuels. Fortunately, IEA (2012b) reported that this type of energy crops will be a

major source of biomass in the future. But then again, it will take time to secure land, arrange planting, confirm sustainability and establish new supply chains (IEA, 2012b).

The environmental impact of harvesting biomass for fuel uses depends on the intensiveness and how widely it is harvested. Before the wood is chipped, the collection of biomass fuels is in the form of branches, canopies and stumps. The collection of wood is from final felling sites and forest management sites, that is the thinning sites of young forests. Section 8.4.1 discusses the effect of soil quality in terms of soil erosion and depletion of nutrients due to ploughing and cropping system, while this section describes the effect of soil due to machines that move at the logging site. Logging residues cannot be collected during winter time. Therefore, the machines have to be used and may cause damages to the soil, which later can lead to soil erosion.

Chipping requires heavy-duty crushers and only possible in centralised chipping facilities. At the moment, chipping is mainly distributed in interim storages, where the load capacity and load size of the truck is fully exploited and transported in long distances to power plants. In Risolog, the transportation of non-chipped biomass is not as efficient as that of chipped biomass. Hence, the distance, where the biomass is chipped is < 100 km and from a < 50 km for non-chipped biomass to the logistic centre. In Pursiala, the chipping is not allowed in the power plant area due to noise caused by the process. Therefore, the raw material is chipped at the logging site.

Forest biomass is usually stored at roadside after harvesting. During the storing, potassium and phosphorus may leach out and eroded into the water system, provided that the biomass are not covered or situated next to ditches. Most biomass would degrade after a few months or even days when they are left exposed after harvest (Brown, 2003). Hence, a proper storage is crucial for the preservation of these biomass fuels for the successful development of bioenergy. To promote long-term storage, these fuels are pre-dried, cooled or processed the fuels to a more stable intermediate product (Brown, 2003). Drying the biomass fuels helps to inhibit the growth of microorganisms. However, this process demands a great amount of energy content. Brown (2003) mentioned that theoretically, 2442 kJ of energy is required for every kilogram of moisture to be removed at 25°C. But in fact, drying requires 50% more heat energy due to the sensible heat of both the biomass and of the air used for drying (Brown, 2003). Furthermore, to dry a ton of biomass that contains 50% moisture down to

10% would require about 1.5 GJ of energy (Brown, 2003). Therefore, field drying is preferred whenever possible. But piling of biomass can cause heat to build up and results in self-ignition. In addition to that, biomass is a very dusty material and the dusts can be more potentially ignited than dusts from coal.

Raw materials are taken from the storage to the power plant in Pursiala by road, using full and semi-trailer trucks. The transportation distance is 30 km. If it was assumed that 50% of the raw materials are transported by full-trailer truck and the other half by semi-trailer trucks, the total carbon dioxide equivalent emissions are approximately 7226 kg per annum. These emissions can be lowered if more of the full-trailer trucks are used. The transportation distance affects the emissions. If it was 50 km, with 50% of both trucks, the emissions can go up to 12044 kg per year. Risolog uses railroad and water way as means of transportation, which are more eco-efficient than road transportation but their transportation distances is likely to be longer. For an average distance of 100 km transported by railroad, carbon dioxide emissions are 338 000 kg per year, while that by water way causes the emissions of 310 000 kg per annum.

8.10.2.2 Torrefaction plant

The location and the land area demand of the plant (whether it is for pilot plant or commercial-use plants) are crucial in a torrefaction industry as this would entirely affect the natural and human activities. Therefore, one should fully analyse the land area prior to construction. For example, the Pursiala pilot plant covers an area of 50 x 20 m and the heights of the units vary from 6 to 9 m except for the stack, which is several metres higher. There were concerns if the pilot plant may cause visual harm such as the Mikkelipuisto Park, which is just distance away but the other existing industrial plants are in the way of the pilot plant, hence the visual harm caused by the pilot plant is minimal.

A typical torrefaction power plant involves six main units that are made for drying, torrefaction, cooling, pelletising (if included), combustion and heat exchange. The environmental impacts of the equipments are taken into consideration as part of the scoping process. For example dryers, where some reviews have discussed about the emissions from drying but the risks caused from the dryers and how they can lead to environmental impacts are not available. Potential risks occur when the equipments are not well-monitored, controlled and maintained. Some of the potential risks are for example, the leakage of air

entering the torrefaction chamber can lead to ignition and even explosion; the uncontrolled settings of the temperatures during drying and torrefaction that could go higher than desired can lead to "over-cooking" of the biomass fuels and may also lead to fires if it was not carefully monitored; the leakage of volatiles (tars and hot gases) during torrefaction process can leach (for tars) and produce odours as well as explosion if in contact with air; problems in the filtration system can cause dusts and more volatiles to escape, which will require intensive cleaning and unequal mixing of fuel and air during combustion leading to incomplete combustion, producing carbon monoxide and other unburned fuels.

8.10.2.3 Stages involved before, during and after torrefaction

Figure 8.7 illustrates the basic concept of torrefaction as drawn in IEA (2012a). The following section only identifies and discusses products that are potentially evolved during drying, torrefaction and cooling as these stages are the main ones that take place in a torrefaction reactor. The effect of pelletisation is also discussed here.

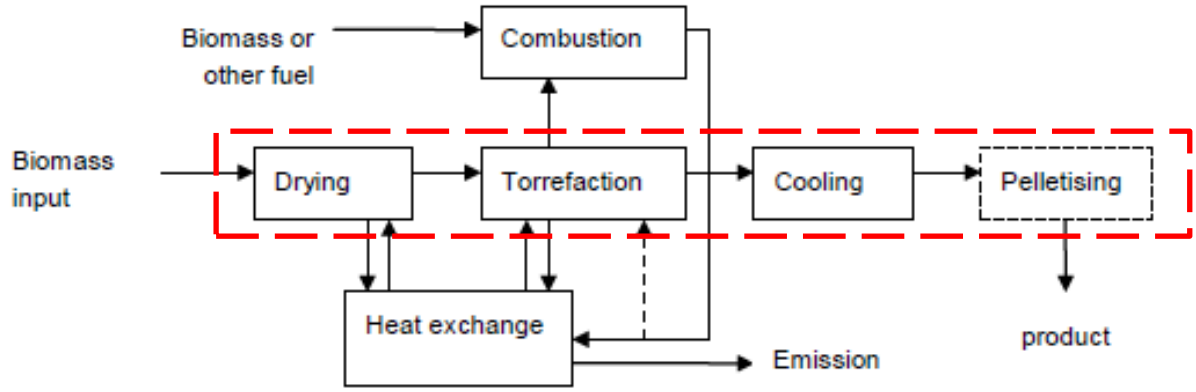

Figure 8.7. Overview of heat integration options (IEA, 2012a). The red dashed lines represent the boundaries at which those enclosed in the red box are discussed in this section.

During biomass growth, alkali metals such as potassium and chlorine are the two most necessary, nutritious elements. However, these elements are also the main contributors of slagging, fouling and corrosion in biomass-fired boilers (Deng *et al*., 2013). An example is when alkali metals react with silica, forming alkali silicates and these compounds melt or soften at temperatures as low as 700°C (Jenkins *et al*., 1998).

With regards to torrefaction, even though this process can greatly improve the properties of a biomass, vast amounts of alkali metals still remain in the torrefied fuel (Saddawi *et al*., 2012). Ash content is a measure of assuming non-combustible inorganics in biomass and it has

significant effects on the energy value of the biomass. The higher the ash content, the lower the energy value (Vassilev *et al*., 2010). Particularly for agricultural residues such as wheat straw, where the ash content goes up to 10.2% after torrefaction at 290°C, in comparison to when it is raw (6.3%) (Bridgeman *et al*., 2008). Therefore, pre-treatment of the raw biomass fuels is necessary to reduce such metals by washing before drying and torrefaction. Saddawi *et al* (2012) studied the effect of washing before and after torrefaction of willow, eucalyptus, wheat straw and *Miscanthus* at 290°C with a residence time of 60 min. Three types of washings were applied, namely water, ammonium acetate and hydrochloric acid and as a result, these procedures have different effects on the reactivity of each fuel. *Miscanthus* and wheat straw have high ash contents (3.7 and 9.2%, dry basis respectively). They also have high silica and potassium oxide contents, hence, are well-known for their high fouling potential. All in all, water washing is suggested to be the most promising pre-treatment for the preparation of torrefied fuels. Water washing seemed to be able to release nutrients depending on the temperature of the water. Potassium, sodium and other elements are readily soluble in water and therefore, they are easily removed.

Furthermore, water washing can increase the higher heating value of the treated biomass due to the reduction of ash content (Saddawi *et al*., 2012; Deng *et al*., 2013). For example, the ash contents of torrefied willow before and after washing were 3.5 and 2.7%, dry basis respectively, while their HHV were 23.6 and 23.9 MJ kg^{-1}, dry basis respectively (Saddawi *et al*., 2012).

Table 8.4 presented data collected from Deng *et al* (2013), who studied the effect of water washing on fuel properties of biomass. The results presented in Deng *et al* (2013) showed that washing can effectively remove ashes from biomass, where SiO_2 and K_2O are the main components of all the ashes. Candlenut wood has the lowest ash content, therefore it is suggested to fire well in boilers without difficulties, while wheat straw, rice straw and corn stalk may result in serious deposition and corrosion (Deng *et al*., 2013). It was also reported that sulphur and chlorine also make a great contribution to deposition and high temperature corrosion in biomass-fired boilers (Baxter *et al*., 1998).

Table 8.4. Ash contents and High Heating Value (HHV), both at dry basis, of biomass before and after water washing at 60°C as determined by Deng *et al* (2013).

Biomass	Ash (wt %, before washing	Ash (wt %, after washing)	HHV (MJ/kg, before washing)	HHV (MJ/kg, after washing)
Wheat straw	6.28	2.49	15.86	16.45
Rice straw	12.53	10.33	14.21	14.65
Corn stalk	6.40	3.36	14.86	15.84
Candlenut wood	1.40	1.00	16.53	17.40

Deng *et al* (2013) reported that silicon in the biomass is present in the form of monosilicic acid. Most of it is deposited on the outer walls of epidermal cells as amorphous silica, while others may polymerise into silica gel in the xylem sap (Deng *et al*., 2013). Silicon is soluble in water, presumably in the form of $Si(OH)_4$. Therefore, when biomass is treated with water washing, a significant decrease of silicon is reported in the study. Potassium is assimilated in the form of K^+ and forms weak complexes with organic anions (Deng *et al*., 2013).More than 80% of K^+ is removed after water washing. Sulphur is assimilated mainly in the form of sulphate anion, SO_4^{2-} by the roots and the rest is taken up in the form of SO_2 by the aerial parts of higher plants. According to Deng *et al* (2013), more than 70% of S is washed out of candlenut wood while 90% is released out of the other three biomass fuels listed in Table 9.1 after the water washing treatment. Chlorine is taken in in the form of chloride ion (Cl^-), where about 80-90% of chlorine is removed from water washing.

In the end, the leachate can be used for irrigation purposes, recycling valuable nutrients into the soil (Deng & Che, 2012; Deng *et al*., 2013). Deng and Che (2012) studied the characterisation of water leachates from biomass and they found out that in the leachate, K^+ was the most abundant cation and inorganic C and P exists in the form of HCO_3^- and $H_2PO_4^-$ respectively. Few organics were found in the leachate as well, in which the authors discovered carbohydrates and carboxylates. The overall pH of the leachate was in the range of 6-8.

8.10.2.3.1Heating and drying

The moisture content of biomass fuels can go up to 50-65%. Before they are fed into thermochemical processes, they have to be dried and reduced their moisture content down to 10-30% (Fagernäs and Sipilä, 1997). Drying increases the efficiency and improves the operation (Bergman, 2005; Roos, 2008). According to Roos (2008), dry biomass can reduce the net emissions of particulates and benefits the environment by reducing carbon emissions.

Following that, drying cuts down transportation costs and biomass will be less prone to degradation and microbial attack upon long storage. However, this approach has its drawbacks. Wimmerstedt (1999) reported that drying has the highest energy consumption worldwide, where most energy is consumed in heating and evaporating moisture (Roos, 2008).

With respect to torrefaction, woods are pre-dried before they enter the torrefaction reactor. Dryers used are based on direct or indirect heating. In direct dryers, hot gas is in contact with the wet biomass via convection, while in indirect dryers, a hot surface will be in contact with the wet biomass via conduction (Fagernäs and Sipilä, 1997). Flue gas drying or steam drying techniques are commonly used for biomass fuels, where the temperature and pressure applied on the dryers differ depending on the type of biomass. However, steam drying is more often used due to environmental reasons. In general, dryers used are based on rotary, fluidized-bed and flash dryers.

Fagernäs and Sipilä (1997) mentioned that wet biomass fuels are usually dried at low temperatures (100-450°C), high heating rates and in short residence times (0.5-60s). However, drying can lead to thermal degradation of the biomass materials releasing water vapour and volatile organic compounds. These compounds may cause environmental problems to the ambient air when the flue gases are led uncondensed into the stack (Fagernäs and Sipilä, 1997; Rupar and Sanati, 2005). The emissions of VOC can also cause tar to build up on low temperatures. VOC begins to release when the temperature of the feedstock is above the boiling point of water and become more significant as temperature increases. Furthermore, they can contribute to the formation of deposits in downstream sections (Fagernäs and Sipilä, 1997).

Emissions of biomass during drying comprised of aqueous and gaseous emissions. Fagernäs and Sipilä (1997) described that the formation of aqueous emissions originates when steam that is liberated condensed and produce condensable compounds. The emissions that remain volatile form the gaseous emissions. Wood, bark and wood-derived residues contain a large percentage of VOC than agricultural wastes, which are primarily consists of both hydrophilic and lipophilic, gaseous and condensable ones (Fagernäs and Sipilä, 1997). These compounds can be listed below:

- Condensable hydrophilic compound groups: Carboxylic acids such as formic acid and acetic acids, alcohols mostly methanol and ethanol, aldehydes, furfurals and carbohydrates such as anhydrosugars.
- Condensable lipophilic compound groups: Fatty acids, hydroxyl fatty acids, fatty alcohols, resin acids and triterpenoid alcohols.

Figure 8.8 presents the most volatile lipophilic compounds consist of monoterpenes (α-pinene and β-pinene). The non-condensing gases consist mainly carbon dioxide and to a lesser amount of hydrogen, carbon monoxide, methane and low hydrocarbons, C_2-C_4 (Fagernäs and Sipilä, 1997).

Figure 8.8. Terpenes (Sell, 2003).

Bridgwater *et al* (1995) provided a review of the origin and characterisation of emissions (solid, liquid wastes and volatiles) from thermochemical processing of biomass, namely combustion, gasification and pyrolysis as well as the environmental evaluation. A study was carried out to determine the organic compounds released from drying of birch bark and pine bark at 150-350°C. The results showed that the amount and composition of compounds released depends on the tree species. The dominant compounds found emitted during the drying of birch bark were carboxylic acids and terpenoids, while those found in pine bark consisted of carboxylic acids, aldehydes and carbohydrates. Furthermore, Bridgwater *et al* (1995) stated that the main classes of emissions from drying of biomass are monoterpenes, other lipid compounds and thermal degradation products, where the latter two released at high drying temperatures that may not be applicable to drying prior to torrefaction. The drying temperatures that are usually used in the study of torrefaction were 95°C (Deng *et al*., 2009), 105°C (Chen *et al*., 2011) and 100°C (Peng *et al*., 2012), all for 24 h.

Samuelsson *et al* (2006) measured the amount of VOC released during the oven drying process at 105°C for 24 h. Different types of woods were selected from various places in Europe. They collected the VOC and analysed using a gas chromatograph, equipped with a mass selective detector and an auto-injector. Brown (2003) stated that terpenes are abundant in softwoods. As a result, 60-80% of VOC released out of softwood consist of different terpene compounds, while in other materials, a much greater variety of compounds was found. Table 8.5 lists VOCs that are emitted (Samuelsson *et al*., 2006).

Table 8.5. Emissions of volatile organic compounds from drying of softwood (Samuelsson *et al*., 2006).

1) α-pinene	11) 1,4-methanoazulene
2) β-pinene	12) 2-cyclohexenecarboxanilide
3) 2,6-dimethylbicyclohept-2-ene	13) Isoparvifuran
4) 1,3,6,10-cyclotetradecatetraene	14) Napthopyran derivative
5) Hexanal	15) 1,4-methanonapthalene
6) 2-pentylfuran	16) 4-hydroxybutanoic acid
7) Furfural	17) Pyrazole
8) Phenol	18) 1-pentanol
9) Piperazine	19) Hexanoic acid
10) 3-carene	20) Nonanal

Rupar and Sanati (2005) used hot air to dry pine and spruce at 140, 170 and 200°C so that their moisture contents went below 10%. They also have identified few monoterpenes, namely α-pinene (~500 kCounts/g), β-pinene (~100 kCounts/g) and 3-carene (~90 kCounts/g). Higher temperatures released sesquiterpenes, namely limonene, calamenene, copaene, longifolene γ-muurolene and α-muurolene. Their environmental impacts will be discussed in the later section.

It is worth mentioning that there are many factors that can influence the emissions formed in drying of biomass such as types of dryers, drying operating conditions (temperature and residence time) and the type of biomass.

Flue gas dryers are based on direct and indirect heating. Emissions from direct and indirect heating consist of terpenes and other non-condensing gases that can be used for combustion,

while the rest are being led into the stack. Water-soluble compounds are also produced and separated as condensates. Steam dryers generally emit condensates, which consist of hydrophilic and lipophilic compounds as listed previously.

The amount and composition of the compounds produced from drying of biomass are greatly influenced by the temperature. In general, the higher the temperature, the higher the amount of emissions produced as illustrated in Figure 8.9. The boiling points of monoterpenes ranged from 150 to 180°C (Fagernäs and Sipilä, 1997). Drying temperatures above 100°C release all of the monoterpene content, fatty and resin acids from wood (Wastney, 1994 in Fagernäs and Sipilä, 1997). At above 150°C, these compounds have significant vapour pressures leading to vapourisation. At above 200°C, thermal degradation of lignocellulosic components of biomass considerably takes place, resulting additional different compound groups.

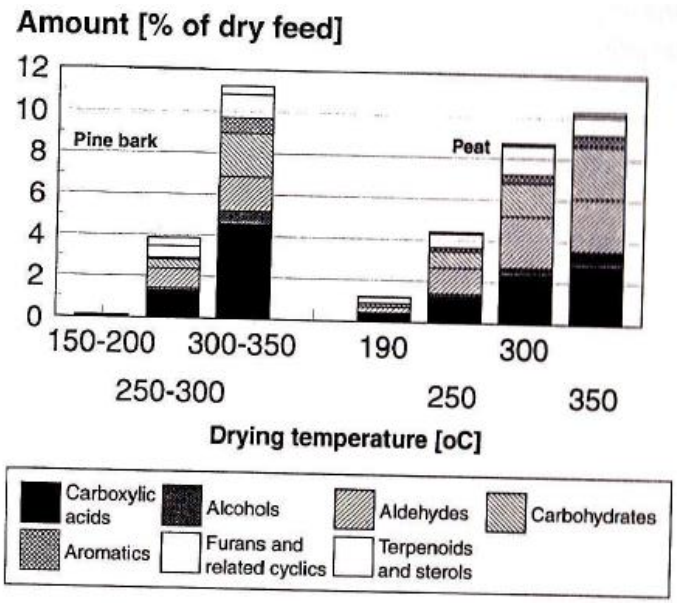

Figure 8.9. Amounts of organic compound groups released from the drying of pine bark and peat in steam dryers (Fagernäs and Sipilä, 1997).

"*Biomass feedstock has a great effect on the emission quality and composition*" but this effect is also highly dependent on the drying temperature (Fagernäs and Sipilä, 1997). The level of condensates produced from drying bark and forest residues is higher than from wood and peat at temperature range 160-200°C (Fagernäs, 1992 in Fagernäs and Sipilä, 1997).

The environmental effects due to biomass drying comprised of organic condensates on natural waters and gaseous emission to the air. The former effect requires the adjustment of

pH and wastewater treatment (Liinanki and Karlsson, 1994 in in Fagernäs and Sipilä, 1997). Blue haze is observed due to discolouration of exhaust gases and it is formed when gases from the exhaust stack of dryers condense to form submicron aerosols in ambient conditions (Wastney, 1994 in in Fagernäs and Sipilä, 1997). Lipids released such as fatty and resin acids have been assumed to contribute to the formation of deposits on the surfaces of peat and bark dryers (Fagernäs, 1992 in Fagernäs and Sipilä, 1997). Moreover, monoterpenes and formaldehyde are strong smelling irritants. Monoterpenes have been found to react with nitrogen oxides and produce ozone in the presence of solar radiation. Some drying produced fumes that are carcinogenic and Kurttio *et al* (1990) discovered that drying spruce and birch at 170C emit mutagenic compounds that are short lived and/or volatile. One of them is 3-carene. Kurttio *et al* (1990) stated that α-pinene and β-pinene are not mutagenic. To reduce the emissions from biomass drying, it is suggested to use lower temperature and reduce the drying time. Furthermore, the gaseous emissions can be minimised by employing steam drying processes or burning the terpenes.

Chapter 6 identified some low molecular weight volatiles/gaseous products evolving during the drying period (carbon dioxide, methanol, water, methane and carbon monoxide). It would be of great interest in future work if VOC can be identified and quantified using the on-line FTIR.

8.10.2.3.2 Torrefaction

Few studies have shown that during torrefaction, a number of volatiles are released after the drying period and they consist of condensable and non-condensable fractions (Prins *et al*., 2006a; Bridgeman *et al*., 2008; Deng *et al*., 2009; Medic *et al*., 2012). Acetic acid and water are the main liquid torrefaction products, while smaller quantities found to be made up of methanol, formic acid, lactic acid, furfural, hydroxyl acetone and traces of phenol (Bergman *et al*, 2005a; Prins *et al*., 2006a).

Prins *et al* (2006a) torrefied willow, beech, larch and straw using a bench scale torrefaction unit and these four fuels were treated as follows. The first two biomass fuels were treated at temperatures in the range of 220-300ºC (with a residence time of 10-60 min). Larch was treated at 230ºC (50 min), 250ºC (30 min), 270ºC (15 min), 290ºC (10 min) and straw at 250ºC (30 min). Thermal decomposition of biomass within torrefaction temperature yields a number of different products. The amount of torrefied solid and volatiles that evolved during

torrefaction depends on the lignocellulosic composition of the biomass fuels. Prins *et al* (2006a) discovered that hardwoods (willow and beech) were found to produce lower solid yields and more volatile yields than softwoods (larch), whereas the results obtained from torrefaction of hardwoods are comparable with those from straw. Prins *et al* (2006a) also observed that the main acid found in the hardwood is acetic acid while that found in the softwood is formic acid. As reported in several literature reviews, hemicellulose experiences the most significant decomposition reactions and it usually starts to decompose at above 200°C. This is basically due to the difference in the hemicellulose composition. The hemicellulose of hardwoods has acetoxy- and methoxy- groups attached to the xylose units and form acetic acid and methanol upon thermal treatment (Prins *et al*., 2006a). The mechanism leading to the production of formic acid is unknown and remains obscure even though it is probably derived from the degradation of hemicellulose (Degroot *et al*., 1988).

Similarly, Bridgeman *et al*'s (2008) torrefaction work for reed canary grass (RCG) at 290°C using TGA-FTIR. In Bridgeman *et al* (2008), the absorbance per mass of the sample detected by the FTIR was recorded and the results can be displayed in Figure 3.25. The figure illustrates the evolution of volatiles during the torrefaction of RCG, starting from the drying period at about 100°C (400 K) to the final temperature, 290°C (563 K). The main gaseous products from the torrefaction of the biomass were carbon dioxide, carbon monoxide and methane. As can be seen in Figure 3.25, carbon dioxide was recorded to have the highest absorbance of IR followed by other organic compounds, namely acetaldehyde, formaldehyde, acetic acid, formic acid, methanol, carbon monoxide and methane.

When volatiles condense, liquids and tars are formed. As described in Section 3.10, Chen *et al* (2011) torrefied Lauan at three temperatures (with residence times of 0.5, 1, 1.5, 2 h). The results showed that the yields of condensed liquid increased with temperature. At 220°C, the weight percentage of condensed liquid was 10-12%. At 250°C, the weight percentage increased from 24-30%, while at 280ºC, the weight percentage increased from 28-46%. These authors have also analysed the composition of condensed liquids of increased torrefaction temperatures, where the heavier components were found to be present at the highest temperature (280°C). Main components contained in the condensed liquid from the torrefaction of Lauan are as listed in Table 8.6. Most of the species were monoaromatics (No. 1-3, 6, 7 and 9). The structures of phenol, eugenol, vanillin and 7,9-dihydroxy-3-methoxy-1-

methyl-6H-dibenzo[b,d]pyran-6-one can be provided in Figure 3.26. The results of the chromatogram were illustrated absorbance against time but no quantification other than that was provided in the paper.

Table 8.6. Composition of condensed liquids upon torrefaction of Lauan (Chen *et al*., 2011).

No.	**Component**
1)	Phenol
2)	2-methoxyphenol
3)	4-methylphenol
4)	2-methoxy-4-methylphenol
5)	4-ethyl-2methoxyphenol
6)	2,6-dimethoxyphenol
7)	2-methoxy-4-prop-2-enylphenol (Eugenol)
8)	2-methoxy-4-propylphenol
9)	4-hydroxy-3-methoxybenzaldehyde (Vanillin)
10)	4-hydroxy-3methoxybenzoic acid
11)	1,2,3,-trimethoxy-5-methylbenzene
12)	2,6-dimethoxy-4-prop-2-enlyphenol
13)	1-(4-hydroxy-3,5-dimethoxyphenyl)ethanone
14)	7,9-dihydroxy-3-methoxy-1-methyl-6H-dibenzo[b,d]pyran-6-one

As can be seen in Figure 1.14, the last stage in torrefaction is cooling, where the process stops and no further mass loss takes place. Most literatures described cooling as lowering the temperature to below 200°C, where it could be assumed that it is just lowering the temperature reading of the furnace. Andritz-ECN technology used a cooling screw technology to cool torrefied material down to temperatures where it is safe enough to handle and store (IEA, 2012a). Unfortunately, not many readings thoroughly explained how they carried out the cooling stage. Moreover, little attention is paid during this stage with respect to evolution of volatiles. Below describes some of the reported cooling techniques.

During the cooling period, the solid product is relatively stable. Therefore, it is assumed that decomposition reactions have slowed down as the temperature decreases. With that said, this period hardly contributes to the decomposition of biomass (Bergman *et al*., 2005a). In other words, any evolution of volatiles is not sourced from the lignocellulose degradation. Bergman

et al (2005a) stated that some evaporation of adsorbed reactions may occur instead but further information to these reactions was not mentioned in their study. In Pursiala pilot plant, water vapour released from drying is allowed to condense and used for cooling torrefied solids. However, the condensing water is acidic (pH 2.7) and may contain dissolved compounds (Nurminen, 2012). Leaching of this water can provide an impact to the environment (adverse and/or benefit).

Another factor that can put into consideration that is outside the torrefaction process is noise pollution. The noise level of the torrefaction pilot plant is found to be not as remarkable as compared to other industrial plants in the area in Pursiala. This is because the duration of the operation is not continuous, where they are operated 16 hours a day.

8.10.2.4 Torrefied biomass materials

The upgraded characteristics of torrefied biomass provide more advantages compared to when it is untreated. However, as mentioned earlier, torrefaction is still under development, where several large pilot scale studies have been constructed or completed using different technologies of torrefaction. In addition to that, information and experience on storage, conveying and handling torrefied biomass in terms of large scale is still limited. IEA (2012b) also addressed that health and security issues for torrefied biomass have just started. Areas of interest are as follows:

i) Fire-related hazards
ii) Self-heating, off-gassing, dust explosions
iii) Mitigation measures and fire fighting
iv) Health concerns
v) Exposure to airborne dust, fungi, moulds
vi) Exposure to off-gassing emissions and oxygen-depleted air
vii) Other risks, including other exposure risks, trauma, etc
viii) Transportation

These issues need to be investigated for permissions to store and trade torrefied biomass fuels. Not all will be discussed in this section due to limited information available.

IEA (2012b) pointed out that transportation of torrefied biomass fuels after torrefaction is not advisable. Torrefied biomass has an attractive feature that is it has improved grindability

behaviour (Bridgeman *et al*., 2010; Arias *et al*., 2008; Chen *et al*., 2011). Unfortunately, because it is brittle and light, transporting and storing it becomes a challenge and costly. Moreover, it can be extremely reactive in the form of powder and prone to explosion in high concentrations (Kleinschmidt, 2011). This has resulted in a fire accident at a torrefaction installation in Amel, Belgium (IEA., 2012a). Therefore, it is suggested that after the milling process, torrefied biomass should be kept inert to avoid spontaneous combustion (Kleinschmidt, 2011). Another caution to take is when the torrefied biomass is still hot and unstable. It has to be cooled before put into storage and expose to air. With regards to outdoor storage and leaching, the concerns are yet to be dealt with and must be well understood (IEA, 2012a).

Torrefied biomass fuels require densification to reduce risks of explosion. The most common techniques are pelletisation and briquetting. Torrefied pellets have better storage properties in comparison to conventional wood pellets (Stelte *et al*., 2012). These pellets contain less moisture due to its improved hydrophobic nature, higher heating value and are less sensitive to moisture uptake and biological degradation. Torrefied pellets also have better grinding properties, at which they can be ground into a dust-like powder with favourable size distribution and spherical particles using conventional coal mills while conventional wood pellets require a hammer mill and higher energy input for grinding (Kleinschmidt, 2011).

Even though they have improved higher heating value, their volumetric energy density is not. Pelletisation becomes more difficult with increased severity of torrefaction (IEA, 2012b). Stelte *et al* (2011) discovered that pellets of different torrefaction conditions have different quality. Their mechanical strength has been reduced and creates more dust formation. High pelletising pressure is required for torrefied spruce due to the lack of water and hemicellulose content. These authors also suggested that it could be due to the removal of extractives as they have been shown to play an important role during the pelletisation process and can act as a lubricant, lowering the friction of the press channel. They found that pellets could not be produced from spruce that was torrefied at 300°C (Figure 8.10). Furthermore, the pellets tend to lengthened upon one month storage as can be seen in spruce torrefied at 250 and 275°C. This is due to the increase lacking of adhesion between the particles. This in effect, requires more energy for pellet compression hence, increases the risk of fires and dust explosion. In addition to that, low pellet strength in torrefied biomass fuels increases the risk for fines and dust formation during handling and transportation (Stelte *et al*., 2013). Several measures have

been suggested to improve the pelletisation of torrefied biomass such as increase moisture content, add lubricant to reduce friction, additives and adjust the temperature and residence time (optimal condition).

Untreated spruce 250°C 275°C 300°C

Figure 8.10. Pellets of spruce and torrefied spruce of increasing temperatures (250, 275 and 300°C) (Stelte *et al*., 2011).

Finally, another potential hazard of torrefied biomass fuels is the increasing ash content, which can cause impacts to the operating systems due to fouling and corrosion. It was already stated that the alkali metal contents of torrefied biomass fuels remains and the disadvantages of such contents can be found in Section 8.10.2.3.

8.10.2.5 Environmental fates of volatiles

Table 8.7 presents a table of environmental fate for some of the identified pollutants that evolved in the torrefaction process. Their environmental fates are based on their reactions when released in water, soil and air. The atmospheric half-life when they react in air is also presented.

Table 8.7. Environmental fate of identified pollutants (Sources: International Programme of Chemical Safety (INCHEM) & PubChem Compounds Database (PUBCHEM)).

Environmental fate					
Name of component	**Exposure limit**	**Reaction in water**	**Reaction in soil**	**Reaction in air**	**Atmospheric half-life**
α-pinene	NA	Likely to adsorb to suspended soils and sediment in water.	Expected to have a slight mobility and may volatilize from dry soil and surfaces.	Vapour phase α-pinene will be degraded in the air by reaction with photochemically-produced hydroxyl radicals. Vapour phase α-pinene will also be degraded upon reaction with ozone (40 min).	7 h
β-pinene	NA	Likely to adsorb to suspended soils and sediment in water.	Expected to have a slight mobility and may volatilize from dry soil and surfaces.	Vapour phase β-pinene will be degraded in the air by reaction with photochemically-produced hydroxyl radicals. Vapour phase β -pinene will also be degraded upon reaction with ozone (23 h).	4.9 h
Hexanal	NA	Likely to adsorb to suspended soils and sediment in water.	Moderate mobility when released to soil.	Degraded with photochemically produced hydroxyl radicals.	13 h
Phenol	250 ppm	It is expected to adsorb to suspended soils and sediment in water.	It is not expected to volatilize from dry soil and surfaces. Its degradation will be completed in 2-5 days.	Degraded by photochemical reactions to dihydroxybenzenes, nitrophenols and ring cleavage.	14 h

Table 8.7. *Continued*

Hexanoic acid	NA	It is not expected to adsorb to suspended soils and sediment in water.	It is expected to have a very high mobility in soil. It is not expected to volatilize from dry soil and surfaces.	Degraded with photochemically produced hydroxyl radicals.	3 days
Furfural	100 ppm	It is not expected to adsorb to suspended soils and sediment in water.	It is expected to have a very high mobility in soil and may volatilize from dry soil.	Degraded with photochemically produced hydroxyl radicals.	5.5 h
Piperazine	NA	It is not expected to adsorb to suspended soils and sediment in water.	It is not expected to volatilize from dry soil and surfaces. It may biodegrade in soil.	Degraded with photochemically produced hydroxyl radicals.	2.3 h
Pentanol	NA	It is not expected to adsorb to suspended soils and sediment in water.	It may volatilize from dry soil and surface.	Degraded with photochemically produced hydroxyl radicals.	2 days
Acetaldehyde	2000 ppm	It is not expected to adsorb to suspended soils and sediment in water. Volatilize rapidly and rapidly undergoes microbial degradation.	It has a very high mobility.	Reacts with OH radicals, NO_3 and NO_2. It also reacts with ozone and absorbs UV.	10-60 h
Acetic acid	50 ppm	It is not expected to adsorb to suspended soils and sediment in water.	It has a very high to moderate mobility. It may volatilize from dry soil and surfaces.	Degraded with photochemically produced hydroxyl radicals.	22 days

Table 8.7. *Continued*

Methanol	6000 ppm	It is not expected to adsorb to suspended soils and sediment in water.	It is expected to have a very high to moderate mobility. It may also volatilize from dry soil.	Readily degraded in the environment by photo-oxidation and biodegradation processes.	7-18 days
Formaldehyde	20 ppm	It is not expected to adsorb to suspended soils and sediment in water.	It is expected to have a very high mobility and volatilizes from dry soil surfaces. It readily biodegrades under both aerobic and anaerobic conditions.	Degraded with photochemically produced hydroxyl radicals. It absorbs UV radiation and is susceptible to direct photolysis. It has a half-life of 6 h in simulated sunlight.	41 h
Acetone	2500 ppm	It is not expected to adsorb to suspended soils and sediment in water.	Volatilization from dry and moist soil surfaces is expected.	Degraded with photochemically produced hydroxyl radicals. It also undergoes photodecomposition by sunlight (80 days).	79 days.
Formic acid	30 ppm	It is not expected to adsorb to suspended soils and sediment in water.	It may volatilize from dry soil surfaces.	Degraded with photochemically produced hydroxyl radicals.	36 days
Ethane	NA	It is not expected to adsorb to suspended soils and sediment in water.	It has a moderate mobility and will volatilize from dry soil surfaces.	Degraded with photochemically produced hydroxyl radicals.	50-70 days

8.10.2.6 Environmental risk assessment and its mitigation measures as well as alternative options

The identification of emission and its source as well as their impacts are based on Pursiala torrefaction pilot plant (Nurminen, 2012). This can act as a guideline for assessing the environmental risks of other existing torrefaction plants (Table 8.8 and 8.9). Table 8.8 also presents additional information of the risks that may affect the human health. Environmental risks identified from other literatures based on exploratory studies are also taken into consideration and listed in the table. Environmental risks are classified according to the probability to expose the sources and consequences.

In general, the risks of identified hazards in Table 8.8 and 8.9 show that there are mostly medium or low risks. Pursiala power plant is small, so the loads of material are relatively low. Nurminen (2012) reported that there are no hazardous materials handled in the process. The main concerns of environmental risks are due to dusts and emission of malodorous gases. If the operation is not well-monitored and controlled, ignition or even explosion may occur. Technical risks and human errors can be avoided by applying security systems and practicing proper training for the workers and develop better communications with one another. If the system is automated, any worst possible scenario can cause it to shut down automatically.

A valuable method in planning a risk assessment is to involve stakeholders and public. The most effective way is to use small discussion groups of 10-20 people. However, during the course of developing the environmental impact assessment for this chapter, this participatory risk assessment is not carried out in this thesis.

8.11 Conclusion

Environmental impact assessment (EIA) of torrefaction of biomass fuels has not been widely. Torrefaction of biomass fuels is still under development that some information has limited access and kept confidential. Scoping as the most critical stage in an EIA process, is the main subject discussed in this chapter. It involves the identification of environmental impacts of the raw materials, torrefaction plant, torrefaction process and products of torrefaction. The identification of impacts from torrefaction plant is mainly reviewed based on a study by Nurminen (2012), who have examined two torrefaction plants in Pursiala and Risolog in Finland, while impacts of torrefaction process and products of torrefaction are based from

exploratory studies and reviews. Data on mitigation measures is currently not available and the information listed in this chapter is just recommendations and open for alterations. This can only be affirmed when the information is readily accessed from torrefaction developers/suppliers.

Table 8.8. Identification of impact (health and environmental) of torrefaction process according to activity associated with the plant.

Zones	**Hazards and their sources**	**Environmental/Health impacts**	**Probability**	**Consequences**	**Mitigation/Measures, where necessary**
Drying	Release of VOC (as identified in Table 8.5) from drying of softwood (Samuelsson *et al*., 2006).	The environmental fates of the listed VOC can be listed in Table 8.7.	Low	Medium	Use lower drying temperatures and reduce the drying time.
	Release of terpenes (Rupar and Sanati, 2005).		Low	Medium	Gaseous emissions can be minimised by employing steam drying processes and burn terpenes as suggested by Kurttio *et al* (1990).
	Fatty and resin acids from biomass fuels that contain high lipid contents (Fagernäs, 1992 in Fagernäs and Sipilä).	May lead to the formation of deposits on the surface of peat and bark dryers.	Low	Low	
	Seasons, for example winter (Nurminen, 2012).	Ignition, increased energy demand.	Medium	Low	If the raw material is frozen, more energy will be required in the drying phase.
Torrefaction	Air leakage to torrefaction chamber	Hot gases may react with air instantaneously and can	Low	High	Careful monitoring of any leakage using a

		lead to ignition or even explosion.			computerised system that can detect any gas leakage in and out of the chamber.
	Release/leakage of permanent gas, carbon monoxide.	Carbon monoxide is odourless and can harm the human health by inhalation. It competes with oxygen upon breathing. Body cannot receive enough oxygen and upon long storage, can cause shortage of breath and death.	Low	Low	Provide sensors that can detect presence of carbon monoxide.
	Release of heavier organic condensables upon severe torrefaction condition (Chen *et al*., 2011).	Vapours of heavier organic condensables can accumulate along the lining of air passage. May cause blockage. Difficulty in breathing.	Low	Low	Provide proper condensation of condensables or filters.
	Torrefied biomass is brittle.	It is reactive in the form of powder and prone to explosion in high concentrations (Kleinschmidt, 2011).	Medium	High	Pelletisation of powdered torrefied biomass.
	If the torrefied biomass is still hot, it is unstable.	Fire-related hazards.	Medium	High	Torrefied biomass has to be cooled before it can be

					stored.
	Storage of torrefied biomass.	Self-heating	Low	High	Long term storage of biomass is well-known to lead to microbial respiration and hence, self-heating but no information is available for storage of torrefied biomass.
	Exposure to airborne dusts.	Inhalation, ingestion and eye-soreness can be the potential pathways as to how dusts can affect the human health.	Medium	High	Proper ventilation.
Cooling	Water vapour released from drying is allowed for cooling torrefied fuels.	The pH of the condensing water is acidic (pH 2.7) and may contain dissolved compounds (Nurminen, 2012).	Low	Low	Proper pipeline may be required to avoid leaching, provided that if it is harmful to the environment.
Other operations	Noise	This may affect those people who live nearby the industrial plant.	Low	Medium	The duration of operation is not continuous. For example, the plant in Pursiala is operated 16 hours a day (Numinen, 2012).

Table 8.9. Environmental risks based on Nurminen (2012) and suggested mitigation measures.

Hazard and its source	**Environmental impacts**	**Probability**	**Consequences**	**Remarks/Mitigation**, where necessary
Materials release from wood chips upon truck unloading	Dusting	Medium	Very low	The amount of dust should be moderate. However, workers are required to use dust masks and goggles to avoid inhalation, ingestion and irritation to the eyes.
Leakage of natural gas due to pipeline breakage, joints	Release of natural gas to the atmosphere	Low	Low	Gas will not explode and fades away quickly when released (Nurminen, 2012). Careful checking for any breakage and proper maintenance of pipelines and joints.
Leakage of additives from pelletisation process	The additives used are either low toxic or non-toxic	Low	Low	Careful monitoring of any leakage.
Leakage of machinery oil	Spillage may seeps into the ground and further affects the drainage system	Low	Low	Careful monitoring of any leakage.
Air leakage to torrefaction chamber	Hot gases may react with air instantaneously and can lead to ignition or even explosion.	Low	High	Careful monitoring of any leakage using a computerised system that can detect any gas leakage in and out of the chamber.
Problems in filtration system of air	Dusting may cause problems to respiratory tract through inhalation. Release of malodorous air that can affect workers and local communities.	Low	High	Proper maintenance of the filtration system.

Table 8.9. *Continued*

Leaching of water; Access of rain water to torrefied materials in outdoor storage	May alter chemical properties of the materials	Low	Medium	Proper storages and coverage where torrefied materials are protected from any access of water.
Lacks in system control; Uncontrolled process in torrefaction chamber; Too high temperature	Ignition or even explosion	Low	High	If it was a technical fault, a proper maintenance and careful monitoring are required. Security system to control the temperature is necessary. For example, torrefaction can shut down automatically once the system detects temperature that is beyond what is desired for torrefaction (Nurminen, 2012).
Incomplete combustion	CO and malodorous gas emission	Low	Low	Some pilot plants include combustion as part of the units after torrefaction. It is important to ensure that there is a sufficient mixing of the biomass fuels and air to prevent incomplete combustion.
Human errors in operating torrefaction; Errors in communication	Almost any kind of hazard from dusting to explosion	Low	High	Provide adequate training and efficient ways to share information (Nurminen, 2012).
Maintenance of work; Opening of torrefaction chamber	Dusting; Release of odours	Low	Low	Maintenance should be done in suitable weather conditions (Nurminen, 2012).

Table 8.9. *Continued*

Torrefied wood pellets	Odours release	Medium	Low	
NO_x	Can lead to ozone formation	High	Low	Adopt low NO_x technology
SO_2	Can lead to acid rain	Very low	Medium	Wood contains either low or no sulphur. Therefore the emissions of SO_2 is present is minimal.
Leakage of tars	Tars can cause clogging to the operating system. It produces odours that can be harmful. If torrefaction is operated at the field, tars may seep to the ground and affects the drainage system.	Medium	Medium	Proper maintenance of the operating system is required.
Seasons (heating up or freezing the raw material)	Ignition; Increased energy demand	Medium	Low	If the raw material is frozen, more energy will be required in drying phase.
Storms and floods	Dusting, whirling of the material. Water may seeps into the soil and carries with it any waste at the torrefaction plant and affects the soil and surface water.	Very low	Medium	Proper drainage system will be required.
Vandalism	Almost any kind of hazard from dusting to explosion	Low	Medium	Sufficient security system is recommended. The place needs to have a well-controlled access to minimize any possibilities of vandalism.
Foreign materials (rocks) in raw materials	Uncontrolled torrefaction process Ignition or even explosion	Low	Medium	Rocks can damage the equipment. Materials must be well-filtered.

CHAPTER 9

SUMMARY OF CONCLUSIONS AND DISCUSSION OF FURTHER WORK

9.1 Introduction

This thesis has covered various objectives that were aimed at investigating the fundamentals of torrefaction and its environmental impacts. Solid characterisation of torrefied biomass fuels was studied in depth, and optimisation of the process for the investigated fuels was determined. This thesis also looked into the influence of particle sizes on torrefaction and compared experimental results to those predicted by the FG-Biomass model. This thesis also provides a short investigation on the behaviour of torrefied biomass fuels in combustion. Finally, an environmental impact assessment of torrefaction of biomass fuels was reviewed, where several areas of interests were considered such as the raw materials, torrefaction plant, processes involved in the torrefaction plant, the products of torrefaction and their environmental fates. Towards the end of this chapter the potential areas that require attention for further work are discussed.

9.2 Torrefaction studies and an investigation of the properties and characterisation of products of torrefaction

To get a better insight of the chemistry of torrefied biomass fuels, their physicochemical characterisations were investigated. The standard fuel analysis showed that there were significant changes in these fuels, where the contents exhibited improvements in comparison to when they were still untreated. Grindability tests were conducted for optimisation of torrefaction and the results demonstrated that optimisation depends on the type of fuel, where in this case, lower temperature (270°C) with a shorter residence time (30 min). This is the condition where the overall energy yield was at its highest (above 80%) with reasonable a mass yield (~70-80%). Further investigation was made for torrefied biomass fuels where spectroscopy and microscopy were utilised. Observations revealed that there were obvious alterations in the structures of the biomass after torrefaction. SEM presented images of torrefied biomass that looked flaky and fragile and these changes became clearer when treated with a more severe condition (condition C). When it was untreated, the biomass looked compact and fibrous. FTIR and XPS proved that there were loss of hydroxyl groups

and an increase in the C=O groups relative to C-O groups. Finally, components of tars were identified, where they were mainly composed of monoaromatics and heavier compounds were found to be present at condition C.

9.3 The investigation of the influence of particle sizes on products from torrefaction of biomass

Larger volumes of willow (*Salix spp.*) and eucalyptus (*Eucalyptus Gunnii*) of particle sizes ≥ 5 mm were studied for torrefaction using a TGA coupled to an FTIR. This part of the thesis was aimed to analyse the evolution behaviour of volatiles of different particle sizes of biomass and to compare the findings with those predicted by FG-Biomass software. Results from the TGA-FTIR showed that there was a significant trend in terms of yields of products, where the larger the volume, the greater the solid yield and the lesser the yields of volatiles. These changes were in line with those observed in the software. Heat transfer limitations in larger biomass fuels were concluded to be the main factor. 14 species (H_2O, CO_2, CO, CH_4, CH_3OH, acetaldehyde, formaldehyde, acetone, acetic acid, formic acid and small amounts of ethane, furfural, phenol and ammonia) were identified. Overall mass balances of torrefaction obtained from reactor, TGA and FG-Biomass were compared and the results showed that TGA and especially the reactor lead to a greater mass loss and yields of permanent gases and condensables were observed to be more than predicted. The existence of temperature gradient in large particles promotes interest in the torrefaction studies.FG-Biomass model was again utilised to determine this phenomenon with the aid of another program, Sphere. The results showed the presence of an increase in the gradual temperature distribution with increased particle sizes. This indicates the presence of heat transfer limitations and hence, affecting the rate of torrefaction in big-sized particles. Therefore, the understanding of such limitations is very important for the future utilisation of biomass fuels in industrial sectors.

9.4 The study of a single particle combustion of willow (*Salix spp.*) and eucalyptus (*E.Gunnii*)

Combustion behaviours of raw and torrefied willow and eucalyptus were examined in a methane air flame using a high speed camera. The observations showed that torrefaction has changed the combustion properties of biomass. Torrefied willow samples have improved ignition delay due to their lower moisture content than the raw willow but the results could not be observed in eucalyptus samples. Moreover, even though this study shows that

torrefaction seemed to not affect the duration of volatile combustion, it produced significant changes to the duration of char combustion, where the time taken is longer in comparison to the raw materials. This could be due to their increasing fixed carbon content as a result of torrefaction. These behavioural changes were more pronouncedly observed in eucalyptus samples of increasing severity of treatment than in willow. With regards to the type of biomass' response to combustion behaviour, lignocellulose composition may have an impact to such changes in the durations of volatile and char combustion. Rate of devolatisation and char combustion were also investigated. FG-Biomass model was used to simulate pyrolysis of raw willow and eucalyptus and the results are compared with the duration of volatile combustion obtained experimentally in order to estimate the heating rate experienced by the particles in the Meker burner. The results showed that the approximate heating rate was 100-200 K s^{-1}. The rate of char combustion of torrefied willow was obtained using the parameters determined in Jones *et al* (2012), as 0.636 s^{-1} when the oxygen content used in the present study was taken into consideration. Plots of the conversion factor with time for both rate constants were illustrated and gave a maximum predicted burnout time of 4.7 s for 95% burnout. Since the actual burnout durations were in the range of 30-65 s, diffusion appears to also contribute to the char combustion rate, that is, the combustion is taking place in zone II.

9.5 Environmental impact assessment of torrefaction of biomass

Health and safety concerns with regards to torrefaction were not well-assessed yet. Torrefaction of biomass fuels is still under development that some information has limited access and kept confidential. This chapter provides a preliminary study of its environmental impact assessment. Scoping as the most critical stage in an EIA process, is the main subject discussed in this chapter. It involves the identification of environmental impacts of the raw materials, torrefaction plant, torrefaction process and products of torrefaction. The identification of impacts from torrefaction plant is mainly reviewed based on a study by Nurminen (2012), who have examined two torrefaction plants in Pursiala and Risolog in Finland, while impacts of torrefaction process and products of torrefaction were based from exploratory studies and reviews. Data on mitigation measures is currently not available and the information listed in this chapter is just recommendations and open for alterations. This can only be affirmed when the information is readily accessed from torrefaction developers/suppliers. Finally, all information is gathered to form an environmental risk assessment that can be used as a guideline for future use.

9.6 Future work

9.6.1 Torrefaction studies and an investigation of properties and characteristics of products of torrefaction

Overall mass balances of torrefaction of willow, a mixture of softwoods and a mixture of hardwoods were the only ones that were carried out in this study. Future work can include that of eucalyptus to allow more comparisons. It would be more interesting if the particle sizes of all the biomass fuels were similar especially eucalyptus. In this study, the particle size of eucalyptus was the smallest in comparison to the other fuels and the outcomes upon torrefaction treatment showed that this parameter plays an important role in the process. Furthermore, more characterisation for all of the biomass fuels could have been made apart from just willow and eucalyptus.

There were leakages and loss of liquids during torrefaction especially those obtained from severe condition (C). Therefore, it is worthwhile to have a proper design for collecting such products as the volumes are important for further analysis. Viscosity tests could have been made if the volume was enough. It requires at least 5 mL of tar in order to conduct the experiment. Tar analysis was only limited to Karl Fischer titration, TOC and liquid-GC-MS. Few literatures only focused on identifying the components of tars and deeper characterisation of such product could be interesting especially when it comes to assessing its impact to the environment.

Gases were detected using the GC-MS chromatography but the data were not available. Careful collection of permanent gases using the chromatography needs to be re-visited for future work.

9.6.2 The investigation of the influence of particle sizes on products from torrefaction of biomass

The FTIR was only calibrated for water vapour, carbon dioxide and carbon monoxide. Further calibrations of the FTIR for more volatiles can be suggested for further work. Apart from that, it was stated that Biot and Pyrolysis numbers are parameters that could influence the torrefaction process. It would be of great interest if these parameters could be determined for this study. Samples of investigations were only on hardwoods. More sample variations would be interesting in order to get better insights of the influence of particle sizes in terms of types of biomass fuels. This study used sample sizes that were greater than 5 mm that

comprised of cubes and cuboids. Torrefaction of smaller than 5 mm (> 1 mm) could be considered for future work in order to see if there is a limiting factor as to where temperature gradients inside the biomass become no longer important.

9.6.3 The study of a single particle combustion of willow (*Salix spp.*) and eucalyptus (*E.Gunnii*)

This chapter deals with a preliminary work for combustion studies of torrefied biomass fuels. This chapter has the potential to be further developed extensively. Future work can include drop tube furnace, looking at the char combustion rate, surface area development, where SEM images of such chars could be of interest to examine.

9.6.4 Environmental impact assessment of torrefaction of biomass

Potential environmental impacts are identified that covers those involve raw materials, torrefaction plant, processes associate with torrefaction as well as hazards of torrefied biomass fuels and environmental fates of emissions (volatiles). Torrefaction is still under development, where demonstration plants are in operation and construction of plants for commercial is not readily available to provide the required information to set an environmental impact assessment. In developing an EIA, it is important to be aware of the factors that affect the level of the risks in terms of engineering (processes, operation), natural and human activities. Obviously, the EIA of torrefaction of biomass fuels requires a collection of more definite data especially those that come from torrefaction developers and suppliers. When they are accessible, this EIA can be developed further in collaboration with other interested parties as earlier mentioned in the overview of the EIA process. A standardised EIA for such pre-treatment process can be established and act as a guideline for future biomass-based power plants.

REFERENCES

2020 SITE. 2012. All About Trees including Palm Trees, Oak Trees, Pines, Willows, Maples and more. [online]. [Accessed 16/1/13]. Available from: http://www.2020site.org/trees/

AGUS, F. and P.L. WATERS. 1971. Determination of the grindability of coal, shale and other minerals by a modified Hardgrove machine method. *Fuel*, **50**(4), pp.405-431.

AHO, A., N. KUMAR, K. ERANEN, B. HOLMBOM, M. HUPA, T. SALMI and D.Y. MURZIN. 2008. Pyrolysis of softwood carbohydrates in a fluidized bed reactor. *International Journal of Molecular Science*, **9**(9), pp.1665-1675.

AILE. 2007. Purification function of short rotation willow coppice. [online]. [Accessed 17/4/13]. Available from: http://ec.europa.eu/environment/life/project/Projects/index.cfm?fuseaction=home.showFile&rep=file&fil=LIFE04ENVFR320_PurificationFonctionofSRC.pdf

ALMEIDA, G., J.O. BRITO and P. PERRE. 2010. Alterations in energy properties of eucalyptus wood and bark subjected to torrefaction: The potential of mass loss as a synthetic indicator. *Bioresource Technology*, **101**(24), pp.9778–9784.

ANDERSSON and LINDVALL. n.d. Use of biomass from reed canary grass (*Phalaris arundinacea*) as raw material for production of paper pulp and fuel. [online].[Accessed 12/4/13]. Available from: http://www.internationalgrasslands.org/files/igc/publications/1997/1-03-003.pdf

ARIAS, B., C. PEVIDA, J. FERMOSA, M.G. PLAZA, F. RUBIERA and J.J. PIS. 2008. Influence of torrefaction on the grindability and reactivity of woody biomass. *Fuel Processing Technology*, **89**(2), pp.169-175.

ARES, E. 2012a. The renewables obligation. [online]. [Accessed 21/4/13]. Available from: http://www.parliament.uk/briefing-papers/SN05870

ARES, E. 2012b. Feed-in tariffs. [online]. [Accessed 21/4/13]. Available from: www.parliament.uk/briefing-papers/SN06200.pdf

ARES, E. 2013. Biomass. [online]. [Accessed 26/9/13]. Available from: www.parliament.uk

AYLÓN. E., M.S. CALLÉN, J.M. LÓPEZ, ANA MARÍA MASTRA, R. MURILLO, M.V. NAVARRO and SLAWOMIR STELMACH. 2005. Assessment of tire devolatization kinetics. *Journal of Analytical and Applied Pyrolysis*, **74**(1-2), pp.259-264.

BAHNG, M-K., B.S. DONOHOE and M.R. NIMLOS. 2011. Application of an Fourier Transform-Infrared imaging tool for measuring temperature or reaction profiles in pyrolysed wood. *Energy and Fuels*, **25**, pp.370-378.

BASU, P. 2013. *Biomass gasification, pyrolysis and torrefaction: Practical design and theory*. 2nd ed. London: Elsevier.

BATES, R.B. and A.F. GHONIEM. 2012. Biomass torrefaction: Modeling of volatile and solid product evolution kinetics. *Bioresource Technology*, **124**, pp.460-469.

BASU, P., R. SHAILENDRA and A. DHUNGHANA. 2013. An investigation into the effect of biomass particle size on its torrefaction. The Canadian Journal of Chemical Engineering, **91**(3), pp. 466-474.

BAUEN, A., G. BERNES, M. JUNGINGER, M. LONDO and R. VUILLE. (2009). Bioenergy – A sustainable and reliable energy source: A review of status and prospects. [online]. [Accessed 06/09/13]. Available from: http://www.globalbioenergy.org/uploads/media/0912_IEA_Bioenergy_-_MAIN_REPORT_-_Bioenergy_-_a_sustainable_and_reliable_energy_source._A_review_of_status_and_prospects.pdf

BAXTER, L.L., T.R. MILES, T.R. MILES JR, B.M. JENKINS, T. MILNE, D. DAYTON, R.W. BRYERS and L.L. ODEN. 1998. The behaviour of inorganic material in biomass-fired power boilers: field and laboratory experiences. *Fuel Processing Technology*, **54**(1-3), pp.47-78.

BEAUMONT, O. and Y. SCHWOB. 1984. Influence of physical and chemical parameters on wood pyrolysis, *Industrial and Engineering Chemistry Process Design and Development*, **23**(4), pp.637-641.

BERGMAN, P.C.A. 2005. *Combined torrefaction and pelletisation: The TOP process*. The Netherlands: Petten.

BERGMAN, P.C.A., A.R. BOERSMA, R.W.R. ZWART and J.H.A. KIEL. 2005a. *Torrefaction for biomass co-firing in existing coal-fired power stations: "Biocoal"*. The Netherlands: Petten.

BERGMAN, P.C.A., A.R. BOERSMA, J.H.A. KIEL, M.J. PRINS, K.J. PTASINKI and F.J.J.G. JANSSEN. 2005b *Torrefaction for entrained-flow gasification of biomass*. The Netherlands: Petten.

BIOMASS ENERGY CENTRE (BEC). 2007a. Planting and growing miscanthus. [online]. [Accessed 15/10/10]. Available from: http://www.biomassenergycentre.org.uk/pls/portal/docs/PAGE/BEC_TECHNICAL/SOURCES%20OF%20BIOMASS/ENERGY%20CROPS/GRASSES%20AND%20NON-WOODY%20ENERGY%20CROPS/MISCANTHUS/MISCANTHUS-GUIDE.PDF

BIOMASS ENERGY CENTRE (BEC). 2007b. Information sheet 3: Short rotation coppice. [online]. [Accessed 12/4/13]. Available from: http://www.biomassenergycentre.org.uk/pls/portal/docs/PAGE/RESOURCES/REF_LIB_RES/PUBLICATIONS/3.%20SRC%20V5%209-2009.PDF

BIRD, N., A. COWIE, F. CHERUBINI and G. JUNGMEIER. 2011. Using a life cycle assessment approach to estimate the net greenhouse gas emissions of bioenergy. [online]. [Assessed 04/09/13]. Available from:

http://www.globalbioenergy.org/uploads/media/1110_IEA_Bioenergy_-_Using_a_LCA_approach_to_estimate_the_net_GHG_emissions_of_bioenergy.pdf

BLAGINI, E., F. BARONTINI and L. TOGNOTTI. 2006. Devolatilization of Biomass Fuels and Biomass Components Studied by TG/FTIR Technique. *Industrial and Engineering Chemistry Research*, **45**(13), pp.4486-4493.

BORMAN, G.L. and K.W. RAGLAND. 1998. *Combustion engineering*. New York: McGraw-Hill.

BOURGOIS, J. and R. GUYONNET. 1988. Characterisation and analysis of torrefied wood. *Wood Science Technology*, **22**(2), pp.143–155.

BP STATISTICAL REVIEW OF WORLD ENERGY. 2013. [online]. [Accessed 26/9/13]. Available from: www.bp.com/content/dam/bp/pdf/statistical-review/statistical_review_of_world_energy_2013.pdf

BRADLEY, R.H., X. LING and I. SUTHERLAND. 1993. An investigation of carbon fibre surface chemistry and reactivity based on XPS and surface free energy. *Carbon*, **31**(7), pp.1115-1120.

BRETT, C. and K. WALDRON. 1996. *Physiology and Biochemistry of Plant Cell Walls. Topics in Plant Functional Biology*. London: Chapman and Hall.

BRIDGEMAN, T.G., L.I. DARVELL, J.M. JONES, P.T. WILLIAMS, R. FAHMI, A.V. BRIDGWATER, T. BARRACLOUGH, I. SHIELD, N. YATES, S.C. THAIN and I.S. DONNISON. 2007. Influence of particle size on the analytical and chemical properties of two energy crops. *Fuel*, **3**(9), pp.60–72.

BRIDGEMAN, T.G., J.M. JONES, I. SHIELD and P.T. WILLIAMS. 2008. Torrefaction of reed canary grass, wheat straw and willow to enhance solid fuel qualities and combustion properties. *Fuel*, **87**(6), pp.844-856.

BRIDGEMAN, T.G., J.M.JONES, A.WILLIAMS and D.J.WALDRON. 2010. An investigation of the grindability of two torrefied energy crops. *Fuel*, **89**(12), pp.3911–3918.

BRIDGWATER, A.V., D.C. ELLIOT, L. FAGERNAS, J.S. GIFFORD, K.I. MACKIF and A.J. TOFT. 1995. The nature and control of solid, liquid and gaseous emissions from the thermochemical processing of biomass. *Biomass and Bioenergy*, **9**(1-5), pp.325-341.

BROWN, R.C. 2003. *Biorenewable resources: Engineering new products from agriculture*. Iowa: Iowa State Press.

CALAHORRO, C.V., V. GÓMEZ SERRANO, J. HERNÁNDEZ ALVARO and A. BERNALTE GARCÍA. 1992. The use of waste matter after olive grove pruning for the preparation of charcoal. The influence of the type of matter, particle size and pyrolysis temperature. *Bioresource Technology*, **40**(1), pp.17-22.

CASLIN, B., J. FINNAN and A. McCRACKEN. 2011. Short rotation coppice willow: Best practice guidelines. [online]. [Accessed 17/4/13]. Available from: http://www.afbini.gov.uk/willowbestpractice.pdf

CHEN, W-H., H-C. HSU, K-M. LU, W-J. LEE and T-C. LIN. 2011. Thermal pretreatment of wood (Lauan) block by torrefaction and its influence on the properties of the biomass. *Energy*, **36**(5), pp.3012-3021.

CHEN, W-H. and P-C, KUO. 2011. Torrefaction and co-torrefaction characterization of hemicellulose, cellulose and lignin as well as torrefaction of some basic constituents in biomass. *Energy*, **36**(2), pp.803-811.

COMMISSION OF THE EUROPEAN COMMUNITIES (CEC). 2008. Proposal for a Directive of the European Parliament and of the Council. [online]. [Accessed 25/01/12]. Available from: http://ec.europa.eu/energy/climate_actions/doc/2008_res_directive_en.pdf

DAVID, K. and A.J. RAGAUKAS. 2010. Switchgrass as an energy crop for biofuel production: A review of its lingo-cellulosic chemical properties. *Energy and Environmental Science*, **3**(9), pp.1182–1190.

DAVIDSSON, K.O., L.E. AMAND, B. LECKNER, B. KOVACEVIK, M. SVANE, M. HAGSTROM, J.B.C. PETTERSSON, J. PETTERSSON, H. ASTEMAN, J.E. SVENSSON and L.G. JOHANSSON. 2007. Potassium, chlorine and sulphur in ash, particles, deposits and corrosion during wood combustion in a circulating fluidized-bed boiler. *Energy and Fuels*, **21**(1), pp.71–81.

DAWSON, M. 2007. Short rotation coppice willow: Best practice guidelines. [online]. [Accessed 11/4/13]. Available from: http://www.afbini.gov.uk/willowbestpractice.pdf

DAYTON, D.C., B.M. JENKINS, S.Q. TURN, R.R. BAKKER, R.B. WILLIAMS, D. BELLE-OUDRY and L.M. HILL. 1999. Release of inorganic constituents from leached biomass during thermal conversion. *Energy and Fuels*, **13**(4), pp.860-870.

DD CENT/TS 14774-2:2004; Solid biofuels. Method for the determination of moisture content – Oven dry method. Part 2: Total moisture content – Simplified method. 2004, British Standards, p. 6.

DD CENT/TS 14775:2004; Solid Biofuels. Method for the determination of ash content. 2004, British Standards, p.12.

DD CENT/TS 15148:2005; Solid biofuels. Method for the determination of volatile matter . 2005, British Standards, p.9.

DE JONG, W., A. PINONE and M.A. WÓJTOWICZ. 2003. Pyrolysis of Miscanthus Giganteus and wood pellets: TG-FTIR analysis and reaction kinetics. *Fuel*, **82**(9), pp.1139-1147.

DEGROOT, W.F., W-P. PAN, M.D. RAHMAN and G.N. RICHARDS. 1988. First chemical events in pyrolysis of wood. *Journal of Analytical and Applied Pyrolysis*, **13**(3), pp.221.231.

DEMIRBAS, A. 2004. Effects of temperature and particle size on bio-char yield from pyrolysis of agricultural residues. *Journal of Analytical and Applied Pyrolysis*, **72**(2), pp.243-248.

DEMIRBAS, A. 2005. Potential applications of renewable energy sources, biomass combustion problems in boiler power systems and combustion related environmental issues. *Progress in Energy and Combustion Science*, **31**(2), pp.171-192.

DENG, J., G-J. WANG, J-H. KUANG, Y-L. ZHANG and Y-H. LUI. 2009. Pre-treatment of agricultural residues for co-gasification via torrefaction. *Journal of Analytical and Applied Pyrolysis*, **86**(2), pp.331-337.

DENG, L., T. ZHANG and D. CHE. 2013. Effect of water washing on fuel properties, pyrolysis and combustion characteristics and ash fusibility of biomass. *Fuel Processing Technology*, **106**, pp.712-720.

DENG, L. and CHE, D. 2012. Chemical, electrochemical and spectral characterization of water leachates from biomass. *Industrial and Engineering Chemistry Research*, **51**(48), pp.15710-15719.

DEPARTMENT OF ENERGY AND CLIMATE CHANGE (DECC) 2009. The UK Renewable Energy Strategy. [online]. [Accessed 8/10/12]. Available from: http://www.decc.gov.uk/en/content/cms/meeting_energy/bioenergy/strategy/strategy.aspx#

DEPARTMENT OF ENERGY AND CLIMATE CHANGE (DECC) 2011. Renewable heat incentive. [online]. [Accessed 25/1/12]. Available from: https://www.gov.uk/government/uploads/system/uploads/attachment_data/file/48041/1387-renewable-heat-incentive.pdf

DEPARTMENT OF ENERGY AND CLIMATE CHANGE (DECC) 2012. Biomass electricity and combined heat and power plants – ensuring sustainability and affordability. [online]. [Accessed 27/9/13]. Available from: https://www.gov.uk/government/uploads/system/uploads/attachment_data/file/66519/6339-consultation-on-biomass-electricity--combined-heat.pdf

DEPARTMENT OF ENERGY AND CLIMATE CHANGE (DECC) 2013a. UK Energy in Brief 2013. [online]. [Accessed 26/9/13]. Available from: https://www.gov.uk/government/uploads/system/uploads/attachment_data/file/224130/uk_energy_in_brief_2013.PDF

DEPARTMENT OF ENERGY AND CLIMATE CHANGE (DECC) 2013b. New biomass sustainability criteria to provide certainty for investors to 2027. [online]. [Accessed 25/9/13]. Available from: https://www.gov.uk/government/news/new-biomass-sustainability-criteria-to-provide-certainty-for-investors-to-2027

DEPARTMENT FOR ENVIRONMENT FOOD AND RURAL AFFAIRS (DEFRA). 2003. Energy White Paper: Our energy future – creating a low carbon economy. [online]. [Accessed 06/05/11]. Available from: http://webarchive.nationalarchives.gov.uk/20121217150421/http://decc.gov.uk/assets/decc/publications/white_paper_03/file10719.pdf

DEPARTMENT FOR ENVIRONMENT, FOOD AND RURAL AFFAIRS (DEFRA). 2005. Biomass task force: Report to government. [online]. [Accessed 3/12/12]. Available from: http://archive.defra.gov.uk/foodfarm/growing/crops/industrial/energy/biomass-taskforce/pdf/btf-finalreport.pdf

DEPARTMENT FOR ENVIRONMENT, FOOD AND RURAL AFFAIRS (DEFRA). 2007. UK Biomass Strategy. [online].[Accessed 2/12/12]. Available from: http://www.biomassenergycentre.org.uk/pls/portal/docs/PAGE/RESOURCES/REF_LIB_RES/PUBLICATIONS/UKBIOMASSSTRATEGY.PDF

DEPARTMENT FOR ENVIRONMENT, FOOD AND RURAL AFFAIRS (DEFRA). 2011. Guidelines for Environmental Risk Assessment and Management: Green Leaves III. [online]. [Assessed 23/9/13]. Available from: https://www.gov.uk/government/uploads/system/uploads/attachment_data/file/69450/pb13670-green-leaves-iii-1111071.pdf

DEPARTMENT OF TRADE AND INDUSTRY (DTI). 2007. Meeting the energy challenge: A white paper on energy. [online]. [Accessed 24/01/11]. Available from: www.berr.gov.uk/files/file39387.pdf

DHUNGANA, A., P. BASU and A. DUTTA. Effects of reactor design on the torrefaction of biomass. *Journal of Energy Resources Technology*, **134**(4). Available from: http://energyresources.asmedigitalcollection.asme.org.

DI BLASI, C. 1996. Heat, momentum and mass transport through a shrinking biomass particle exposed to thermal radiation. *Chemical Engineering Science*, **51**(7), pp.1121-1132.

DI BLASI, C. and M. LANZETTA. 1997. Intrinsic kinetics of isothermal xylan degradation in inert atmosphere. *Journal of Analytical and Applied Pyrolysis*, **40-41**, pp.287-303.

DI BLASI, C. 2008. Modeling chemical and physical processes of wood and biomass pyrolysis. *Progress in Energy and Combustion Science*, **34**(1), pp.47-90.

DRAX. 2011. Biomass: The fourth energy source. [online]. [Accessed 11/01/12]. Available from: http://www.draxpower.com/biomass/

ENVIRONMENTAL AGENCY (EA). 2002. *Environmental Impac Assessment (EIA): A handbook for scoping projects*. London: Environmental Agency.

ENERGY INFORMATION ADMINISTRATION (EIA). 2013. International Energy Outlook 2013. [online]. [Accessed 26/9/13]. Available from: http://www.eia.gov/forecasts/ieo/pdf/0484(2013).pdf

ENERGY WHITE PAPER (EWP). 2011. An energy white paper: A package of reforms to encourage investment in electricity generation. [online]. [Accessed 21/4/13]. Available from: http://www.sse.com/uploadedFiles/Controls/Lists/Resources/_Sample_resources(1)/AnEnergyWhitePaper.pdf

ENVIRONMENTAL PROTECTION UNIT (EPU). 2009. Biomass and air quality guidance for Scottish local authorities. [online]. [Accessed 18/10/12]. Available from: http://www.iaqm.co.uk/text/guidance/epuk/biomass_guidance_scotland.pdf

ESSENDELFT, D.T.V., X. ZHOU and B.S.J. KANG. 2013. Grindability determination of torrefied biomass materials using the Hybrid Work Index. *Fuel*, **105**, pp.103-111.

EUROPEAN COMMISSION (EC). 2010a. Report from the commission to the council and the European parliament on sustainability requirements for the use of solid and gaseous biomass sources in electricity, heating and cooling. [online]. [Accessed 26/9/13]. Available from: www.emissions-euets.com/attachments/259_Report%20from%20the%20Commission%20of%2025%20February/%202010%20COM(2010)11%20final.pdf

EUROPEAN COMMISSION (EC). 2010b. Commission staff working document: Impact assessment. [online]. [Accessed 26/9/13]. Available from: www.eurosfaire.prd.fr/7pc/doc/1267520101_sec_2010_65_en.pdf

FAGERNÄS, L. and K. SIPILÄ. 1997. Emissions of biomass drying. *In* Bridgwater, A.V. and Boocock, D.G.B. *Developments in thermochemical biomass conversion*. Volume 1. London: Blackie Academic and Professional. pp. 783-797.

FORESTRY COMMISION SCOTLAND (FCS). 2010. Interim guidance on the grant aiding and planting of eucalypts in Scotland. [online]. [Accessed 11/4/13]. Available from: http://www.forestry.gov.uk/pdf/InterimEucalyptusGuidance.pdf/$FILE/InterimEucalyptusGuidance.pdf

FELFLI, F.F., C.A. LUENGO, J.A. SUDREZ and P.A. BEATON. 2005. Wood briquette torrefaction. *Energy for Sustainable Development*, **IX**(3), pp.19-22.

FERRO, D.T., V. VIGOUROUX, A. GRIMM and R. ZANZI. 2004. Torrefaction of agricultural and forest residues. Guantánamo, Cuba.

FOREST PRODUCTS COMMISSION'S TREE FARMING AND INDUSTRY DEVELOPMENT PLAN: A 35 YEAR VISION (FPC). 2006. Maritime Pine – Esperance. [online]. [Accessed 15/4/13]. Available from: http://www.fpc.wa.gov.au/content_migration/_assets/documents/plantations/industry_plans/EucalyptSawlog-CentralSouthWestRecoveryCatchments.pdf

FRANCESCATO, V., E. ANTONINI and L.Z. BERGOMI. 2008. *Wood fuels handbook*. Italy: AIEL-Italian Agriforestry Energy Association.

FREDERICK JR, W.J., S.J. LIEN, C.E. COURCHENE, N.A. DEMARTINI, A.J. RAGAUKAS and K. LISA. 2008. Production of ethanol from carbohydrates from loblolly pine: A technical and economic assessment. *Bioresource Technology*, **99**(11), pp.5051-5057.

FREUDENBERG, K. and A.A. NEISH. 1968. *The Constitution and Biosynthesis of Lignin*. New York: Springer-Verlag,

FRIEDL, A., E. PADOUVAS, H. ROTTER and K. VARMUZA. 2005. Prediction of heating values of biomass fuel from elemental composition. *Analytica Chimica Acta*, **544**(1-2), pp.191-198.

GLASSON, J., R. THERIVEL and A. CHADWICK. 2012. Introduction to environmental impact assessment. New York: Routledge.

GONZALEZ, R., R. PHILLIPS, D. SALONI, H. JAMEEL, R. ABT, A. PIRRAGLIA and J. WRIGHT. 2011. Biomass to energy in the Southern United States: Supply chain and delivered cost. *Bioresources*, **6**(3), pp.2954-2976.

GÜLLÜ, D. and A. DEMIRBAŞ. 2011. Biomass to methanol via pyrolysis process. *Energy Conversion and Management*, **42**(11), pp.1349-1356.

HALFORD, N.G. and A. KARP (ed). 2011. *Energy crops*. London: Royal Society of Chemistry.

HARDCASTLE, P.D. 2006. A review of the potential impacts of short rotation forestry. [online]. [Accessed 17/4/13]. Available from: http://www.forestry.gov.uk/pdf/SRFFinalreport27Feb.pdf/$FILE/SRFFinalreport27Feb.pdf

HARMSEN, P.F.H., W.J.J. HUIJGEN, L.M. BERMUDEZ LOPEZ and R.R.C. BAKKER. 2011. Literature review of physical and chemical pre-treatment processes for lignocellulosic biomass. [online]. [Accessed 19/4/13]. Available from: http://www.ecn.nl/docs/library/report/2010/e10013.pdf

HAYKIRI-ACMA, H. 2006. The role of particle size in the non-isothermal pyrolysis of hazelnut shell, *Journal of Analytical and Applied Pyrolysis*, **75**(2), pp. 211-216.

HEO, H.S., H.J. PARK, J-H, YIM, J.M. SOHN, S-S. KIM, C. RYU, J-K. JEON and Y-K. PARK. 2010. Influence of operation variables on fast pyrolysis of *Miscanthus sinensis var. purpurascens*, *Bioresource Technology*, **101**(10), pp.3672-3677.

HON, D.N.S. and N. SHIRAISHI. 2001. *Wood and cellulosic chemistry*. New York: Marcel Dekker.

HUGHES, L. and J. RUDOLPH. 2011. Future world oil production: growth, plateau or peak? *Current opinion in environmental sustainability*, **3**(4), pp.225-234.

HUSTAD, J.E., Ø, SKREIBERG and O.K. SØNJU. 1995. Biomass combustion research and utilisation in IEA countries. *Biomass and Bioenergy*, **9**(1-5), pp.235-255.

IBRAHIM, R.H.H., L.I. DARVELL, J.M. JONES and A. WILLIAMS. 2013. Physicochemical characterisation of torrefied biomass. *Journal of Analytical and Applied Pyrolysis*. **103**, pp.21-30.

INTERNATIONAL PROGRAMME OF CHEMICAL SAFETY (INCHEM). [online]. [Accessed 29/11/12]. Available from: inchem.org

INARI, G.N., M. PETRISSANS, J. LAMBERT, J.J. EHRHARDT and P. GERARDIN. 2006. XPS characterisation of wood chemical composition after heat-treatment. *Surface and Interface Analysis,* **38**(10), pp.1336-1342.

INTERNATIONAL ENERGY AGENCY (IEA). 2012a. IEA Bioenergy Task 32: Status overview of torrefaction technologies. [online]. [Accessed 1/8/13]. Available from: www.ieabcc.nl/publications/IEA_Bioenergy_T32_Torrefaction_review.pdf

INTERNATIONAL ENERGY AGENCY (IEA). 2012b. IEA Bioenergy Task 40: Possible effect of torrefaction on biomass trade. [online]. [Accessed 26/9/13]. Available from: bioenergytrade.org/downloads/t40-torrefaction-2012.pdf

INTERNATIONAL ENERGY AGENCY (IEA). 2013a. IEA Bioenergy Task 40: Large industrial users of energy biomass. [online]. [Accessed 27/9/13]. Available from: bioenergytrade.org/downloads/t40-large-industrial-biomass-users.pdf

INTERNATIONAL ENERGY AGENCY (IEA). 2013b. IEA Bioenergy Task 32, 36, 47 and 40: Health and safety aspects of solid biomass storage, transportation and feeding. [online]. [Accessed 29/9/13]. Available from: www.ieabcc.nl/publications/IEA_Bioenergy_Health_and_Safety_Report_(final).pdf

JAMES, P. and P. HOWES. 2006. Regulation of energy from solid biomass plants. [online]. [Accessed 19/12/11]. Available from: http://www.biomassenergycentre.org.uk/pls/portal/docs/PAGE/RESOURCES/REF_LIB_RES/PUBLICATIONS/REGULATION%20OF%20ENERGY%20DEFRA.PDF

JENKINS, B.M., R.R. BAKKER and J.B. WEI. 1998. On the properties of washed straw. *Biomass and Bioenergy*, **10**(4), pp.177-200.

JOHANSSON, T. 1999. Biomass production of Norway spruce (*Picea abies (L.) Karst.*) growing on abandoned farmland. *Silva Fennica,* **33**(4), pp.261-280.

JONES, J.M., L.I. DARVELL, T.G. BRIDGEMAN, M. POURKASHANIAN and A. WILLIAMS. 2007. An investigation of the thermal and catalytic behaviour of potassium in biomass combustion. *Proceedings of the Combustion Institute*, **31**, pp.1955-1963.

JONES, J.M., T.G. BRIDGEMAN, T.G., L.I. DARVELL, B. GUDKA, A. SADDAWI and A. WILLIAMS. 2012. Combustion properties of torrefied willow compared with bituminous coals. *Fuel Processing Technology*, **101**, pp.1-9.

JOSHI, N.R. 1979. Relative grindability of bituminous coals on volume basis. *Fuel*, **58**(6), pp.477-478.

KARP, A. and N.G. HALFORD. 2011. Energy Crops: Introduction. *In*: KARP, A and N.G.HALFORD. *Energy Crops*. London: RSC Publishing. pp.1-12.

KIM, Y-H., S-M, L, H-W, L and J-W, L. 2012. Physical and chemical characteristics of products from the torrefaction of yellow poplar (*Liriodendron tulipifera*). *Bioresource Technology,* **116**, pp.120-125.

KLASS, D.L. 1998. *Biomass for renewable energy, fuels and chemicals*. London: Academic Press.

KLEINSCHMIDT, C.P. n.d. Overview of international developments in torrefaction. [online]. [Accessed 01/05/13]. Available from: http://www.ieabcc.nl/workshops/task32_2011_graz_torrefaction/Kleindschmidt_Paper.pdf

KOPPEJAN, J. 2012. Safety aspects of solid biomass storage, transportation and feeding. [online]. [Accessed 1/8/13]. Available from: http://www.ieabcc.nl/workshops/task32_Dublin_SSC/07%20Koppejan.pdf

KURTTIO, P., P. KALLIOKOSKI, S. LAMPELO and M.J. JANTUNEN. 1990. Mutagenic compounds in wood-chip drying fumes. *Mutation Research*, **242**, pp.9-15.

LANDSTRÖM, S., L. LOMAKKA and S. ANDERWIN. 1996. Harvest in spring improves yield and quality of reed canary grass as a bioenergy crop. *Biomass and Bioenergy*, **11**(4), pp.333-341.

LAVERGNE, S. and J. MOLOFSKY. 2004. Reed canary grass (*Phalaris arundinacea*) as a biological model in the study of plant invasions. *Critical Reviews in Plant Sciences*, **23**(5), pp.415–429.

LESLIE, A.D., M. MENCUCCINI and M. PERKS. 2012. The potential for Eucalyptus as a wood fuel in the UK. *Applied Energy*, **89**(1), pp.176-182.

LEWIN, M. and I.S. GOLDSTEIN. 1991. *Wood structure and composition*. New York: Marcel Dekker.

LEWANDOWSKI, I., J.C. CLIFTON-BROWN, J.M.O. SCURLOCK and W. HUISMAN. 2000. Miscanthus: European experience with a novel energy crop. *Biomass and Bioenergy*, **19**(4), pp.209-227.

LIPINSKY, E.S., J.R. ARCATE and T.B. REED. 2002. Enhanced wood fuels via torrefaction. *Abstracts of Papers American Chemical Society*, **223**(1-2), pp.FUEL 171.

LIVINGSTON, W.R. 2012. Recent developments in biomass co-firing in large coal-fired utility boilers. [online]. [Accessed 18/1/13]. Available from: http://www.ieabcc.nl/workshops/task32_2012_Copenhagen/Livingston-1.pdf

LU, H., W. ROBERT, G. PEIRCE, B. RIPA and L.L. BAXTER. 2008. Comprehensive study of biomass particle combustion. *Energy and Fuels*, **22**(4), pp.2826-2839.

MANI, S., L.G. TABIL and S. SOKHANSANJ. 2004. Grinding performance and physical properties of wheat and barley straws, corn starch and switchgrass. *Biomass and Bioenergy*, **27**(4), pp.339 -352.

MANI, T., P. MURUGAN, J. ABEDI and N. MAHINPEY. 2010. Pyrolysis of wheat straw in a thermogravimetric analyser: Effect of particle size and heating rate on devolatisation and estimation of global kinetics. *Chemical Engineering Research and Design*, **88**(8), pp.952-958.

McCRACKEN, A.R. 2006. Growing willow for energy. [online]. [Accessed 16/1/13]. Available from: http://localplanet.ie/index.php?option=com_content&task=view&id=210

McKAY, H. 2006. Environmental, economic, social and political drivers for increasing use of wood fuel as a renewable resource in Britain. *Biomass and Bioenergy*, **20**(4), pp.308-315.

McKAY, H. 2011. *Short rotation forestry: Review of growth and environmental impacts*. Surrey: Forest Research.

MCKENDRY, P. 2002. Energy production from biomass (part 1): Overview of biomass. *Bioresource Technology*, **83**(1), pp.37-46.

MEDIC, D., M. DARR, A. SHAH, B. POTTER and J. ZIMMERMAN. 2012. Effects of torrefaction process parameters on biomass feedstock upgrading. *Fuel*, **91**(1), pp.147-154.
MELKIOR, T., S. JACOB, G. GERBAUD, S. HEDIGER, L. LE PAPE and L. BONNEFOIS. 2012. NMR analysis of the transformation of wood constituents by torrefaction. *Fuel*, **92**(1), pp.271-280.

MITCHELL, C.P., E.A. STEVENS and M.P. WATTERS. 1999. Short-rotation forestry - operations, productivity and costs based on experience gained in the UK. *Forest Ecology and Management*, **121**(1-2), pp.123-136.

MONTROSS, M. and C. CZARENA. Energy crops for the production of biofuels. *In*: CROCKER, M, ed. 2010. *Thermochemical Conversion of Biomass to Liquid Fuels and Chemicals*. London: The Royal Society of Chemistry, pp.26-45.

MORTERRA, C. and M.J.D. LOW. 1983. IR studies of carbons – II. The Vacuum pyrolysis of cellulose. *Carbon*, **21**(3), pp. 283-288.

MUCSI, G. 2008. Fast test method for the determination of the grindability of fine materials. *Chemical Engineering Research and Design*, **86**(4A), pp.395-400.

MURPHY, D.P.L., A. BRAMM and K.C. WALKER. 1996. *Energy from crops*. Cambridge: Semundo.

NATIONAL NON FOOD CROPS CENTRE (NNFCC). 2009. Marketing study for biomass treatment technology. [online]. [Accessed 6/2/12]. Available from: http://www.nebr.co.uk/_cmslibrary/files/marketingstudynnfccappendix2.pdf

NORDH, N-E and I. DIMITRIOU. 2003. Harvest techniques in Europe. Short Rotation Crops for Bioenergy: New Zealand. [online]. [Accessed 11/4/13]. Available from: http://www.shortrotationcrops.org/PDFs/2003Mtg/18-SimsTransportEconomics.pdf

NOWAKOWSKI, D.J., J.M. JONES, R.M.D. BRYDSON and A.B. ROSS. 2007. Potassium catalysis in the pyrolysis behaviour of short rotation willow coppice. *Fuel*, **86**(15), pp.2389-2402.

NURMINEN, F. 2012. Environmental impacts of torrefied wood pellet production: Cases Risolog and Pursiala pilot plant. [online]. [Accessed 23/9/13]. Available from: www.miktech.fi/media/getfile.php?file=271

OSAZUWA-PETERS, O. and A.E. ZANNE. 2011. Wood density protocol. [online]. [Accessed 14/11/11]. Available from: http://prometheuswiki.publish.csiro.au/tiki-index.php?page=Wood+density+protocol.

PAULY, M. and K. KEEGSTRA. 2008. Cell-wall carbohydrates and their modification as a resource for biofuels. *The Plant Journal*, **54**(4), pp.559–568.

PARLIAMENTARY OFFICE OF SCIENCE AND TECHNOLOGY (POST). 2004. The future of UK gas supplies. *postnote*, **230**, pp.1-4.

PENG, J.H., H.T. BI, S. SOKHANSANJ and C. LIM. 2012. A study of particle size effect on biomass torrefaction and densification. *Energy and Fuels*, **26**(6), pp.3826-3839.

PENTANANUNT, R., A.N.M. MIZANUR RAHMAN and S.C. BHATTACHARYA. 1990. Upgrading of biomass by means of torrefaction. *Energy*, **15**(12), pp.1175–1179.

PHANPHANICH, M. and S. MANI. 2011. Impact of torrefaction on the grindability and fuel characteristics of forest biomass. *Bioresource Technology*, **102**(2), pp.1246-1253.

PIERRE, F., G. ALMEIDA, J.O. BRITO and P. PERRĖ. 2011. Influence of torrefaction on some chemical and energy properties of maritime pine and pedunculate oak. *Bioresource*s, **6**(2), pp.1204-1218.

PIMCHUAI, A., A. DUTTA and P. BASU. 2010. Torrefaction of agriculture residue to enhance combustible properties. *Energy and Fuels*, **24**, pp.4638–4645.

PIRRAGLIA, A., R. GONZALEZ, D. SALONI, J. WRIGHT and J. DENIG. 2012. Fuel properties and suitability of *Eucalyptus Benthamii* and *Eucalyptus Macarthurii* for torrefied wood and pellets. *Bioresources*, **7**(1), pp.217-235.

PRINS, M.J., K.J. PTASINSKI and F.J.J.G. JANSSEN. 2006a. Torrefaction of wood: Part 2. Analysis of products. *Journal of Analytical and Applied Pyrolysis*, **77**(1), pp.35-40.

PRINS, M.J., J. K.J. PTASINKI and F.J.J.G. JANSSEN. 2006b. Torrefaction of wood. Part 1: Weight loss kinetics. *Journal of Analytical and Applied Pyrolysis*, **77**(1), pp.28-34.

PUBCHEM COMPOUND (PUBCHEM). [online]. [Accessed 29/11/12]. Available from: www.ncbi.nlm.nih.gov/pccompound

RAVINDRANATH, N.H. and D.O. HALL. 1995. *Biomass, energy and environment: A developing country perspective from India*. New York: Oxford University Press.

REPELLIN, V., A. GOVIN, M. ROLLAND and R. GUYONNET. 2010. Energy requirement for the fine grinding of torrefied wood. *Biomass and Bioenergy*, **34**(7), pp.923–930.

ROCKWOOD, D.L., A.W. RUDIE, S.A. RALPH, J.Y. ZHU and J.E. WINANDY.2008. Energy product options for *Eucalyptus* species grown as short rotation woody crops. *International Journal of Molecular Sciences*, **9**(8), pp.1361-1378.

RODRIGUES, T.O. and P.L.A. ROUSSET. 2009. Effects of torrefaction on energy properties of *Eucalyptus grandis* wood. *Cerne*, **15**(4), pp.446-452.

ROSILLO-CALLE, F., S.V. BAJAY and H. ROTHMAN. 2000. *Industrial uses of biomass energy.* New York: Taylor and Francis.

ROUSSET, P., C. AGUIAR, N. LABBĖ and J-M. COMMANDRĖ. 2011. Enhancing the combustible properties of bamboo by torrefaction. *Bioresource Technology*, **102**(17), pp.8225-8231.

RUBIERA, F., A. ARENILLAS, E. FUENTE, N. MILES and J.J. PIS. 1999. Effect of the grinding behaviour of coal blends on coal utilization for combustion. *Powder Technology*, **105**(1-3), pp.351-356.

RUPAR, K. and M. SANATI. 2003. The release of organic compounds during biomass drying depends upon the feedstock and/or altering drying heating medium. *Biomass and Bioenergy*, **25**(6), pp.615-622.

ROOS. C.J. 2008. Biomass drying and dewatering for clean heat and power. [online]. [Accessed 10/10/12]. Available from: http://chpcenternw.org/NwChpDocs/BiomassDryingAndDewateringForCleanHeatAndPower.pdf

SADAKA, S. and S. NEGI. 2009. Improvements of biomass physical and thermochemical characteristics via torrefaction process. *Environmental Progress & Sustainable Energy*, **28**(3), pp.427-434.

SADDAWI, A., J.M. JONES, A. WILLIAMS and C. Le COEUR. 2012. Commodity fuels from biomass through pretreatment and torrefaction: Effects of mineral content on torrefied fuel characteristics and quality. *Energy and Fuels*, **26**(11), pp.6466-6474.

SCIENTIFIC APPLICATIONS INTERNATIONAL CORPORATION (SAIC). 2006. Lifecycle assessment: Principles and Practice. [online]. [Assessed 06/09/13]. Available from: http://www.epa.gov/nrmrl/std/lca/pdfs/chapter1_frontmatter_lca101.pdf

SAMUELSSON, R., C. NILSSON and J. BURVALL. 2006. Sampling and GC-MS as a method for analysis of volatile organic compounds (VOC) emitted during oven drying of biomass materials. *Biomass and Bioenergy*, **30**(11), pp.923-928.

SCHOBERT, H.H. 1990. *The chemistry of hydrocarbon fuels*. London: Butterworths.

SELL, C. 2003. *A fragnant introduction to terpenoid chemistry.* Cambridge: The Royal Society of Chemistry.

SHANG, L., J. AHRENFELDT, J.K. HOLM, A.R. SANADI, S. BARSBERG, T. THOMSEN, W. STELTE and U.B. HENRIKSEN. 2012. Changes of chemical and mechanical behaviour of torrefied wheat straw. *Biomass and Bioenergy*, **40**, pp.63-70.

SHOULAIFAR, T.K., N. DEMARTINI, A. IVASKA, P. FARDIM and M. HUPA. 2012. Measuring the concentration of carboxylic acid groups in torrefied spruce wood. *Bioresource Technology*, **123**, pp.338-343.

SIMPENDORFER, K.J. 1992. *An introduction to trees for South-Eastern Australia*. Melbourne: Inkata Press.

SJÖSTÖRM, L. 1981. *Wood chemistry: Fundamentals and applications*. New York: Academic Press.

SREEKANTH, M. and A.K. KOLAR. Progress of conversion in a shrinking wet cylindrical wood particle pyrolyzing in a hot fluidized bed. *Journal of Analytical and Applied Pyrolysis*, **84**(1), pp.53.67.

STELTE, W., C. CLEMONS, J.K. HOLM, A.R. SANADI, J. AHRENFELDT, L. SHANG and U.B. HENRIKSEN. 2011. Pelletizing properties of torrefied spruce. *Biomass and Bioenergy*, **35**(11), pp.4690-4698.

STELTE, W., A.R. SANADI, L. SHANG, J.K. HOLM, J. AHRENFELDT and U.B. HENRIKSEN. 2012. Recent developments in biomass pelletization – A review. *BioResources*, **7**(3), pp.4451-4490.

STELTE, W., N.P.K. NIELSEN, H.O. HANSEN, J. DAHL, L. SHANG and A.R. SANADI. 2013. Reprint of: Pelletizing properties of torrefied wheat straw. *Biomass and Bioenergy*, **53**, pp.105-112.

TAPASVI, D., R. KHALIL, Ø. SKREIBERG, K-Q, TRAN and M. GRØNLI. 2012. Torrefaction of Norwegian birch and spruce: An experimental study using macro-TGA. *Energy and Fuels*, **26**(8), pp.5232-5240.

THE RENEWABLES OBLIGATION (AMENDMENT) ORDER (RO) 2011. 2011. Electricity. [online]. [Accessed 10/01/12]. Available from: http://www.legislation.gov.uk/uksi/2011/984/pdfs/uksi_20110984_en.pdf

THE RENEWABLES TRANSPORT FUEL OBLIGATIONS (AMENDMENT) ORDER (RTFO) 2011. 2011. Transport. [online]. [Accessed 10/01/12]. Available from: http://www.legislation.gov.uk/uksi/2011/2937/pdfs/uksi_20112937_en.pdf

THORNLEY, P. 2006. Increasing biomass based power generation in the UK. *Energy Policy*, **34**(15), pp.2087-2099.

TILMAN, D.A., J.R. AMADEO and D.K. WILLIAM. 1981. *Wood combustion: Principles, processes and economics*. New York: Academic Press.

TUMULURU, J.S., R.D. BOARDMAN, C.T. WRIGHT and J.R. HESS. 2012. Some chemical compositional changes in Miscanthus and white oak sawdust samples during torrefaction. *Energies*, **5**(10), pp.3928-3947.

TURNS, S.R. 2000. *An introduction to combustion*. New York: Mc-Graw Hill.

UNITED NATIONS. 1998. Kyoto Protocol to the United Nations Framework Convention on Climate Change. [online]. [Accessed 02/05/11]. Available from: http://unfccc.int/resource/docs/convkp/kpeng.pdf

VAN DER STELT, M.J.C., H. GERHAUSER, J.H.A. KIEL and K.J. PTASINSKI. 2011. Biomass upgrading by torrefaction for the production of biofuels: A review. *Biomass and Bioenergy*, **35**(9), pp.3748-3762.

VASSILEV, S.V., D. BAXTER, L.K. ANDERSEN and C.G. VASSILEVA. 2010. An overview of the chemical composition of biomass. *Fuel*, **89**, pp.913-933.

VIANA, H., W.B. COHEN, D. LOPES and J. ARANHA. 2010. Assessment of forest biomass for use as energy, GIS-based analysis of geographical availability and locations of wood-fired power plants in Portugal. *Applied Energy*, **87**(8), pp.2551-2560.

WANNAPEERA, J., B. FUNGATAMMASAN and N. WORASUWANNARAK. 2011. Effects of temperature and holding time during torrefaction on the pyrolysis behaviors of woody biomass. *Journal of Analytical and Applied Pyrolysis*, **92**(1), pp.99-105.

WEI, L., S. XU, L. ZHANG, H. ZHANG, C. LIU, H. ZHU and S. LIU. 2006. Characteristics of fast pyrolysis of biomass in a free fall reactor. *Fuel Processing Technology*, **87**(10), pp. 863- 871.

WERKELIN, J., B-J. SKRIFVARS, M. ZEVENHOVEN, B. HOLMBOM and M, HUPA. 2010. Chemical forms of ash-forming elements in woody biomass fuels. *Fuel*, **89**(2), pp.481-493.

WILLIAMS, A., J.M. JONES, L. MA and M. POURKASHANIAN. 2012. Pollutants from the combustion of solid biomass fuels: Review. *Progress in Energy and Combustion Science*, **38**(2), pp.113-137.

WIMMERSTEDT, R. 1999. Recent advances in biofuel drying. *Chemical Engineering and Processing*, **38**(4-6), pp.441-447.

WORLD COAL INSTITUTE (WCI). n.d. The coal resource: A comprehensive overview of coal. [online]. [Accessed 3/4/13]. Available from: http://www.scribd.com/doc/18825349/The-Coal-Resource-A-Comprehensive-Overview-of-Coal-World-Coal-Institute

WÓJTOWICZ, M,A., X. SHI and M.A. SERIO. 2011. *Premium upgraded biomass solid fuels: Fundamentals of torrefaction and performance of torrefied fuels*. USA: Advanced Fuel Research.

WU, K-T., C-J. TSAI, C-S. CHEN and H-W. CHEN. 2012. The characteristics of torrefied microalgae. *Applied Energy*, **100**, pp.52-57.

YAN, W., T.C. ACHARJEE, C.J. CORONELLA and V.R.VASQUEZ. 2009. Thermal pretreatment of lignocellulosic biomass. *Environmental Progress & Sustainable Energy*, **28**(3), pp.435-440.

YANG, H., R. YAN, H. CHEN, D.H. LEE and C. ZHENG. 2007. Characteristics of hemicellulose, cellulose and lignin pyrolysis. *Fuel*, **86**(12-13), pp.1781-1788.

YIN, R., R. LIU, J. WU, X. WU, C. SUN and C. WU. 2012. Influence of particle size on performance of a pilot-scale fixed-bed gasification system. *Bioresource Technology*, **119**, pp.15-21.

ZANZI, E., M. PACH and E. BJØRNBOM. 2002. Biomass torrefaction. Proceedings of the Sixth Asia-Pacific International Symposium on Combustion and Energy Utilization, Kuala Lumpur, Malaysia.

ZAWADZKI, J. 1989.Infrared-Spectroscopy in surface-chemistry of carbons. *Chemistry and Physics of Carbon*, **21**, pp.147-380.

Appendix 5.1. Temperature profile of biomass fuels upon torrefaction.

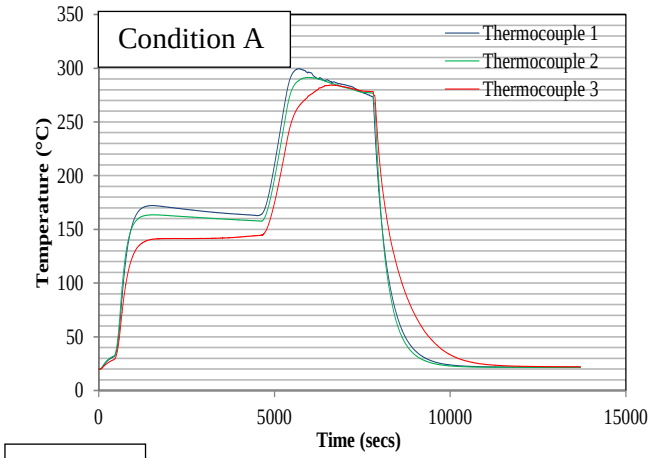

Willow

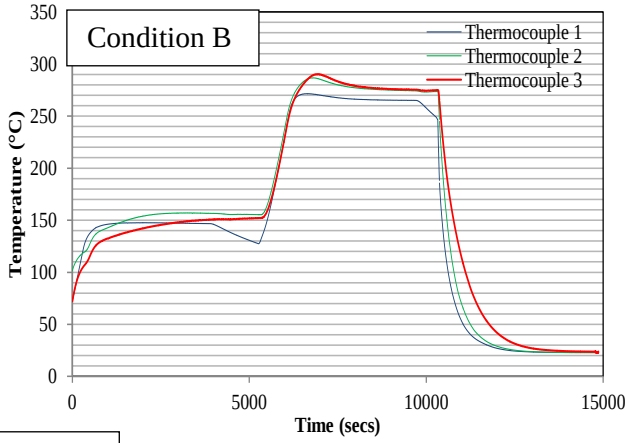

Willow

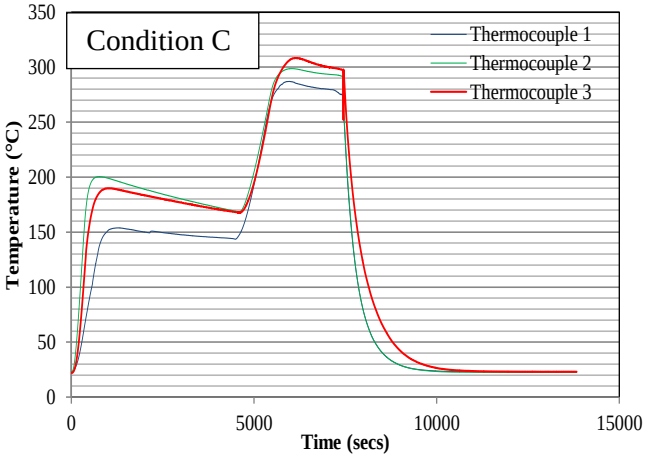

Willow

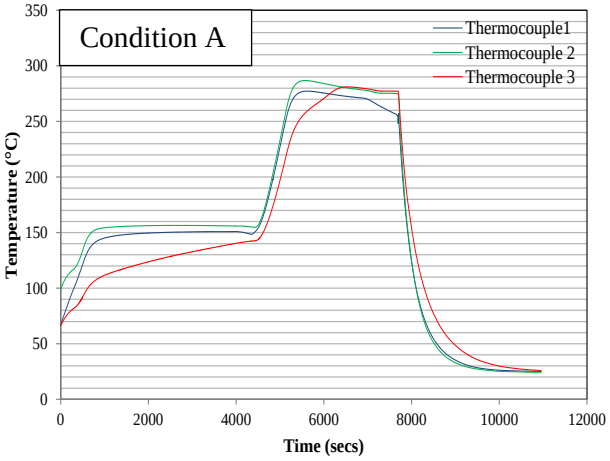

Eucalyptus

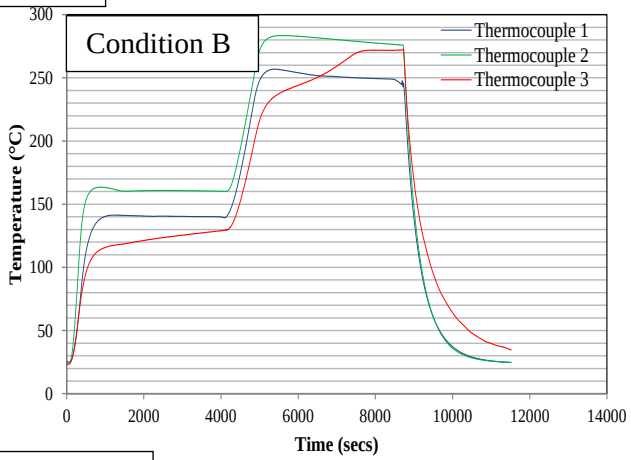

Eucalyptus

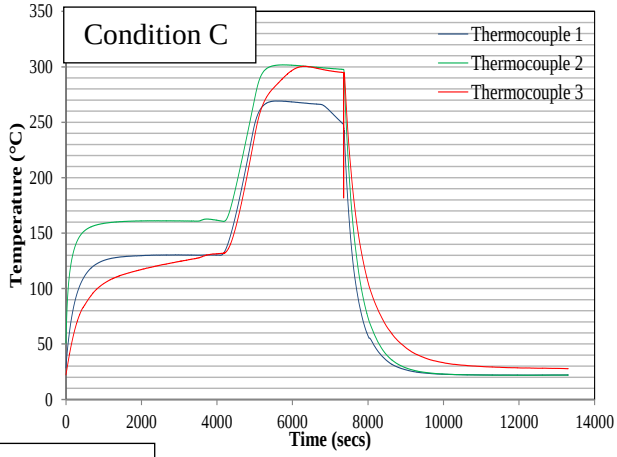

Eucalyptus

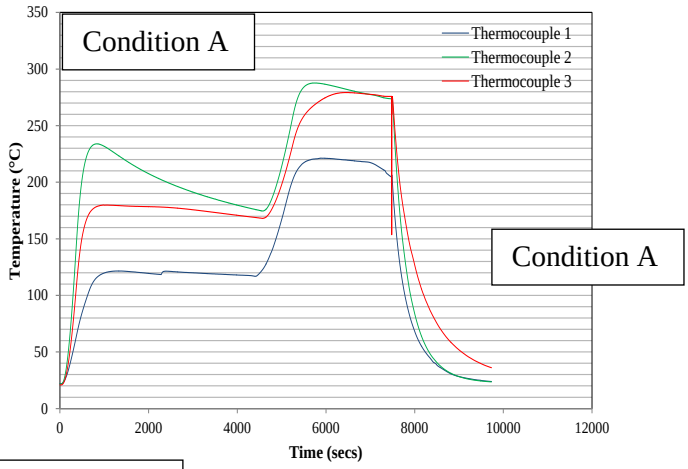

Condition A

Hardwood

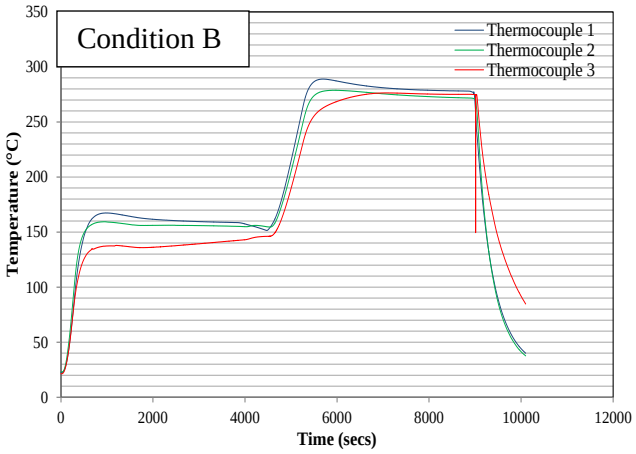

Hardwood

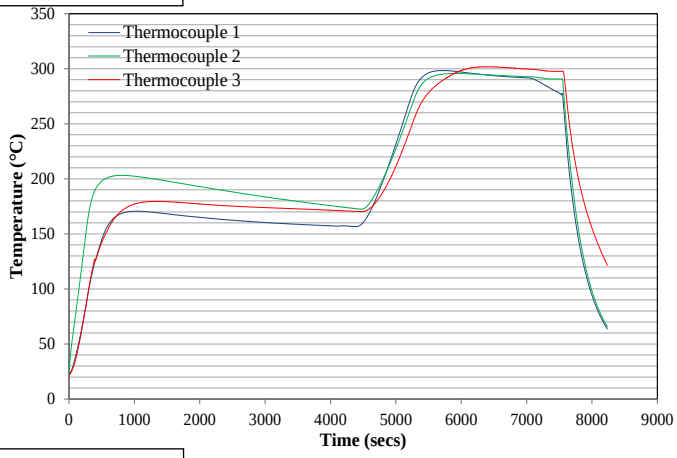

Hardwood

Appendix 5.2. Ash elemental composition (%m/m).

Elemental oxides	Willow	Eucalyptus	Hardwood	Softwood
SiO_2	2.2	3.3	5.0	17.2
Al_2O_3	0.5	0.3	1.0	3.5
Fe_2O_3	0.4	1,3	1.0	2.2
TiO_2	<0.1	<0.1	<0.1	0.2
CaO	33.8	30.6	29.9	24.3
MgO	4.0	2.4	2.7	5.8
Na_2O	1.2	1.7	0.8	0.8
K_2O	18.1	19.0	17.7	14.8
Mn_3O_4	0.4	0.5	1.1	3.0
P_2O_5	16.1	3.1	2.6	3.7
SO_3	5.6	2.8	3.5	4.7

Appendix 5.3. Grindability performance of biomass.

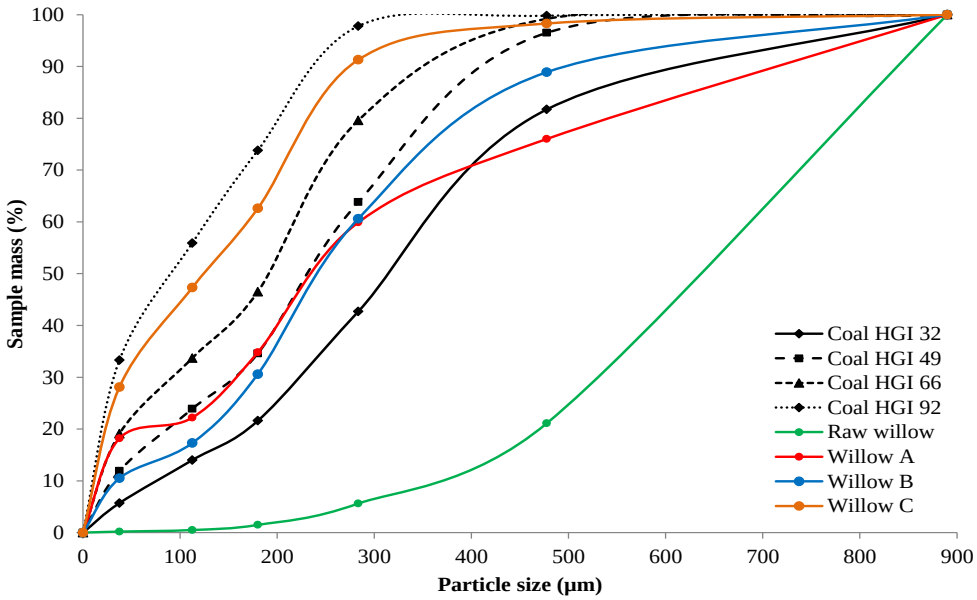

Figure A-5.3.1. Cumulative particle size distributions resulting from milling tests of raw and torrefied willow under conditions A, B and C and compared with standard reference coals of known HGI values.

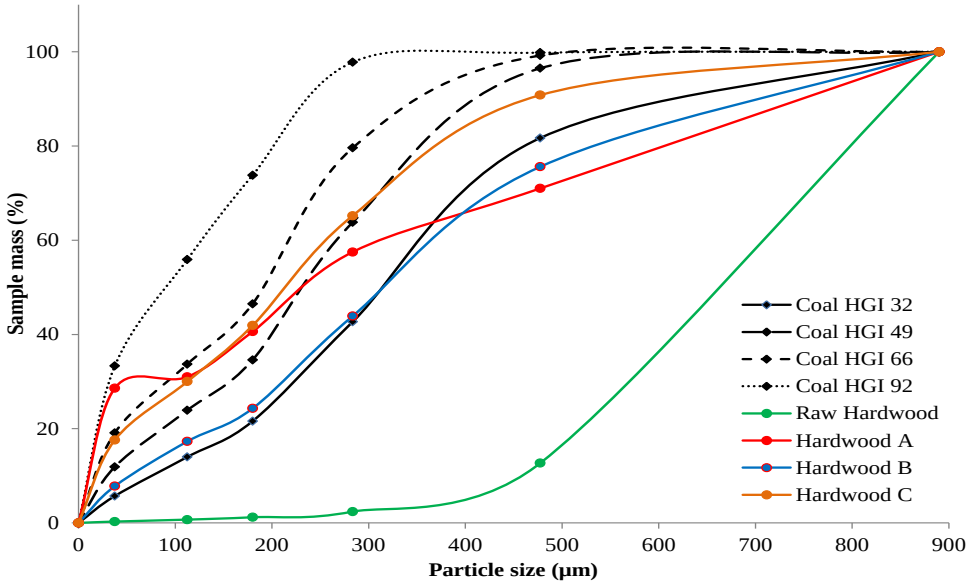

Figure A-5.3.2. Cumulative particle size distributions resulting from milling tests of raw and torrefied hardwood under conditions A, B and C and compared with standard reference coals of known HGI values.

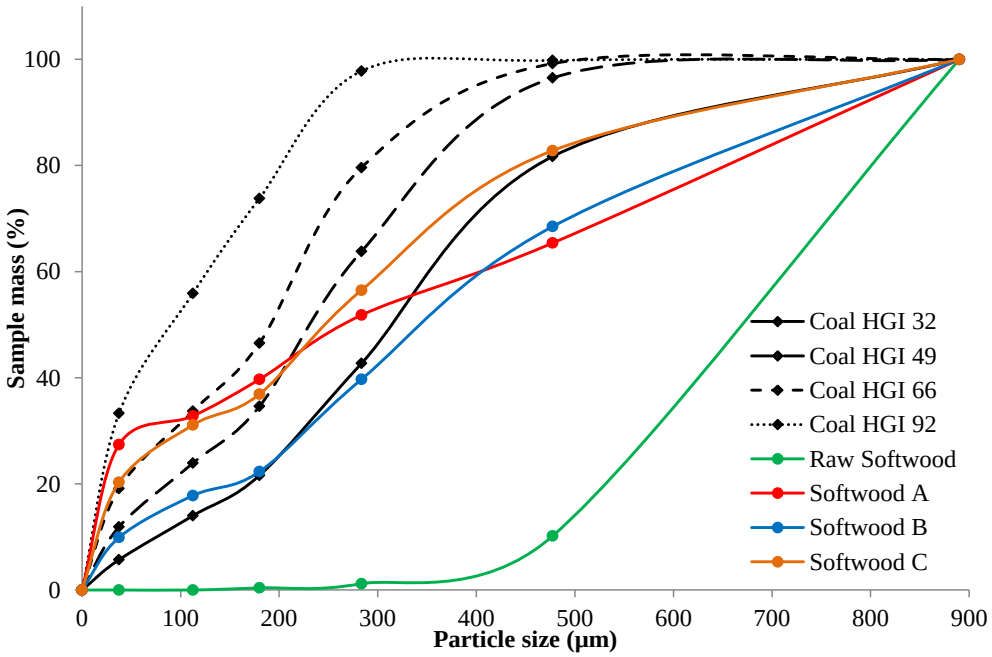

Figure A-5.3.3. Cumulative particle size distributions resulting from milling tests of raw and torrefied softwood under conditions A, B and C and compared with standard reference coals of known HGI values.

Appendix 5.4. FTIR Spectra of raw and torrefied willow and eucalyptus samples.

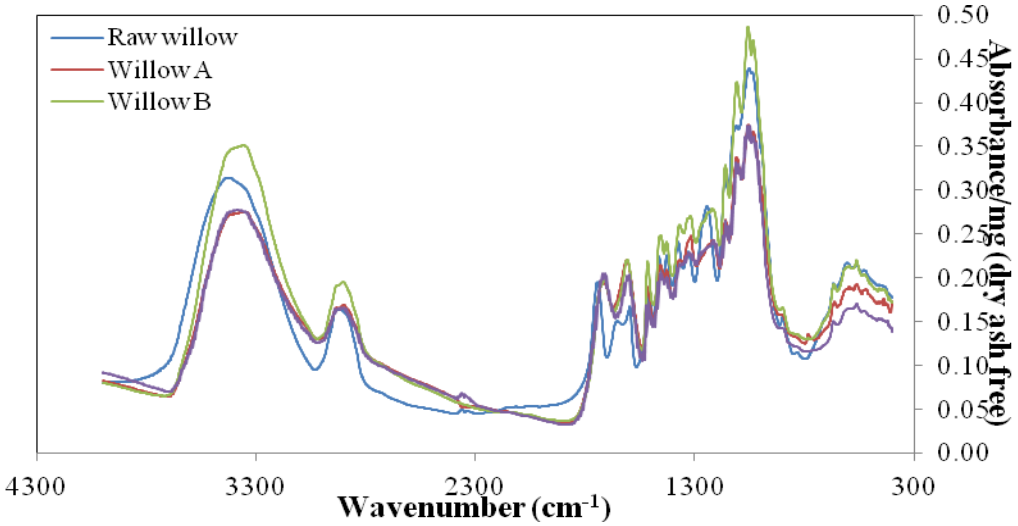

Figure A-5.4.1. FTIR spectra of raw and torrefied willow

.

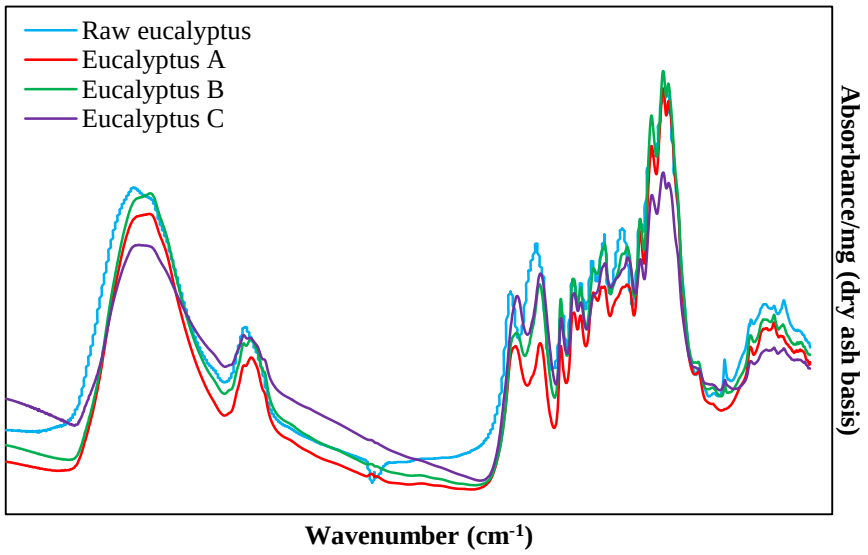

Figure A-5.4.2. FTIR spectra of raw and torrefied eucalyptus.

Appendix 5.5. X-ray Photoelectron Spectroscopy survey spectra of eucalyptus samples.

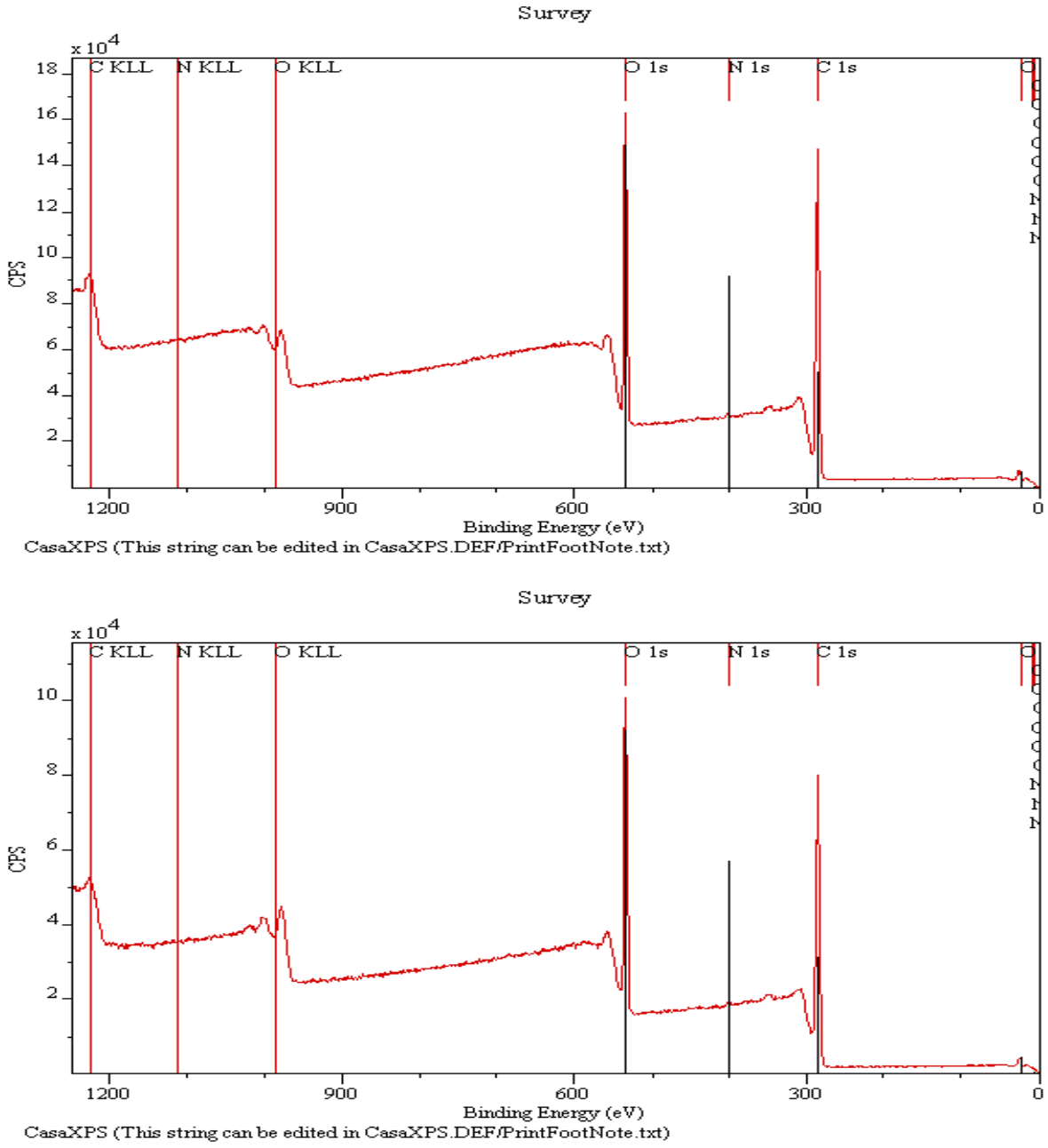

Figure A-5.5.1. XPS Survey spectra of raw (top) and torrefied eucalyptus C (bottom).

Appendix 5.6. List of components contained in tar, obtained from torrefaction of hardwood and softwood.

Table A-5.6.1. Main components that contained in the tar from hardwood.

PK	RT	Area Pct	Library/ID	Ref	CAS	Qual
1	26.3989	3.2345	Phenol, 2-methoxy-4-methyl-	16763	000093-51-6	98
2	30.4045	7.2981	2-Methoxy-4-vinylphenol	23425	007786-61-0	87
3	30.8715	2.0754	Phenol, 2-methoxy-4-(1-propenyl)-, (Z)-	31881	005912-86-7	94
4	31.8365	8.9816	Phenol, 2,6-dimethoxy-	26272	000091-10-1	95
5	32.0597	0.9332	Phenol, 2,6-dimethoxy-	26272	000091-10-1	89
6	34.1559	11.73	Phenol, 2-methoxy-4-(1-propenyl)-, (Z)-	31881	005912-86-7	98
7	34.3997	10.8476	4-Methoxy-2-methyl-1-(methylthio)benzene	35577	022583-04-6	74
8	36.4492	7.8281	5-tert-Butylpyrogallol	44207	020481-17-8	72
9	38.3379	4.3102	2,3,5,6-Tetrafluoroanisole	43464	002324-98-3	72
10	38.6077	5.3174	2,4-Hexadienedioic acid, 3-methyl-4-propyl-, dimethyl ester, (E,Z)-	75567	058367-44-5	38
11	38.8516	6.412	(+)-s-2-Phenethanamine, 1-methyl-N-vanillyl-	106254	1000127-89-6	72
12	40.2422	3.0499	Phenol, 2,6-dimethoxy-4-(2-propenyl)-	52464	006627-88-9	78
13	41.9025	14.5664	Phenol, 2,6-dimethoxy-4-(2-propenyl)-	52459	006627-88-9	94
14	44.2634	2.6954	Benzene, 1,1'-(3-methylbutylidene)bis-	74549	026466-27-3	49
15	45.8978	10.7202	Desaspidinol	63949	000437-72-9	80

Table A-5.6.2. Main components that contained in the tar from softwood.

PK	RT	Area Pct	Library/ID	Ref	CAS	Qual
1	17.3188	2.2575	2-Furanmethanol	3020	000098-00-0	87
2	19.4202	1.238	1,2-Cyclopentanedione	3030	003008-40-0	83
3	21.0961	0.7758	1H-Imidazole, 4,5-dihydro-2-methyl-	1343	000534-26-9	72
4	21.5423	1.259	1,4-Butanediamine, 2,3-dimethoxy-N,N,N',N'-tetramethyl-, [S-(R*,R*)]-	59321	026549-21-3	78
5	22.2376	1.3719	1,2-Cyclopentanedione, 3-methyl-	6225	000765-70-8	81
6	23.4206	4.1037	Phenol, 2-methoxy-	10081	000090-05-1	95
7	26.0824	3.1059	Phenol, 2-methoxy-4-methyl-	16763	000093-51-6	97
8	26.5182	2.0937	4-Cyclopentene-1,3-diol, trans-	3638	000694-47-3	22
9	28.438	1.4467	Phenol, 4-ethyl-2-methoxy-	24916	002785-89-9	91
10	28.7493	1.1841	3-Aminopiperidin-2-one	6918	1000302-88-7	43
11	30.2022	6.8493	2-Methoxy-4-vinylphenol	23425	007786-61-0	91
12	30.7054	3.8758	Phenol, 2-methoxy-4-(1-propenyl)-, (Z)-	31881	005912-86-7	97
13	30.9753	1.6349	5-Acetoxymethyl-2-furaldehyde	35414	010551-58-3	87
14	31.8729	2.1026	2-Furancarboxaldehyde, 5-(hydroxymethyl)-	10778	000067-47-0	70
15	32.4488	1.9321	Phenol, 2-methoxy-4-(1-propenyl)-, (Z)-	31881	005912-86-7	98
16	34.0002	22.2023	Phenol, 2-methoxy-4-(1-propenyl)-, (E)-	31883	005932-68-3	98
17	35.204	5.6293	Vanillin	24745	000121-33-5	96
18	36.7658	1.9501	Phenol, 2-methoxy-4-propyl-	33184	002785-87-7	91
19	37.2431	0.8006	Benzoic acid, 4-hydroxy-3-methoxy-, methyl ester	45107	003943-74-6	96
20	37.5233	4.1295	Ethanone, 1-(4-hydroxy-3-methoxyphenyl)-	34048	000498-02-2	93
21	38.6908	7.87	Homovanillyl alcohol	35473	002380-78-1	72
22	39.7596	1.515	4-[(1-Carboxy-2-methylpropyl)amino]-2(1H)-pyrimidinone	65266	024604-80-6	47
23	40.071	2.0473	3,7-Benzofurandiol, 2,3-dihydro-2,2-dimethyl-	42754	017781-15-6	62
24	44.087	0.9867	Benzeneacetamide, N-(aminocarbonyl)-4-hydroxy-3-methoxy-	73846	015324-70-6	62
25	46.1053	17.2694	4-Hydroxy-2-methoxycinnamaldehyde	41242	127321-19-1	91
26	54.9831	0.3691	1-Phenanthrenecarboxylic acid, 1,2,3,4,4a,9,10,10a-octahydro-1,4a-dimethyl-7-(1-methylethyl)-, methyl ester, [1R-(1.alpha.,4a.beta.,10a.alpha.)]-	133618	001235-74-1	97

Appendix 6.1. A procedure to conduct a torrefaction/pyrolysis simulation using an FG-Biomass model.

Open FG-Biomass program.

Under '**Config'**, click onto '**Load Input File**' and pick an input file. An input file is usually saved as '*.kin' for example, willow_e.kin. Sample properties of willow will be displayed under '**File Header**'.

Then click onto '**Build Single-Step TTH'** to set up the temperature profile. Another window will be displayed and this is where the desired values for parameters are keyed in. The description for each parameter is given below:

- Hold time: the reaction time in seconds.
- Tfinal (C): Desired final temperature in degrees celcius.
- Tinit (C): Initial temperature in degrees celcius.
- Heating rate (C/s): Heating rate in degrees celcius per second
- Time step: The interval time it takes to collect data during the thermal process.

Click '**OK**'.

Then, click '**RUN MODEL**'.

'**Plots**' of evolution rates and yields of each evolution species will be resulted.

The values of rates and yields at a given time will be provided in '**Table**'. The values are expressed in dry ash free basis. Click onto '**EXPORT XY**' to export the data. It is important to note that the data exported are saved in the form of a text. To convert it to Excel, open the MS Excel and convert the text file to a tabulated form.

Elemental composition of the thermal treated solid can be provided in '**Elemental**'. The changes in the elemental composition for gases, tar and char can also be obtained in that section.

Appendix 6.2. Calculated volumes of willow and eucalyptus samples.

Table A-6.2.1. Calculated volumes of willow, treated at conditions A, B and C.

Condition A

Size	*M %*	f_m	*Mass, ar (mg)*	*Mass, db (mg)*	*Mass, db (kg)*	$\rho_{particle}$	*Volume (m^3)*	*Volume (mm^3)*	*MY (ar)*	*MY (db)*
150-300 µm_A	1.5	0.0150	21.35	21.03	0.000021	527.0	0.00000004	39.9	77.4	78.6
5x5x5_A	2.0	0.0199	81.09	79.48	0.000079	529.3	0.00000015	150.1	80.7	82.3
6x6x6_A	3.5	0.0352	136.74	131.93	0.000132	536.5	0.00000025	245.9	81.6	78.6
5x5x10_A	6.3	0.0630	206.35	193.35	0.000193	549.5	0.00000035	351.9	76.1	81.2
7x7x7_A	6.3	0.0630	242.21	226.95	0.000227	549.5	0.00000041	413.0	78.5	83.8
6x6x10_A	5.9	0.0590	161.82	152.27	0.000152	547.6	0.00000028	278.1	79.3	84.3
7x7x10_A	3.3	0.0330	257.03	248.55	0.000249	535.5	0.00000046	464.2	81.7	84.5
8x8x8_A	5.9	0.0590	302.61	284.76	0.000285	547.6	0.00000052	520.0	76.9	81.7

Density of water at 20°C = 998.2071 kg m^{-3}

Condition B

Size	*M %*	f_m	*Mass, ar (mg)*	*Mass, db (mg)*	*Mass, db (kg)*	$\rho_{particle}$	*Volume (m^3)*	*Volume (mm^3)*	*MY (ar)*	*MY (db)*
150-300 µm	0.7	0.0070	21.13	20.98	0.000021	523.3	0.00000004	40.1	72.6	73.1
5x5x5										75.4
6x6x6	2.7	0.0270	155.72	151.52	0.000152	532.6	0.00000028	284.5	75.5	77.6
5x5x10	2.7	0.0270	114.5	111.41	0.000111	532.6	0.00000021	209.2	75.5	77.6
7x7x7	6.1	0.0610	200.12	187.91	0.000188	548.6	0.00000034	342.6	71.8	76.5
6x6x10		0.0000								
7x7x10	5.6	0.0560	257.03	242.64	0.000243	546.2	0.00000044	444.2	76.1	80.6
8x8x8	4.9	0.0490	302.61	287.78	0.000288	542.9	0.00000053	530.0	73.9	77.7

Condition C

Size	M %	f_m	Mass, ar (mg)	Mass, db (mg)	Mass, db (kg)	$\rho_{particle}$	Volume (m^3)	Volume (mm^3)	MY (ar)	MY (db)
150-300 µm	0.6	0.0060	21.21	21.08	0.000021	522.8	0.00000004	40.3	68.6	69.0
5x5x5	4.2	0.0420	88.42	84.71	0.000085	539.7	0.00000016	157.0	71.2	74.3
6x6x6	3.6	0.0356	138.95	134.00	0.000134	536.7	0.00000025	249.7	70.7	73.3
5x5x10	2.7	0.0268	197.31	192.02	0.000192	532.5	0.00000036	360.6	73.1	75.1
7x7x7	6.0	0.0597	195.69	184.01	0.000184	548.0	0.00000034	335.8	68.6	73.0
6x6x10	3.8	0.0380	213.91	205.78	0.000206	537.8	0.00000038	382.6		76.2
7x7x10	6.7	0.0670	291.05	271.55	0.000272	551.4	0.00000049	492.5	69.26	74.2
8x8x8	2.2	0.0220	236.73	231.52	0.000232	530.3	0.00000044	436.6	72.9	74.5

Table A-6.2.2. Calculated volumes of eucalyptus, treated at conditions A, B and C.

Condition A

Size	M %	f_m	Mass, ar (mg)	Mass, db (mg)	Mass, db (kg)	$\rho_{particle}$	Volume (m^3)	Volume (mm^3)	MY (db)
5x5x5_A	5.9	0.0593	73.92	69.54	0.000070	717.1	0.00000010	97.0	79.2
6x6x6_A	3.2	0.0318	116.79	113.08	0.000113	709.2	0.00000016	159.4	81.0
5x5x10_A	5.7	0.0568	141.73	133.68	0.000134	716.4	0.00000019	186.6	79.6
7x7x7_A	2.9	0.0293	178.24	173.02	0.000173	708.4	0.00000024	244.2	81.2
6x6x10_A	1.1	0.0114	175.43	173.43	0.000173	703.3	0.00000025	246.6	80.6
7x7x10_A	3.65	0.0365	253.75	244.49	0.000244	710.5	0.00000034	344.1	81.3
8x8x8_A	1.42	0.0142	225.35	222.15	0.000222	704.1	0.00000032	315.5	81.5

Condition B

Size	M %	f_m	Mass, ar (mg)	Mass, db (mg)	Mass, db (kg)	$\rho_{particle}$	Volume (m^3)	Volume (mm^3)	MY (db)
5x5x5	1.3	0.0131	51.99	51.31	0.000051	703.8	0.00000007	72.9	74.6
6x6x6	1.1	0.0114	111.76	110.49	0.000110	703.3	0.00000016	157.1	76.2
7x7x7	5.9	0.0589	162.05	152.51	0.000153	717.0	0.00000021	212.7	75.6
8x8x8	3.49	0.0349	250.31	241.57	0.000242	710.1	0.00000034	340.2	77.3

Condition C

Size	M %	f_m	Mass, ar (mg)	Mass, db (mg)	Mass, db (kg)	$\rho_{particle}$	Volume (m^3)	Volume (mm^3)	MY (db)
5x5x5	5.8	0.0582	72.11	67.91	0.000068	716.8	0.00000009	94.7	71.4
6x6x6	8.5	0.0852	133.61	122.23	0.000122	724.6	0.00000017	168.7	72.0
5x5x10	0.9	0.0088	132.86	131.69	0.000132	702.5	0.00000019	187.5	72.8
7x7x7	0.4	0.0043	179.79	179.02	0.000179	701.2	0.00000026	255.3	73.6
6x6x10	1.4	0.0139	180.19	177.69	0.000178	704.0	0.00000025	252.4	73.2
7x7x10	3.32	0.0332	247.58	239.36	0.000239	709.6	0.00000034	337.3	73.0
8x8x8	2.12	0.0212	264.08	258.48	0.000258	706.1	0.00000037	366.1	74.8

Appendix 6.3. Mass yields of torrefied willow and eucalyptus, obtained from TGA-FTIR.

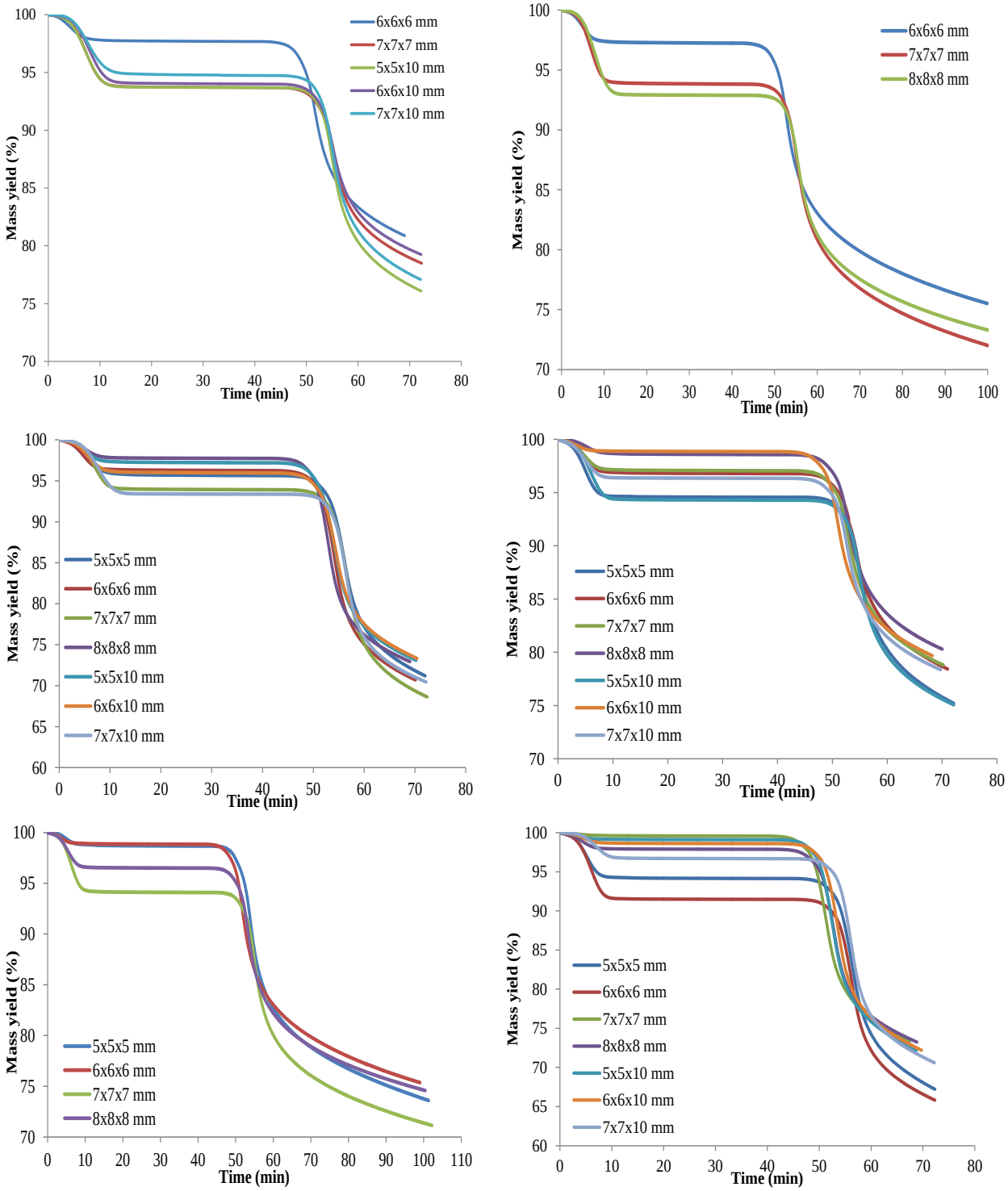

Figure A-6.3.1. Plots of mass yield vs time of torrefied willow and eucalyptus of different particle sizes at different conditions.

Appendix 6.4. Yields of products of torrefaction of biomass as predicted by FG-Biomass model.

Table A-6.4.1. Product distribution of torrefaction of willow and eucalyptus at different conditions, where A is at 270°C with a reaction time of 30 min, B is at 270°C with a reaction time of 60 min and C is at 290°C with a reaction time of 30 min (dry ash free basis).

	Conditions					
Products	**Willow - A (%)**	**Willow - B (%)**	**Willow - C (%)**	**Eucalyptus - A (%)**	**Eucalyptus - B (%)**	**Eucalyptus - C (%)**
Char	79.73	74.01	67.34	73.24	68.56	62.45
Carbon monoxide	0.62	0.77	0.97	0.55	0.71	0.93
Carbon dioxide	1.50	1.81	2.18	1.84	2.08	2.44
Tars	11.47	14.47	17.95	19.44	22.67	26.76
Water	1.33	1.83	2.53	2.96	3.48	4.19
Methane	0.01	0.02	0.03	0.01	0.02	0.03
Ethylene	0.00	0.00	0.00	0.00	0.00	0.00
Phenol	0.53	0.76	1.05	0.24	0.36	0.54
Acetone	0.66	0.91	1.21	0.11	0.15	0.21
Methanol	0.61	0.68	0.75	0.51	0.57	0.62
HCN	0.01	0.02	0.02	0.00	0.00	0.00
Ammonia	0.01	0.01	0.01	0.00	0.00	0.00
Formaldehyde	0.63	0.85	1.12	0.78	1.01	1.29
Formic acid	0.38	0.54	0.72	0.10	0.12	0.14
Acetic acid	1.57	1.90	2.18	0.18	0.22	0.27
Acetaldehyde	0.94	1.43	1.93	0.03	0.06	0.13

Appendix 8.1. Potential stakeholders and sources of environmental information (EA, 2002).

Issues	Potential stakeholders and sources of environmental information (inc. statutory consultees and other organisations)
WATER	• Environment Agency {http://www.environment-agency.gov.uk/} • Water companies • British Geological Survey {http://www.bgs.ac.uk/} • British Waterways {http://www.british-waterways.org/}

Issues	Potential stakeholders and sources of environmental information (inc. statutory consultees and other organisations)
AIR	• Local authority {http://www.tagish.co.uk/tagish/links/localgov.htm} • Meteorological Office {http://www.meto.gov.uk/home.html} • Environment Agency {http://www.environment-agency.gov.uk/} • Academic institutions {http://www.scit.wlv.ac.uk/ukinfo/uk.map.html} • UK National Air Quality Information Archive {http://www.aeat.co.uk/netcen/airqual/} • Welsh Air Quality Forum {http://whoweb.uwic.ac.uk/airquality/}
LAND USE AND DESIGNATIONS	• Local authority {http://www.tagish.co.uk/tagish/links/localgov.htm} • Environment Agency {http://www.environment-agency.gov.uk/} • Department for Environment, Food and Rural Affairs (DEFRA) {http://www.defra.gov.uk/} • National Assembly for Wales Agriculture Department {http://www.wales.gov.uk/subiagriculture/index.htm} • The Countryside Agency {http://www.countryside.gov.uk/} • Countryside Council for Wales {http://www.ccw.gov.uk/} • English Nature {http://www.english-nature.org.uk/} • Royal Society for Nature Conservation/Local Wildlife Trusts {http://www.rsnc.org/} • Electricity companies • Gas companies • Water companies • Telecommunications companies • Forestry Commission {http://www.forestry.gov.uk/} • Farming and Wildlife Advisory Group {http://www.fwag.org.uk/} • National Farmers' Union {http://www.nfu.org.uk/} • Farmers' Union of Wales {http://www.fuw.org.uk/} • County minerals officers {http://www.tagish.co.uk/tagish/links/localgov.htm} • British Geological Survey {http://www.bgs.ac.uk/} • Soil Survey and Land Research Centre {http://www.cranfield.ac.uk/sslrc/} • Royal Agricultural Society of England {http://www.rase.org.uk}

FAUNA AND FLORA	• Environment Agency {http://www.environment-agency.gov.uk/} • English Nature {http://www.english-nature.org.uk/} • Countryside Council for Wales {http://www.ccw.gov.uk/} • Royal Society for Nature Conservation/local wildlife trusts {http://www.rsnc.org/} • Royal Society for the Protection of Birds {http://www.rspb.com/}